THE *SLEEPING BEAUTY* TRANSPOSON SYSTEM FOR FORWARD AND REVERSE GENETIC STUDIES OF LIVER CANCER

A THESIS

SUBMITTED TO THE FACULTY OF THE GRADUATE SCHOOL OF

THE UNIVERSITY OF MINNESOTA

BY

BARBARA RYAN TSCHIDA

IN PARTIAL FULFILLMENT OF THE REQUIREMENTS

FOR THE DEGREE OF

DOCTOR OF PHILOSOPHY

DAVID A. LARGAESPADA, PH.D., ADVISOR

APRIL 2017

Copyright page

ACKNOWLEDGEMENTS

In addition to Barbara Ryan Tschida, the following people and groups contributed to the work described here:

Khalid Amin, Pauline J. Beckmann, Caitlin B. Conboy, Adam J. Dupuy, Rachel A. Heuer, Hsiangyu D. Hu, Wendy A. Hudson, Robert Hullsiek, Carlyn Iverson, Vincent W. Keng, Timothy P. Kuka, David A. Largaespada, Lindsey A. Lee, Michael A. Linden, Joseph H. Nadeau, Jesse D. Riordan, Lewis R. Roberts, N. Alpay Temiz, Carlos A. Tierrablanca, Sandra Wagner, Ju Dong Yang

Contributions:

CI provided Illustration assistance with the preparation of some of the figures presented in chapter 2. BRT, AJD, VWK, and DAL contributed to the chapter 2 study concept and design. BRT, CBC, AJD, VWK, DAL, and LDR contributed to the chapter 3 study concept and design. BRT, KA, PJB, CBC, AJD, RAH, HDH, WAH, RH, VWK, TPK, LAL, MAL, NAT, JDR, CAT, SW, and JDY contributed to data acquisition. BRT, KA, CBC, AJD, WAH, VWK, DAL, MAL, JHN, JDR, LRR, NAT, SW, and JDY contributed to the analysis and interpretation of data. BRT, AJD, JDR, and NAT contributed to statistical analysis. BRT, DAL, and JDR obtained funding. AJD, DAL, JHN, and LRR contributed to study supervision. BRT wrote the thesis.

The results published here are in part based upon public data generated by the TCGA Research Network: http://cancergenome.nih.gov/. This work utilized computing resources at the University of Minnesota Supercomputing Institute. The University Of Minnesota Genomics Center provided Illumina sequencing, Sanger sequencing, and primer synthesis services.

ABSTRACT

Hepatocellular carcinoma (HCC) is the second leading cause of death from cancer globally and increasing in prevalence. HCC usually occurs in the context of chronic liver damage. The specific genetic alterations promoting HCC have been difficult to identify due to the genetic heterogeneity of HCC and the prevalence of large chromosome aberrations. To study the pathogenesis of HCC, we used *Sleeping Beauty* (SB) transposons for both a forward genetic screen and reverse genetic studies of genes identified in HCC mouse models, altered in human HCC, or components of the Hepatitis B virus, a major HCC risk factor. Hepatic steatosis is a common chronic liver disease linked to HCC development. We used conditional SB transposon insertional mutagenesis in mice with diet and ethanol induced hepatic steatosis to model steatosis-associated HCC and perform a forward genetic screen for molecular drivers. We compared the results from this screen to human HCC data from multiple sources. We found an increase in HCC in females in both mice and humans with hepatic steatosis, reducing the typical male sex bias of HCC. We identified over 200 genes candidate steatosis-associated HCC genes in mice, many of which are altered in human steatosis and alcohol associated HCC. We identified an association between protein kinase A/cyclic AMP signaling pathway alterations and steatosis-associated HCC, and *NAT10* overexpression and HCC, both of which could potentially be targeted therapeutically. We used SB transposon-based gene delivery for reverse genetic studies testing candidate oncogenes identified in human HCC, complementary mouse models including the steatosis-associated HCC screen, and Hepatitis B viral genes for their roles in promoting liver tumorigenesis. These studies revealed new oncogenic roles for genes tested in normal livers, in mice of both sexes, in steatotic livers, and in fibrotic livers. We generated several new mouse models of HCC that could be used for mechanistic studies or therapeutic testing.

TABLE OF CONTENTS

LIST OF TABLES

LIST OF FIGURES

ABBREVIATIONS

BH, Benjamini-Hochberg

CCl4, carbon tetrachloride

cDNA, complementary DNA

CIS, common insertion site

DEN, N-nitrosodiethylamine

DNA, deoxyribonucleic acid

eCDD, 5% ethanol and choline-deficient diet

gCIS, gene-centric CIS

GFP, green fluorescent protein

H&E, hematoxylin and eosin

HBsAg, HBV surface antigen

HBV, hepatitis B virus

HBx, HBV regulatory protein X

HCV, hepatitis C virus

HCC, hepatocellular carcinoma

IHC, immunohistochemistry

IPA, Ingenuity Pathway Analysis

IR/DR, inverted repeat/direct repeat

Lsl, loxP-flanked stop cassette

ND, normal diet

p-FOXA2, FOXA2 phosphorylated at T156

p-PKA, PKA phosphorylated at T197

qRT-PCR, quantitative reverse-transcriptase polymerase chain reaction

RNA, ribonucleic acid

rRNA, ribosomal RNA

SB, Sleeping Beauty

shRNA, short hairpin RNA

TCGA, The Cancer Genome Atlas Consortium

tdCIS, TAPDANCE CIS

CHAPTER 1: INTRODUCTION

Sleeping Beauty transposon-driven models of hepatocellular carcinoma

*Contains material from previously published work:

Tschida BR, Largaespada DA, Keng VW. Mouse models of cancer: *Sleeping Beauty* transposons for insertional mutagenesis screens and reverse genetic studies.
Semin Cell Dev Biol 2014;27:86–95.

I. Hepatocellular carcinoma

1. Hepatocellular carcinoma pathophysiology

Hepatocellular carcinoma (HCC), the major type of primary malignant liver cancer, is composed of cells resembling hepatocytes with abnormal appearance and organization.[1] Studies examining restriction fragment length polymorphisms[2] or Hepatitis B virus (HBV) genome integration sites[3–5] in tumor cells suggest most HCCs are monoclonal. The cell of origin can be either a mature hepatocyte or hepatic progenitor cell that accumulates genetic mutations leading to dysregulation of proliferation and survival.[1] Both hepatocytes and hepatic progenitor cells are proliferative cells capable of acquiring these mutations and are susceptible to transformation. Although hepatocytes are highly differentiated, they can regenerate liver tissue by self-replication in response to most forms of liver damage and can give rise to HCC in some instances.[1] Hepatic progenitor cells, or oval cells, are activated and proliferate in response to extensive liver damage or when liver regeneration by hepatocytes is compromised. These give rise to more oval cells, the number of which increases with increasing severity of liver injury,[6] and to intermediate hepatocytes which proliferate and differentiate into hepatocytes.[7] Oval cells are believed to be the cell of origin for most cases of HCC.[1] Hepatic carcinogenesis is a multistep process, most often occurring in the setting of chronic liver damage and regeneration.[8] Acquisition of mutations in proliferating oval cells or hepatocytes gives rise to dysplastic focal lesions which develop into HCC after multiple rounds of damage, mutation, and clonal expansion.[9]

HCC tumors commonly contain a mixture of cells resembling hepatocytes and oval cells, with some organization into plate-like structures around sinusoids.[1] The development of multiple tumor nodules is common in HCC.[10] HCCs are classified as either early HCCs which are small, vaguely nodular tumors with poorly defined margins, or progressed

HCCs, which vary in size and are moderately differentiated, distinctly nodular, infiltrative, and characterized by neovascularization.[10] The 4-scale HCC grading system described by Edmondson and Steiner in 1954[11] remains the most commonly used HCC grading system.[10] This system defines Grade I HCCs as tumors consisting of small cells with abundant cytoplasm and a minimal amount of nuclear irregularity that resemble normal liver tissue. Grade II HCC tumors have nuclear irregularity and excessive nuclear staining. Grade III HCC tumor cells are variable in size and shape and have irregular nuclei of variable sizes and shapes. Grade IV HCCs have cells that are highly variable in size and shape and often contain giant anaplastic cells.[11] HCC tumors are highly heterogeneous; one tumor often contains regions that resemble multiple tumor grades.[12]

2. Major risk factors for hepatocellular carcinoma

A. Overview

HCC is the second leading cause of death from cancer in the world, with a staggering mortality to incidence ratio of 0.95.[13] Unlike most cancers, it is increasing in prevalence in the United States.[14–16] The risk for HCC development in men is 2-4 times higher than in women, with limited molecular data explaining this sex bias.[8,17] HCC almost always develops in the context of chronic liver damage and cirrhosis, major causes of which include Hepatitis B Virus (HBV) infection, Hepatitis C Virus (HCV) infection, alcoholic liver disease, and hepatic steatosis.[8] Chronic liver damage leads to excess extracellular matrix accumulation, scarring the liver parenchyma and leading to increasing severity of fibrosis. With ongoing injury, fibrosis can eventually progress to cirrhosis, which is characterized by distortion of the liver parenchyma and vascular structure and by nodules of regenerating hepatocytes surrounded by scar tissue.[18,19]

B. Hepatitis B Viral infection

Viral infection with HBV or HCV accounts for approximately 85% of the world total liver cancer cases, 42.5% of the cases in developed countries and 92% of the cases in developing countries, with only a small proportion of cases resulting from joint infections.[20] Over half of HCC cases globally are attributable to HBV infection.[20] HBV is a partially double-stranded DNA virus in the *Hepadnaviridae* family.[21] HBV promotes HCC through various indirect and direct mechanisms that are not fully understood. HBV infection causes chronic liver inflammation and hepatocyte injury, leading to hepatocyte proliferation. This increases the chances for the accumulation of transforming mutations and the development of fibrosis and cirrhosis.[22] Hepatic cirrhosis often accompanies HBV-associated HCC development, but HBV can also cause HCC in the absence of cirrhosis.[23] The HBV genome can integrate into the host genome, leading to insertion mutations and altered gene expression, such as activation of *TERT* expression.[24,25] The HBV regulatory protein, HBx, required for the transcription of the viral genome, can transactivate host genes controlling proliferation, survival, and DNA repair,[26] altering expression of genes that can lead to hepatocarcinogenesis.

C. Hepatitis C Viral infection

Approximately one-third of HCC cases worldwide are attributable to HCV infection.[20] HCV is an RNA virus in the *Flaviviridae* family that can induce HCC through indirect mechanisms.[27] HCV infection causes chronic inflammation and hepatocyte injury, leading to hepatocyte and proliferation, fibrosis, and cirrhosis.[22] The HCV core protein localizes to the host cell mitochondrial membrane and endoplasmic reticulum, where it promotes oxidative stress.[27] The immune response to HCV infection induces insulin resistance, increased levels of inflammatory cytokines, and fibrosis.[28,29] The relationship between

HCV infection, immune response, insulin resistance, inflammation, and HCC has not been fully characterized.[27]

D. Alcoholic liver disease

Chronic heavy alcohol intake is one of the most common causes of cirrhosis and an established risk factor for HCC development.[30,31] Heavy alcohol intake also enhances hepatocarcinogenesis due to HBV, HCV, or non-alcoholic fatty liver disease.[31] Alcohol can promote HCC through DNA damage due to acetaldehyde, oxidative stress, and chronic inflammation due to alcoholic steatohepatitis.[31] Acetaldehyde is a major metabolite produced during ethanol oxidation. It can interfere with DNA synthesis and repair, leading to mutations and tumor formation.[32] Chronic alcohol consumption increases levels of Cytochrome P-4502E1, which creates oxidative stress as it metabolizes ethanol to acetaldehyde.[31,33] Ethanol is a substantial source of calories (7.1 kcal per gram). It comprises, on average, half of an alcoholic's caloric intake, displacing normal nutrients and leading to nutritional deficiencies which can cause liver damage.[33] Even in the presence of adequate dietary nutrition, ethanol metabolism can induce fatty liver.[34] Ethanol oxidation through the alcohol dehydrogenase pathway produces NADH, stimulating fatty acid synthesis.[33] Chronic heavy alcohol intake induces fatty liver disease in almost all cases, itself risk factor for HCC (reviewed below).[31,33,35] Alcoholic fatty liver progresses to alcoholic steatohepatitis in approximately 30% of cases and to hepatic cirrhosis in 10-20% of cases.[35]

E. Hepatic steatosis

A strong risk factor for HCC development, hepatic steatosis, or fatty liver disease, is the most common chronic liver disease in the United States and becoming increasingly

common in the United States and worldwide.[36–39] Hepatic steatosis can be induced by chronic heavy alcohol intake or due to metabolic syndrome in the absence of chronic alcohol use.[31,33,35] Metabolic syndrome is characterized by obesity, diabetes, insulin resistance, dyslipidemia, and non-alcoholic fatty liver disease.[40] Obesity is the biggest risk factor for non-alcoholic hepatic steatosis.[39] With the rise of obesity, fatty liver disease has become the most common chronic liver disease in Western countries,[39] partially accounting for the increase in HCC. Obese individuals are at a 2-4 fold relative risk for HCC and a 5-6 fold relative risk for HCC-related mortality.[41]

Fatty liver disease due to alcohol and non-alcoholic steatosis appear similar histologically,[42] and can develop inflammation, hepatocyte injury, and fibrosis.[27] Hepatic steatosis progresses to steatohepatitis in approximately 30% of cases, and approximately 30% of those progress to cirrhosis.[40] Cirrhotic livers can have varying degrees of steatosis ranging from focal steatosis in regenerative nodules to more substantial steatosis.[19] High intrahepatic levels of fatty acids creates oxidative stress that can induce DNA damage and inflammatory cytokines. This can lead to hepatocyte and oval cell proliferation and accumulation of mutations, leading to tumor formation.[27] Alcohol consumption further increases the risk of HCC development steatotic livers and was found to be among the most significant factors associated with progression of fatty liver disease to HCC.[37]

3. Molecular drivers of hepatocellular carcinoma

    A. Known drivers of hepatocellular carcinoma

Cancer arises from a series of molecular changes inheritable by progeny cells that confer selective advantages by corrupting normal cellular processes including proliferation, survival, migration, replicative immortality, angiogenesis, and metabolism.[43,44] A small number of alterations driving HCC have been identified. These include inactivation of

TP53 which confers a survival advantage,[43,45,46] Wnt/β-catenin signaling activation through *CTNNB1* activating mutations and *AXIN1* inactivating mutations conferring a proliferation and survival advantage,[45–47] *TERT* amplification and promoter mutations which confer replicative immortality,[43,46] and *EGFR* amplification and activating mutations conferring a proliferative advantage.[43,46,48] Pro-angiogenic receptor tyrosine kinases *VEGFR2* and *PDGFRβ* are commonly overexpressed in HCC,[49,50] and downstream regulators of receptor tyrosine kinase signaling like *PTEN* and *RSK2* often have inactivating mutations.[51,52] Five major molecular subtypes of HCC have been defined by gene expression analysis, characterized by Wnt/β-catenin signaling, high proliferation, interferon signaling, polysomy of chromosome 7, and an unannotated class. The Wnt/β-catenin signaling subtype is often driven by *CTNNB1* mutations.[53] The driving events for the other subtypes are not fully understood. The highly proliferative subtype is likely driven by receptor tyrosine kinase activation, and the polysomy of chromosome 7 subtype is likely driven by overexpression of *EGFR* along with an unidentified set of other oncogenes on chromosome 7.[53,54]

B. Molecularly targeted therapies

Therapeutic options currently available for HCC are insufficient. Only 30-40% of HCC cases in Western countries are diagnosed at early stages and suitable for the potentially curative locoregional therapies of local ablation, surgical resection, chemoembolization, radioembolization, and liver transplantation.[55–57] For later stage HCC patients not eligible for locoregional therapies, only two systemic treatments have been shown to provide improvement in HCC survival, targeted multikinase inhibitors sorafenib and regorafenib.[56,57] Sorafenib is the only approved molecularly targeted HCC therapy. It inhibits the pro-angiogenetic receptor tyrosine kinases VEGFR1, VEGFR2, and VEGFR3

and PDGFRβ, as well as serine/threonine kinases RAF1 and BRAF which signal downstream of receptor tyrosine kinases.[50,57] Sorafenib is approved as a first line treatment for HCC and significantly extends median survival by almost 3 months.[57] Regorafenib is another molecularly targeted therapy that, like sorafenib, inhibits pro-angiogenic kinases VEGFR1, VEGFR2, and VEGFR3 and PDGFRβ, as well as c-KIT, RET, BRAF, and a constitutively active mutant form of BRAF.[56,58] It has been shown to improve lifespan by almost 3 months in patients with HCC disease progression during sorafenib treatment.[56] Learning more about the molecular alterations driving HCC is needed to provide targets for the development of more effective therapies.

C. Challenges for driver alteration identification

Genomic and gene expression data has revealed a great amount of heterogeneity in the many mutated and misexpressed genes in HCC.[59–61] Sequencing of over 500 HCC cases revealed only a small number of genes were mutated in more than five percent of cases, including *TERT*, *CTNNB1*, *TP53*, and *AXIN1*, while the vast majority of mutations occurred infrequently.[46] Chromosome aberrations involving copy number variations or large regions and whole chromosomes are highly prevalent in HCC, making the identification of the specific tumor-promoting changes difficult as these large regions harbor many genes, multiple of which may be involved in tumorigenesis.[45,46,53,62] Altered gene expression due to epigenetic changes such as hyper- or hypo-methylation is also common in HCC.[63] Thus, distinguishing molecular drivers of HCC from passenger alterations presents a challenge. Complementary experimental methods are needed to identify and validate the molecular alterations and processes operative in HCC that could serve as a basis for new targeted HCC prevention or treatment strategies.

4. Progress and limitations modeling HCC in mice

A. Genetically modified mouse models

Genetically modified mouse models can be engineered to express oncogenes in a tissue-specific manner, often using the *Albumin* promoter to restrict transgene expression to hepatocytes for modeling HCC.[64] HBV-driven HCC has been modeled using transgenic mice expressing whole fragments of the HBV genome, the surface antigen, or the *HBx* gene.[65–67] Mouse models of HCV-induced HCC have been generated expressing the complete set of viral proteins,[68] the core protein alone,[69,70] or the core with envelope proteins 1 and 2.[71] Transgenic mice expressing well-characterized oncogenes such as *Myc*, *Egf*, and an activating *Ctnnb1* mutation in combination with an *HRas* mutation have also been used to model HCC.[72–74] Genetically engineered mice have been generated with liver-specific tumor suppressor gene loss, such as liver-specific *Pten*-deficient mice which develop hepatic steatosis and liver tumors.[75] Genetically modified mouse models allow tumor development *in situ* in immunocompetent animals. They can be engineered to express multiple oncogenes, facilitating the investigation of cooperation between oncogenic alterations. They are, however, slow and costly to generate, so are typically used to study known oncogenes and tumor suppressor genes rather than novel genes involved in tumor development and maintenance. They do not model the acquisition of transforming alterations by individual somatic cells, since the whole liver is typically engineered to express the genetic modification, nor do they reflect the heterogeneity of tumor cells in which multiple mutations drive tumorigenesis.[64]

B. Mosaic mouse models

To overcome the cost and time obstacles of generating conventional genetically modified mouse models, a mosaic mouse model was developed where liver progenitor cells

(hepatoblasts) are genetically modified in culture, then transplanted into syngeneic recipient mice and assessed for tumor formation.[76] Hepatoblasts from *Trp53*-deficient mice modified to express oncogenes like *Myc*, *Ras*, or *Akt* and wildtype hepatoblasts engineered to express oncogenes and shRNA knockdown constructs against the tumor suppressor *Trp53* can form tumors when seeded into recipient mouse livers.[76,77] These tumors resemble human HCC and can acquire additional spontaneous genetic lesions like focal amplifications promoting tumorigenesis, modeling the genetic heterogeneity of HCC.[77] This model has been used to screen genes by shRNA knockdown for tumor suppressor identification and by overexpression of cDNAs for HCC oncogene identification.[78,79] These models overcome the time and cost associated with the generation of genetically engineered mouse models, but do not recapitulate the typical development of HCC in context of chronic liver disease.

C. Xenograft models

In xenograft models, human HCC cells from a biopsy or cell line are injected into immunodeficient mice either ectopically in the flank or orthotopically in the liver. These models have the advantages of rapid tumor development and allowing the study of human tumor cells *in vivo*. Xenografts neither model the immune response to tumor cells, nor the natural tumor progression in which neoplastic cells interact with the surrounding environment as tumors develop.[64] This system can be improved by implanting tumor cells in an environment with liver damage that more closely resembles the conditions under which HCC typically develops. HCC cells have been implanted into livers with fibrosis induced by carbon tetrachloride or alcohol. The resulting tumors better model HCC development, grow larger than in normal livers, and are capable of metastasizing.[80]

D. Chemically induced models

Hepatocyte injury by chemical compounds can lead to liver tumor formation, modeling the development of liver cancer in context of liver damage typically occurring in humans.[64] N-nitrosodiethylamine (DEN) is a DNA-damaging agent commonly used to induce liver tumors in mice. Repeated DEN administration can result in tumor development in 100% of male mice and 30% of female mice.[81] Carbon tetrachloride (CCl4) is a hepatotoxin that induces fibrosis and HCC by repeated cycles of liver injury, inflammation, and repair, modeling liver disease progression in humans.[64] Although choline-deficiency is not a major cause of hepatic steatosis in humans, a choline-deficient diet is commonly used to model steatosis-associated HCC in rodents; it induces hepatic steatosis with 100% penetrance and liver tumors with approximately 20% penetrance.[82] The addition of ethionine or ethanol to this diet can increase both tumor formation and steatosis severity.[83,84] Choline-deficient diets are a particularly useful model for alcohol-associated hepatic steatosis because, like alcohol, choline-deficiency decreases the synthesis of phosphatidylcholine, causing fatty acids to accumulate in hepatocytes.[33,83] These systems model HCC development in context of liver damage, but it can be difficult to determine the mutations driving tumor formation using these models. The interaction between tumor-promoting mutations and the influence of the environment of liver damage in which tumors arise could be addressed by using these liver damaging agents on genetically-driven mouse models of HCC, like those listed above. This would be useful to study the influence of chronic liver damage on HCC induction driven by known cancer genes, but would be inefficient for identifying new HCC oncogenes or tumor suppressors in the context of liver damage.

II. The *Sleeping Beauty* (SB) transposon system for cancer studies

1. SB transposon system overview

The *Sleeping Beauty* (SB) transposon system is a useful tool for both forward and reverse genetic studies to elucidate cancer genes *in vivo*. The SB transposable element is a synthetic DNA transposon belonging to the Tc1/Mariner family that mobilizes in a cut-and-paste fashion. It was awakened from millions of years of evolutionary sleep by correcting the mutations responsible for its transposase inactivity.[85] The current SB transposon system consists of two parts: firstly, a transposon vector containing any DNA sequence that is flanked by SB inverted repeat/direct terminal repeat (IR/DR) sequences and secondly, the SB transposase enzyme that is responsible for excision and reintegration of the transposon placed under the control of a promoter. When both these components are present in a cell, a cut-and-paste transposition reaction occurs in which the transposon is excised from its original location and re-integrated at a new "TA" dinucleotide location within the genome. The mobilization process is relatively random, although it has the propensity for local hopping, a phenomenon in which a transposon reintegrates in close vicinity to the donor locus.[86] SB transposition can be active in both transgenic mouse germline and somatic cells.[86–89]

2. SB transposon insertional mutagenesis for forward genetic cancer screens

A. Body wide SB insertional mutagenesis

Comparative analysis of molecular alterations in human tumors to data obtained through unbiased transposon-based insertional mutagenesis screens in mice is a method that can be used to identify driver genes for a variety of cancer types.[90,91] In transposon-based mutagenesis screens, the random insertion of mutagenic transposons alters normal endogenous genes in mouse cells and induces cancer. The mutagenic transposon called

T2/Onc (Figure 1.1A), designed to cause both gene gain- and loss-of-function insertional mutations, contains a strong promoter that can induce gene overexpression and stop cassettes that can truncate gene expression. Insertion of T2/Onc near or within a gene can lead to tumor formation when proto-oncogenes are overexpressed or tumor suppressor genes are inactivated. The genetic changes that drive tumor progression can then be identified by the locations of transposon insertions in the genome.[87,88,92] (Figure 1.1B-C) T2/Onc combined with transgenes ubiquitously expressing SB transposase in wild-type or cancer predisposed mice have induced or accelerated sarcoma and T-cell leukemia.[87,88] In both cases, the SB initiated or accelerated tumors were characterized by somatic, tumor specific transposon insertions that were shown to occur at dozens of recurrently mutated known and novel cancer genes.[87,88] SB insertion sites are readily cloned and can be characterized rapidly to implicate new genes in solid tumor development using a forward genetic approach. Next-generation sequencing platforms allow rapid and adequate coverage for identifying transposon insertion sites. Sites mutated by insertions significantly more frequently in tumors than predicted by random chance are called common insertion sites (CIS) and are hypothesized to reveal potential driver mutations. These data can be compared to human cancer mutation data to elucidate which alterations found in human tumors may be important cancer drivers. (Figure 1.2) These transposon-based systems, therefore, provide powerful genetic tools for identifying cancer-promoting mutations.

B. Conditionally expressed SB transposon system

Tissue specific mutagenesis with SB has developed informative models of various types of human solid tumors. In these studies, mice conditionally express the catalytically improved SB transposase, *SB11*,[93] from the endogenous *Rosa26* locus after Cre

recombinase has excised a loxP flanked stop cassette (lsl) separating the *SB11* cDNA from the *Rosa26* promoter. Thus, using these *Rosa26*-lsl-*SB11* mice, SB mutagenesis can be restricted to tissues expressing the Cre recombinase from a tissue-specific promoter. Conditional SB transposition systems have been used to generate various solid tumors and screen for genes associated with these cancer types.[48,92,94] In addition to tissue-specific promoters driving Cre recombinase, predisposed genetic backgrounds have also been incorporated into these screens to elucidate mutations cooperating with common cancer initiating mutations.[48,95] Variations of this mutagenesis system have been used to reveal both known and novel oncogenes as well as tumor suppressors in solid tumors and leukemias.[48,87,92,94–97]

C. Forward genetic screens for hepatocellular carcinoma drivers

Hepatocellular carcinoma (HCC) is the second leading cause of cancer-related mortality worldwide.[13] The pathogenic changes underlying the development and progression of HCC are complex and incompletely understood. To specifically model HCC in mice and identify driver mutations, we previously used the conditional SB transposon system for insertional mutagenesis. Mice were generated carrying the conditional *Rosa26*-lsl-*SB11* transposase transgene, the T2/Onc2 transposon, and the hepatocyte specific *Albumin*-Cre to limit transposase expression and subsequent transposon mobilization to hepatocytes. In addition, because *TP53* is frequently mutated in human HCC, a conditional dominant negative *Trp53* transgene, p53-lsl-R270H,[98] was added along with the transposition system. Both the three transgene mutagenesis system and the mutagenesis system on the *Trp53* mutated background produced tumors in mice that modeled all stages of liver cancer progression including neoplastic nodules, adenomas, HCC, and lung metastasis.[48] These models recapitulated the sex bias seen in humans,

with higher tumor burdens occurring in males than females.[48,54] This screen uncovered 19 candidate HCC-associated loci including known oncogenes such as *Egfr* and *Met* and novel candidate genes associated with HCC including *Ube2H* and *Zbtb20*.[48]

HCC has also been generated in mice using a modified mutagenic transposon, T2/Onc3, in which oncogene overexpression is driven by the CAGGS promoter, which is more active in epithelial cells than the murine stem cell virus 5' long-terminal repeat promoter used in T2/Onc2.[92] As expected, body wide mobilization of T2/Onc3 produced more carcinomas[92] than T2/Onc2, which induced mainly hematopoietic malignancies.[87] Of the tumors generated by body wide mobilization of T2/Onc3, liver tumors occurred most frequently.[92] A CIS identified in this screen was the complex Dlk1-Dio3 imprinted domain which contains protein-coding genes, long non-coding RNAs, microRNAs, and small nucleolar RNAs, and which is aberrantly expressed in human HCC.[99]

The *MYC* oncogene is amplified in 30% and overexpressed in a majority of HCC.[63] To identify genetic alterations cooperating with *MYC* overexpression, a transposon based mutagenesis screen was performed on a *MYC* overexpression mouse model of liver cancer. Transgenic mice were generated carrying the mutagenic SB transposon T2/Onc2, ubiquitously expressed *Rosa26-SB11* transposase, tetracycline-repressible *MYC*, and liver specific tet-transactivator transgenes.[95] *MYC*-overexpressing mice undergoing transposition had an accelerated rate of tumorigenesis, with 65% of mice developing tumors before 16 weeks of age compared to 29% of *MYC*-overexpressing controls without transposition. Fourteen CISs were identified from tumors in the mice undergoing transposition. Of these, three were validated as tumor suppressor genes by shRNA knockdown in *Trp53*-null hepatoblasts immortalized by *MYC* overexpression. Hepatoblasts with *Ncoa2*, *Zfx*, or *Dtnb* shRNA knockdown gave rise to tumors when

injected into nude mice. Therefore, this study identified 14 candidate *MYC*-cooperating liver cancer driver mutations, three of which were shown to act as tumor suppressors in context of *MYC* overexpression.[95]

While these SB mutagenesis studies in context of an otherwise normal liver, in context of known HCC-promoting gene expression, and in mice of both sexes provide useful information about HCC genetics, HCC most often develops in the context of chronic liver damage and cirrhosis. SB mutagenesis in chronically damaged livers could reveal unique genetic changes in response to the unique selective pressure nascent HCC cells encounter in damaged livers. These specific changes may have relevance for the prevention and treatment of HCC in patients.

In two studies, SB insertional mutagenesis in mouse livers expressing the HBV surface antigen (HBsAg) has been used identify genes promoting HCC in the context of HBV induced liver inflammation. [100,101] In one of these studies, transgenic mice were generated with the mutagenic T2/Onc2 transposon, expression of the conditional *Rosa26*-lsl-*SB11* transposase transgene restricted to hepatocytes by *Albumin*-Cre, and hepatic expression of *HBsAg* to induce liver inflammation.[100] Transposon mutagenesis in context of *HBsAg* expression in this study revealed over 2,800 candidate liver cancer genes, over 1000 of which have altered expression or mutations in human HCC. Well-characterized pathways involved in HCC like Wnt/β-catenin, p53, and Ras signaling were altered by transposon insertions in most of the tumors. More than 1000 of the candidate cancer genes identified in this study were involved in cellular metabolism.[100] Another study used the mutagenic T2/Onc3 transposon, conditional *Rosa26*-lsl-*SB11* transposase, *Albumin*-Cre, and hepatically expressed *HBsAg* transgenes to induce HCC and identified over 1000 CIS genes, 410 of which were mutated in human HCC.[101] Tumor suppressor gene candidates

from both screens were tested *in vivo* by shRNA knockdown in immortalized mouse liver cells which were then injected into nude mice for a tumor formation assay. This assay validated 27 candidate genes as tumor suppressors.[101] These studies demonstrated the use of SB mutagenesis to identify mutations promoting HCC in context of liver damage. More studies in damaged liver contexts such as hepatic fibrosis and steatosis would be highly relevant to human HCC.

3. SB transposon system for reverse genetic studies of cancer

    A. Selection of candidate genes for study

Transposon-based forward genetic screens and human HCC mutation and expression data have generated a wealth of candidate cancer-promoting alterations with possible relevance for human disease. This can make prioritizing these genes for further study challenging. To select candidate cancer genes for testing, we propose that SB CIS genes found in mouse models should be compared to human cancer genetic data, when available, to identify the strongest candidate genes. Transposon insertions in the 5' region of a gene with the promoter in the forward orientation relative to the gene likely drive overexpression, while transposon insertions scattered throughout a gene likely disrupt expression. (Figure 1.1) This allows CIS genes to be identified as candidate oncogenes or tumor suppressors based on insertion site profiles.[90] CIS genes without a clear trend of alteration in human cancer should be considered weaker candidate cancer genes. CIS genes with known roles as human oncogenes or tumor suppressors are not novel, but can be useful as controls or for proof-of-principle experiments. CIS genes found as candidate oncogenes in SB screens that are amplified, overexpressed, or have activating mutations in human cancer can be considered strong candidate oncogenes that should be prioritized for study. Likewise, candidate tumor suppressor CIS genes from SB screens that are

deleted, under-expressed, or have inactivating mutations in human cancer can be considered strong candidate tumor suppressor genes that should be prioritized for further study. (Figure 1.2)

B. SB gene delivery-based reverse genetic cancer models

The roles of candidate cancer genes selected for study can be tested *in vivo* using reverse genetic models. Transgenic mice provide the advantage of allowing development of orthotopic cancer models in immunocompetent mice. Generating transgenic mice, however, is costly and slow, making it an impractical method for addressing a large number of candidate cancer genes. SB-mediated gene delivery may provide a more efficient method to generate reverse genetic cancer models. In addition to its use as a mutagen, SB can be used to deliver genes-of-interest or knockdown vectors for stable expression within cells *in vivo*.[102–106] SB can excise a cDNA sequence or shRNA sequence that is flanked by inverted repeat/direct terminal repeat (IR/DR) sequences from a plasmid and reintegrate it at a random "TA" dinucleotide in the genome.[106] SB transposon plasmids have been delivered to the brain by intracranial injection of DNA-polyethylenimine complexes,[103,105] lung by intravenous injection of DNA-polyethylenimine complexes,[104] and liver by hydrodynamic injection of plasmid DNA,[102,107] while SB has been expressed from a transgene[48,108] or plasmid,[102–104] allowing reverse genetic studies of brain, lung, and liver cancer genes. In this way, SB can be used to generate reverse genetic models of cancer in tissue types for which efficient methods of plasmid delivery exist.

C. SB and the selective Fah-deficient mouse model for hepatic gene expression

A unique mouse model for validating candidate liver cancer genes that uses *Fah* mutant mice expressing SB for gene delivery (*Fah*$^{-/-}$/*SB11*) has been established.[48,54,102,108] *Fah*

mutant mice have a defect in the tyrosine metabolic pathway similar to the human hereditary tyrosinemia type I disease and require maintenance on 2-(2-nitro-4-fluoromethylbenzoyl)-1,3-cyclohexanedione (nitisinone) water. While on nitisinone water, these animals are physiologically normal. Candidate liver oncogene cDNAs or short-hairpin RNAs against putative tumor suppressor gene homologues can be introduced into the livers of Fah/SB11 mice for validation along with the *Fah* cDNA on SB transposon plasmid vectors flanked by SB IRDRs. The plasmids are introduced into the livers of *Fah*$^{-/-}$/*SB11* mice by hydrodynamic tail vein injection,[107] and then nitisinone is removed. As hepatocytes lacking *Fah* die, the livers of the *Fah*$^{-/-}$/*SB11* mice are repopulated by hepatocytes in which transposon vectors are integrated by SB and stably express the *Fah* cDNA and gene-of-interest. This results in generating mice with almost entirely transgenic livers in 6–8 weeks. (Figure 1.3A-B) This system can be used to efficiently test the role of novel HCC-associated genes identified in insertional mutagenesis screens that are altered in human disease to determine their importance as driver mutations. An advantage of using this animal model is that the cost and effort associated with the generation of germline transgenic animals harboring the genes-of-interest can be avoided. Genes-of-interest can be cloned into SB transposon vectors and introduced into the livers of *Fah*$^{-/-}$/*SB11* animals by a relatively simple technique involving hydrodynamic tail vein injection. Live imaging can be used to monitor the pathogenicity of the genes-of-interest by including a luciferase reporter on the gene delivery vector and mice are sacrificed when a phenotype is observed. Most importantly, this approach allows the rapid generation of liver cancer mouse models driven by various genetic alterations. This system has been used to model liver cancer driven by known liver oncogenes,[102] genes identified in a forward genetic screen[48] and the HBV viral gene *HBx*.[108] It could prove useful for efficiently testing liver

cancer drivers discovered in other studies, in mice of both sexes, and in context of liver steatosis and fibrosis, conditions highly relevant to human HCC.

III. Hypothesis

1. SB insertional mutagenesis in steatotic livers will reveal a distinct set of steatosis-associated HCC genes.
2. SB gene delivery can be used to efficiently test candidate HCC genes discovered in a variety of disease-relevant contexts.

IV. Objectives

1. Use SB insertional mutagenesis to model hepatic steatosis-associated HCC and compare to human HCC data to identify steatosis-associated HCC genes. (Figure 1.4)
2. Use SB gene delivery to test a candidate steatosis-associated HCC oncogene in steatotic livers *in vivo*. (Figure 1.4)
3. Use SB gene delivery to test candidate HCC oncogenes in a variety of disease relevant contexts *in vivo*. (Figure 1.4)

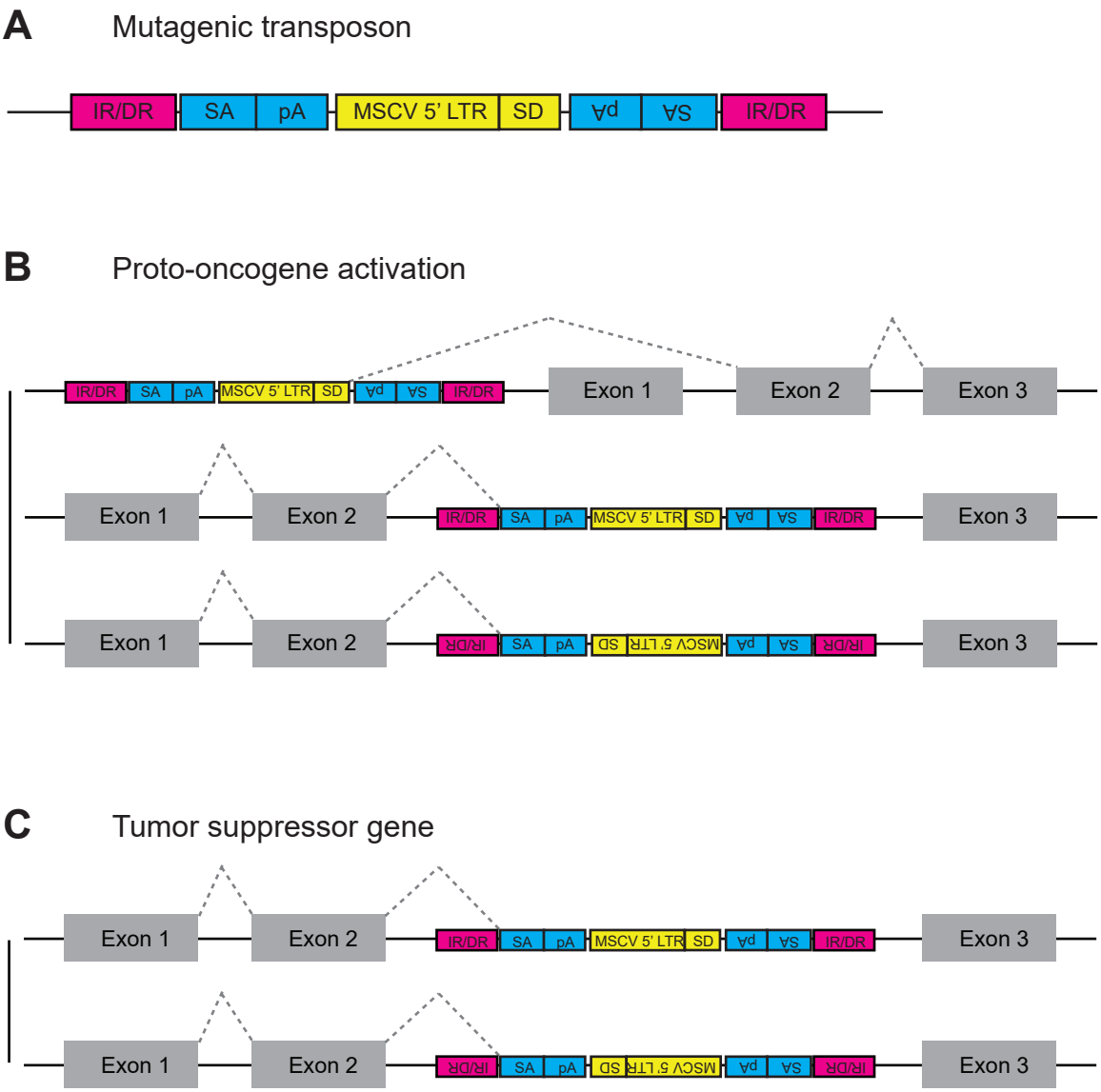

Figure 1.1. Mutagenic transposon vector for gain- and loss-of-function screen. (A) The mutagenic T2/Onc transposon contains splice acceptors (SAs) followed by poly-adenylation (pA) signals in both orientations, which are designed to elicit premature transcript truncation. The 5'- long terminal repeat (LTR) of the murine stem cell virus (MSCV) fused with a splice donor (SD) was placed in between the two SAs to drive misexpression of genes. This MSCV contains enhancer and strong cis-regulatory elements that have been shown to be active and methylation-resistant in pluripotent cells. IR/DR, inverted repeat/direct terminal repeat sequences. (B) Gain-of-function screen for proto-oncogenes. The mutagenic transposon vector can integrate upstream of a proto-oncogene and cause misexpression or create truncated versions by integrating withintronic sequences of the endoenous gene. (C) Loss-of-function screen for tumor suppressor genes. The mutagenic transposon can integrate within intronic sequences and disrupt expression of tumor suppresor genes.

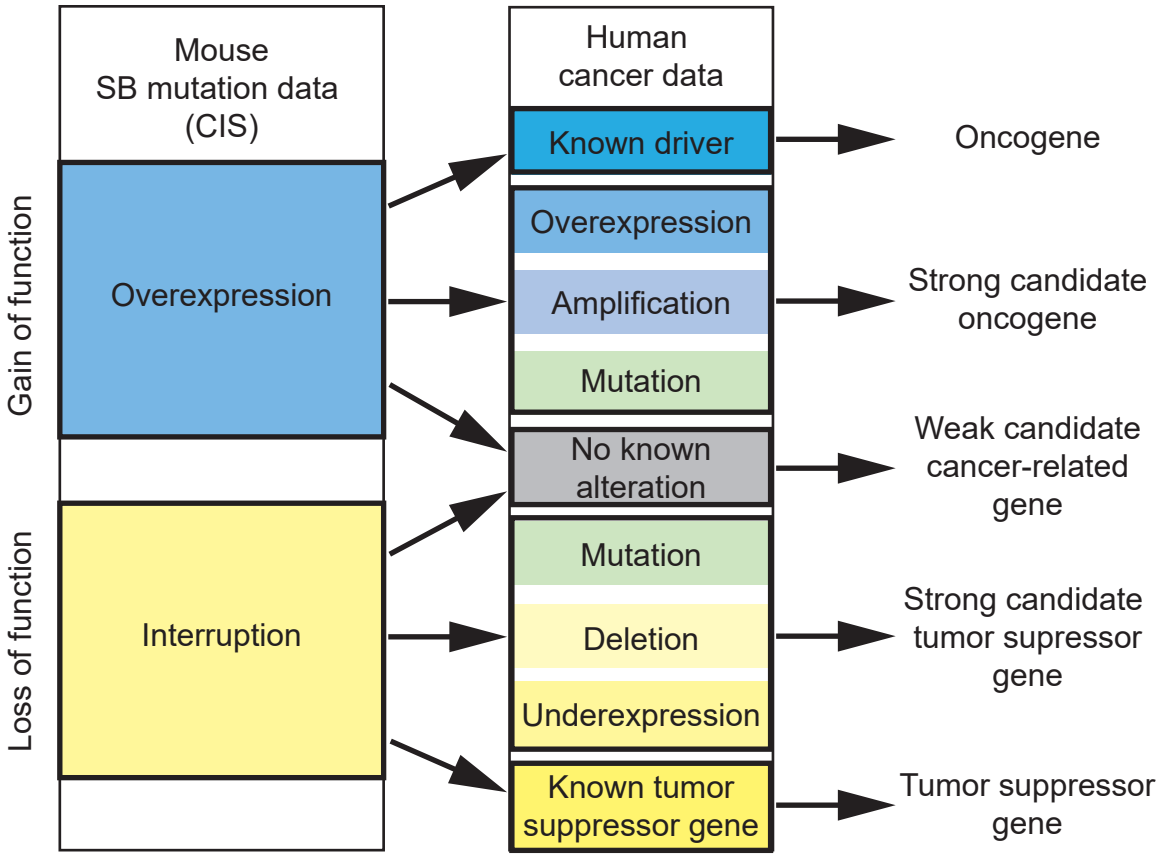

Figure 1.2. Pipeline for selecting candidate cancer genes from SB screens for further study. SB insertion mutations can result in gene overexpression or disruption. Human molecular cancer data can likewise reveal potential gain-of-function or loss-of-function alterations. To determine which common insertion sites (CISs) are most likely relevant oncogenes or tumor suppressors in human cancer, human cancer data is analyzed for gain- or loss-of-function alterations in CIS genes. Genes overexpressed by transposon insertions that have gain-of-function alterations in human cancer are considered to be strong candidate oncogenes, and genes interrupted by transposon insertions that have loss-of-function alterations in human cancer are considered strong candidate tumor suppressor genes. These strong candidate cancer genes should be prioritized for further study.

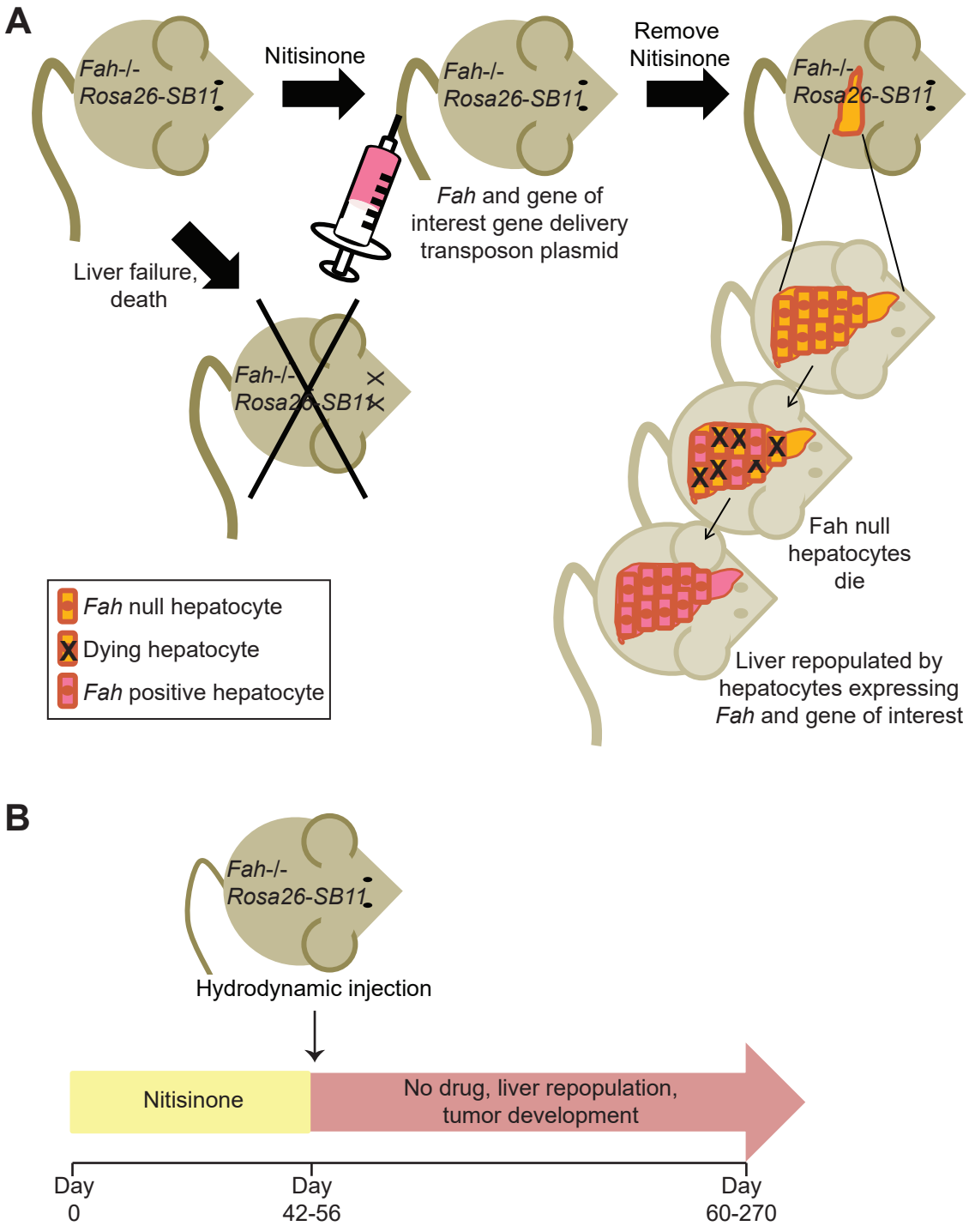

Figure 1.3. Validation of candidate liver cancer genes using the *Fah* mutant mouse model. (A) Schematic of the selective *Fah* mutant mouse model. (B) Schematic of time-line for validation of candidate liver cancer genes using the *Fah* mutant mouse model.

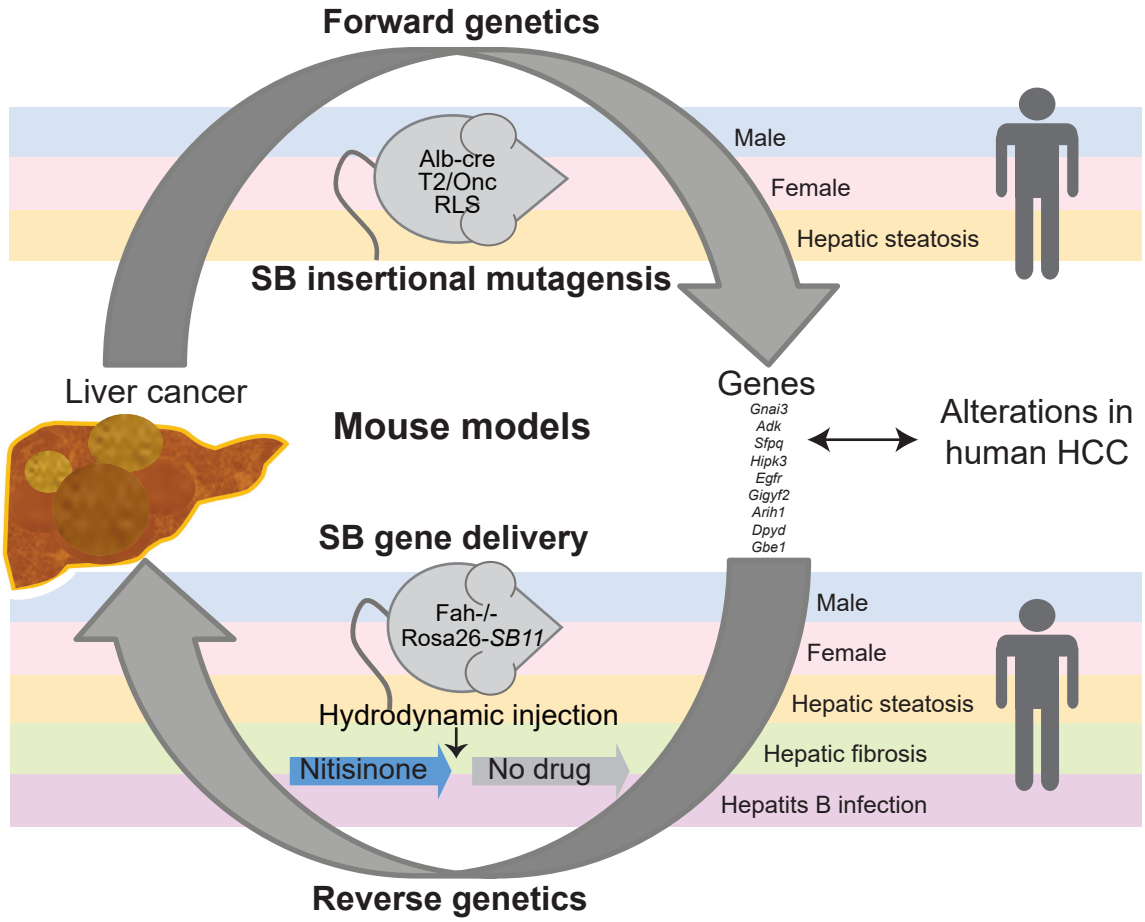

Figure 1.4. Thesis objectives.
Objective 1: Perform a forward genetic screen using SB insertional mutagenesis in mice of both sexes with hepatic steatosis to model hepatic steatosis-associated HCC, then compare to human HCC data to identify steatosis-associated HCC genes.
Objective 2: Use SB gene delivery to test a candidate steatosis-associated HCC driver gene in steatotic livers in mice of both sexes.
Objective 3: Use SB gene delivery to test candidate HCC driver genes in a variety of disease relevant contexts *in vivo*.

CHAPTER 2:

Sleeping Beauty insertional mutagenesis in mice identifies steatosis-associated hepatocellular carcinoma drivers

*The following chapter contains material from a manuscript under review:

Tschida BR, Keng VW, Temiz NA, Kuka TP, Lee LA, Riordan JD, Tierrablanca CA, Hullsiek R, Wagner S, Hudson WA, Linden MA, Amin K, Beckmann PJ, Heuer RA, Yang JD, Roberts LR, Nadeau JH, Dupuy AJ, Largaespada DA. Sleeping Beauty insertional mutagenesis in mice identifies steatosis-associated hepatocellular carcinoma drivers. Under review.

Abstract

To study the molecular pathology of HCC in the context of hepatic steatosis, we performed a forward genetic screen using conditional *Sleeping Beauty* (SB) transposon insertional mutagenesis in mice with diet and ethanol-induced hepatic steatosis and compared the results to human HCC data from public databases and clinical samples. In humans, we found the proportion of female patients developing HCC increased in the context of steatosis. Experimental steatosis similarly reduced the male liver tumor burden sex bias in mice. We identified 203 candidate steatosis-associated HCC genes, many of which are altered in human HCC and are members of established HCC-driving signaling pathways. In particular, the protein kinase A/cyclic AMP signaling pathway was frequently altered in mouse and human steatosis-associated HCC. *NAT10*, a candidate HCC driver identified in mice, was overexpressed in human HCC, was associated with decreased survival, and drove liver tumorigenesis in a steatotic mouse model *in vivo*.

Statement of significance: Hepatic steatosis, a common chronic liver disease increasing in prevalence, is a strong risk factor for hepatocellular carcinoma (HCC). This study identifies genes and pathways that promote HCC and may represent novel targets for prevention and treatment, particularly in the increasingly relevant context of hepatic steatosis.

Introduction

Hepatocellular carcinoma (HCC) is the second leading cause of death from cancer worldwide.[13] HCC is sex biased, occurring in men 2-4 times more frequently than women.[8] Hepatic steatosis, or fatty liver disease, is an increasingly common and strong risk factor for HCC.[37] Alcohol consumption further increases the risk of HCC and is among the most significant factors associated with progression of hepatic steatosis to HCC.[37]

There is considerable genetic heterogeneity in HCC.[60] The vast majority of mutations occur infrequently[46] and chromosome aberrations involving large gains and losses are prevalent,[46,53] making the distinction between molecular drivers of tumorigenesis and passenger alterations challenging. In addition, limited data is available on steatosis-associated HCC; only 12 cases with hepatic steatosis as the sole predisposing condition have been characterized by The Cancer Genome Atlas Consortium (TCGA) (TCGA Research Network: http://cancergenome.nih.gov/). Comparative methods are needed to identify specific genes and processes operative in HCC and provide a basis for new prevention and treatment strategies.

Comparative analysis of molecular alterations in human tumors to data obtained through *Sleeping Beauty* (SB) transposon-based insertional mutagenesis in mice has identified HCC drivers in normal livers, in the context of commonly known HCC-promoting mutations, and in mice of both sexes.[48] Mutagenic transposons contain a strong promoter that can induce gene overexpression and stop cassettes that can truncate gene expression, leading to tumor formation when proto-oncogenes are overexpressed or tumor suppressor genes are inactivated. The locations of these transposon insertions tag cancer genes in resulting tumor cells.[87] While earlier studies have provided useful information about HCC genetics, few recapitulate the environment of chronic liver damage

in which human tumors almost always develop, which changes the selective pressures that nascent HCC cells encounter.[8] SB insertional mutagenesis in mouse livers expressing the Hepatitis B virus surface antigen protein to model Hepatitis B-induced liver inflammation identified a distinct set of HCC promoting mutations, many of which were linked to cellular metabolic processes.[100] We expected SB mutagenesis in steatotic livers would reveal unique genetic drivers not identified in earlier SB screens for HCC that may have relevance for HCC prevention and treatment in patients, particularly those with steatosis.

In this study, we aimed to identify molecular alterations that promote HCC in the context of diet and alcohol-associated hepatic steatosis using liver-specific SB insertional mutagenesis in mice treated with ethanol and a choline-deficient diet. Choline-deficient diets are an established model for hepatic steatosis, and ethanol treatment acts additively to increase steatosis severity and susceptibility to liver tumor formation.[83,84] This is a particularly useful model for alcohol-associated steatosis because both alcohol ingestion and choline-deficiency decrease phosphatidylcholine synthesis, causing fatty acid accumulation in hepatocytes.[33,83] Using this system, we modeled steatosis-associated HCC in mice and found over 200 candidate driving mutations, many of which affected genes altered in human steatosis-associated HCC. The protein kinase A/cyclic AMP (PKA/cAMP) signaling pathway was altered frequently in mouse and human steatosis-associated HCC. *NAT10*, identified as a candidate oncogene in mice, is overexpressed in human steatosis-associated HCC and associated with decreased survival, and we validated its oncogenic role in steatosis-associated liver cancer *in vivo*.

Results

A transposon insertional mutagenesis-driven mouse model of hepatic steatosis-associated liver cancer

We used a previously described conditional SB transposon-based insertional mutagenesis system to induce liver adenomas and HCC, generating a mutagenized transgenic mouse cohort with one copy each of *Albumin*-cre, mutagenic transposon (T2/onc), and transposase expressing *Rosa26*-lsl-SB11 transgenes and a control cohort carrying two of the three transgenes (thereby lacking transposition).[48] All mutagenized and control mice were treated with a diet designed to induce hepatic steatosis (eCDD) consisting of 5% ethanol in the drinking water *ad libitum* for two months after weaning followed by untreated drinking water and a modified choline-deficient diet for the remainder of the study (Figure 2.1A). Choline-deficient diet treatment reliably induces hepatic steatosis and leads to liver tumor formation in 22% of mice after 19 months.[82] The addition of 5% ethanol increases steatosis severity and sensitization to ethionine-induced tumor formation.[83,84] In our study, we used SB transposon insertional mutagenesis in place of ethionine to induce tumorigenesis in eCDD-treated mice.

Mice treated with eCDD developed hepatic steatosis (Figure 2.1E, 2.2A-B). All livers examined histopathologically from eCDD-treated mice displayed fatty change (34/34). We measured the lipid droplet percentage of liver tissue from representative eCDD-treated and normal diet (ND)-treated control mouse liver sections by quantifying the percent of unstained pixels from hematoxylin and eosin (H&E)-stained slides using Aperio Positive Pixel Count software. Lipid droplet percentage of liver tissue was approximately 8-fold higher in eCDD-treated than ND-treated mice (P = .012, Student's t test). (Figure 2.2A-B)

To determine whether SB insertional mutagenesis drove liver tumor formation, tumor penetrance and average tumor burden were compared between eCDD-treated SB-mutagenized mice and age-matched control mice. Mutagenized mice had higher tumor penetrance than control mice, with 75.5% (n = 49) vs. 21.9% (n = 32) developing tumors by 436 days ($P < .0001$, Chi-square test). (Figure 2.1B) Average tumor burden was also higher in mutagenized mice, 4.76 tumors per mouse vs. 0.28 tumors per control mouse ($P = .002$, Student's t test). (Figure 2.1C) SB transposase expression was confirmed by immunohistochemistry (IHC). (Figure 2.1E) Liver tumors that developed in mutagenized mice and were examined histopathologically were classified as well-differentiated hepatocellular neoplasms, analogous to adenomas (81%), or as hepatocellular carcinomas (19%). (Figure 2.1D-E) Albumin expression was detected in tumors by IHC, confirming their hepatocyte origin.[48] (Figure 2.1E) Thus, SB transposon insertional mutagenesis plus treatment with eCDD induced steatosis-associated liver cancer in our mouse model.

Increased HCC incidence in females with hepatic steatosis

The sex distribution of a previously described[109] cohort of 460 adult patients diagnosed with HCC between January 2007 and December 2009 at the Mayo Clinic, Rochester followed the typical bias, with 72% (332) males and 28% (128) females. We examined the sex distribution among subsets of patients with and without hepatic steatosis as the primary predisposing factor. The 397 HCC patients without steatosis were 74.6% (296) men and 25.4% (101) women. The 63 HCC patients with steatosis were 57.1% (36) men and 42.9% (27) women, a significantly higher female proportion than the non-steatotic subset and the overall cohort ($P = .004$, and $P = .014$, respectively, Chi-square test). (Figure 2.3A)

We previously induced liver tumors in mice fed a normal diet using transgenes for hepatic insertional mutagenesis identical to those used in the current study.[48,54] (Table 2.1) The sex distribution of SB-induced liver tumors in ND-treated mice modeled the typical human sex bias, with an average tumor burden of 8.15 tumors per male (n = 27) and 2.27 tumors per female (n = 11) (*P* = .024, Student's t test). (Figure 2.3B) This sex bias was absent in SB-induced liver tumors in eCDD-treated mice, with an average tumor burden for males (n = 23) and females (n = 26) of 3.26 and 6.04, respectively (*P* = .213, Student's t test). (Figure 2.3C) Tumor penetrance in male mice decreased non-significantly from 84.6% with ND to 65.2% with eCDD treatment (*P* = .115, Chi-square test) and increased non-significantly in female mice from 63.6% with ND to 80.8% with eCDD treatment (*P* = .267, Chi-square test). Thus, the SB system models the human HCC sex bias, with higher prevalence of non-steatosis associated liver cancer in males than females, and a reduction of the male sex bias in steatosis-associated liver cancer.

FoxA1 and FoxA2 are repressed in steatotic liver

Forkhead box transcription factors *FoxA1* and *FoxA2* contribute to the liver cancer sex bias in mice.[110] Their activities are metabolically regulated in human liver, where FOXA1 transcript is down-regulated with steatosis[111] and FOXA2 function is negatively regulated by phosphorylation at T156 downstream of the insulin signaling pathway.[112]

In our mouse model, *FoxA1* expression was reduced and phosphorylated T156 FOXA2 (p-FOXA2) increased in mice with hepatic steatosis. As detected by qRT-PCR, *FoxA1* transcript levels were lower in eCDD- than ND-treated mouse livers (*P* = .014, Student's t test). (Figure 2.2F) In humans and mice, hepatic steatosis increases with age[113,114] and in ND-treated mice, *FoxA1* expression significantly decreased with age (Pearson's correlation coefficient, r = -.823, *P* = .002). (Figure 2.2G). We examined FOXA1

expression by IHC and quantified staining using Aperio Positive Pixel Count in serial sections from the same liver samples used to quantify lipid droplet percentage of liver tissue, finding a non-significant inverse correlation between the two measures. (Pearson's correlation coefficient, r = -.624, *P* = .261). (Figure 2.2A, C) Serial sections from the same samples were stained for p-FOXA2 by IHC, average staining was quantified using ImageJ (National Institutes of Health), and the percentage of cells with nuclear p-FOXA2 was measured with Aperio Positive Pixel Count. Intensity of p-FOXA2 staining increased (Pearson's correlation coefficient, r = .890, *P* = .043) and nuclear p-FOXA2 increased non-significantly (Pearson's correlation coefficient, r = .775, *P* = .124) with lipid droplet liver tissue percentage. (Figure 2.2A, D-E) We analyzed expression of *ApoM*, a transcriptional target of FOXA1 and FOXA2, by qRT-PCR, finding reduced expression in eCDD- versus ND-treated control mouse livers (*P* = .022, Student's t test). (Figure 2.2H) Collectively, these data suggest FOXA1 and FOXA2 are repressed in steatotic liver. Since loss of *FoxA1* and *FoxA2* eliminates sex bias in chemically-induced HCC in mice,[110] repression of FOXA1 and FOXA2 may contribute to the reduction in HCC sex bias with steatosis.

Common transposon insertion sites identify genes relevant to human steatosis-associated HCC

To identify common transposon insertion sites (CIS) harboring liver cancer genes, transposon insertions from 159 tumors collected from 36 eCDD-treated transposition mice of both sexes (15 males and 21 females) (Table 2.1) were amplified and sequenced on the Illumina platform, revealing 7010 non-redundant insertions. From these, TAPDANCE analysis[115] identified 67 CIS with 73 associated genes and gene centric CIS (gCIS) analysis[87] identified 188 CIS genes. 58 CIS genes were identified by both methods, so 203 candidate steatosis-associated liver cancer genes were identified in total. (Table 2.2)

Many steatosis-associated liver cancer CIS genes were altered in human HCC cases profiled by TCGA (TCGA Research Network: http://cancergenome.nih.gov/). Of all TCGA HCC cases, 68% (139/203) CIS genes were significantly misexpressed ($P < .05$ by Benjamini-Hochberg (BH)-adjusted Student's t test) in tumors compared to average expression in normal livers, 14% (29) were misexpressed in HCC cases with steatosis as the sole predisposing condition, and 62% (125) were misexpressed in alcohol-associated HCC cases. (Figure 2.4A, Table 2.3) Examining mutation and copy number changes for all TCGA HCC cases, 10% of CIS genes (20) were altered in more than 5% of tumors, 15% (30) were altered in more than 5% of alcohol-associated HCC cases, and 29% (59) were altered in more than 5% of steatosis-associated HCC cases. (Figure 2.4B, 2.5-7, Table 2.3) This overlap shows the relevance of genes altered in our mouse model to human HCC.

The majority of CIS gene expression changes in human steatosis or alcohol-associated TCGA HCC cases were consistent with the gene's predicted role as an oncogene or tumor suppressor, as based on transposon insertion locations and orientations (i.e. predicted oncogenes were overexpressed in human HCC and predicted tumor suppressors under-expressed). Of the 29 significant CIS gene expression changes in steatosis-associated HCC, 69% (20) were consistent with the predicted effect of transposon insertions. (Figure 2.8A) Of the 125 significant CIS gene expression changes in alcohol-associated HCC, 66% (83) were consistent with the predicted effect of transposon insertions. (Table 2.3) Nineteen CIS genes had significant expression changes greater than 2-fold in alcohol-associated HCC, of which 74% (14) were consistent with the predicted effect of transposon insertions. (Figure 2.8B) These genes represent the most promising human steatosis-associated HCC driver candidates to be prioritized for further study.

Many CIS are enriched in steatosis-associated HCC

To differentiate CIS specifically relevant to steatosis-associated HCC from those likely to drive HCC regardless of steatotic context, we performed an enrichment analysis. We compared the prevalence of steatosis-associated liver cancer CIS insertions in tumors generated in the eCDD HCC screen and a previously conducted, otherwise identical SB screen for HCC drivers in ND-treated mice[48] using Fisher's exact test with Benjamini-Hochberg correction and a significance threshold of $P < .05$. We found 49 steatosis-enriched TAPDANCE CIS genes and 79 steatosis-enriched gCIS with 30 overlapping, for a total of 98 steatosis-enriched CIS genes. (Table 2.4)

Wnt/β-catenin signaling pathway genes altered in steatosis-associated HCC

Ingenuity Pathway Analysis (IPA) indicated the Wnt/β-catenin signaling pathway was significantly associated with the steatosis-associated CIS gene list ($P = .001$) and the steatosis-enriched CIS gene list ($P = .007$). To assess the generalizability of this finding, we analyzed genes with significant expression changes between tumor and adjacent tumor-free liver from an independent mouse model of steatosis-associated HCC in which wild-type C57BL/6J mice were treated with a diet high in saturated fat and sucrose to induce liver cancer. Several Wnt/ β-catenin signaling genes showed significant expression changes in tumors from this cohort. We also analyzed human TCGA HCC data by IPA for pathways associated with genes with significant expression changes in steatosis-associated (all differentially expressed genes) alcohol-associated (>2-fold change) HCC. Similar to the mouse tumors, we found Wnt/β-catenin signaling was significantly associated with genes altered in human alcohol-associated HCC ($P = .015$) and several pathway genes had expression changes in human steatosis-associated HCC. (Figure 2.9, Table 2.5) The association of this well-characterized HCC-promoting pathway with the

candidate genes identified in our screen highlights the relevance of this mouse model to human HCC.

PKA/cAMP signaling pathway genes altered in steatosis-associated HCC

IPA indicated the PKA/cAMP signaling pathway was significantly associated with the steatosis-associated (P = .003) and the steatosis-enriched (P < .0001) CIS gene lists, and several pathway genes had altered expression in wild-type, high-fat diet-fed mouse liver tumors. PKA/cAMP signaling was associated with genes with significant expression changes in human steatosis-associated (all differentially expressed genes) or alcohol-associated (>2-fold change) HCC from TCGA (P = .016 and P < .0001, respectively). (Figure 2.10, Table 2.6)

Phosphorylation of the catalytic subunit of PKA at T197 is required for enzyme activation.[116] Activated PKA phosphorylated at T197 (p-PKA) was examined by IHC analysis of a tissue microarray of human HCC cases, and staining intensity was quantified using ImageJ. We detected a significant increase in p-PKA in HCC, with 75 of 99 tumors displaying stronger p-PKA staining than matched normal liver. (Wilcoxon signed rank test, P < .0001). (Figure 2.11A) Five cases on the tissue microarray had steatosis indicated in the pathology reports, 3 displaying stronger p-PKA staining than paired tumor-free liver (Wilcoxon signed rank test, P =.005) (Figure 2.11A-B), further supporting a role for the activation of PKA/cAMP signaling in steatosis-associated HCC.

PKA activation promotes steatosis-associated hepatocarcinogenesis in vivo

To test the effects of PKA activation on tumor formation in steatotic livers, we used an *in vivo* model of activated mutant *PRKACA* overexpression in livers of mice with diet-induced hepatic steatosis. A mutation in *PRKACA* leading to a substitution of leucine at position

206 with arginine in the catalytic subunit of PKA (*PRKACA*$_{L206R}$) is constitutively active.[117] We used SB transposon-based gene delivery to stably overexpress *PRKACA*$_{L206R}$ in the selective *Fah*-deficient mouse model as described previously.[48,54,108] *Fah*-deficient male mice expressing *SB* transposase knocked into the *Rosa26* locus (*Fah*/*SB11*)[48] were maintained on the protective drug nitisinone until delivery of transposon vectors by hydrodynamic tail vein injection[107] at 8 weeks and selection of hepatocytes with stable *Fah*-rescue transgene expression by nitisinone withdrawal. Mice were treated with either eCDD or ND. For each diet, negative control mice were injected with an SB transposon-based GFP expression vector co-expressing *Fah* (pKT2/GD-GFP)[108] and short hairpin against *Trp53* (pT2/shp53)[108] (*GFP*/shp53) and experimental mice were injected with an SB transposon-based expression vector for mouse *PRKACA*$_{L206R}$ cDNA co-expressing *Fah* with a GFP reporter (pT2/GD-PRKACA$_{L206R}$) plus pT2/shp53 (*PKA*/shp53). (Figure 2.12A) As shown previously,[108] the use of pT2/shp53 in this model sensitizes to, but is not sufficient to induce, tumorigenesis. With eCDD-treatment, the use of pT2/shp53 is still not sufficient to induce tumorigenesis. *GFP*/shp53-injected eCDD-treated mice of both sexes develop a mean of 0.73 tumors, and pKT2/GD-GFP-injected eCDD-treated mice develop a mean of 0.08 tumors (No significant difference, Student's t test). (Data not shown)

Mice were sacrificed between 150 and 180 days post-injection. eCDD-treated *PKA*/shp53 mice (n = 13) developed more tumors than eCDD-treated *GFP*/shp53 mice (n = 20), with a mean of 3.85 vs 0.85 tumors per mouse (P = .008, Student's t test). (Figure 2.12B) In ND-treated mice, a mean of 0.64 versus 0.00 tumors per *PKA*/shp53 (n = 14) and *GFP*/shp53 (n = 18) mouse. (P = .006, Student's t test) developed. (Figure 2.12B) Treatment with eCDD significantly increased tumor formation in *PKA*/shp53-injected mice compared to ND treatment (P = .009, Student's t test). (Figure 2.12B)

NAT10 is over-expressed in human hepatic steatosis-associated HCC

In eCDD-treated transposition mice, *Nat10* was identified as a candidate gene by both TAPDANCE and gCIS (P = .049 and P < .0001, respectively) (Table 2.2) for which the predicted effect of transposon insertions was to drive overexpression. (Figure 2.13) *Nat10* insertions were enriched in tumors from eCDD-treated versus ND-treated SB-mutagenized mice (Q = .038, BH corrected Fisher's exact test). (Table 2.4)

Nat10 was selected for further study based on alterations in human HCC supporting its predicted role as an oncogene. Of 357 human HCC cases on TCGA, 6.72% (24) overexpressed *NAT10* more than 2-fold, which was associated with decreased survival (P = .0124, Log-rank Mantel-Cox test).(Figure 2.14A) Ten cases additionally had copy number gains that corresponded with overexpression (P < .0001, One-way ANOVA with post-hoc test). (Figure 2.14B) Among steatosis-associated HCC cases on TCGA, *NAT10* transcript was even more significantly overexpressed in tumors (P < .0001, Student's t-test). (Figure 2.14C)

NAT10 protein expression was examined by IHC analysis of a human HCC tissue microarray, and staining intensity was quantified using ImageJ. NAT10 was overexpressed in a majority of HCC cases, with 82 of 99 HCC cases and 3 of 5 steatosis-associated cases displaying stronger NAT10 staining than paired tumor-free liver (Wilcoxon signed rank test, P < .0001; and P = .003, respectively). (Figure 2.14D-E)

Nat10 overexpression promotes steatosis-associated hepatocarcinogenesis in vivo

To test the effects of *Nat10* on tumor formation in steatotic livers, we used SB transposon-based gene delivery to stably overexpress *Nat10* in the selective *Fah*-deficient mouse model as described above. Mice were treated with either eCDD or ND. For each diet,

negative control mice of both sexes were injected with pKT2/GD-GFP and pT2/shp53 (*GFP*/shp53) and experimental mice of both sexes were injected with an SB transposon-based expression vector for mouse *Nat10* cDNA co-expressing *Fah* with a GFP reporter (pT2/GD-Nat10) plus pT2/shp53 (*Nat10*/shp53). (Figure 2.15A)

Mice were sacrificed between 150 and 180 days post-injection. Six of 7 eCDD treated- and 4 of 10 ND treated- mouse livers examined histopathologically showed fatty change. The increased hepatic steatosis in eCDD- compared to ND- treated regenerated *Fah*-deficient mouse livers was not statistically significant (P = .060, Chi-square test).

eCDD-treated *Nat10*/shp53 mice (n = 24) developed more tumors than eCDD-treated *GFP*/shp53 mice (n = 25), with a mean of 4.42 vs 0.84 tumors per mouse (P = .014, Student's t test). (Figure 2.15B) Similar results were observed in ND-treated mice, with a mean of 2.76 versus 0.14 tumors per *Nat10*/shp53 (n = 25) and *GFP*/shp53 (n = 29) mouse. (P < .0001, Student's t test). (Figure 2.15B) Treatment with eCDD did not significantly increase tumor formation in *Nat10*/shp53 mice compared to ND treatment (P = .267, Student's t test).

Nat10/shp53-induced liver tumors were classified as well-differentiated hepatocellular neoplasms, analogous to adenomas (57%), or as hepatocellular carcinomas (43%) by histopathological analysis. *Nat10*/shp53-injected mouse livers and liver tumors overexpressed *Nat10* compared to *GFP*/shp53 mouse livers (P < .0001 and P = .027, respectively, Student's t test) as measured by qRT-PCR. (Figure 2.15C) Higher NAT10 IHC staining levels were detected in *Nat10*/shp53 than *GFP*/shp53 mouse livers by ImageJ quantification (P = .004, Wilcoxon rank sum test). (Figure 2.16A) Both *Nat10*/shp53 and *GFP*/shp53 mouse livers expressed normal levels of *Fah* transcript (Figure 2.16B) and FAH protein expression was detected by IHC in *GFP*/shp53 and

Nat10/shp53 mouse livers and *Nat10*/shp53 mouse liver tumors, indicating efficient liver repopulation with transfected cells. (Figure 2.15D) Albumin expression was detected in *Nat10*/shp53 mouse liver tumors by IHC, confirming hepatocyte tissue origin of tumors.[48] (Figure 2.15D)

Discussion

Hepatic steatosis is a major and increasingly widespread HCC risk factor.[37] Here we report the results of a forward genetic screen for HCC drivers in mouse livers with diet and alcohol-induced steatosis. Because HCC occurs most frequently in men, many mouse models of HCC include only males.[64] We found, however, that the proportion of women developing HCC is higher in the context of hepatic steatosis than in the general population. Our steatosis-associated HCC model recapitulated the reduction of male HCC sex bias observed in human steatosis-associated HCC. The inclusion of females in studying HCC pathogenesis is, therefore, particularly important in this context. We found estrogen and androgen receptor pioneer factors FOXA1 and FOXA2 are negatively regulated in steatotic livers, which may contribute to the reduction in sex bias. Based on these similarities to human disease, HCC genes discovered in this screen may have broader relevance to human steatosis-associated HCC than those identified by studies conducted exclusively in males.

The considerable genetic heterogeneity in human HCC necessitates the use of methods complementary to direct profiling of patient samples to identify driver alterations, such as mouse models.[60] Analysis of recurrently mutated genes in liver tumors undergoing hepatocyte-specific transposition in steatotic livers identified over 200 candidate steatosis-associated HCC genes, the majority of which are altered by expression change, copy number alteration, or mutation in human HCC. Most expression changes in human

steatosis and alcohol-associated HCC were also consistent with predicted roles of CIS genes as either oncogenes or tumor suppressors, providing additional evidence that our screen identified a subset of alterations in human steatosis and alcohol associated HCC that are promising candidate drivers of human hepatocarcinogenesis.

PKA/cAMP signaling pathway genes were commonly altered in SB-induced steatosis-associated mouse tumors and human steatosis-associated HCC. Similar disruption of this pathway in an independent mouse model of high fat diet-induced steatosis-associated HCC further supported its importance and demonstrated the broader relevance of our model to hepatocarcinogenesis in steatotic livers. We showed expression of a constitutively active PKA catalytic subunit induced tumorigenesis in steatotic livers *in vivo*. The PKA/cAMP signaling pathway regulates glucose and lipid metabolism, proliferation, and cell survival in the liver.[118–120] Activating mutations in the PKA catalytic subunit, *PRKACA*, are common in adrenocortical tumors,[117] and recurrent translocations in fibrolamellar HCC lead to *DNAJB1-PRKACA* chimeric transcripts associated with PKA upregulation.[117,121] β-adrenergic receptors activate PKA/cAMP signaling in many cell types including hepatocytes and regulate many cancer-relevant cellular processes including growth, metabolism, DNA damage repair, cell motility, survival, and inflammation.[122] Several retrospective studies have found inhibition of β-adrenergic receptor signaling by the non-selective β-blocker, propranolol, in patients with cirrhosis may decrease HCC incidence, an effect that might involve PKA/cAMP signaling.[123–125] To our knowledge, a prospective clinical trial has yet to be completed. Our identification of frequent alterations in human and mouse tumors support a role for PKA/cAMP signaling in steatosis-associated HCC.

We identified *NAT10* as a steatosis-associated HCC oncogene. In a study of human HCC, NAT10 protein was found to be overexpressed in HCC compared to normal liver, and high expression was found to correlate with high TNM classification and poor survival outcomes.[126] NAT10 expression has been shown to promote invasion and migration of HCC cells.[127] Our data demonstrates a direct role for *Nat10* overexpression in driving liver tumorigenesis *in vivo* in a mouse model with hepatic steatosis. NAT10 is a lysine and RNA acetyltransferase that acetylates histones, alpha tubulin, and RNA, thereby regulating gene expression, cell division, and precursor rRNA processing.[128–130] Normal expression is required for the formation of N4-Acetylcytidine, a highly conserved modification of eukaryotic 18S rRNAs with an important role in ribosome biogenesis.[130] N4-Acetylcytidine formation by NAT10 may be a nutrient-responsive RNA modification regulating translational output by promoting ribosome biogenesis only in the presence of acetylCoA,[131] which is highly abundant in steatotic liver.[132] In steatotic livers, NAT10 overexpression may allow cells to respond to the abundance of acetylCoA by promoting increased ribosome biosynthesis, potentially bypassing a rate-limiting step in the process of hepatocarcinogenesis.

NAT10 is a candidate for therapeutic targeting in HCC. Our study and other published work[126] found NAT10 protein overexpression in over 60% of HCC cases, indicating a higher rate of NAT10 activation than is indicated by transcript expression levels on TCGA (6.7%). *NAT10* knockdown has been demonstrated to decrease growth rates of several cancer cell types.[130,133] Importantly, a chemical inhibitor of NAT10 acetyltransferase activity, Remodelin, has been characterized.[134] Our *Nat10* overexpression mouse model could be used to test the efficacy of Remodelin for preventing or treating NAT10-driven HCC. The rate of ribosome biogenesis regulates cell proliferation[135] and could be rate

limiting in HCC. Inhibition of this process using the RNA polymerase I specific inhibitor, CX-5461, reduces proliferation and induces senescence in many cancer cell types *in vitro* and *in vivo*.[135,136] The efficacy of CX-5461 for inhibiting NAT10-overexpressing HCC cell proliferation could be evaluated to clarify the mechanism by which NAT10 drives tumorigenesis and for potential therapeutic benefit.

The candidates we identified in this forward genetic screen for HCC drivers in the highly relevant context of hepatic steatosis may provide insight into which of the many genes altered in human HCC are likely drivers, the pathways promoting HCC in steatotic livers, and potential strategies for HCC prevention or treatment to investigate. We identified activation of the PKA/cAMP signaling pathway and overexpression of *NAT10* as important steatosis-associated HCC-promoting events, both of which could potentially be targeted therapeutically.

Methods

Generation and maintenance of transposition and control transgenic animals

Animal studies were conducted using procedures approved and monitored by the Institutional Animal Care and Use Committee at the University of Minnesota. Transgenic mice with Cre-inducible *SB* transposase and T2/Onc transposon concatemer on chromosome 15 (*Rosa26*-lsl-*SB11*$^{Tg/Tg}$; T2/Onc$^{Tg/Tg}$) rederived from lines previously generated[48] were bred to mice with one copy of Cre recombinase expressed from the liver specific *Albumin* promoter (*Alb*-Cre$^{Tg/WT}$) rederived from lines previously generated.[48] These crosses produced SB-mutagenized mice (*Alb*-Cre$^{Tg/WT}$; *Rosa26*-lsl-*SB11*$^{Tg/WT}$; T2/Onc$^{Tg/WT}$) and control mice lacking transposon mobilization (*Rosa26*-lsl-*SB11*$^{Tg/WT}$; T2/Onc$^{Tg/WT}$). Genotyping for *Alb*-Cre, *Rosa26*-lsl-*SB11*, and T2/Onc was performed as

described previously.[48] After weaning at 21 days, mice were placed on 5% v/v ethanol drinking water for 2 months, then normal drinking water and a modified choline-deficient diet (#0296021050, MP Biomedicals) *ad libitum* for the remainder of the study. Mutagenized mice were sacrificed with age-matched control mice at approximately 60 day intervals (to assess tumor formation), when mice became moribund, or by 400-436 days and liver tumor analysis was performed as described.[48]

Fah-deficient mouse model

Animal studies were conducted using procedures approved and monitored by the Institutional Animal Care and Use Committee at the University of Minnesota. Transgenic mice deficient for *Fah* and expressing *SB11* transposase (*Fah*$^{-/-}$*; Rosa26-SB11*$^{Tg/WT}$) were generated and maintained as described.[108] Mice were assigned to either a normal diet (ND) or ethanol treatment and choline-deficient diet (eCDD). ND mice were maintained on nitisinone drinking water until injection with plasmid DNA at 8 weeks of age, then placed on normal drinking water and standard diet. After weaning at 21 days of age, eCDD mice were placed on 5% v/v ethanol plus nitisinone drinking water. After plasmid injection at 8 weeks of age, eCDD mice were placed on normal drinking water and a modified choline-deficient diet (#0296021050, MP Biomedicals) *ad libitum* for the remainder of the study. We generated an SB transposon-based expression vector for *Nat10* co-expressing *Fah* with a *GFP* reporter (pT2/GD-Nat10) as follows. A *Nat10* cDNA clone was purchased (#MC202909, Origene) and cloned into pENTR entry vector (#A10462, Invitrogen) to get pENTR-Nat10. The *Nat10* component from pENTR-Nat10 was cloned into the previously generated pT2/GD-IRES-GFP[54] Gateway destination SB transposon plasmid co-expressing *Fah* and *GFP* using Gateway LR clonase mix II (#11791-020, Thermo Fisher Scientific) according to the manufacturer's instructions to get pT2/GD-Nat10. The mouse

PRKACA transcript variant 1 (Accession # NM008854) open reading frame with nucleotides 616 and 617 mutated from TT to CG to generate the L206R mutation flanked by Gateway cloning sequences was ordered as a gBlock, cloned into the pENTR entry vector (#A10462, Invitrogen), then into the Gateway destination SB transposon plasmid co-expressing *Fah* and *GFP* using Gateway LR clonase mix II (#11791-020, Thermo Fisher Scientific) according to the manufacturer's instructions to get pT2/GD/PRKACA$_{L206R}$. The pKT2/GD-GFP and pT2/shp53 plasmids were generated previously.[108] Plasmids used for *in vivo* studies were prepared using endotoxin-free maxi-preparation kits (#740424.50, Macherey-Nagel). Twenty µg of each plasmid was delivered by hydrodynamic tail vein injection as described.[107] At 150-180 days post-injection, liver tumor analysis was performed as described.[48] Livers were examined using GFP goggles (#FHS/EF-2G2, BLS-ltd), and GFP-positive tumors were counted and collected.

Quantitative reverse transcriptase PCR (qRT-PCR)

RNA was extracted from mouse liver tissue using the TRIzol reagent (#15596026, Invitrogen) or the RNeasy kit (#74106, Qiagen) and DNase treated with the DNA-free kit (#AM1906, Ambion) using protocols described by the manufacturers. cDNA was synthesized using the Transcriptor First Strand cDNA Synthesis Kit (#04379012001, Roche) or SuperScript IV VILO Master Mix (#11756050, Invitrogen) according the manufacturers' instructions. Primer sequences are listed in Table 2.7. qPCR was performed on a C1000 Touch Thermal Cycler with CFX96 Real-Time System (#1855195, Bio Rad) using SYBR Green Master Mix (#4309155, Applied Biosystems) according to manufacturer's instructions.

Tissue Microarray Preparation

A human HCC tissue microarray was procured from the University Of Washington Department Of Pathology. HCC and paired tumor-free liver tissue cores from cases with etiologies of Hepatitis B (11), Hepatitis C (58), autoimmune hepatitis (3), alcohol (1), a combination thereof (9), or unknown (18) collected from surgeries performed between 1999 and 2007 were formalin fixed, paraffin embedded, sectioned at 5 microns on a standard microtome, and heat-fixed onto glass slides.

Histological Staining

Formalin fixed, paraffin embedded tissue section slides were either stained with H&E and analyzed by color bright-field microscopy by two board-certified pathologists (KA and ML, American Board of Pathology) or stained by IHC as described[108] using the antibodies listed in Table 2.8. Stained tissue section slides were photographed at 10x magnification and representative fields are displayed.

Histological stain quantification with Aperio

When specified, slides were scanned at 20x magnification with Aperio ScanScope XT (Leica) and analyzed using Aperio ImageScope Positive Pixel Count software (Leica). Measurements were taken from 5 representative 1000 by 1000 pixel boxes per section and averaged. To quantify fat percentage of liver tissue from H&E stained sections, the hue value was set to 0.05 and hue width 0.999999 to include all stained pixels. Intensity threshold of negative pixels was 255 to include all pixels. The white color of fat droplets was defined as weak positive pixels (wpp), with intensity threshold upper limit 255 and lower limit 218. Stained tissue was defined as strong positive pixels (spp), with intensity threshold lower limit 0. Liver fat percentage was defined as the percentage of spp out of

the total positive pixels (wpp plus spp). To quantify positive IHC staining for FOXA1, the hue value was set to 0.1 and hue width 0.16. Color saturation threshold was 0.04. Upper limit of intensity threshold for positive pixels was 230 and lower limit was 0. Negative pixel intensity threshold was 230. The average stained pixel intensity was measured as brown stained pixel intensity divided by the number of positive pixels to exclude fat droplets. FOXA1 IHC stain level was defined as 1000 divided by the average stained pixel intensity. To quantify the percent of p-FoxA2 IHC stained nuclei, OD values for nuclear hematoxylin (negative IHC stain) were 0.706 for red, 0.629 for green and 0.33 for blue. OD values for nuclear DAB (positive IHC stain) were 0.244583 for red, 0.509334 for green, 0.825081 for blue. The cytoplasm intensity threshold value was 230. The upper limit intensity threshold was 220 for weak, 188 for medium, and 162 for strong positive nuclei. The lower limit intensity threshold for strong positive nuclei was 0. Minimum elongation, compactness, and roundness was 0.4. Maximum nuclear size was set to 300 um^2 and minimum nuclear size 20 um^2. The upper limit for intensity thresholding was 164 and lower limit 0. Cytoplasmic rejection was the nuclear segmentation type. The percent positive nuclei was defined as the percent of positive stained nuclei out of the total nuclei (negative stained plus positive stained).

Histological stain quantification with ImageJ

When specified, images of IHC stained tissue section slides taken at 10x magnification were analyzed using ImageJ software (National Institutes of Health), to measure IHC stain level. We used the IHC Image Analysis Toolbox[137] (available from imagej.nih.gov/ij/plugins/ihc-toolbox/index.html) default H-DAB settings to detect brown staining. The brown stain image was then converted to 32-bit grayscale. Lower intensity threshold was set to 10, upper threshold 185. Background pixels were set to NaN to

exclude fat droplets. Measurements were taken from 3 representative 100 by 100 pixel boxes per tissue section and averaged. IHC stain level was defined as 1000 divided by the average stained pixel intensity.

Transposon insertion site analysis

Transposon-genomic DNA junctions were amplified from genomic DNA isolated from SB-induced liver tumor samples by linker-mediated PCR as described,[138] and sequenced on the Illumina MiSeq with 150 cycle paired end reads. Identification of TAPDANCE CIS and gene centric CIS was performed as previously described.[87,115] To account for T2/Onc local-hopping, the donor chromosome 15 was excluded from analysis. Known CIS artifacts caused by T2/Onc sequence elements (*En2*, *Foxf2*) or amplified regions within the mouse genome (*Serinc3*, *Sfi*) were excluded.[87,115]

CIS enrichment analysis

For each CIS gene with more than 3 transposon insertions in SB-induced liver tumors in eCDD-treated mice, the number of SB-induced liver tumors in eCDD-treated mice with and without insertions was compared to the number of SB-induced liver tumors in ND-treated mice from a previous study[48] with and without insertions. Steatosis-enriched CIS were defined as CIS with a significantly higher proportion of tumors with insertions in eCDD treated than ND treated mice with a *Q* value < .05 by Benjamini-Hochberg-corrected Fisher's exact test.

Sex distribution of human HCC cases by presence of steatosis

Clinical information abstracted from records of 460 HCC patients at the Mayo Clinic, Rochester between January 2007 and December 2009 was reported previously.[109] The number of male and female HCC cases in the overall cohort and in the subset without

hepatic steatosis was compared to the subset with non-alcoholic hepatic steatosis as the primary HCC etiology by Chi squared test.

Analysis of genomic data from TCGA

RNA-seq normalized counts, copy number variation, mutation, and survival data generated by TCGA Research Network (http://cancergenome.nih.gov/) were extracted from TCGA and cBioportal.[139,140] Normalized expression count values under 0.1 were adjusted to 0.1 to minimize the effects of low count genes in differential expression analysis. Genes with significant expression changes between tumor and normal liver were identified by Benjamini-Hochberg adjusted Student's t test.

Generation and RNA-sequencing of high fat diet-fed wildtype mouse liver tumors

Animal studies were conducted using procedures approved and monitored by the Institutional Animal Care and Use Committee at the Pacific Northwest Research Institute. Starting at five weeks of age, male C57BL/6J mice were fed a high saturated fat and sucrose diet for 400 days (#D12331; Research Diets) *ad libitum*, after which mice were euthanized for liver tissue collection. Tumors and adjacent tumor free liver samples were frozen in liquid nitrogen and stored at -80˚C. RNA was extracted from liver samples using the Direct-zol RNA Miniprep kit (#R2050, Zymo Research). Library preparation was performed with the TruSeq Stranded mRNA kit (#RS-122-2101, Illumina) and samples were sequenced on the Illumina NextSeq 500 platform with a high output 2x75bp paired-end kit. Quantification of all RefSeq genes from the GRCm38/mm10 genome assembly was performed using the kallisto algorithm.[141]

Ingenuity Pathway Analysis

Gene lists specified in the results section were subjected to a core analysis including direct and indirect relationships using Ingenuity Pathway Analysis (IPA) Software (Ingenuity Systems, Redwood City, CA, USA; www.ingenuity.com).

Acknowledgments

The results published here are in part based upon public data generated by the TCGA Research Network: http://cancergenome.nih.gov/. This work utilized computing resources at the University of Minnesota Supercomputing Institute. The University of Minnesota Genomics Center provided Illumina sequencing, Sanger sequencing, and primer synthesis services. Carlyn Iverson provided Illustration assistance with the preparation of some of the figures presented in this work.

Table 2.1: Frequency of liver tumor nodules in experimental mice

Experimental mouse*	Sex	Age (days)	Diet	# of visible tumors
ATR M121	Male	82	eCDD	0
ATR M122	Male	154	eCDD	0
ATR M132	Male	189	eCDD	0
ATR M133	Male	189	eCDD	0
ATR M146	Male	213	eCDD	1
ATR M147	Male	213	eCDD	1
ATR M172	Male	260	eCDD	2
ATR M181	Male	300	eCDD	1
ATR M182	Male	340	eCDD	0
ATR M184	Male	340	eCDD	0
ATR M204	Male	377	eCDD	5
ATR M194	Male	380	eCDD	38
ATR M201	Male	381	eCDD	1
ATR M202	Male	381	eCDD	4
ATR M203	Male	381	eCDD	2
ATR M211	Male	400	eCDD	1
ATR M216	Male	400	eCDD	5
ATR M221	Male	400	eCDD	1
ATR M223	Male	400	eCDD	0
ATR M221*	Male	429	eCDD	0
ATR M225	Male	434	eCDD	3
ATR M226	Male	434	eCDD	5
ATR M227	Male	434	eCDD	5
ATR F123	Female	82	eCDD	0
ATR F124	Female	154	eCDD	0
ATR F151	Female	359	eCDD	2
ATR F153	Female	359	eCDD	0
ATR F154	Female	359	eCDD	2
ATR F134	Female	375	eCDD	4
ATR F171	Female	380	eCDD	1
ATR F173	Female	380	eCDD	1
ATR F174	Female	380	eCDD	7
ATR F162	Female	381	eCDD	3
ATR F163	Female	381	eCDD	0
ATR F164	Female	382	eCDD	17
ATR F175	Female	400	eCDD	2
ATR F177	Female	400	eCDD	0
ATR F221*	Female	429	eCDD	8
ATR F223*	Female	429	eCDD	29
ATR F224*	Female	430	eCDD	12
ATR F225*	Female	431	eCDD	4
ATR F185	Female	431	eCDD	20
ATR F221	Female	434	eCDD	20
ATR F191	Female	434	eCDD	9
ATR F195	Female	434	eCDD	4
ATR F211	Female	435	eCDD	5
ATR F212	Female	435	eCDD	1
ATR F222	Female	436	eCDD	3
ATR F223	Female	436	eCDD	3
ATR M11	Male	105	ND	0
ATR M15	Male	105	ND	0
ATRP M66	Male	160	ND	3

ATR M36	Male	215	ND	0
ATRP M134	Male	223	ND	30
ATR M325	Male	231	ND	5
ATR M31	Male	250	ND	3
ATR M41	Male	289	ND	0
ATR M362	Male	317	ND	8
ATRP M51	Male	330	ND	22
ATRP M175	Male	375	ND	1
ATR M71	Male	440	ND	1
ATR M81	Male	460	ND	1
ATR M93	Male	471	ND	17
ATR M341	Male	472	ND	1
ATR M296	Male	492	ND	16
ATR M297	Male	511	ND	13
ATRP M254	Male	528	ND	14
ATRP M292	Male	539	ND	5
ATR M312	Male	600	ND	15
ATR M302	Male	603	ND	13
ATRP M353	Male	611	ND	3
ATR M271	Male	623	ND	17
ATRP M362	Male	652	ND	9
ATR M352	Male	668	ND	18
ATRP M301	Male	700	ND	2
ATR M364	Male	702	ND	3
ATRP F121	Female	178	ND	0
ATR F13	Female	285	ND	0
ATR F1	Female	310	ND	0
ATR F42	Female	342	ND	0
ATR F106	Female	512	ND	5
ATRP F31	Female	575	ND	2
ATR F115	Female	588	ND	6
ATRP F183	Female	596	ND	6
ATRP F143	Female	612	ND	4
ATRP F115	Female	621	ND	1
ATRP F362	Female	652	ND	1

*Experimental mice carrying *albumin*-Cre (*Alb*-Cre), T2Onc and *Rosa26*-lsl-SB11 transgenes

Table 2.2: Steatosis-associated CIS list

CIS-associated gene	Tumors with tdCIS	tdCIS p value	Tumors with gCIS	gCIS q value	Predicted effect on gene function	Predicted Oncogene or TSG?
Gnai3	9	7.14E-11	9	0.00E+00	Disrupts	TSG
Adk	14	5.69E-09	14	6.83E-23	Disrupts	TSG
Sfpq	5	3.02E-06	4	1.07E-32	Disrupts	TSG
Hipk3	5	3.02E-06	5	2.25E-16	Truncates C terminus or disrupts	TSG
Egfr	5	3.02E-06	6	1.60E-11	Truncates C terminus	Oncogene
Gigyf2	6	2.24E-05	7	9.34E-18	Disrupts	TSG
Arih1	8	0.0002	7	1.07E-20	Disrupts	TSG
Dpyd	10	0.0002	18	1.42E-13	Disrupts	TSG
Gbe1	9	0.0003	9	2.16E-13	Disrupts	TSG
Dhx9	4	0.0004	4	1.08E-18	Disrupts	TSG
Ubl3	4	0.0004	4	4.64E-16	Disrupts	TSG
Palmd	4	0.0004	4	2.35E-14	Disrupts	TSG
Mkln1	4	0.0004	6	9.43E-14	Disrupts	TSG
Pafah1b1	5	0.0011	5	4.72E-20	Disrupts	TSG
Ppp2r2a	5	0.0011	5	1.83E-19	Disrupts	TSG
Ppm1b	5	0.0011	5	1.57E-17	Disrupts	TSG
Arhgap5	5	0.0011	5	2.95E-16	Disrupts	TSG
Rundc3b	6	0.0021	3	8.96E-06	Drives N terminal truncation	Oncogene
Mtus1	7	0.0031	7	1.34E-18	Disrupts	TSG
Kynu	7	0.0031	5	9.66E-08	Disrupts	TSG
Cfh	7	0.0031	4	5.12E-06	Disrupts	TSG
Zbtb20	7	0.0031	7	4.98E-05	Disrupts	TSG
Atrn	8	0.0262	5	2.98E-09	Disrupts	TSG
Ddrgk1			-	-	Drives N terminal truncation	Oncogene
Prr16	8	0.0262	-	-	Disrupts	TSG

Acbd5	6	0.0485	4	2.02E-14	Disrupts	TSG
Ranbp9	6	0.0485	5	2.12E-14	Disrupts	TSG
Rnf111	6	0.0485	5	3.88E-14	Disrupts	TSG
Mllt10	6	0.0485	6	2.41E-10	Disrupts	TSG
Suclg2	6	0.0485	7	2.93E-10	Disrupts	TSG
Gfi1	6	0.0485	5	1.40E-08	Drives	Oncogene
Chchd3	6	0.0485	6	8.71E-06	Disrupts	TSG
Bmpr2	6	0.0485	-	-	Drives N terminal truncation	Oncogene
Thrap3	5	0.0486	4	4.93E-20	Drives/ Drives N terminal truncation	Oncogene
Sh3d21			-	-	Drives N terminal truncation	Oncogene
Atp2a2	5	0.0486	4	2.19E-16	Disrupts	TSG
Usp47	5	0.0486	5	1.51E-11	Disrupts	TSG
Cacul1	5	0.0486	4	1.51E-11	Drives N terminal truncation	Oncogene
Grb14	5	0.0486	5	1.05E-10	Disrupts	TSG
Gopc	5	0.0486	3	2.07E-07	Disrupts	TSG
Rhobtb1	5	0.0486	3	8.24E-06	Drives	Oncogene
Trip11			3	4.53E-05	Disrupts	TSG
Cpsf2			-	-	Drives	Oncogene
Yeats2	5	0.0486	-	-	Disrupts	TSG
Sucla2	4	0.0489	4	1.37E-15	Disrupts	TSG
Scyl2	4	0.0489	4	8.94E-15	Disrupts	TSG
Rnf169	4	0.0489	4	1.70E-13	Drives N terminal truncation	Oncogene
Notch2	4	0.0489	5	6.81E-12	Disrupts	TSG
Tax1bp1	4	0.0489	4	1.01E-11	Disrupts	TSG
Nat10	4	0.0489	3	9.06E-11	Drives	Oncogene
Caprin1			3	1.81E-09	Disrupts	TSG
Nrip1	4	0.0489	4	1.60E-09	Disrupts	TSG
Ahr	4	0.0489	3	1.63E-09	Disrupts	TSG
Sec63	4	0.0489	4	2.99E-09	Disrupts	TSG
Zeb1	4	0.0489	5	7.27E-06	Drives N terminal truncation	Oncogene
No results within 20000 bp window	4	0.0489	-	-	-	-

Ctif	4	0.0489	-	-	Disrupts	TSG
Stag2	4	0.0489	-	-	Disrupts	TSG
Dgkq	3	0.0490	3	5.86E-26	Disrupts	TSG
Idua			3	6.94E-25	Drives	Oncogene
Ube2b	3	0.0490	3	5.89E-19	Disrupts	TSG
Klf3	3	0.0490	3	9.46E-17	Disrupts	TSG
Nploc4	3	0.0490	3	6.77E-09	Drives N terminal truncation	Oncogene
Cdk13	3	0.0490	4	1.64E-06	Disrupts	TSG
Abcd3	3	0.0490	3	2.99E-06	Disrupts	TSG
Ell2	3	0.0490	3	1.98E-05	Disrupts	TSG
Cnot1	3	0.0490	-	-	Disrupts	TSG
Kbtbd3	3	0.0490	-	-	Drives	Oncogene
Rabl3	3	0.0490	-	-	Drives N terminal truncation	Oncogene
Xbp1	3	0.0490	-	-	Drives N terminal truncation	Oncogene
Ankrd36			-	-	Drives N terminal truncation	Oncogene
Lgi2	3	0.0490	-	-	Drives N terminal truncation	Oncogene
Nr1i2	7	0.0497	3	1.86E-10	Disrupts	TSG
Gsk3b			-	-	Disrupts	TSG
4933406I18Rik	-	-	16	0.00E+00	Drives 5' truncation	-
Stard4	-	-	5	8.37E-57	Truncates C terminus	TSG
Fgf2	-	-	7	1.61E-51	Truncates C terminus	TSG
Cited2	-	-	3	1.30E-37	Drives	Oncogene
Mrpl27	-	-	3	9.30E-37	Truncates C terminus	TSG
Nckap1	-	-	8	2.30E-35	Drives N terminal truncation	Oncogene
Gaa	-	-	3	7.93E-34	Disrupts	TSG
Ube2r2	-	-	6	1.16E-32	Disrupts	TSG
Cntd1	-	-	3	2.24E-31	Drives N terminal truncation	Oncogene
Acadm	-	-	4	5.30E-29	Disrupts	TSG
Xylb	-	-	4	1.82E-28	Disrupts	TSG
Cntf	-	-	3	1.26E-27	Disrupts	TSG
Rabggtb	-	-	3	2.33E-26	Drives N terminal truncation	Oncogene

Prpf6	-	-	5	1.31E-23	Disrupts	TSG
Nat2	-	-	3	1.66E-23	Disrupts	TSG
Arl1	-	-	3	3.38E-23	Disrupts	TSG
Paip1	-	-	4	3.23E-18	Disrupts	TSG
Mgat1	-	-	3	5.93E-18	Disrupts	TSG
Ube2d3	-	-	4	8.09E-18	Disrupts	TSG
Polr2a	-	-	3	1.08E-17	Disrupts	TSG
Rp9	-	-	3	1.16E-17	Disrupts	TSG
Ppp2r5e	-	-	7	1.43E-16	Disrupts	TSG
Esd	-	-	3	3.45E-16	Disrupts	TSG
Csnk1d	-	-	3	9.21E-16	Disrupts	TSG
Rab2a	-	-	5	2.82E-15	Disrupts	TSG
Atg14	-	-	3	4.83E-15	Disrupts	TSG
Bcar3	-	-	5	5.90E-15	Disrupts	TSG
Sec16a	-	-	3	3.35E-14	Disrupts	TSG
Rab1	-	-	3	8.91E-14	Disrupts	TSG
Timm23	-	-	3	1.93E-13	Disrupts	TSG
Mgea5	-	-	3	3.12E-13	Disrupts	TSG
Arcn1	-	-	3	5.45E-13	Disrupts	TSG
Ptp4a2	-	-	3	5.68E-13	Disrupts	TSG
Uox	-	-	3	1.41E-12	Disrupts	TSG
Ddi2	-	-	3	6.02E-12	Disrupts	TSG
Dnajc5	-	-	3	6.85E-12	Drives	Oncogene
G3bp2	-	-	3	9.08E-12	Disrupts	TSG
Abhd2	-	-	4	1.70E-11	Disrupts	TSG
Cyp2b13	-	-	3	4.84E-11	Disrupts	TSG
Vangl1	-	-	3	1.36E-10	Disrupts	TSG
Wbp1l	-	-	3	1.84E-10	Disrupts	TSG
Rcor3	-	-	3	2.42E-10	Disrupts	TSG
Acsl5	-	-	3	3.90E-10	Disrupts	TSG
Elavl1	-	-	3	5.00E-10	Drives	Oncogene

Hadha	-	-	3	5.72E-10	Disrupts	TSG
Zfp91	-	-	3	7.50E-10	Disrupts	TSG
Ash1l	-	-	5	8.16E-10	Disrupts	TSG
Slc35d1	-	-	3	1.28E-09	Disrupts	TSG
Fbxo3	-	-	3	1.67E-09	Disrupts	TSG
Celf1	-	-	4	2.51E-09	Disrupts	TSG
Aadat	-	-	3	3.16E-09	Disrupts	TSG
Eif4enif1	-	-	3	3.43E-09	Disrupts	TSG
Prkd3	-	-	4	3.50E-09	Disrupts	TSG
Larp4b	-	-	4	4.36E-09	Disrupts	TSG
Dnajb6	-	-	3	6.92E-09	Disrupts	TSG
Zranb1	-	-	3	1.56E-08	Drives	Oncogene
Fbxo38	-	-	3	1.62E-08	Disrupts	TSG
Nr2c1	-	-	3	2.16E-08	Disrupts	TSG
Ncor1	-	-	5	2.66E-08	Disrupts	TSG
Ube2e1	-	-	3	2.66E-08	Drives	Oncogene
Dag1	-	-	3	3.07E-08	Drives	Oncogene
Wdfy3	-	-	6	3.27E-08	Disrupts	TSG
D17Wsu92e	-	-	3	4.40E-08	Disrupts	TSG
Smek1	-	-	3	4.79E-08	Disrupts	TSG
Txnrd1	-	-	3	9.68E-08	Disrupts	TSG
Fbxo36	-	-	3	1.04E-07	Disrupts	TSG
Ptprd	-	-	12	1.04E-07	Disrupts	TSG
Txlnb	-	-	3	1.18E-07	Disrupts	TSG
Aldh1a1	-	-	3	1.29E-07	Disrupts	TSG
Kdm1a	-	-	3	1.30E-07	Disrupts	TSG
Foxj3	-	-	4	1.37E-07	Disrupts	TSG
Vps54	-	-	4	1.41E-07	Disrupts	TSG
Txlng	-	-	3	1.81E-07	Drives N terminal truncation	Oncogene
Pex14	-	-	4	1.82E-07	Disrupts	TSG
Rreb1	-	-	4	1.99E-07	Disrupts	TSG

Pde3b	-	-	5	2.11E-07	Disrupts	TSG
Kcmf1	-	-	3	2.24E-07	Drives N terminal truncation	Oncogene
Bmpr1a	-	-	4	2.37E-07	Disrupts	TSG
Tmem135	-	-	6	2.41E-07	Disrupts	TSG
Dicer1	-	-	3	2.65E-07	Disrupts	TSG
Btbd7	-	-	4	3.97E-07	Disrupts	TSG
D330022K07Rik	-	-	4	4.65E-07	Disrupts	TSG
Iqgap2	-	-	6	4.81E-07	Disrupts	TSG
Taok3	-	-	4	5.46E-07	Disrupts	TSG
Arid1a	-	-	3	5.84E-07	Disrupts	TSG
Rtf1	-	-	3	5.90E-07	Disrupts	TSG
Tcf12	-	-	7	8.13E-07	Disrupts	TSG
Dennd4c	-	-	4	1.03E-06	Disrupts	TSG
Nsd1	-	-	4	1.20E-06	Disrupts	TSG
Pah	-	-	3	1.21E-06	Disrupts	TSG
Cnot6l	-	-	4	1.23E-06	Drives	Oncogene
2610018G03Rik	-	-	3	1.43E-06	Disrupts	TSG
Tbca	-	-	3	1.48E-06	Drives N terminal truncation	Oncogene
Rock2	-	-	4	1.53E-06	Disrupts	TSG
Shb	-	-	3	2.12E-06	Disrupts	TSG
Adcy9	-	-	4	2.20E-06	Disrupts	TSG
Mtmr3	-	-	4	2.70E-06	Disrupts	TSG
Cnot2	-	-	4	2.76E-06	Disrupts	TSG
Gnaq	-	-	6	2.76E-06	Disrupts	TSG
Lnpep	-	-	4	3.00E-06	Disrupts	TSG
Fam193a	-	-	4	3.30E-06	Disrupts	TSG
U2surp	-	-	3	3.43E-06	Disrupts	TSG
Chd2	-	-	4	4.46E-06	Disrupts	TSG
Scp2	-	-	3	4.87E-06	Disrupts	TSG
Pan3	-	-	4	5.48E-06	Disrupts	TSG
Cep85l	-	-	4	5.85E-06	Disrupts	TSG

Lpgat1	-	-	3	8.78E-06	Disrupts	TSG
Phf3	-	-	3	9.33E-06	Disrupts	TSG
Thrb	-	-	7	9.66E-06	Disrupts	TSG
Snx13	-	-	4	9.93E-06	Disrupts	TSG
Ubr4	-	-	3	1.24E-05	Disrupts	TSG
Lcorl	-	-	5	1.35E-05	Disrupts	TSG
Stard13	-	-	4	2.27E-05	Disrupts	TSG
Kcnn2	-	-	4	2.66E-05	Disrupts	TSG
Stim2	-	-	4	3.26E-05	Disrupts	TSG
Tek	-	-	4	3.30E-05	Disrupts	TSG
Ugt1a6a	-	-	3	3.37E-05	Disrupts	TSG
Slc22a23	-	-	4	4.18E-05	Disrupts	TSG
Arntl	-	-	3	4.43E-05	Disrupts	TSG
Ablim1	-	-	4	4.71E-05	Disrupts	TSG
Tcf7l2	-	-	4	4.96E-05	Disrupts	TSG
Frs2	-	-	3	5.80E-05	Drives	Oncogene
Brd4	-	-	3	5.88E-05	Drives	Oncogene
Rc3h1	-	-	3	6.35E-05	Disrupts	TSG
Wac	-	-	3	7.46E-05	Disrupts	TSG
Mkl2	-	-	4	8.10E-05	Disrupts	TSG
Brwd1	-	-	3	8.28E-05	Disrupts	TSG
Mon2	-	-	3	9.47E-05	Disrupts	TSG
Kmt2E	-	-	3	0.0001	Disrupts	TSG
Insc	-	-	3	0.0001	Disrupts	TSG

Table 2.3: CIS genes altered in human HCC. Gene expression changes, CNV, and mutation in TCGA HCC cases

ECDD-treated mouse insertions		TCGA HCC gene expression vs normal liver						Percent of TCGA tumors with amplification, deletion, mutation		
		All TCGA tumor		Alcohol associated tumor		Steatosis-associated tumor				
CIS-associated gene	**Predicted oncogene or TSG**	**Fold change**	**BH q value**	**Fold change**	**BH q value**	**Fold change**	**BH q value**	**All TCGA HCC**	**TCGA alcohol-associated**	**TCGA steatosis-associated**
2610018G03Rik	TSG	-	-	-	-	-	-	0%	0%	0%
4933406I18Rik	-	-	-	-	-	-	-	0%	0%	0%
AADAT	TSG	0.15	3.1E-22	0.14	3.8E-22	0.08	8.4E-20	1%	1%	0%
ABCD3	TSG	0.59	1.1E-15	0.61	1.3E-13	0.54	1.5E-02	1%	2%	0%
ABHD2	TSG	0.54	1.5E-14	0.56	4.7E-12	-	-	1%	3%	0%
ABLIM1	TSG	-	-	-	-	-	-	1%	2%	0%
ACADM	TSG	0.43	2.4E-20	0.45	7.9E-19	0.35	3.5E-03	1%	0%	0%
ACBD5	TSG	0.66	1.1E-12	0.70	8.3E-08	-	-	1%	2%	8%
ACSL5	TSG	0.66	6.3E-06	0.70	2.0E-03	-	-	1%	1%	0%
ADCY9	TSG	-	-	-	-	-	-	2%	3%	0%
ADK	TSG	0.51	2.0E-17	0.50	1.4E-17	0.40	7.4E-05	2%	3%	8%
AHR	TSG	0.64	4.4E-09	0.66	1.1E-06	0.57	3.7E-02	1%	2%	0%
ALDH1A1	TSG	-	-	-	-	-	-	1%	1%	0%
ANKRD36	Oncogene	2.03	1.5E-15	1.75	9.0E-06	-	-	1%	1%	0%
ARCN1	TSG	0.81	9.6E-10	0.80	3.7E-08	-	-	1%	1%	0%
ARHGAP5	TSG	0.82	4.6E-05	0.83	1.6E-03	-	-	2%	3%	0%
ARID1A	TSG	-	-	-	-	-	-	10%	15%	17%
ARIH1	TSG	-	-	-	-	-	-	2%	4%	0%
ARL1	TSG	-	-	-	-	-	-	1%	1%	0%
ARNTL	TSG	-	-	-	-	-	-	0%	0%	0%
ASH1L	TSG	1.44	2.4E-09	1.45	1.2E-06	-	-	16%	20%	42%
ATG14	TSG	-	-	-	-	-	-	1%	3%	0%
ATP2A2	TSG	1.31	9.8E-07	1.30	3.4E-05	1.85	1.2E-03	2%	2%	0%
ATRN	TSG	1.20	5.2E-03	1.33	2.0E-03	-	-	1%	1%	0%
BCAR3	TSG	-	-	-	-	-	-	0%	0%	0%
BMPR1A	TSG	1.13	1.7E-02	-	-	-	-	1%	1%	0%
BMPR2	Oncogene	0.67	6.4E-12	0.66	1.8E-10	-	-	2%	2%	8%
BRD4	Oncogene	-	-	-	-	-	-	3%	6%	0%
BRWD1	TSG	0.79	9.7E-09	0.80	1.1E-06	-	-	2%	2%	0%
BTBD7	TSG	1.14	2.8E-03	1.14	5.0E-02	-	-	2%	3%	0%
CACUL1	Oncogene	-	-	-	-	-	-	1%	1%	0%
CAPRIN1	TSG	1.28	3.3E-09	1.31	7.0E-07	2.12	4.2E-02	1%	2%	0%

CDK13	TSG	-	-	-	-	-	-	1%	2%	0%
CELF1	TSG	0.82	6.3E-06	0.83	3.1E-04	-	-	1%	2%	0%
CEP85L	TSG	-	-	-	-	-	-	2%	3%	8%
CFH	TSG	0.76	5.2E-07	0.81	1.1E-03	-	-	13%	17%	33%
CHCHD3	TSG	1.41	2.3E-14	1.43	1.4E-09	-	-	2%	3%	0%
CHD2	TSG	-	-	-	-	-	-	4%	8%	0%
CITED2	Oncogene	0.50	3.8E-08	0.50	1.3E-07	-	-	2%	2%	0%
CNOT1	TSG	-	-	-	-	-	-	3%	3%	0%
CNOT2	TSG	1.08	4.2E-03	-	-	-	-	2%	3%	0%
CNOT6L	Oncogene	0.76	6.7E-07	0.76	2.3E-05	-	-	2%	3%	0%
CNTD1	Oncogene	1.91	1.8E-13	2.00	1.2E-05	-	-	2%	3%	8%
CNTF	TSG	1.43	2.7E-04	1.51	7.1E-04	-	-	1%	0%	0%
CPSF2	Oncogene	-	-	-	-	-	-	2%	3%	0%
CSNK1D	TSG	1.41	2.3E-15	1.38	1.7E-10	-	-	8%	8%	17%
CTIF	TSG	-	-	-	-	-	-	2%	2%	0%
Cyp2b13	TSG	-	-	-	-	-	-	0%	0%	0%
D17Wsu92e	TSG	-	-	-	-	-	-	0%	0%	0%
D330022K07Rik	TSG	-	-	-	-	-	-	0%	0%	0%
DAG1	Oncogene	1.14	7.9E-03	1.17	1.1E-02	-	-	2%	1%	0%
DDI2	TSG	0.61	1.5E-05	0.61	5.9E-05	-	-	2%	3%	0%
DDRGK1	Oncogene	1.17	1.1E-03	1.12	5.0E-02	-	-	1%	1%	0%
DENND4C	TSG	0.82	3.7E-06	0.85	1.0E-03	-	-	2%	3%	0%
DGKQ	TSG	1.90	2.0E-27	1.92	5.0E-14	-	-	1%	1%	0%
DHX9	TSG	1.29	1.1E-14	1.27	1.4E-07	1.81	2.5E-02	13%	16%	25%
DICER1	TSG	0.68	4.3E-11	0.66	1.7E-10	-	-	2%	1%	0%
DNAJB6	TSG	1.52	4.0E-33	1.50	2.1E-15	-	-	2%	1%	0%
DNAJC5	Oncogene	1.69	6.4E-20	1.70	3.9E-13	-	-	2%	5%	0%
DPYD	TSG	0.54	2.0E-16	0.53	3.6E-15	-	-	2%	3%	0%
EGFR	Oncogene	0.66	2.8E-05	0.71	6.5E-03	-	-	4%	4%	0%
EIF4ENIF1	TSG	1.34	1.5E-16	1.33	2.0E-06	1.70	4.5E-02	2%	3%	0%
ELAVL1	Oncogene	1.24	5.4E-13	1.23	9.3E-08	-	-	1%	4%	17%
ELL2	TSG	0.66	1.1E-04	0.62	4.5E-05	-	-	2%	3%	0%
ESD	TSG	0.76	3.5E-16	0.73	4.2E-13	0.64	3.7E-02	2%	2%	0%
FAM193A	TSG	1.33	4.1E-18	1.27	4.9E-06	-	-	2%	3%	0%
FBXO3	TSG	0.74	1.3E-13	0.74	5.7E-10	-	-	1%	3%	0%
FBXO36	TSG	-	-	-	-	-	-	1%	1%	0%
FBXO38	TSG	-	-	-	-	-	-	3%	4%	0%
FGF2	TSG	-	-	-	-	-	-	1%	1%	0%
FOXJ3	TSG	-	-	-	-	-	-	1%	1%	0%
FRS2	Oncogene	-	-	-	-	-	-	2%	3%	0%

G3BP2	TSG	0.79	1.1E-08	0.83	4.6E-05	-	-	1%	3%	0%
GAA	TSG	1.14	3.1E-03	-	-	-	-	6%	6%	0%
GBE1	TSG	0.67	6.1E-07	0.69	1.5E-05	-	-	1%	1%	0%
GFI1	Oncogene	1.78	9.0E-03	-	-	-	-	1%	0%	0%
GIGYF2	TSG	-	-	-	-	-	-	2%	2%	0%
GNAI3	TSG	-	-	-	-	-	-	1%	1%	0%
GNAQ	TSG	0.82	4.6E-05	0.83	5.6E-04	-	-	3%	2%	0%
GOPC	TSG	0.86	1.3E-05	0.83	4.0E-05	-	-	2%	2%	0%
GRB14	TSG	0.79	4.7E-06	0.79	3.5E-04	-	-	4%	5%	0%
GSK3B	TSG	1.13	1.3E-04	1.16	4.2E-04	-	-	1%	2%	0%
HADHA	TSG	0.76	1.6E-10	0.78	4.0E-07	-	-	2%	3%	8%
HIPK3	TSG	0.54	3.1E-07	0.55	1.9E-06	-	-	1%	2%	0%
IDUA	Oncogene	2.55	2.2E-39	2.39	2.9E-15	-	-	1%	2%	0%
INSC	TSG	2.52	3.4E-03	-	-	-	-	0%	0%	0%
IQGAP2	TSG	0.57	4.8E-16	0.58	1.5E-13	-	-	2%	3%	0%
KBTBD3	Oncogene	-	-	-	-	0.64	6.4E-03	2%	3%	0%
KCMF1	Oncogene	1.19	1.3E-11	1.16	1.1E-06	-	-	1%	1%	8%
KCNN2	TSG	0.10	6.4E-13	0.07	4.9E-13	0.05	6.9E-12	2%	1%	8%
KDM1A	TSG	1.34	1.5E-16	1.34	1.6E-05	-	-	1%	3%	0%
KLF3	TSG	0.68	6.9E-09	0.68	2.7E-08	-	-	1%	1%	0%
KMT2E	TSG	-	-	-	-	-	-	4%	5%	0%
KYNU	TSG	0.66	1.9E-10	0.60	9.2E-09	-	-	2%	3%	8%
LARP4B	TSG	1.43	1.5E-24	1.41	4.7E-13	1.91	4.0E-02	2%	3%	17%
LCORL	TSG	0.84	4.0E-03	0.82	2.3E-02	-	-	2%	1%	0%
LGI2	Oncogene	3.07	1.2E-11	2.41	2.0E-06	-	-	2%	3%	0%
LNPEP	TSG	-	-	-	-	-	-	2%	3%	8%
LPGAT1	TSG	1.72	1.9E-16	1.80	1.9E-10	-	-	9%	14%	8%
MGAT1	TSG	-	-	0.92	4.5E-02	0.66	1.2E-02	2%	3%	17%
MGEA5	TSG	0.92	4.7E-02	-	-	-	-	1%	1%	0%
MKL2	TSG	-	-	-	-	-	-	2%	2%	0%
MKLN1	TSG	0.80	5.4E-11	0.81	8.6E-07	-	-	3%	3%	8%
MLLT10	TSG	1.12	1.6E-02	-	-	1.47	3.4E-02	2%	4%	17%
MON2	TSG	0.83	5.6E-06	0.82	3.6E-05	-	-	2%	3%	0%
MRPL27	TSG	1.33	4.8E-06	1.29	9.0E-03	-	-	2%	3%	8%
MTMR3	TSG	1.18	1.6E-05	1.16	5.5E-03	-	-	1%	2%	0%
MTUS1	TSG	0.69	2.3E-07	0.76	5.7E-04	-	-	7%	6%	8%
NAT10	Oncogene	1.34	3.5E-16	1.30	7.3E-08	1.64	3.4E-02	1%	3%	0%
NAT2	TSG	0.14	4.4E-18	0.16	9.9E-18	0.08	2.9E-17	7%	6%	8%
NCKAP1	Oncogene	1.09	2.1E-02	-	-	1.50	3.5E-02	2%	3%	0%
NCOR1	TSG	0.53	2.7E-16	0.58	3.0E-11	-	-	6%	9%	17%

NOTCH2	TSG	-	-	-	-	-	-	12%	15%	8%
NPLOC4	Oncogene	1.84	2.2E-39	1.92	1.6E-20	1.72	1.9E-03	8%	8%	17%
NR1I2	TSG	0.40	7.8E-17	0.44	9.2E-14	0.27	1.1E-02	1%	0%	0%
NR2C1	TSG	1.22	2.3E-07	1.18	7.5E-04	-	-	1%	2%	0%
NRIP1	TSG	0.61	1.9E-08	0.62	1.3E-07	-	-	1%	1%	0%
NSD1	TSG	1.60	1.7E-16	1.54	5.4E-10	-	-	4%	7%	17%
PAFAH1B1	TSG	0.79	4.5E-15	0.82	1.2E-08	-	-	2%	2%	0%
PAH	TSG	0.54	4.7E-15	0.53	1.4E-13	-	-	1%	1%	0%
PAIP1	TSG	1.10	5.7E-04	1.13	4.5E-03	-	-	1%	2%	0%
PALMD	TSG	0.85	2.4E-02	0.80	1.5E-02	-	-	3%	3%	0%
PAN3	TSG	1.12	2.4E-02	-	-	-	-	2%	4%	8%
PDE3B	TSG	0.63	2.9E-09	0.65	9.6E-06	-	-	1%	3%	8%
PEX14	TSG	0.75	2.6E-08	0.77	1.5E-05	0.56	3.7E-02	3%	3%	0%
PHF3	TSG	0.88	1.3E-02	-	-	-	-	5%	3%	8%
POLR2A	TSG	0.83	3.2E-05	0.82	1.7E-04	-	-	4%	8%	0%
PPM1B	TSG	0.89	1.1E-03	0.90	2.4E-02	-	-	2%	2%	0%
PPP2R2A	TSG	0.59	7.8E-12	0.61	3.8E-10	-	-	7%	8%	8%
PPP2R5E	TSG	0.84	1.0E-02	0.82	8.9E-03	-	-	1%	2%	0%
PRKD3	TSG	-	-	-	-	-	-	1%	1%	0%
PRPF6	TSG	1.48	3.9E-21	1.41	8.9E-11	-	-	2%	4%	0%
PRR16	TSG	2.75	8.5E-18	2.74	2.2E-09	-	-	2%	3%	17%
PTP4A2	TSG	0.92	3.7E-02	-	-	-	-	1%	2%	0%
PTPRD	TSG	0.54	3.2E-08	0.58	1.5E-05	-	-	3%	3%	0%
RAB1	TSG	-	-	-	-	-	-	1%	1%	0%
RAB2A	TSG	1.24	4.4E-09	1.26	2.5E-05	-	-	8%	7%	0%
RABGGTB	Oncogene	1.32	3.7E-13	1.31	1.1E-06	-	-	0%	0%	0%
RABL3	Oncogene	-	-	-	-	-	-	0%	1%	8%
RANBP9	TSG	-	-	-	-	-	-	5%	7%	25%
RC3H1	TSG	0.89	3.7E-03	0.90	1.5E-02	-	-	10%	14%	33%
RCOR3	TSG	1.71	2.0E-27	1.71	2.5E-13	-	-	11%	14%	17%
RHOBTB1	Oncogene	2.39	6.4E-06	2.28	4.9E-03	-	-	2%	2%	0%
RNF111	TSG	-	-	-	-	-	-	2%	3%	8%
RNF169	Oncogene	-	-	-	-	-	-	2%	3%	8%
ROCK2	TSG	-	-	-	-	-	-	4%	3%	0%
RP9	TSG	1.47	6.8E-11	1.42	7.9E-06	-	-	2%	2%	0%
RREB1	TSG	-	-	-	-	-	-	5%	5%	8%
RTF1	TSG	-	-	-	-	-	-	1%	1%	0%
RUNDC3B	Oncogene	0.50	1.4E-16	0.54	3.0E-11	-	-	2%	3%	0%
SCP2	TSG	0.41	3.0E-19	0.43	3.9E-18	0.34	3.8E-03	1%	1%	0%
SCYL2	TSG	0.78	3.2E-04	0.79	1.9E-03	-	-	2%	6%	0%

SEC16A	TSG	-	-	-	-	-	-	2%	1%	0%
SEC63	TSG	0.86	3.0E-06	0.82	2.0E-06	-	-	3%	1%	0%
SFPQ	TSG	1.13	1.3E-02	-	-	-	-	2%	3%	17%
SH3D21	Oncogene	-	-	-	-	-	-	1%	3%	0%
SHB	TSG	0.63	1.8E-05	0.63	4.7E-05	0.40	2.4E-06	1%	0%	0%
SLC22A23	TSG	1.75	2.5E-20	1.90	4.7E-12	3.25	3.8E-02	7%	8%	42%
SLC35D1	TSG	0.41	5.4E-22	0.42	6.2E-22	0.37	1.7E-06	2%	2%	0%
SMEK1	TSG	-	-	-	-	-	-	0%	0%	0%
SNX13	TSG	-	-	-	-	-	-	1%	4%	8%
STAG2	TSG	-	-	-	-	-	-	3%	4%	8%
STARD13	TSG	-	-	-	-	-	-	2%	3%	8%
STARD4	TSG	0.71	7.5E-04	0.67	3.9E-04	-	-	2%	2%	8%
STIM2	TSG	-	-	-	-	-	-	1%	3%	0%
SUCLA2	TSG	0.75	1.1E-13	0.76	5.5E-09	-	-	3%	3%	0%
SUCLG2	TSG	0.51	4.9E-21	0.58	4.3E-16	-	-	1%	2%	0%
TAOK3	TSG	-	-	-	-	-	-	1%	3%	0%
TAX1BP1	TSG	1.27	8.4E-07	1.29	1.4E-05	-	-	2%	3%	0%
TBCA	Oncogene	1.24	2.9E-06	1.23	4.7E-03	-	-	0%	0%	0%
TCF12	TSG	-	-	-	-	-	-	2%	3%	8%
TCF7L2	TSG	0.86	1.3E-03	-	-	-	-	2%	1%	0%
TEK	TSG	0.41	5.5E-14	0.43	1.3E-11	-	-	2%	4%	0%
THRAP3	Oncogene	0.88	4.0E-05	0.87	1.8E-04	-	-	1%	3%	8%
THRB	TSG	0.72	4.7E-10	0.70	1.1E-09	-	-	1%	1%	8%
TIMM23	TSG	-	-	-	-	-	-	0%	1%	0%
TMEM135	TSG	0.87	2.9E-03	-	-	-	-	1%	0%	0%
TRIP11	TSG	-	-	-	-	-	-	2%	3%	0%
TXLNB	TSG	-	-	-	-	-	-	2%	2%	0%
TXLNG	Oncogene	-	-	-	-	-	-	2%	1%	8%
TXNRD1	TSG	2.66	2.0E-22	2.53	1.0E-09	-	-	1%	1%	0%
U2SURP	TSG	-	-	-	-	-	-	2%	5%	8%
UBE2B	TSG	-	-	-	-	-	-	1%	2%	8%
UBE2D3	TSG	0.74	3.9E-16	0.75	9.7E-14	0.74	4.4E-02	2%	1%	0%
UBE2E1	Oncogene	1.27	6.2E-14	1.21	2.0E-06	-	-	1%	1%	0%
UBE2R2	TSG	-	-	-	-	-	-	1%	2%	0%
UBL3	TSG	0.63	1.1E-16	0.63	6.2E-15	-	-	2%	1%	0%
UBR4	TSG	0.85	7.7E-04	0.83	6.7E-04	-	-	4%	7%	8%
UGT1A6A	TSG	-	-	-	-	0.38	4.4E-02	0%	0%	0%
UOX	TSG	-	-	-	-	-	-	0%	0%	0%
USP47	TSG	0.84	2.7E-05	0.83	4.5E-05	-	-	2%	3%	8%
VANGL1	TSG	1.29	3.2E-06	1.22	7.4E-03	-	-	1%	0%	0%

VPS54	TSG	1.32	8.0E-08	1.24	4.1E-04	-	-	1%	2%	0%
WAC	TSG	1.08	4.6E-03	1.09	2.5E-02	1.48	4.8E-02	2%	3%	8%
WBP1L	TSG	-	-	-	-	-	-	1%	0%	0%
WDFY3	TSG	0.80	1.3E-03	0.76	1.6E-03	-	-	3%	3%	0%
XBP1	Oncogene	0.65	7.0E-09	0.66	9.3E-08	0.60	3.3E-02	2%	3%	0%
XYLB	TSG	0.76	7.9E-06	0.75	7.7E-05	-	-	1%	1%	0%
YEATS2	TSG	2.29	2.2E-39	2.22	1.9E-18	-	-	3%	5%	17%
ZBTB20	TSG	0.73	7.0E-04	0.64	3.7E-05	-	-	2%	3%	8%
ZEB1	Oncogene	-	-	-	-	-	-	2%	4%	8%
ZFP91	TSG	0.90	1.5E-02	-	-	-	-	1%	0%	0%
ZRANB1	Oncogene	0.75	5.8E-06	0.75	4.9E-05	-	-	1%	2%	8%

Table 2.4: Steatosis-enriched CIS list

	TAPDANCE CIS enrichment			gCIS enrichment		
Gene	% eCDD tumors with CIS	% ND tumors with CIS	BH q value	% eCDD tumors with CIS	% ND tumors with CIS	BH q value
Gnai3	9.1	0.0	1.6E-04	9.1	0.0	3.7E-04
Gbe1	9.1	0.0	1.6E-04	9.1	0.0	3.7E-04
Arih1	8.1	0.0	3.1E-04	7.1	0.0	1.9E-03
Atrn	8.1	0.0	3.1E-04	5.1	0.0	9.5E-03
Prr16	8.1	0.0	3.1E-04	-	-	-
Mtus1	7.1	0.0	7.9E-04	7.1	0.0	1.9E-03
Kynu	7.1	0.0	7.9E-04	5.1	0.0	9.5E-03
Cfh	7.1	0.0	7.9E-04	4.0	0.0	1.4E-02
Suclg2	6.1	0.0	1.5E-03	7.1	0.0	1.9E-03
Chchd3	6.1	0.0	1.5E-03	6.1	0.0	5.1E-03
Mllt10	6.1	0.0	1.5E-03	6.1	0.0	5.1E-03
Rnf111	6.1	0.0	1.5E-03	5.1	0.0	9.5E-03
Gfi1	6.1	0.0	1.5E-03	5.1	0.0	9.5E-03
Acbd5	6.1	0.0	1.5E-03	4.0	0.0	1.4E-02
Bmpr2	6.1	0.0	1.5E-03	-	-	-
Gigyf2	6.1	0.0	1.5E-03	-	-	-
Rundc3b	6.1	0.0	1.5E-03	-	-	-
Ppm1b	5.1	0.0	3.1E-03	5.1	0.0	9.5E-03
Hipk3	5.1	0.0	3.1E-03	5.1	0.0	9.5E-03
Usp47	5.1	0.0	3.1E-03	5.1	0.0	9.5E-03
Grb14	5.1	0.0	3.1E-03	5.1	0.0	9.5E-03
Thrap3	5.1	0.0	3.1E-03	4.0	0.0	1.4E-02
Sh3d21				-	-	-
Atp2a2	5.1	0.0	3.1E-03	4.0	0.0	1.4E-02
Sfpq	5.1	0.0	3.1E-03	4.0	0.0	1.4E-02
Yeats2	5.1	0.0	3.1E-03	-	-	-
Trip11	5.1	0.0	3.1E-03	-	-	-
Gopc	5.1	0.0	3.1E-03	-	-	-
Ppp2r2a	5.1	0.0	3.1E-03	-	-	-
Cacul1	5.1	0.0	3.1E-03	-	-	-
Rhobtb1	5.1	0.0	3.1E-03	-	-	-
Pafah1b1	5.1	0.0	3.1E-03	-	-	-
Zeb1	4.0	0.0	7.8E-03	5.1	0.0	9.5E-03
Dhx9	4.0	0.0	7.8E-03	4.0	0.0	1.4E-02
Nrip1	4.0	0.0	7.8E-03	4.0	0.0	1.4E-02
Sec63	4.0	0.0	7.8E-03	4.0	0.0	1.4E-02
Ubl3	4.0	0.0	7.8E-03	4.0	0.0	1.4E-02
Sucla2	4.0	0.0	7.8E-03	4.0	0.0	1.4E-02
Scyl2	4.0	0.0	7.8E-03	4.0	0.0	1.4E-02
Palmd	4.0	0.0	7.8E-03	4.0	0.0	1.4E-02
Rnf169	4.0	0.0	7.8E-03	4.0	0.0	1.4E-02
Tax1bp1	4.0	0.0	7.8E-03	4.0	0.0	1.4E-02
Nat10	4.0	0.0	7.8E-03	-	-	-
Caprin1				-	-	-
Ctif	4.0	0.0	7.8E-03	-	-	-
Notch2	4.0	0.0	7.8E-03	-	-	-
Stag2	4.0	0.0	7.8E-03	-	-	-
Mkln1	4.0	0.0	7.8E-03	-	-	-
Ahr	4.0	0.0	7.8E-03	-	-	-
4933406I18Rik	-	-	-	16.2	0.0	9.3E-08
Ptprd	-	-	-	12.1	0.0	1.2E-05
Nckap1	-	-	-	8.1	0.0	1.1E-03
Fgf2	-	-	-	7.1	0.0	1.9E-03
Tcf12	-	-	-	7.1	0.0	1.9E-03
Thrb	-	-	-	7.1	0.0	1.9E-03
Wdfy3	-	-	-	6.1	0.0	5.1E-03
Tmem135	-	-	-	6.1	0.0	5.1E-03

Gnaq	-	-	-	6.1	0.0	5.1E-03
Stard4	-	-	-	5.1	0.0	9.5E-03
Prpf6	-	-	-	5.1	0.0	9.5E-03
Rab2a	-	-	-	5.1	0.0	9.5E-03
Bcar3	-	-	-	5.1	0.0	9.5E-03
Ncor1	-	-	-	5.1	0.0	9.5E-03
Pde3b	-	-	-	5.1	0.0	9.5E-03
Lcorl	-	-	-	5.1	0.0	9.5E-03
Acadm	-	-	-	4.0	0.0	1.4E-02
Xylb	-	-	-	4.0	0.0	1.4E-02
Paip1	-	-	-	4.0	0.0	1.4E-02
Ube2d3	-	-	-	4.0	0.0	1.4E-02
Abhd2	-	-	-	4.0	0.0	1.4E-02
Celf1	-	-	-	4.0	0.0	1.4E-02
Prkd3	-	-	-	4.0	0.0	1.4E-02
Larp4b	-	-	-	4.0	0.0	1.4E-02
Vps54	-	-	-	4.0	0.0	1.4E-02
Pex14	-	-	-	4.0	0.0	1.4E-02
Rreb1	-	-	-	4.0	0.0	1.4E-02
Bmpr1a	-	-	-	4.0	0.0	1.4E-02
Btbd7	-	-	-	4.0	0.0	1.4E-02
D330022K07Rik	-	-	-	4.0	0.0	1.4E-02
Dennd4c	-	-	-	4.0	0.0	1.4E-02
Nsd1	-	-	-	4.0	0.0	1.4E-02
Rock2	-	-	-	4.0	0.0	1.4E-02
Cdk13	-	-	-	4.0	0.0	1.4E-02
Adcy9	-	-	-	4.0	0.0	1.4E-02
Mtmr3	-	-	-	4.0	0.0	1.4E-02
Cnot2	-	-	-	4.0	0.0	1.4E-02
Lnpep	-	-	-	4.0	0.0	1.4E-02
Fam193a	-	-	-	4.0	0.0	1.4E-02
Chd2	-	-	-	4.0	0.0	1.4E-02
Pan3	-	-	-	4.0	0.0	1.4E-02
Snx13	-	-	-	4.0	0.0	1.4E-02
Kcnn2	-	-	-	4.0	0.0	1.4E-02
Stim2	-	-	-	4.0	0.0	1.4E-02
Tek	-	-	-	4.0	0.0	1.4E-02
Slc22a23	-	-	-	4.0	0.0	1.4E-02
Ablim1	-	-	-	4.0	0.0	1.4E-02
Tcf7l2	-	-	-	4.0	0.0	1.4E-02
Mkl2	-	-	-	4.0	0.0	1.4E-02

Table 2.5: Wnt/β-catenin pathway genes altered in liver cancer

		CIS genes		Genes with altered expression in tumor vs normal liver									
				Mouse				Human					
Wnt/β-catenin signaling pathway protein/family indicated in Figure 2.9	**Gene(s) altered**	**Steatosis-associated CIS**	**Predicted Oncogene or TSG?**	**Steatosis-enriched CIS**	**C57BL/6J HFD tumors**	**Average fold change**	**p value**	**Alcohol-associated HCC**	**Average fold change**	**BH q value**	**Steatosis-associated HCC**	**Average fold change**	**BH q value**
APC	*APC2*	N	-	-	N	-	-	Y	4.28	3.1E-07	N	-	-
AXIN2	*AXIN2*	N	-	-	N	-	-	Y	4.28	1.7E-04	N	-	-
BCL9	*BCL9*	N	-	-	N	-	-	Y	2.63	6.0E-11	N	-	-
CDH	*Cdh5*	N	-	-	Y	2.09	1.2E-02	N	-	-	N	-	-
	CDH12	N	-	-	N	-	-	Y	31.05	1.9E-02	N	-	-
CCND1	*Ccnd1*	N	-	-	Y	9.86	4.2E-02	N	-	-	N	-	-
CK1	*Csnk1d*	Y	TSG	-	N	-	-	N	-	-	N	-	-
	CSNK1G3	N	-	-	N	-	-	N	-	-	Y	0.75	1.3E-02
CK1D	*Csnk1d*	Y	TSG	-	N	-	-	N	-	-	N	-	-
DKK	*DKK1*	N	-	-	N	-	-	Y	50.64	9.9E-03	N	-	-
	DKK2	N	-	-	N	-	-	Y	4.21	8.9E-05	N	-	-
	DKK3	N	-	-	N	-	-	Y	2.31	4.5E-03	N	-	-
	DKKL1	N	-	-	N	-	-	Y	5.76	3.3E-03	N	-	-
DKK1	*DKK1*	N	-	-	N	-	-	Y	50.64	9.9E-03	N	-	-
DSH	*DVL2*	N	-	-	N	-	-	Y	2.05	6.6E-19	Y	2.23	3.4E-02
FOS/JUN	*FOS, Fos*	N	-	-	Y	3.88	2.9E-02	Y	0.12	8.9E-09	Y	0.06	3.1E-08
	JUN	N	-	-	N	-	-	Y	0.36	7.8E-10	Y	0.27	1.9E-07
FZD	*FZD2*	N	-	-	N	-	-	Y	2.40	1.4E-03	N	-	-
	FZD6	N	-	-	N	-	-	Y	2.11	4.0E-09	N	-	-
	FZD9	N	-	-	N	-	-	Y	4.11	7.0E-03	N	-	-
	FZD10	N	-	-	N	-	-	Y	13.41	1.8E-02	N	-	-
	Smo	N	-	-	Y	4.99	5.4E-03	N	-	-	N	-	-
Gαq/o	*GNAO1*	N	-	-	N	-	-	Y	0.26	1.6E-10	Y	0.08	6.9E-12
	Gnaq	Y	TSG	Y	N	-	-	N	-	-	N	-	-
GJA1	*GJA1*	N	-	-	N	-	-	N	-	-	Y	2.17	4.4E-02
GSK3	*Gsk3b*	Y	TSG	-	N	-	-	N	-	-	N	-	-
KREMEN	*KREMEN2*	N	-	-	N	-	-	Y	8.06	1.7E-03	N	-	-
LRP1	*LRP1*	N	-	-	N	-	-	N	-	-	Y	0.54	4.2E-03
MARK2	*Mark2*	N	-	-	Y	2.19	4.1E-02	N	-	-	N	-	-
MDM2	*Mdm2*	N	-	-	Y	2.57	4.3E-03	N	-	-	N	-	-
MYC	*MYC*	N	-	-	N	-	-	Y	0.43	1.2E-06	Y	0.38	3.4E-02
OCT4	*POU5F1*	N	-	-	N	-	-	Y	4.83	3.8E-09	N	-	-
p14/ARF	*CDKN2A*	N	-	-	N	-	-	Y	15.33	5.4E-10	N	-	-
PP2A	*Ppm1j*	N	-	-	Y	2.38	7.0E-04	N	-	-	N	-	-
	Ppp2r2a	Y	TSG	Y	N	-	-	N	-	-	N	-	-
	PPP2R2C	N	-	-	N	-	-	Y	32.75	1.5E-05	N	-	-
	PPP2R3B	N	-	-	N	-	-	Y	2.14	6.1E-14	N	-	-
	PPP2R5D	N	-	-	N	-	-	N	-	-	Y	1.95	2.7E-02
	Ppp2r5e	Y	TSG	-	N	-	-	N	-	-	N	-	-

RAR	*RARB*	N	-	-	N	-	-	N	-	-	Y	0.47	1.1E-02
	Rarg	N	-	-	Y	4.61	1.0E-02	N	-	-	N	-	-
SFRP	*SFRP1*	N	-	-	N	-	-	Y	0.18	1.3E-14	Y	0.22	2.3E-05
	SFRP4	N	-	-	N	-	-	Y	7.98	3.8E-06	N	-	-
SFRP1	*SFRP1*	N	-	-	N	-	-	Y	0.18	1.3E-14	Y	0.22	2.3E-05
SOX	*SOX2*	N	-	-	N	-	-	Y	5.72	1.5E-02	N	-	-
	SOX4	N	-	-	N	-	-	Y	2.71	1.1E-05	N	-	-
	SOX6	N	-	-	N	-	-	Y	0.36	4.9E-10	N	-	-
	SOX9, Sox9	N	-	-	Y	4.27	2.1E-04	Y	2.18	7.9E-06	N	-	-
	SOX10	N	-	-	N	-	-	Y	0.21	4.8E-06	N	-	-
	SOX11	N	-	-	N	-	-	Y	13.52	6.9E-06	N	-	-
	SOX12	N	-	-	N	-	-	Y	2.40	3.8E-10	N	-	-
SRC	*SRC*	N	-	-	N	-	-	Y	2.15	3.1E-09	N	-	-
TCF/LEF	*LEF1*	N	-	-	N	-	-	Y	9.77	1.7E-09	N	-	-
	TCF3	N	-	-	N	-	-	Y	2.17	1.1E-16	Y	2.56	3.8E-02
	Tcf7l2	Y	TSG	Y	N	-	-	N	-	-	N	-	-
UB	*UBB*	N	-	-	N	-	-	N	-	-	Y	0.57	5.2E-03
	UBD	N	-	-	N	-	-	Y	6.43	3.4E-11	N	-	-
WNT	*WNT2*	N	-	-	N	-	-	Y	0.42	4.2E-04	N	-	-
	WNT4	N	-	-	N	-	-	Y	3.27	4.1E-03	N	-	-
	WNT6	N	-	-	N	-	-	Y	6.70	3.6E-02	N	-	-
	WNT8B	N	-	-	N	-	-	Y	4.63	1.2E-02	N	-	-
	WNT11	N	-	-	N	-	-	Y	0.45	2.2E-03	Y	0.34	2.0E-02

Protein product/family	**Gene(s) not significantly altered**												
AKT	*AKT1, AKT2, AKT3*	N	-	-	N	-	-	N		-	N	-	-
APC	*APC*	N	-	-	N	-	-	N		-	N	-	-
APPL	*APPL1, APPL2*	N	-	-	N	-	-	N		-	N	-	-
AXIN1	*AXIN1*	N	-	-	N	-	-	N		-	N	-	-
BTRC	*BTRC, BTrCP, bTrCP1, FBW1A, FBXW1, FBXW1A, FWD1, HOS, Slim*	N	-	-	N	-	-	N		-	N	-	-
CBP	*CREBBP, EP300*	N	-	-	N	-	-	N		-	N	-	-
CDH	*CDH1, CDH2, CDH3*	N	-	-	N	-	-	N		-	N	-	-
CK1	*CSNK1A1, CSNK1E, CSNK1G1, CSNK1G2*	N	-	-	N	-	-	N		-	N	-	-
CK2	*CSNK2A1, CSNK2A2, CSNK2B*	N	-	-	N	-	-	N		-	N	-	-
CTNNB1	*CATNB, CTNNB, CTNNB1*	N	-	-	N	-	-	N		-	N	-	-
DKK	*DKK4*	N	-	-	N	-	-	N		-	N	-	-
DSH	*DVL1, DVL3*	N	-	-	N	-	-	N		-	N	-	-
FZD	*FZD1, FZD3, FZD4, FZD5, FZD7, FZD8*	N	-	-	N	-	-	N		-	N	-	-
GBP	*FRAT1, FRAT2*	N	-	-	N	-	-	N		-	N	-	-
Groucho	*TLE1, TLE3, TLE4*	N	-	-	N	-	-	N		-	N	-	-
Gsk3	*GSK3A, H2BFM*	N	-	-	N	-	-	N		-	N	-	-
HDAC1	*HDAC, HDAC1*	N	-	-	N	-	-	N		-	N	-	-
ILK	*ILK1, ILK2*	N	-	-	N	-	-	N		-	N	-	-

KREMEN	*KREMEN1*	N	-	-	N	-	-	N	-	N	-	-
LRH1	*LRH1*	N	-	-	N	-	-	N	-	N	-	-
LRP	*LRP5, LRP6*	N	-	-	N	-	-	N	-	N	-	-
MMP7	*MMP7*	N	-	-	N	-	-	N	-	N	-	-
P53	*P53, TP53, Trp53*	N	-	-	N	-	-	N	-	N	-	-
PP2A	*PPM1L, PPP2CA, PPP2CB, PPP2R1A, PPP2R1B, PPP2R2B, PPP2R3A, PPP2R5A, PPP2R5B, PPP2R5C, PTPA*	N	-	-	N	-	-	N	-	N	-	-
PPARD	*PPARD*	N	-	-	N	-	-	N	-	N	-	-
RAR	*RARA*	N	-	-	N	-	-	N	-	N	-	-
SFRP	*FRZB, SFRP2, SFRP5*	N	-	-	N	-	-	N	-	N	-	-
SOX	*SOX1, SOX3, SOX5, SOX7, SOX8, SOX13, SOX14, SOX15, SOX17, SOX18, Sox19*	N	-	-	N	-	-	N	-	N	-	-
TCF/LEF	*HNF1A, TCF1, TCF4, Tcf7, TCF7L1*	N	-	-	N	-	-	N	-	N	-	-
UB	*UBC*	N	-	-	N	-	-	N	-	N	-	-
UBL5	*UBL5*	N	-	-	N	-	-	N	-	N	-	-
WIFI	*WIFI*	N	-	-	N	-	-	N	-	N	-	-
Wnt	*WNT1, WNT2B, WNT3, WNT3A, WNT5A, WNT5B, WNT7A, WNT7B, WNT8A, WNT9A, WNT9B, WNT10A, WNT10B, WNT16*	N	-	-	N	-	-	N	-	N	-	-

Table 2.6: PKA/cAMP pathway genes altered in liver cancer

		CIS genes			Genes with altered expression in tumor vs normal liver								
		Mouse						Human					
PKA/cAMP signaling pathway protein/ family indicated in	**Gene(s) altered**	**Steatosis-associated CIS**	**Predicted Oncogene or TSG?**	**Steatosis enriched CIS**	**C57BL/6J HFD tumors**	**Average fold change**	**p value**	**Alcohol-associated HCC**	**Average fold change**	**BH q value**	**Steatosis-associated HCC**	**Average fold change**	**BH q value**
14-3-3	*SFN*	N	-	-	N	-	-	Y	13.58	1.6E-04	N	-	-
	YWHAH	N	-	-	N	-	-	N	-	-	Y	1.87	8.8E-04
ADCY	*Adcy1*	N	-	-	Y	86.02	3.2E-02	N	-	-	Y	0.10	3.4E-08
	ADCY2	N	-	-	N	-	-	Y	2.73	5.0E-03	N	-	-
	ADCY6	N	-	-	N	-	-	Y	2.35	5.5E-22	Y	2.75	1.4E-03
	ADCY8	N	-	-	N	-	-	Y	17.56	3.7E-02	N	-	-
	Adcy9	Y	TSG	Y	N	-	-	N	-	-	N	-	-
AKAP	*AKAP2*	N	-	-	N	-	-	Y	0.48	5.2E-09	N	-	-
	AKAP3	N	-	-	N	-	-	Y	0.45	1.8E-07	Y	0.32	2.9E-04
	Akap12	N	-	-	Y	3.98	3.5E-02	N	-	-	N	-	-
	AKAP14	N	-	-	N	-	-	Y	5.15	2.8E-03	N	-	-
APC	*ANAPC4*	N	-	-	N	-	-	N	-	-	Y	1.62	1.6E-02
	ANAPC13	N	-	-	N	-	-	N	-	-	Y	0.74	1.9E-02
CALM	*CALM1*	N	-	-	N	-	-	N	-	-	Y	0.67	6.3E-05
CAMK	*CAMK4*	N	-	-	N	-	-	Y	0.28	4.6E-08	Y	0.29	1.2E-04
	CAMK2A	N	-	-	N	-	-	Y	6.56	2.2E-02	N	-	-
	CAMK2B	N	-	-	N	-	-	Y	0.25	1.0E-12	Y	0.11	2.6E-11
	CAMK2G	N	-	-	N	-	-	N	-	-	Y	1.67	2.2E-03
CNG	*CNGA1*	N	-	-	N	-	-	Y	0.42	1.6E-09	Y	0.40	3.6E-02
	CNGB3	N	-	-	N	-	-	Y	5.75	1.2E-03	N	-	-
CREB	*CREB3L4*	N	-	-	N	-	-	Y	2.01	1.4E-14	Y	1.82	1.7E-02
	Creb5	N	-	-	Y	8.05	1.9E-02	N	-	-	N	-	-
DCC	*DCC*	N	-	-	N	-	-	Y	16.85	4.7E-02	N	-	-
EPAC	*RAPGEF3*	N	-	-	N	-	-	Y	2.00	5.1E-09	N	-	-
FLN	*Flnb*	N	-	-	Y	2.07	3.8E-02	N	-	-	N	-	-
	FLNC	N	-	-	N	-	-	Y	11.92	2.2E-04	N	-	-
Gαi	*Gnai3*	Y	TSG	Y	N	-	-	N	-	-	N	-	-
	GNAL	N	-	-	N	-	-	Y	5.00	1.0E-07	N	-	-
	GNAO1	N	-	-	N	-	-	Y	0.26	1.6E-10	Y	0.08	6.9E-12
Gαq	*GNA14*	N	-	-	N	-	-	Y	0.30	8.1E-21	Y	0.27	6.4E-05
	Gnaq	Y	TSG	Y	N	-	-	N	-	-	N	-	-
Gβ	*GNB1L*	N	-	-	N	-	-	Y	2.05	1.4E-11	N	-	-
Gγ	*GNG4*	N	-	-	N	-	-	Y	50.28	9.2E-05	N	-	-
	ADORA1	N	-	-	Y	0.41	2.0E-02	Y	2.75	4.7E-03	N	-	-
	ADORA3	N	-	-	N	-	-	Y	0.47	5.4E-04	Y	0.35	1.9E-02
	ADRA1A	N	-	-	Y	0.39	2.7E-02	Y	0.12	6.4E-15	Y	0.09	1.1E-10
	ADRA1B	N	-	-	N	-	-	Y	0.36	5.2E-14	Y	0.19	1.9E-07
	ADRA1D	N	-	-	N	-	-	Y	9.36	1.0E-02	N	-	-
	ADRA2B	N	-	-	N	-	-	Y	0.23	7.7E-11	Y	0.17	1.3E-09
	ADRA2C	N	-	-	N	-	-	Y	8.46	1.1E-06	N	-	-
	ADRB1	N	-	-	N	-	-	Y	0.33	1.2E-05	Y	0.15	3.6E-05
	ADRB2	N	-	-	Y	3.16	2.1E-02	Y	0.49	5.6E-06	Y	0.23	7.1E-04
	ADRB3	N	-	-	Y	0.45	3.8E-02	Y	2.00	8.2E-03	N	-	-
	AGTR1	N	-	-	N	-	-	Y	0.39	4.6E-16	N	-	-

GPCR	*AVPR1A*	N	-	-	N	-	-	Y	0.16	4.6E-06	Y	0.04	3.0E-06
	AVPR2	N	-	-	N	-	-	Y	2.88	9.2E-06	N	-	-
	CHRM2	N	-	-	N	-	-	Y	0.05	5.9E-09	Y	0.02	4.6E-08
	CHRM3	N	-	-	N	-	-	Y	3.57	2.6E-03	N	-	-
	CNR1	N	-	-	N	-	-	Y	5.65	1.5E-03	N	-	-
	CXCR2	N	-	-	N	-	-	Y	0.19	2.4E-04	Y	0.19	3.4E-03
	DRD4	N	-	-	N	-	-	Y	3.34	4.3E-02	N	-	-
	FPR1	N	-	-	N	-	-	Y	0.26	2.0E-08	Y	0.17	2.5E-08
	FPR2	N	-	-	N	-	-	Y	0.14	3.6E-06	Y	0.06	6.6E-06
	GABBR2	N	-	-	N	-	-	Y	21.22	1.8E-02	N	-	-
	GLP1R	N	-	-	N	-	-	Y	52.49	3.9E-02	N	-	-
	GRM1	N	-	-	N	-	-	Y	2.26	4.1E-02	N	-	-
	GRM2	N	-	-	N	-	-	Y	3.53	7.0E-04	N	-	-
	Grm8	N	-	-	Y	9.59	2.0E-02	N	-	-	N	-	-
	HTR1D	N	-	-	N	-	-	Y	19.46	1.7E-03	N	-	-
	HTR1F	N	-	-	N	-	-	Y	3.16	4.1E-05	N	-	-
	HTR4	N	-	-	N	-	-	Y	5.56	7.9E-04	N	-	-
	HTR7	N	-	-	N	-	-	N	-	-	Y	0.51	3.4E-02
	MC1R	N	-	-	N	-	-	Y	2.63	2.6E-06	N	-	-
	NPY1R	N	-	-	N	-	-	Y	0.23	1.3E-13	N	-	-
	P2RY12	N	-	-	N	-	-	Y	0.18	4.3E-07	Y	0.11	9.0E-07
	P2RY13	N	-	-	N	-	-	Y	0.24	3.9E-07	Y	0.27	4.5E-05
	PTGDR	N	-	-	N	-	-	Y	0.37	1.0E-04	Y	0.23	1.8E-04
	PTGER2	N	-	-	N	-	-	Y	0.42	2.7E-06	Y	0.34	1.4E-02
	PTGIR	N	-	-	N	-	-	Y	0.48	8.2E-10	N	-	-
	PTH1R	N	-	-	N	-	-	Y	0.12	1.8E-17	Y	0.08	7.8E-17
	TBXA2R	N	-	-	N	-	-	Y	0.30	4.5E-19	Y	0.31	3.9E-05
	VIPR1	N	-	-	N	-	-	Y	0.10	1.5E-19	Y	0.05	6.2E-20
	XCR1	N	-	-	N	-	-	Y	0.35	1.5E-02	N	-	-
GRK4	*GRK4*	N	-	-	N	-	-	N	-	-	Y	1.43	3.6E-02
GSK3	*Gsk3b*	Y	TSG	-	N	-	-	N	-	-	N	-	-
GYS	*GYS2*	N	-	-	N	-	-	Y	0.26	5.9E-23	Y	0.18	1.6E-04
ITPR	*Itpr3*	N	-	-	Y	7.94	1.1E-02	Y	4.12	1.3E-03	N	-	-
KDELR	*KDELR3*	N	-	-	N	-	-	Y	2.02	1.1E-05	N	-	-
MEK1	*MAP2K1*	N	-	-	N	-	-	Y	0.46	1.2E-11	Y	0.48	4.3E-06
MKP 1/2/3/4	*DUSP1*	N	-	-	N	-	-	Y	0.31	1.2E-12	Y	0.28	3.4E-04
	DUSP6	N	-	-	N	-	-	Y	0.35	6.3E-11	Y	0.31	7.1E-07
	DUSP9	N	-	-	N	-	-	Y	25.19	2.1E-05	N	-	-
NFAT	*NFATC4*	N	-	-	N	-	-	Y	2.34	6.5E-09	N	-	-
NGFR	*NGFR*	N	-	-	N	-	-	Y	0.28	1.1E-18	N	-	-
PDE	*ENPP6*	N	-	-	N	-	-	Y	6.83	5.3E-03	N	-	-
	PDE1B	N	-	-	N	-	-	N	-	-	Y	0.55	4.8E-02
	Pde1c	N	-	-	Y	37.14	1.7E-02	N	-	-	N	-	-
	PDE2A	N	-	-	N	-	-	Y	0.38	1.5E-12	N	-	-
	PDE3B	Y	TSG	Y	N	-	-	N	-	-	N	-	-
	PDE4C	N	-	-	N	-	-	Y	4.26	1.9E-06	N	-	-
	PDE6A	N	-	-	N	-	-	Y	2.28	1.3E-02	N	-	-
	PDE6B	N	-	-	N	-	-	N	-	-	Y	0.48	1.4E-02
	PDE6C	N	-	-	N	-	-	Y	3.40	4.7E-02	N	-	-
	PDE6G	N	-	-	N	-	-	Y	0.42	5.6E-06	Y	0.27	1.1E-03
	PDE7A	N	-	-	N	-	-	N	-	-	Y	2.06	3.9E-02
	PDE7B	N	-	-	N	-	-	Y	0.32	7.2E-12	Y	0.33	6.2E-03
	PDE11A	N	-	-	N	-	-	Y	0.49	3.0E-04	Y	0.11	4.3E-10

	SMPDL3B	N	-	-	N	-	-	Y	2.58	5.4E-03	N	-	-
PHK	*PHKG1*	N	-	-	N	-	-	Y	2.08	4.1E-04	N	-	-
PKAr	*PRKAR2B*	N	-	-	N	-	-	Y	0.27	1.9E-15	Y	0.31	8.6E-04
	PRKCB	N	-	-	N	-	-	Y	0.37	4.8E-07	Y	0.36	1.6E-02
PKC	*PRKD1*	N	-	-	N	-	-	Y	2.13	1.6E-05	N	-	-
	PRKD3	Y	TSG	Y	N	-	-	N	-	-	N	-	-
PKI	*PKIA*	N	-	-	N	-	-	Y	4.46	1.9E-02	N	-	-
	PKIB	N	-	-	N	-	-	Y	3.33	2.9E-04	N	-	-
	PLCB1	N	-	-	N	-	-	Y	2.68	2.6E-08	N	-	-
	PLCB2	N	-	-	N	-	-	N	-	-	Y	0.47	2.4E-02
	PLCB4	N	-	-	N	-	-	Y	2.74	1.4E-03	N	-	-
	PLCD3	N	-	-	Y	5.42	4.7E-02	Y	2.97	2.8E-04	N	-	-
PLC	*PLCD4*	N	-	-	Y	5.39	1.7E-02	Y	3.46	3.1E-02	Y	2.03	2.7E-02
	PLCE1	N	-	-	N	-	-	Y	4.31	2.0E-12	Y	7.32	4.6E-02
	PLCG1	N	-	-	N	-	-	Y	2.07	2.0E-13	Y	2.59	2.2E-02
	PLCH2	N	-	-	N	-	-	Y	6.39	3.2E-05	N	-	-
	PLCL1	N	-	-	N	-	-	N	-	-	Y	2.04	2.8E-02
	PLCZ1	N	-	-	N	-	-	N	-	-	Y	0.31	2.0E-02
	PPP1CC	N	-	-	N	-	-	N	-	-	Y	1.97	4.3E-02
PP1	*PPP1R7*	N	-	-	N	-	-	N	-	-	Y	0.76	3.7E-02
	PPP1R14D	N	-	-	N	-	-	Y	17.04	3.6E-02	N	-	-
	PPP3CA	N	-	-	N	-	-	N	-	-	Y	0.70	5.2E-03
PP2B	*PPP3CB*	N	-	-	N	-	-	N	-	-	Y	1.28	4.1E-02
	PPP3R2	N	-	-	N	-	-	Y	4.02	2.8E-02	N	-	-
	CDC14B	N	-	-	N	-	-	N	-	-	Y	0.45	3.2E-02
	CDC25A	N	-	-	N	-	-	Y	4.54	1.7E-07	N	-	-
	CDC25B	N	-	-	N	-	-	Y	2.12	2.8E-09	N	-	-
	CDC25C	N	-	-	N	-	-	Y	18.81	1.8E-14	N	-	-
	CDKN3	N	-	-	N	-	-	Y	16.16	1.0E-15	Y	44.90	3.1E-02
	DUSP2	N	-	-	N	-	-	Y	0.43	2.0E-04	Y	0.23	3.8E-05
	DUSP5	N	-	-	N	-	-	Y	0.34	2.2E-06	N	-	-
	Dusp6	N	-	-	N	-	-	Y	0.35	6.3E-11	Y	0.31	7.1E-07
	Dusp7	N	-	-	Y	3.05	2.2E-02	N	-	-	N	-	-
	DUSP10	N	-	-	N	-	-	Y	0.48	1.1E-07	Y	0.33	1.8E-07
PTP	*DUSP15*	N	-	-	N	-	-	Y	3.22	1.4E-02	N	-	-
	Dusp16	N	-	-	Y	2.23	1.4E-02	N	-	-	Y	0.64	1.9E-02
	EPM2A	N	-	-	N	-	-	N	-	-	Y	0.47	1.0E-02
	MTMR3	Y	TSG	Y	N	-	-	N	-	-	N	-	-
	PGP	N	-	-	N	-	-	Y	2.36	4.0E-06	N	-	-
	PTP4A1	N	-	-	N	-	-	N	-	-	Y	0.52	6.9E-03
	PTPN5	N	-	-	N	-	-	Y	3.61	3.7E-06	N	-	-
	PTPN23	N	-	-	N	-	-	N	-	-	Y	1.46	3.9E-02
	PTPRC	N	-	-	N	-	-	Y	0.47	1.9E-04	N	-	-
	PTPRD	Y	TSG	Y	N	-	-	N	-	-	N	-	-
	PTPRN	N	-	-	N	-	-	Y	3.73	4.6E-03	N	-	-
PYG	*Pygb*	N	-	-	Y	7.74	1.7E-03	Y	2.63	4.5E-13	N	-	-
	Pygl	N	-	-	N	-	-	N	-	-	Y	0.59	4.7E-02
RAP1GAP	*RAP1GAP*	N	-	-	N	-	-	Y	2.12	2.6E-04	N	-	-
RHOA	*RHOA*	N	-	-	N	-	-	N	-	-	Y	1.37	2.4E-02
RGS14	*RGS14*	N	-	-	N	-	-	N	-	-	Y	0.59	3.7E-03
RGS18	*RGS18*	N	-	-	N	-	-	Y	0.38	2.8E-07	Y	0.36	8.1E-05
ROCK	*ROCK2*	Y	TSG	Y	N	-	-	N	-	-	N	-	-
RYR	*RYR2*	N	-	-	N	-	-	Y	4.81	2.4E-02	N	-	-

TCF/LEF	*LEF1*	N	-	-	N	-	-	Y	9.77	1.7E-09	N	-	-
	TCF3	N	-	-	N	-	-	Y	2.17	1.1E-16	Y	2.56	3.8E-02
	TCF7L2	Y	TSG	Y	N	-	-	N	-	-	N	-	-
	TCF12	Y	TSG	Y	N	-	-	N	-	-	N	-	-
TH	*TH*	N	-	-	N	-	-	N	-	-	Y	0.14	3.2E-06
TNI	*TNNI2*	N	-	-	N	-	-	Y	4.12	1.9E-03	N	-	-
VASP	*Vasp*	N	-	-	Y	3.30	1.4E-02	N	-	-	N	-	-
Protein product/family	**Gene(s) not significantly altered**												
14-3-3	*PRKCZ, YWHAB, YWHAE, YWHAG, YWHAQ, YWHAZ*	N	-	-	N	-	-	N		-	N	-	-
ADCY	*ADCY3, ADCY4, ADCY5, ADCY7, ADCY10*	N	-	-	N	-	-	N		-	N	-	-
ADD	*ADD1, ADD2, ADD3*	N	-	-	N	-	-	N		-	N	-	-
AKAP	*AKAP1, AKAP4, AKAP5, AKAP6, AKAP7, AKAP8, AKAP9, AKAP10, AKAP11, AKAP13*	N	-	-	N	-	-	N		-	N	-	-
APC	*ANAPC1, ANAPC10, ANAPC11, ANAPC2, ANAPC5, ANAPC7, CDC16, CDC23, CDC26, CDC27*	N	-	-	N	-	-	N		-	N	-	-
ATF1	*ATF1*	N	-	-	N	-	-	N		-	N	-	-
BAD	*BAD*	N	-	-	N	-	-	N		-	N	-	-
BRAF	*BRAF*	N	-	-	N	-	-	N		-	N	-	-
CALM	*CALML5*	N	-	-	N	-	-	N		-	N	-	-
CAMK	*CAMK1, CAMK1D, CAMK1G,CAMK2D*	N	-	-	N	-	-	N		-	N	-	-
CaN	*CHP1*	N	-	-	N	-	-	N		-	N	-	-
CNG	*CNGA2, CNGA3, CNGA4, CNGB1*	N	-	-	N	-	-	N		-	N	-	-
CRAF	*RAF1*	N	-	-	N	-	-	N		-	N	-	-
CREB	*ATF2, ATF4, CREB1, CREB3, CREBBP, EP300*	N	-	-	N	-	-	N		-	N	-	-
CREM	*CREM*	N	-	-	N	-	-	N		-	N	-	-
CTNNB1	*CATNB, CTNNB, CTNNB1*	N	-	-	N	-	-	N		-	N	-	-
ELK1	*ELK, ELK1*	N	-	-	N	-	-	N		-	N	-	-
EPAC	*RAPGEF4*	N	-	-	N	-	-	N		-	N	-	-
ERK 1/2	*MAPK1, MAPK3*	N	-	-	N	-	-	N		-	N	-	-
FAK	*PTK2, PTK2B*	N	-	-	N	-	-	N		-	N	-	-
FLN	*FLNA*	N	-	-	N	-	-	N		-	N	-	-
Gαi	*GNAI1, GNAI2*	N	-	-	N	-	-	N		-	N	-	-
Gαq	*GNA11, GNA15*	N	-	-	N	-	-	N		-	N	-	-
Gαs	*GNAS*	N	-	-	N	-	-	N		-	N	-	-
Gβ	*GNB1, GNB2, GNB3, GNB4, GNB5, RACK1*	N	-	-	N	-	-	N		-	N	-	-

Gγ	*GNG13, GNG2, GNG3, GNG5, GNG7, GNG10, GNG11, GNG12*	N	-	-	N	-	-	N	-	N	-	-
GNA13	*GNA13*	N	-	-	N	-	-	N	-	N	-	-
GPCR	*ADORA2A, ADORA2B, ADRA2A, Agtr1b, AGTR2, APLNR, AVPR1B, CALCR, CCR4, CHRM1, CHRM4, CHRM5, CNR2, CRHR1, DRD1, DRD2, DRD3, DRD5, FFAR3, FSHR, GABBR1, GPER1, GPR17, GRM3, GRM4, GRM5, GRM6, GRM7, HCAR2, HCAR3, HRH1, HRH2, HRH3, HTR1A, HTR1B, HTR1E, HTR2A, HTR2B, HTR2C, HTR5A, Htr5b, HTR6, LHCGR, LPAR1, LTB4R, MC2R, MC3R, MC4R, MC5R, NPR3, OPRD1, OPRK1, OPRL1, OPRM1, P2RY14, PTGER3, PTGER4, RXFP4, S1PR1, S1PR3, SSTR3, TAAR1, VIPR2*	N	-	-	N	-	-	N	-	N	-	-
GRK	*GRK1, GRK7*	N	-	-	N	-	-	N	-	N	-	-
GSK3	*GSK3A, H2BFM*	N	-	-	N	-	-	N	-	N	-	-
GYS	*GYS1*	N	-	-	N	-	-	N	-	N	-	-
ITPR	*ITPR1, ITPR2*	N	-	-	N	-	-	N	-	N	-	-
KDELR	*KDELR1, KDELR2*	N	-	-	N	-	-	N	-	N	-	-
MEK2	*MAP2K2*	N	-	-	N	-	-	N	-	N	-	-
MKP 1/2/3/4	*DUSP4*	N	-	-	N	-	-	N	-	N	-	-
MP1	*MP1*	N	-	-	N	-	-	N	-	N	-	-
NFAT	*NFATC1, NFATC2, NFATC3, NFAT5*	N	-	-	N	-	-	N	-	N	-	-
NOS3	*NOS3*	N	-	-	N	-	-	N	-	N	-	-
NTN1	*NTN1*	N	-	-	N	-	-	N	-	N	-	-
PDE	*APEX1, MPPE1, PDE1A, PDE3A, PDE4A, PDE4B, PDE4D, PDE5A, PDE6D, PDE6H, PDE8A, PDE8B, PDE9A, PDE10A, PDE12, SMPDL3A, TDP2, TULP2*	N	-	-	N	-	-	N	-	N	-	-

PHK	*PHKA2, PHKB, PHKG2*	N	-	-	N	-	-	N	-	N	-	-
PKAc	*PRKACA, PRKACB, PRKACG*	N	-	-	N	-	-	N	-	N	-	-
PKAg	*PRKAG1, PRKAG2*	N	-	-	N	-	-	N	-	N	-	-
PKAr	*PRKAR1A, PRKAR1B, PRKAR2A*	N	-	-	N	-	-	N	-	N	-	-
PKC	*PRKCA, PRKCD, PRKCE, PRKCG, PRKCH, PRKCI, PRKCQ, PRKCZ*	N	-	-	N	-	-	N	-	N	-	-
PKI	*PKIG*	N	-	-	N	-	-	N	-	N	-	-
PLC	*NOTUM, PDIA3, PLCB3, PLCD1, Plcd2, PLCG2, PLCL2*	N	-	-	N	-	-	N	-	N	-	-
PLN	*PLB, Plm, PLN*	N	-	-	N	-	-	N	-	N	-	-
PP1	*PPP1CA, PPP1CB, PPP1R1B, PPP1R3A, PPP1R3C, PPP1R3D, PPP1R10, PPP1R11, PPP1R12A, PPP1R14A, PPP1R14B, PPP1R14C*	N	-	-	N	-	-	N	-	N	-	-
PP2B	*PPP3CC, PPP3R1*	N	-	-	N	-	-	N	-	N	-	-
PTP	*ACP1, DUSP1, DUSP3, DUSP4, DUSP8, DUSP9, DUSP11, DUSP12, DUSP18, DUSP21, DUSP22, DUSP26, EYA1, EYA2, EYA3, PTEN, PTPDC1, PTPN1, PTPN2, PTPN3, PTPN4, PTPN6, PTPN7, PTPN9, PTPN11, PTPN12, PTPN13, PTPN14, PTPN18, PTPN21, PTPN22, PTPRA, PTPRB, PTPRE, PTPRF, PTPRG, PTPRH, PTPRJ, PTPRK, PTPRM, PTPRO, PTPRR, PTPRS, PTPRT, PTPRU, PTPRZ1, SIRPA, TIMM50, UBASH3B*	N	-	-	N	-	-	N	-	N	-	-
PXN	*PXN*	N	-	-	N	-	-	N	-	N	-	-
PYG	*PYGM*	N	-	-	N	-	-	N	-	N	-	-
RAP1	*RAP1A, RAP1B*	N	-	-	N	-	-	N	-	N	-	-

RGS	*RGS2, RGS4, RGS7, RGS10, RGS12, RGS18*	N	-	-	N	-	-	N	-	N	-	-
ROCK	*ROCK1*	N	-	-	N	-	-	N	-	N	-	-
RYR	*RYR1, RYR3*	N	-	-	N	-	-	N	-	N	-	-
TCF/LEF	*HNF1A, TCF4, Tcf7, TCF7L1*	N	-	-	N	-	-	N	-	N	-	-
TNI	*TNNI1, TNNI3*	N	-	-	N	-	-	N	-	N	-	-

Table 2.7: Primer sequneces for RT-PCR

Transcript	Primer sequences	Amplicon size	Annealing temperature (°C)
β-actin	5′-TCCAGCCTTCCTTCTTGGGTATGGA-3′ 5’-CGCAGCTCAGTAACAGTCCGCC-3’	*365 bp*	*57*
FoxA1	5’-GGATGGTTGTGTCGGCCGGG-3’ 5’-AGGAGTAGGCCTCCTGCGTGT-3’	*113bp*	*60*
ApoM	5’- ACTGCAGAGCACCAACTCTC-3’ 5’-GGGTGTGGTGACCGATTGTA-3’	*492 bp*	*57*
Nat10	5’-GGCCTTGCTGTCATACCAGT-3’ 5’- TTCCCAAGAGAAGAGCCGAC-3’	*281 bp*	*57*
Fah	5’-TTACTCCCACAGCTCCTGG-3’ 5’-TGGCTTTGGGTTGCTTTGAG-3’	*275 bp*	*55*

PCR was performed with an initial denaturing step of 95°C for 15 min; 40-cycles of denaturing at 94°C for 15 sec, annealing at above specified temperatures, and extension at 72°C for 30 sec with optics on.

Table 2.8: Antibodies for IHC

Protein	Antibody	Dilution
SB	R&D Systems MAB2798	1:100
ALB	Novus Biologicals NBP132458	1:200
FOXA1	Abcam AB23738	1:200
phospho T156 FOXA2	Abgent AP13206C	1:100
NAT10	Abcam AB194297	1:250
FAH	AbboMax 602-910	1:250
phospho T197 PKA	Abcam AB59218	1:1000

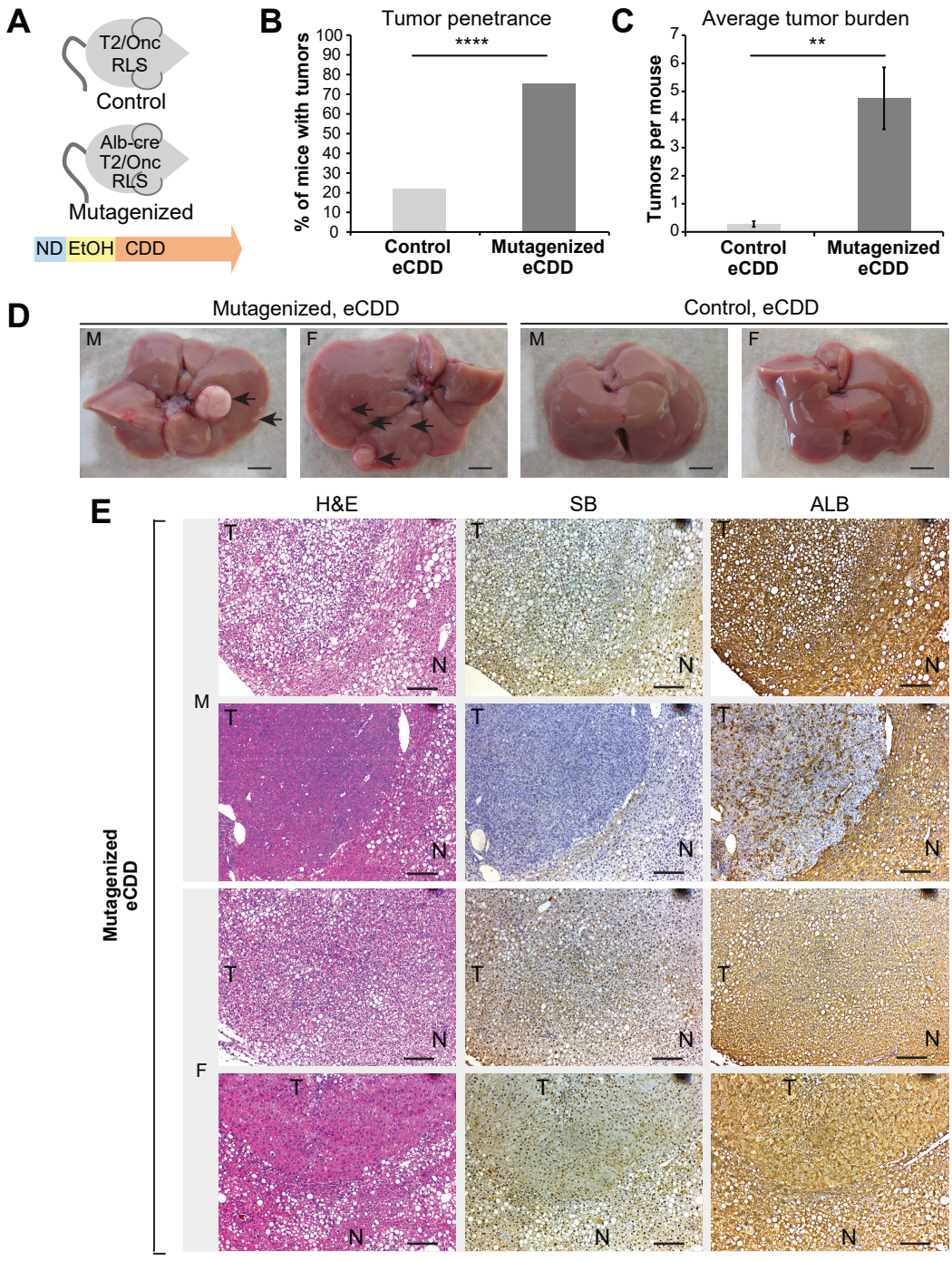

Figure 2.1. SB transposition and eCDD treatment in mice promotes steatosis-associated liver tumorigenesis. (A) Mouse genotype and treatment model. EtOH, 5% ethanol drinking water. CDD, choline-deficient diet. RLS, *Rosa26*-Lsl-SB11. Alb-cre, *Albumin*-cre. (B) Tumor penetrance and (C) average tumor burden in control (n = 32) and SB-mutagenized mice (n = 49) treated with eCDD. (D) Gross livers from SB-mutagenized and control mice treated with eCDD. Arrows, tumors. Gross liver scalebars, 0.5 cm. (E) H&E and IHC for SB and ALB stained mouse liver sections. Liver section scale bars, 100 μm. T, tumor. N, non-tumor tissue. $^{**}P < .01$. $^{****}P < .0001$. Error bars represent SEM. M, male mouse. F, female mouse.

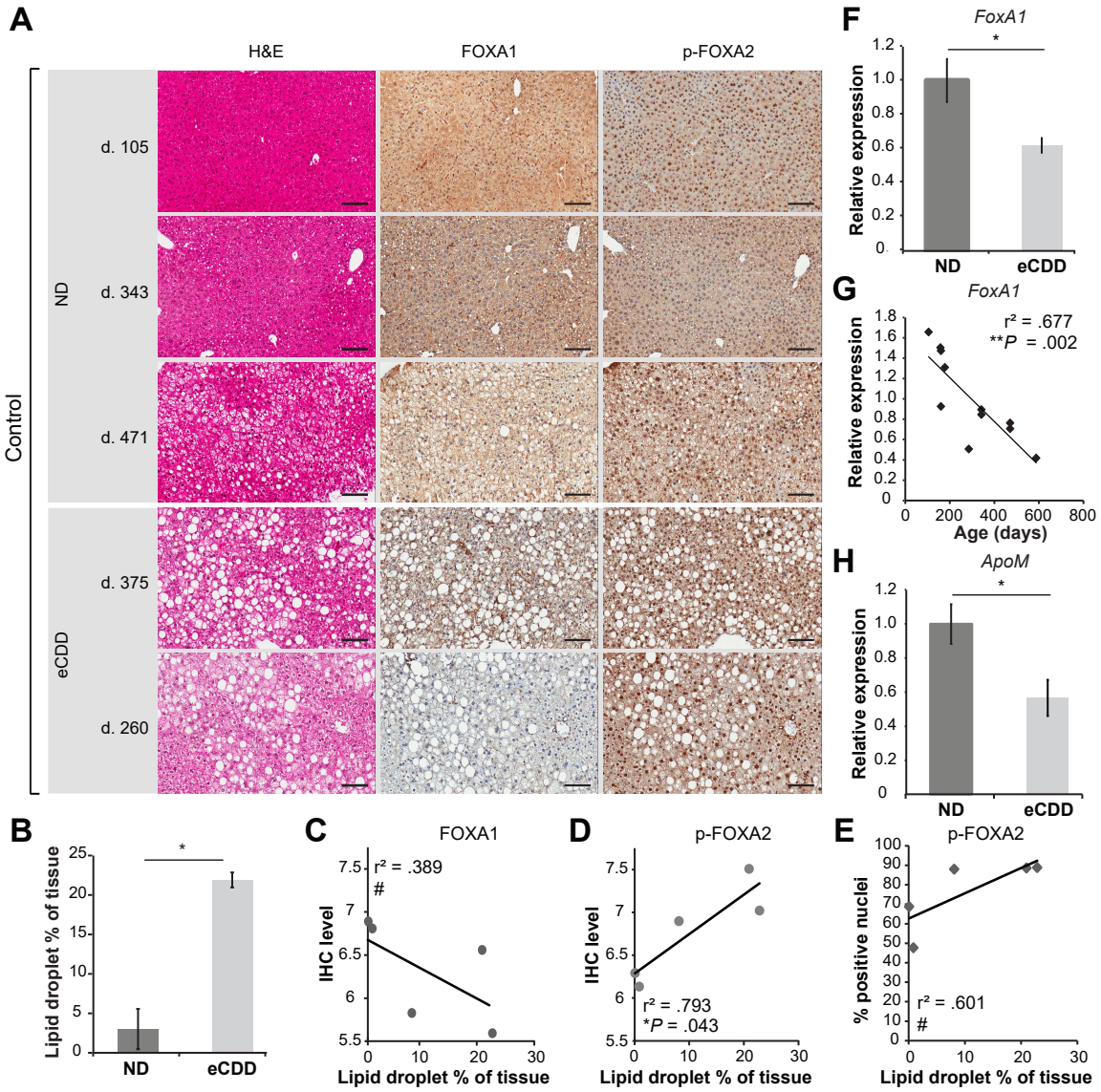

Figure 2.2. FOXA1 and FOXA2 repressed in steatotic liver. (A) Hematoxylin and eosin (H&E) and IHC for FOXA1 (FOXA1) and phosphorylated T156 FOXA2 (p-FOXA2) stained liver sections from control mice treated with ND, ages 105, 343, 471 days (top three rows) or eCDD, ages 375, 260 days (bottom two rows). Scalebars, 100μm. (B) Lipid droplet percent of liver tissue from the H&E stained liver slides from mice on ND vs eCDD pictured in panel A. (C) FOXA1 IHC stain level vs lipid droplet percent of liver tissue measured from the mouse liver slides pictured in panel A. (D) p-FOXA2 IHC stain level vs lipid droplet % of liver tissue from the mouse liver slides pictured in panel A. (E) Percent of cells with p-FOXA2 stained nuclei vs lipid droplet % of liver tissue from the mouse liver slides pictured in panel A. (F) qRT-PCR of control liver tissue from mice treated with ND vs eCDD for *FoxA1*, normalized to *Actb* and average ND level. (G) qRT-PCR of control mouse liver tissue from mice treated with ND for *FoxA1*, normalized to *Actb* average ND level, vs mouse age. (H) qRT-PCR of control mouse liver tissue from mice treated with ND vs eCDD for *ApoM*, normalized to *Actb* and average ND level. r, Pearson's correlation coefficient. #*P* > .05. **P* < .05. ***P* < .01. Error bars represent SEM.

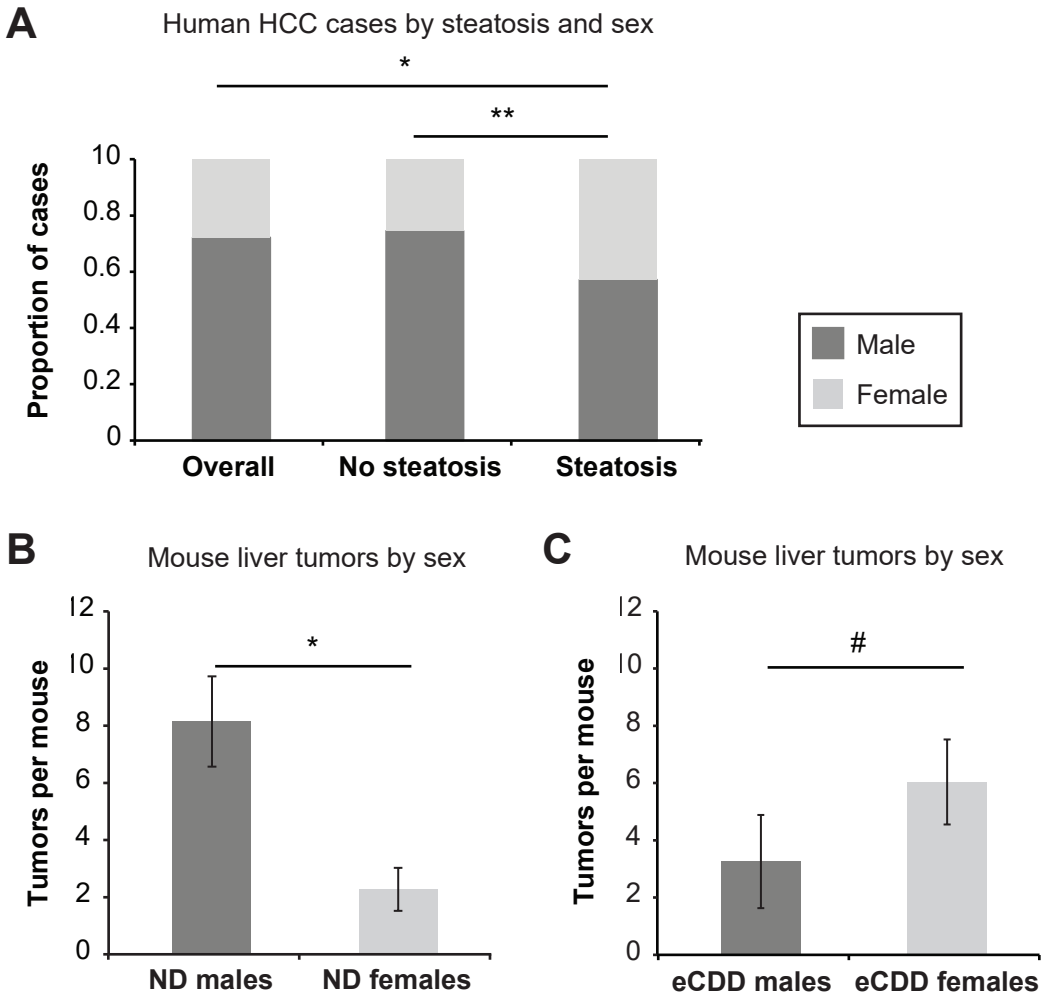

Figure 2.3. Reduced male HCC sex bias in fatty liver. (A) Male and female proportions of human HCC cases by steatosis status. (B) Average tumor burden per ND treated, SB-mutagenized male (n = 27) and female (n = 11) mouse. (C) Average tumor burden per eCDD treated, SB-mutagenized male (n = 23) and female (n = 26) mouse. #*P* > .05. **P* < .05. ***P* < .01. Error bars represent SEM.

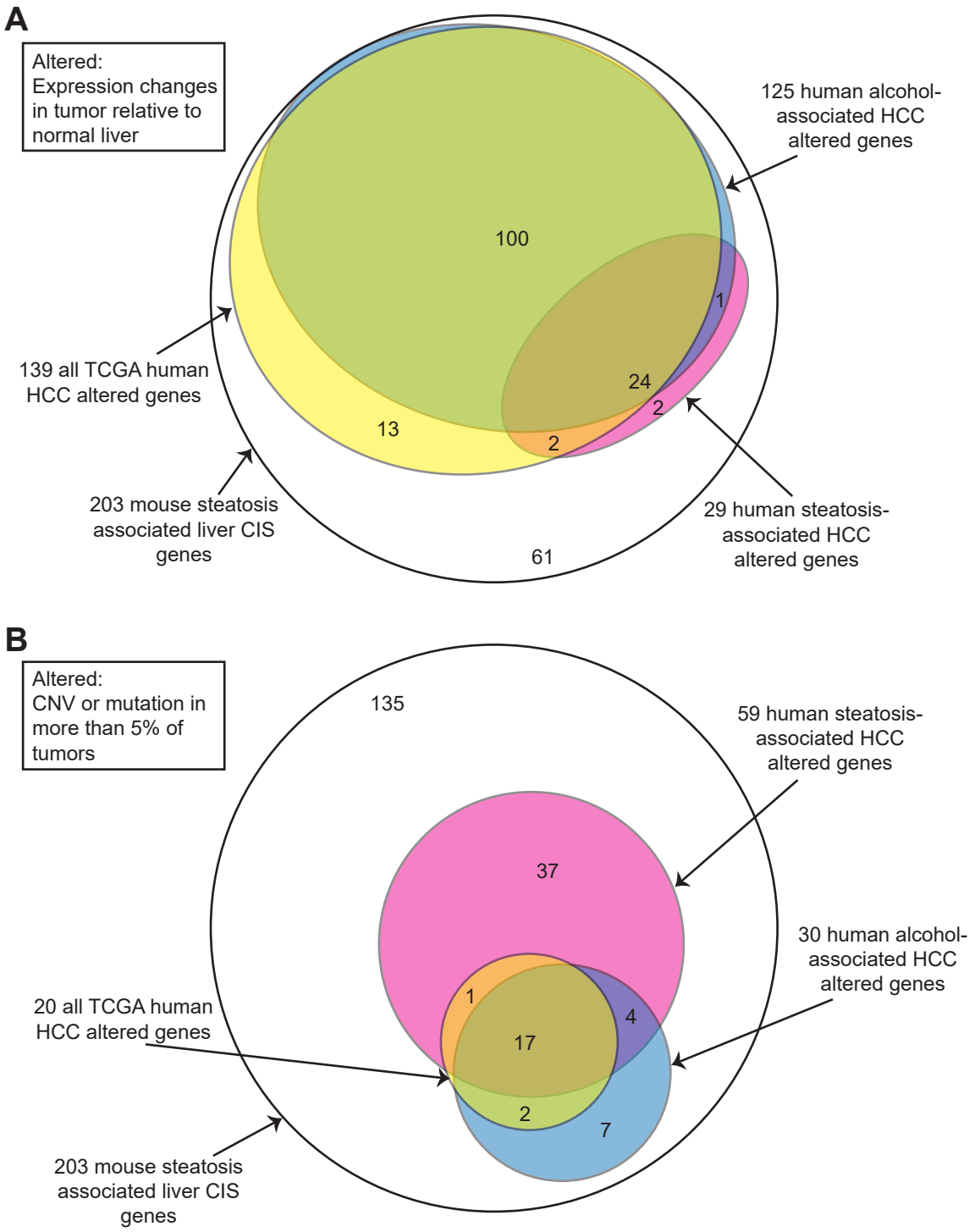

Figure 2.4. Steatosis-associated liver cancer CIS genes altered in human HCC. (A) Representation of the 203 CIS genes and subsets with significant expression changes in and (B) subsets altered in more than 5% of tumors by amplification, mutation, or deletion in all TCGA HCC cases, steatosis- associated HCC, and alcohol-associated HCC.

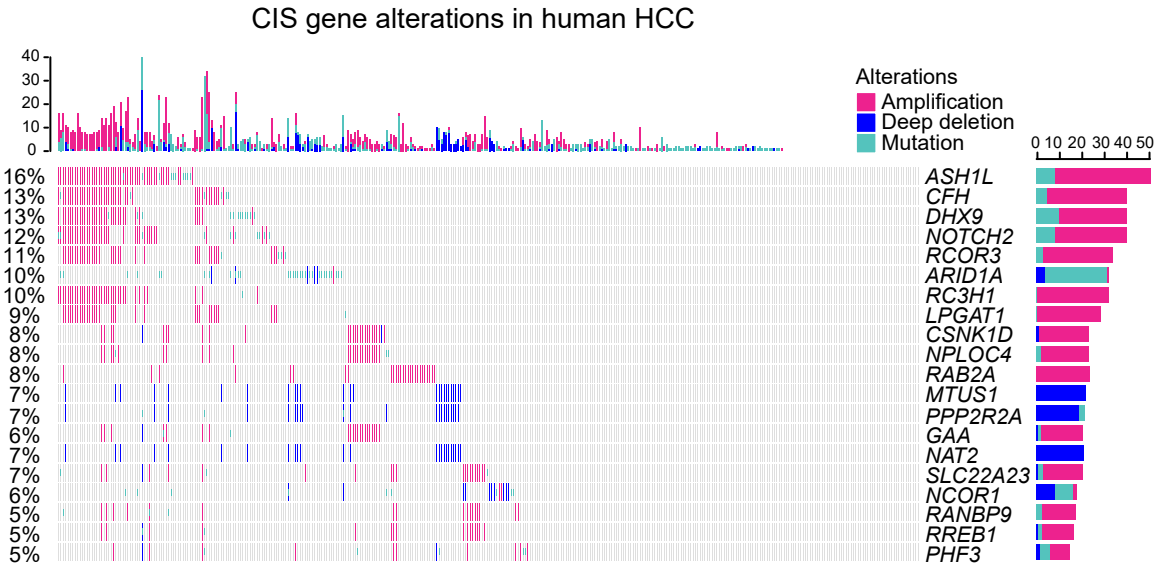

Figure 2.5. Oncoprint showing steatosis-associated CIS gene amplifications, deep deletions, and mutations occurring in at least 5% of all TCGA HCC cases. Amplification, high copy number change. Mutation, any frame shift, stop, or amino acid change.

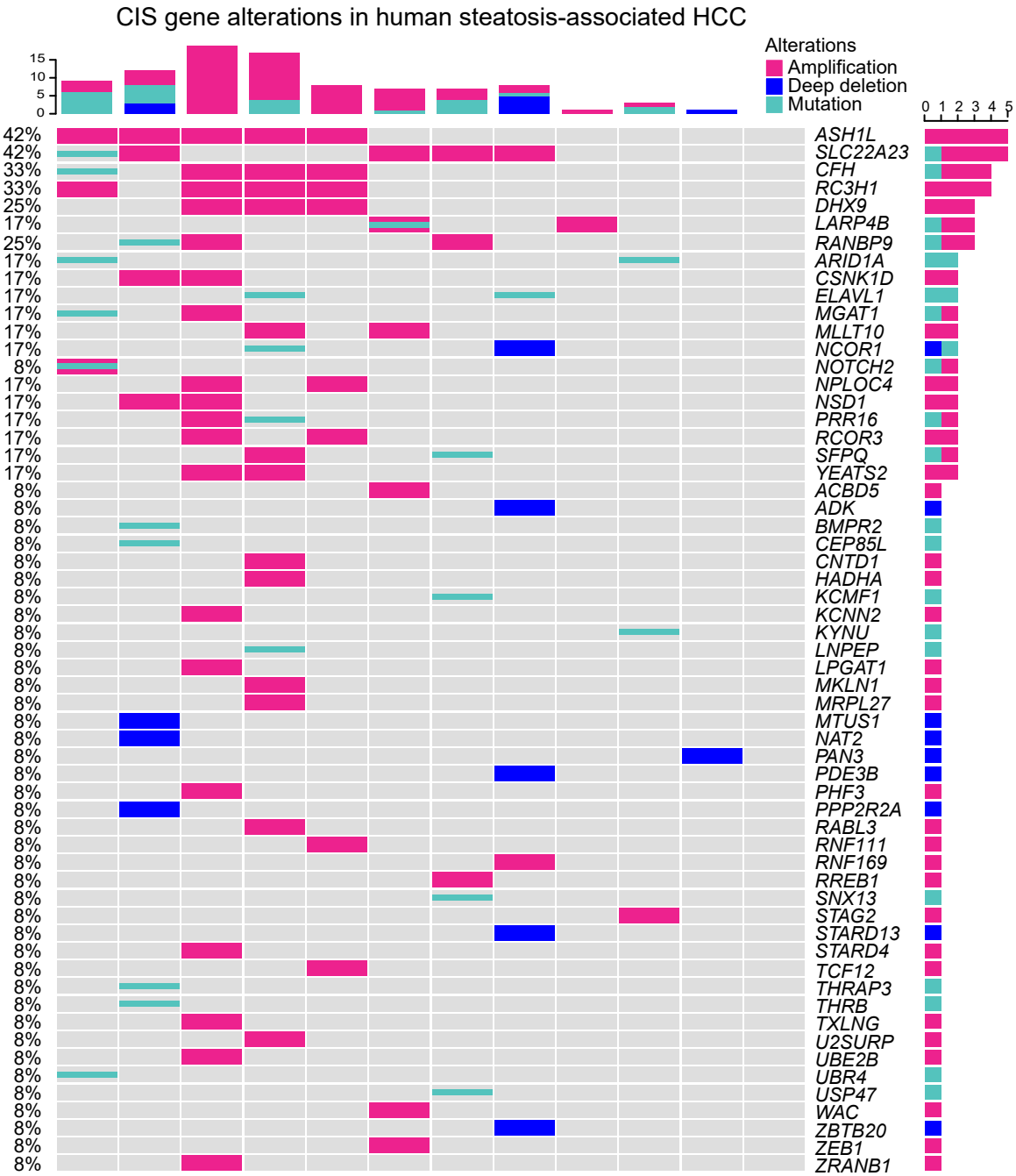

Figure 2.6. Oncoprint showing steatosis-associated CIS gene amplifications, deep deletions, and mutations occurring in at least 5% of steatosis-associated TCGA HCC cases. Amplification, high copy number change. Mutation, any frame shift, stop, or amino acid change.

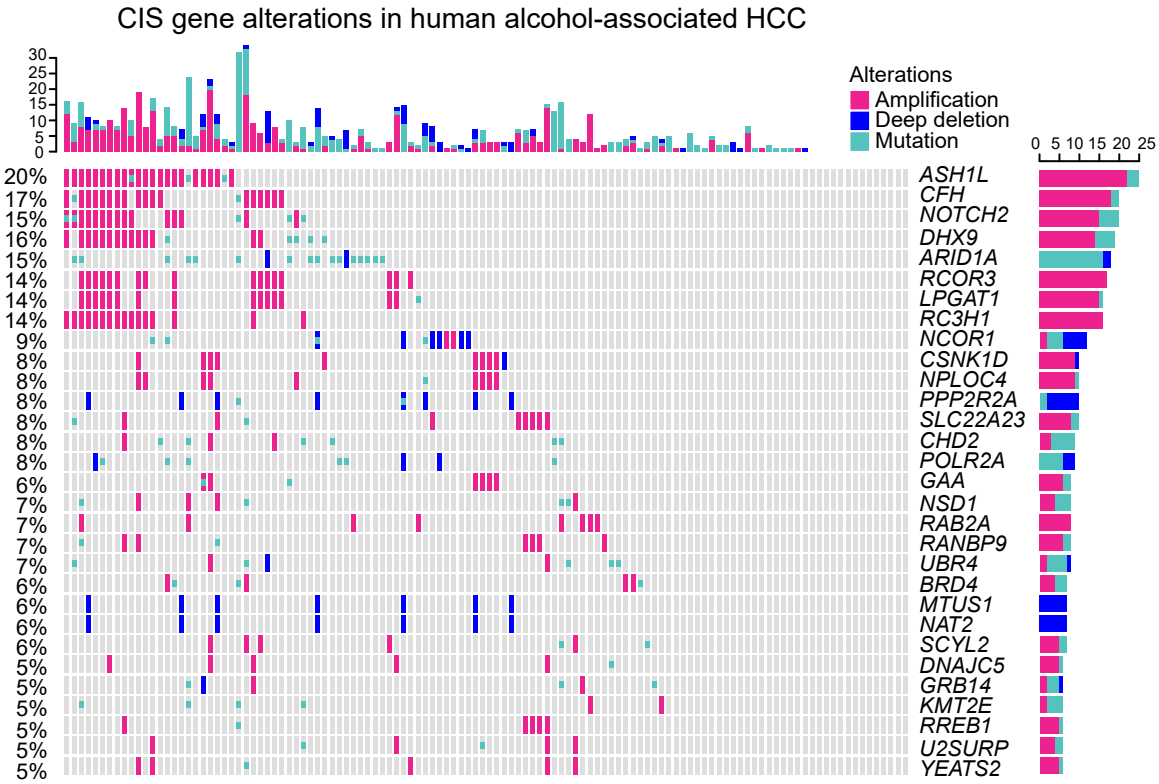

Figure 2.7. Oncoprint showing steatosis-associated CIS gene amplifications, deep deletions, and mutations occurring in at least 5% of alcohol-associated TCGA HCC cases. Amplification, high copy number change. Mutation, any frame shift, stop, or amino acid change.

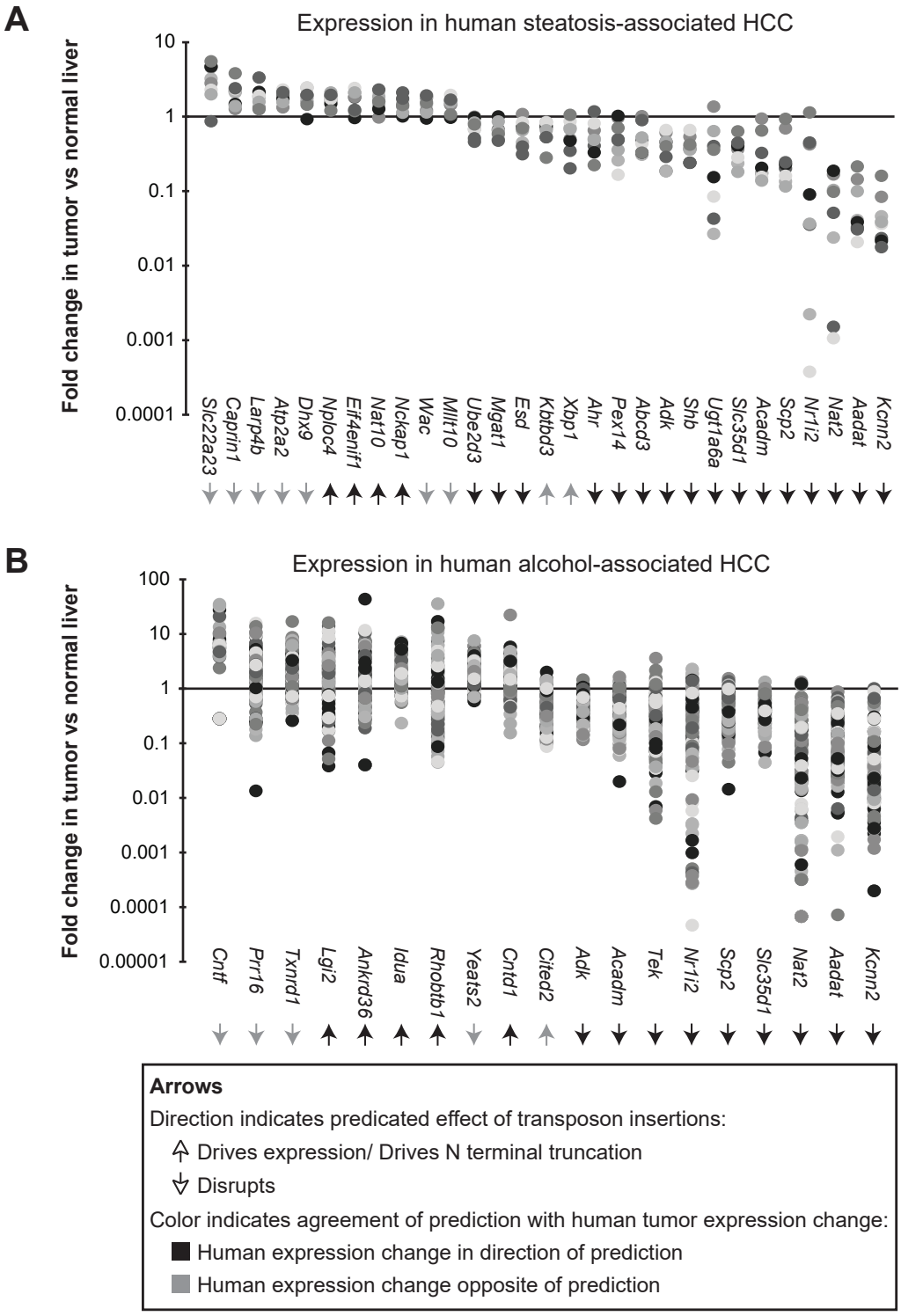

Figure 2.8. Transposon insertions in CIS genes predict expression changes in human HCC. RNA expression fold change in tumor vs normal liver of the steatosis associated CIS genes with (A) significant expression changes in TCGA steatosis-associated HCC cases or (B) significant expression changes more than 2 fold in TCGA alcohol-associated HCC cases.

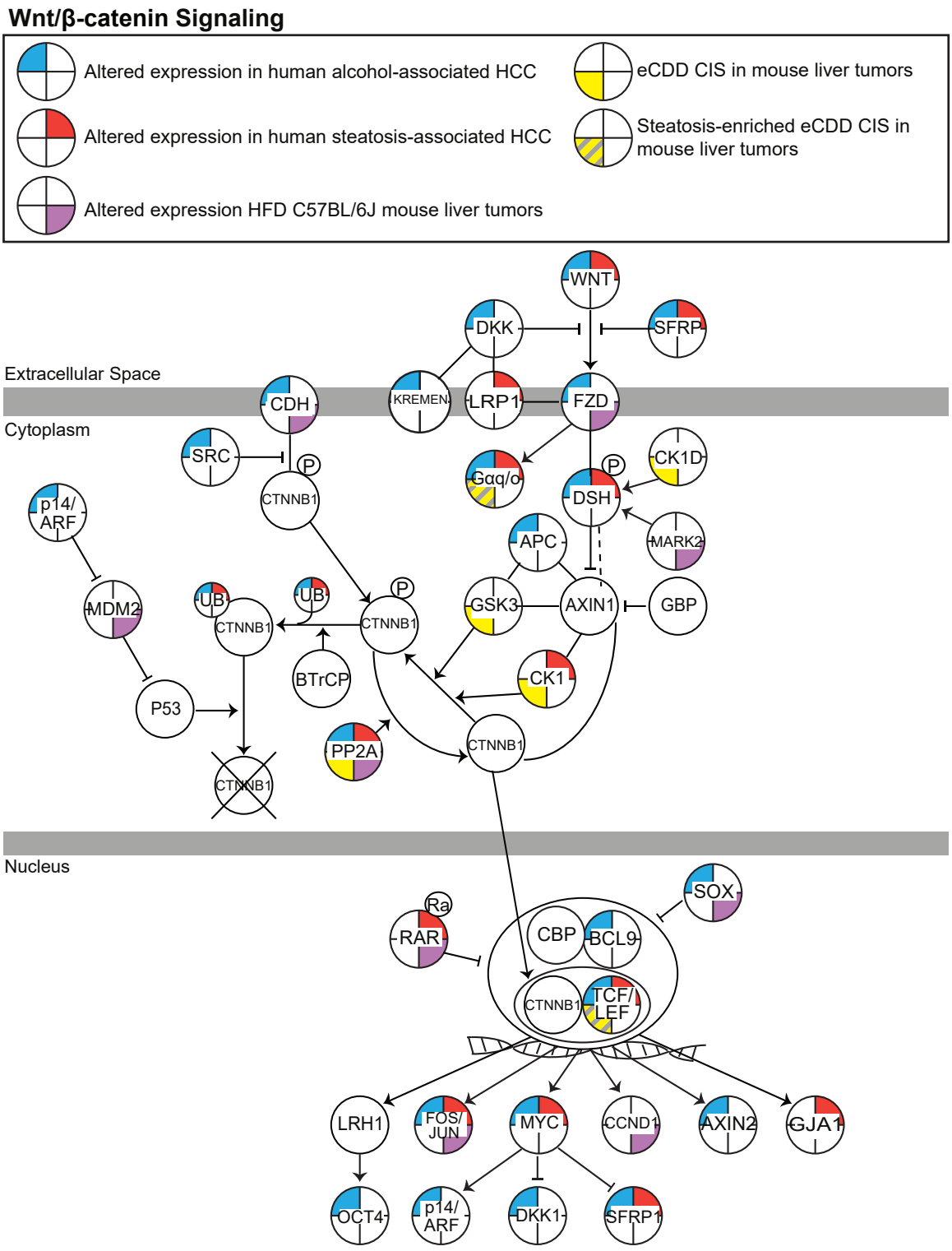

Figure 2.9. Wnt/β-catenin signaling alterations in steatosis-associated liver cancer. Schematic of the Wnt/β-catenin signaling pathway with protein families represented as circles. Proteins or families for which genes are altered in steatosis HCC mouse models or human HCC indicated by colored quadrants. HFD C57BL/6J, high fat diet-fed wildtype C57BL/6J mouse strain.

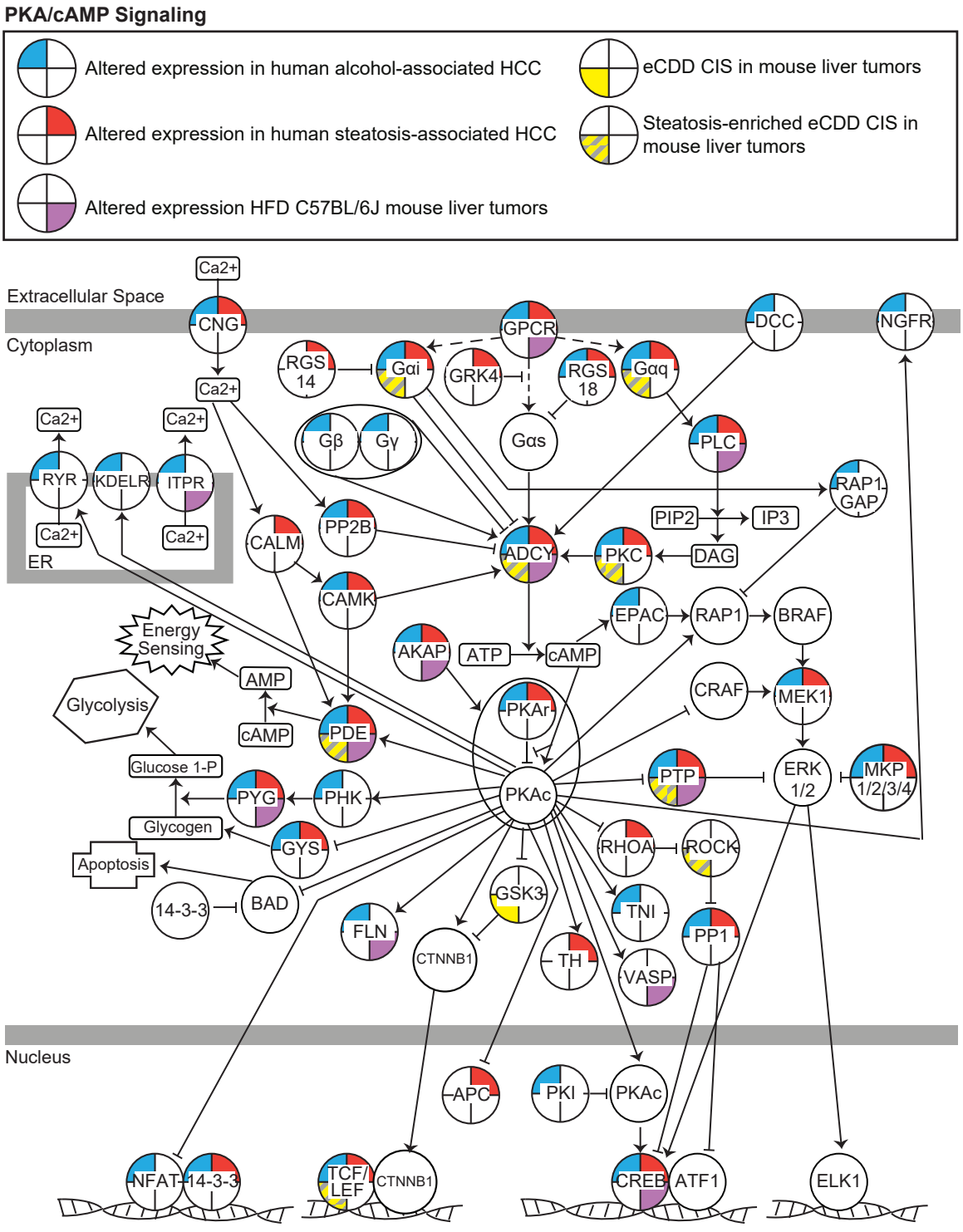

Figure 2.10. PKA/cAMP signaling alterations in steatosis-associated liver cancer. Schematic of the PKA/cAMP signaling pathway with protein families represented as circles. Proteins or families for which genes are altered in steatosis HCC mouse models or human HCC indicated by colored quadrants. HFD C57BL/6J, high fat diet-fed wildtype C57BL/6J mouse strain.

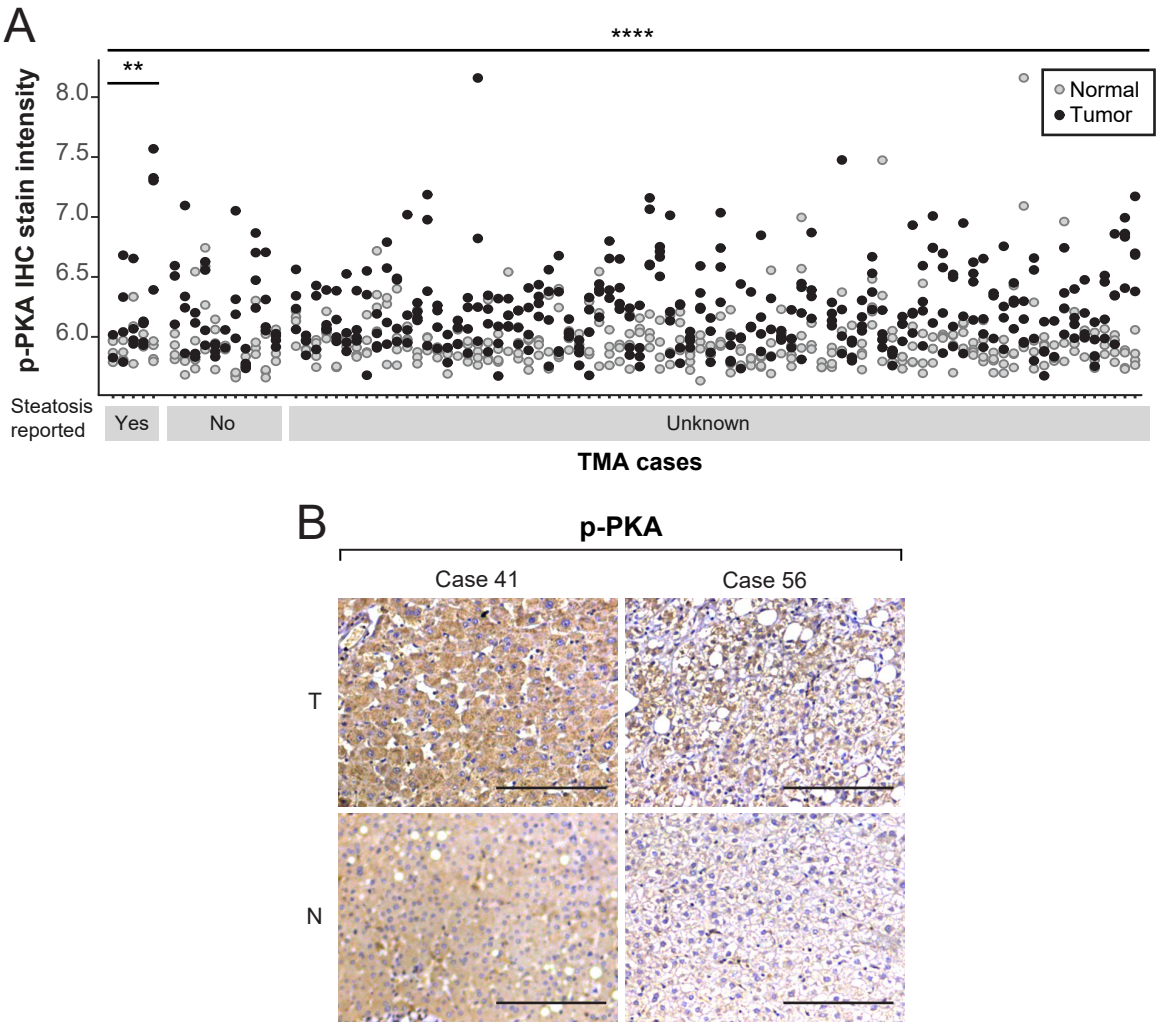

Figure 2.11. PKA is activated in HCC. (A) Phospho T197 PKA (p-PKA) IHC stain intensity of tumor and matched non-tumor liver samples on a tissue microarray (TMA) of human HCC cases stratified by mention of steatosis in pathology report. Yes, steatosis reported. No, no mention of steatosis or steatosis reported absent. Unknown, pathology report not available. (B) Representative IHC for p-PKA stained sections of human HCC (top) or matched normal liver (bottom) from TMA cases with hepatic steatosis indicated in pathology report. Scalebars, 100μm. T, tumor. N, non-tumor liver tissue. ***P* > .01. *****P* < .0001.

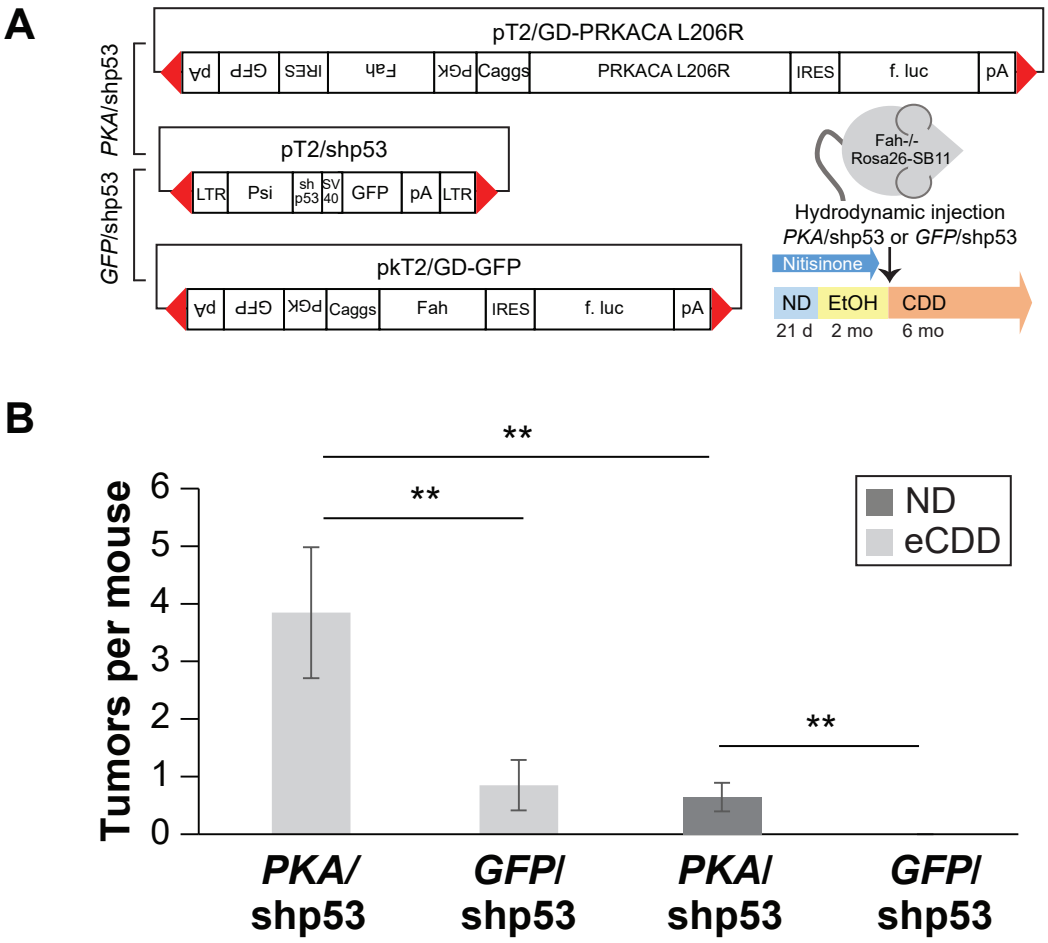

Figure 2.12. *PRKACA L206R* overexpression drives tumorigenesis in steatotic mouse livers. (A) Transposons for tumor induction and treatment plan. EtOH, 5% ethanol CDD, choline-deficient diet. Red triangles, SB inverted repeat/ direct repeat sequences. Caggs, Caggs promoter. PRKACA L206R, mouse *PKA* cDNA sequence with L206R mutation. IRES, internal ribosomal entry site. F. luc, firefly luciferase gene sequence. pA, polyadenylation signal. PGK, *PGK* promoter. Fah, mouse *Fah* cDNA. GFP, *GFP* cDNA sequence. d, days. mo, months. (B) Average tumors per *PKA*/shp53-injected mouse treated with eCDD (n = 13) or ND (n = 14) or *GFP*/shp53-injected mouse treated with eCDD (n = 20) or ND (n = 18). ***P* < .01. Error bars represent SEM.

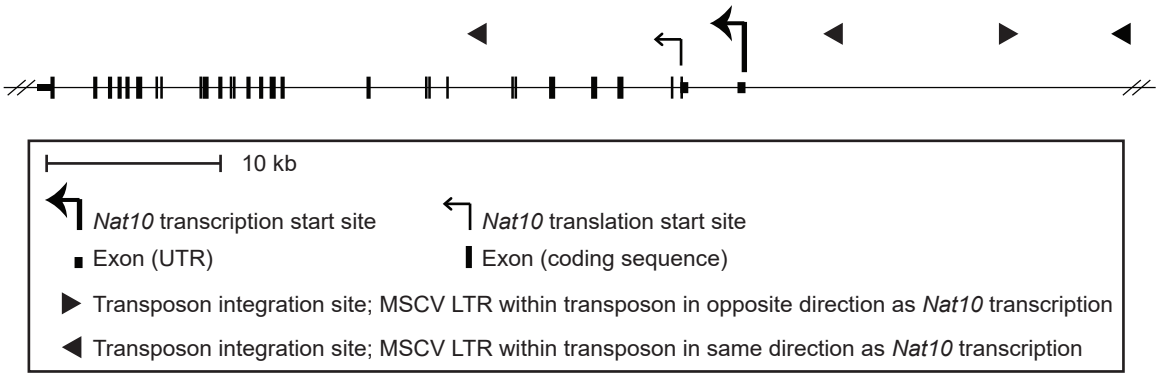

Figure 2.13. *Nat10* is a candidate oncogene in a mouse model of steatosis-associated HCC. Schematic of *Nat10* gene with transposon insertions eCDD treated SB mutagenized mice.

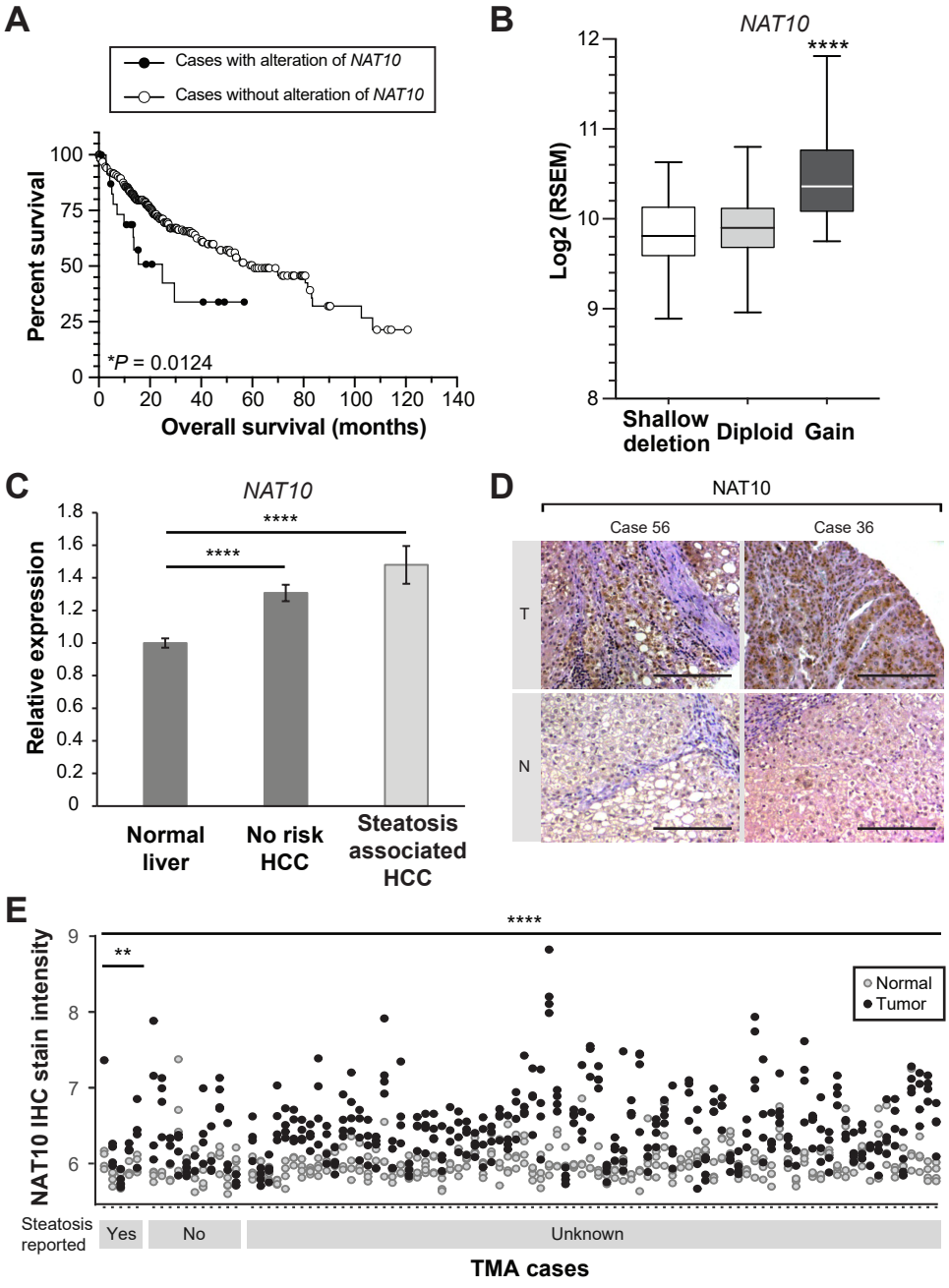

Figure 2.14. *NAT10* is altered in human steatosis-associated HCC. (A) Overall survival for TCGA HCC cases with and without *NAT10* overexpression or copy number gain alteration. (B) *NAT10* gene expression by copy number for TCGA HCC cases. (C) *NAT10* expression in TCGA no risk HCC and steatosis-associated HCC cases compared to normal liver. D) Representative IHC for NAT10 stained sections of human HCC (top) or matched normal liver (bottom) from TMA cases with hepatic steatosis indicated in pathology report. Scalebars, 100μm. T, tumor. N, non-tumor liver tissue. E) NAT10 IHC stain intensity of tumor and matched normal liver samples on TMA of human HCC cases stratified by mention of steatosis on pathology report. Yes, steatosis reported. No, no mention of steatosis or steatosis reported absent. Unknown, pathology report not available. *P < .05. **P < .01. ****P < .0001.

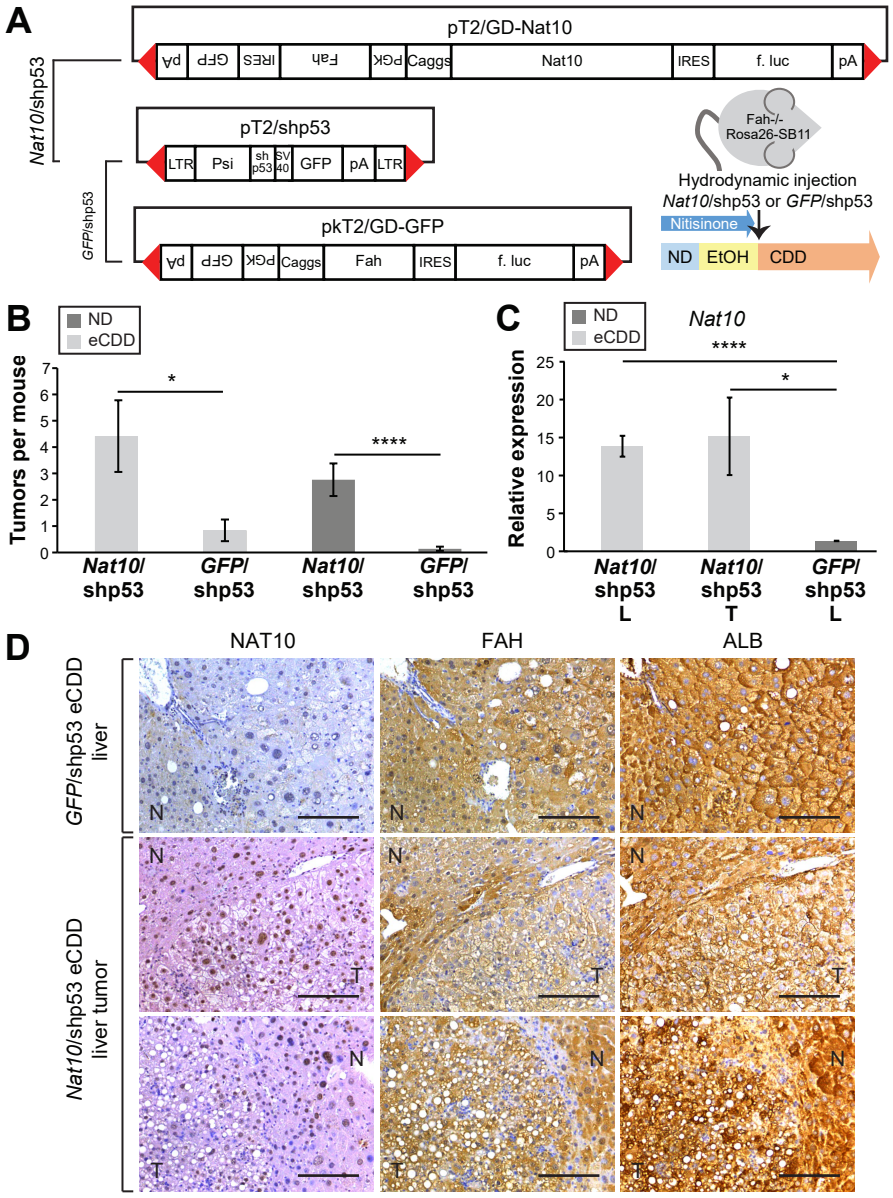

Figure 2.15. *Nat10* overexpression drives tumorigenesis in steatotic mouse livers. (A) Transposons for tumor induction plus treatment plan. EtOH, 5% ethanol CDD, choline-deficient diet. Red triangles, SB inverted repeat/ direct repeat recognition sequences. Caggs, Caggs promoter. Nat10, mouse *Nat10* cDNA sequence. IRES, internal ribosomal entry site. F. luc, firefly luciferase gene sequence. pA, polyadenylation signal. PGK, *PGK* promoter. Fah, mouse *Fah* cDNA. GFP, Green fluorescent protein gene sequence. (B) Average tumors per *Nat10*/shp53 injected mouse treated with eCDD (n = 24) or ND (n = 25) or *GFP*/shp53 injected mouse treated with eCDD (n = 25) or ND (n = 29). (C) *Nat10* RNA expression from non-tumor liver tissue (L) or liver tumor (T) from *Nat10*/shp53 or *GFP*/shp53 injected eCDD treated mice, normalized to *Actb* and to wild type mouse liver *Nat10* (n = 5 each). (D) Immunohistochemistry for NAT10, FAH, and ALB stained liver sections from eCDD treated mice injected with *GFP*/shp53 showing non-tumor liver tissue (top), or injected with *Nat10*/shp53 showing tumor plus adjacent non-tumor liver (middle and bottom). Scalebars, 100μm. T, tumor. N, non-tumor liver tissue. **P* < .05. *****P* < .0001. Error bars represent SEM.

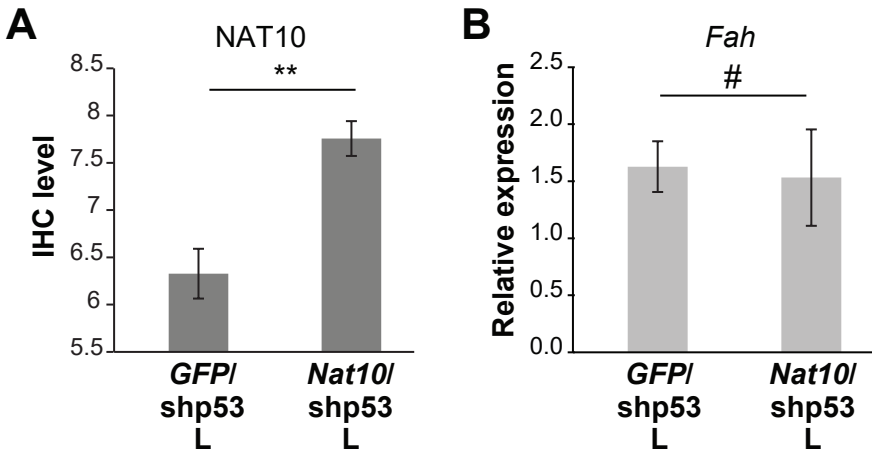

Figure 2.16. Transgenes are expressed in livers of *Fah* deficient mice after hydrodynamic injection (A) NAT10 IHC stain level in mouse livers from injected with *Nat10*/shp53 or *GFP*/shp53 from both diets combined. (B) *Fah* transcript expression from liver tissue from mice treated with eCDD injected with *Nat10*/shp53 or *GFP*/shp53, normalized to *Actb* and to wild type mouse liver *Fah*. #$P > .05$. **$P < .01$.

CHAPTER 3:

Sleeping Beauty transposon-based gene delivery for reverse genetic liver cancer models

*The following chapter contains material from previously published work and manuscripts in preparation:

Riordan JD, Keng VW, **Tschida BR**, Scheetz TE, Bell JB, Podetz-Pedersen KM, Moser CD, Copeland NG, Jenkins NA, Roberts LR, Largaespada DA, Dupuy AJ. Identification of rtl1, a retrotransposon-derived imprinted gene, as a novel driver of hepatocarcinogenesis. PLoS Genet 2013;9:e1003441.

Keng VW, Sia D, Sarver AL, **Tschida BR**, Fan D, Alsinet C, Solé M, Lee WL, Kuka TP, Moriarity BS, Villanueva A, Dupuy AJ, Riordan JD, Bell JB, Silverstein KA, Llovet JM, Largaespada DA. Sex bias occurrence of hepatocellular carcinoma in Poly7 molecular subclass is associated with EGFR. Hepatology 2013;57:120–30.

Jesse D. Riordan JD, Feddersen CR, **Tschida BR**, Beckmann PJ, Keng VW, Largaespada DA, Dupuy AJ. Liver fibrosis alters driver mutation profile in transposon-induced hepatocellular carcinoma. Under review.

Conboy CB, **Tschida BR**, Hu H, Alsinet C, Cornellà H, Pinyol R, Burns MB, Rathe SK, Abrahante J, Temiz NA, Linden MA, Amin K, Kuka T, Vélez Reyes GL, Keng VW, Harris RS, Llovet J, Starr TK, Largaespada DA. R-spondin 2 drives Wnt signaling and tumorigenesis in multiple tissues. In preparation.

Abstract

Hepatocellular carcinoma (HCC) is the second most common cancer-related cause of death globally and is occurring with increasingly frequency. To better understand the pathogenesis of HCC, candidate oncogenes identified in human HCC, complementary mouse models, and tumor-promoting viruses need to be functionally tested to determine their roles in driving liver tumorigenesis. New models need to be generated to study disease mechanisms and test prevention and treatment strategies in context of the relevant tumor-promoting molecular alterations. *Sleeping Beauty* transposon-based gene delivery to hepatocytes using the selective *Fah*-mutant mouse model allows rapid generation of mice with livers expressing transgenes of interest. We used this model to study the roles of candidate oncogenes identified by forward genetic screens, genes and pathways altered in human HCC, or components of a known oncogenic virus in promoting HCC in several different contexts relevant to the human disease. We showed the Dlk1-Dio3 domain gene *Rtl1* can drive hepatocarcinogenesis in otherwise normal male mouse livers, partially explaining the link between aberrant Dlk1-Dio3 domain gene expression and HCC. We showed *EGFR*, which is amplified and overexpressed in the male sex biased Poly7 molecular subclass of HCC, promotes hepatocarcinogenesis more efficiently in males than females. In contrast, both *CTNNB1* and *RSPO2*, which promote Wnt/β-catenin signaling, induced HCC without sex bias. We functionally validated the role of *Gli2* in promoting fibrosis-associated HCC *in vivo*. We also evaluated the oncogenic potential of a mutant variant of the Hepatitis B Virus *HBx* gene and found it to be more oncogenic than the wildtype gene. This selective mouse model allowed us to test several candidate oncogenes in otherwise normal livers, in both male and female mice, and in fibrotic livers, making this a versatile as well as efficient mouse model of HCC.

Introduction

Hepatocellular carcinoma (HCC) is a deadly disease with a 95% case fatality rate.[13] It is the second most common cause death from cancer worldwide, and is one of few cancer types that is becoming more prevalent in the United States.[14–16] HCC develops more frequently in males than females, although the molecular data explaining this sex bias is limited.[8,17] Chronic liver disease and cirrhosis usually precede HCC development. Common causes of liver damage include Hepatitis B Virus (HBV) infection, Hepatitis C Virus (HCV) infection, alcoholic liver disease, and non-alcoholic fatty liver disease.[8]

The high genetic complexity of liver tumors is being revealed by large-scale sequencing projects by The Cancer Genome Atlas Consortium (TCGA) and other groups which have identified a great number of genes mutated or with altered expression levels in a small proportion of HCC cases,[59–61] making the distinction between cancer-promoting events and passenger alterations challenging. It can be difficult to determine the specific driving alterations with gain or loss of large regions or whole chromosomes, a common occurrence in HCC.[45,46,53,62] Gene expression profiling of HCC has facilitated the identification of 5 major molecular subtypes, but the tumor promoting alterations have not been defined for each subtype. The Wnt/β-catenin signaling subtype is often driven by *CTNNB1* mutation, the proliferative subtype is likely driven by tyrosine kinase activation, and the polysomy of chromosome 7 subtype is likely driven by overexpression of *EGFR* and a set of other unknown oncogenes on chromosome 7. Drivers of the interferon signaling and unannotated classes are unknown.[53,54]

Comparative analysis of molecular data from human tumors and *Sleeping Beauty* (SB) transposon insertional mutagenesis-based animal models is useful for identifying cancer promoting alterations for many types of cancer.[90,91] Mutagenic transposons can cause

gain- or loss-of-function, depending on the location and orientation of transposon insertion relative to a gene, and can tag cancer genes within tumor cells. Genes associated with common insertion sites (CISs), representing regions of the genome with higher frequency of transposon integration than would be expected by random chance, may confer a proliferative advantage leading to tumor formation.[87,88,92,142] Forward genetic screens using SB insertional mutagenesis have revealed many candidate liver cancer drivers. These have been conducted in context of an otherwise normal liver, predisposing known HCC-promoting mutations, liver fibrosis (manuscript under review), hepatic steatosis (manuscript in preparation), and with HBV-induced liver inflammation.[48,92,95,100,101]

One such SB transposon-based mutagenesis screen, in which a mutagenic transposon was mobilized by ubiquitously expressed SBase, generating HCC in mice, identified the Dlk1-Dio3 imprinted domain as a site commonly mutated by transposon insertions.[92] This domain contains genes encoding protein-coding transcripts, long non-coding RNAs (lncRNAs), microRNAs, and small nucleolar RNAs.[143] Gene expression profiling of the SB-induced HCCs revealed that transposon insertions in the Dlk1-Dio3 domain consistently drove overexpression of one poorly characterized gene, Retrotransposon-like 1 (*Rtl1*), that is predicted to encode a transmembrane protein with protease activity. *RTL1* transcript was also found to be overexpressed in 30% of human HCC samples.[99] Correlative studies have shown a link between aberrant Dlk1-Dio3 domain gene expression and HCC, but few functional studies have addressed the tumorigenic role of these changes.[144–147]

A conditional forward genetic screen for HCC identified CIS genes in liver tumors isolated from both sexes of mice. In accordance with the pattern seen in humans, tumor incidence was higher in males than females. *Egfr* was identified as a CIS gene that was enriched for insertions in tumors from male compared to female mice.[54] The Poly7 molecular subclass

of HCC, which occurs more frequently in men than women, is associated with *EGFR* copy number gains and increased *EGFR* mRNA expression.[53,54] Studies functionally evaluating the differential hepatocarcinogenic effects of *Egfr* in males and females are lacking.

The Wnt/β-catenin signaling is an important HCC-promoting pathway. Gene expression profiles of approximately half of HCC cases reflect activation of the Wnt/β-catenin signaling pathway, and approximately one third have activating mutations in *CTNNB1*.[148,149] R-spondins are secreted proteins that can activate Wnt/β-catenin signaling *in vitro.*[150] *Rspo2* was identified as CIS genes in gastrointestinal tract cancer and breast cancer insertional mutagenesis screens.[94,151–153] There is evidence that *RSPO2* is involved in HCC. Copy number analysis of 231 human HCC samples revealed recurrent high copy amplifications of *RSPO2* in 3% of cases.[154] Analysis of over 450 HCC samples and 90 non-tumor liver tissue samples revealed *RSPO2* overexpression in HCC samples and associated expression of Wnt/β-catenin signaling target genes (manuscript in preparation). We sought to determine if *Rspo2* overexpression could induce liver tumorigenesis *in vivo*.

Approximately 90% of HCC cases develop in context of liver fibrosis, a condition caused by chronic liver damage leading to excessive extracellular matrix accumulation and scarring of the liver parenchyma.[18,19,31] While HCC is clearly associated with fibrosis, the direct contribution of fibrosis to HCC development is unclear. To address this and identify genetic drivers of HCC in the relevant context of hepatic fibrosis, a liver specific conditional forward genetic SB mutagenesis screen was conducted in the presence or absence of carbon tetrachloride (CCl_4)-induced hepatic fibrosis (manuscript under review). *Gli2* was identified as a candidate oncogene enriched for mutations in the CCl4-treated compared to the untreated mouse cohort. There is evidence that Hedgehog (Hh) signaling and GLI2

expression are involved in HCC. GLI2 protein is overexpressed in HCC and associated with poor survival[155,156] and Hh signaling inhibition can inhibit HCC cell growth,[157,158] but the role of GLI2 overexpression in promoting hepatic tumorigenesis has not been established. Based on transposon insertion data, we hypothesized that *Gli2* overexpression *in vivo* in context of hepatic fibrosis would induce HCC formation.

Approximately 50% of HCC cases worldwide are attributable to HBV infection.[14,20,159,160] There is evidence that HBV viral gene expression, mutations resulting from integration of the viral genome, and chronic inflammation in response to viral infection all contribute to hepatocarcinogenesis, although the mechanisms by which HBV infection promotes HCC are not fully understood.[24–26] The HBV regulatory gene X (*HBx*) encodes a protein that is needed for HBV replication and can induce proliferation and transformation of hepatocytes.[23] We have shown *HBx* overexpression can promote tumorigenesis in the mouse liver.[108] A mutant form of *HBx* with 2 point mutations resulting in 2 amino acid substitutions in the C-terminal transactivation domain of the protein is associated with increased liver damage and HCC.[161] Whether this variant is more oncogenic than wildtype *HBx* has yet to be determined.

While comparative genomic approaches help to distinguish driver from passenger genetic alterations in HCC, reverse genetic approaches are still needed to validate and study the oncogenic roles of the candidate drivers identified by forward genetic studies and to study the roles of specific components from cancer-promoting viruses. Germline transgenic mouse models are powerful tools for studying cancer genes in an orthotopic setting and in immunocompetent animals. They are, however, expensive and slow to generate, and do not reflect the acquisition of transforming alterations by individual somatic cells.[64] Mosaic mouse models in which genetically modified liver progenitor cells are transplanted

into the livers of syngeneic recipient mice help to overcome the time and cost associated with generation of genetically engineered mouse models but do not recapitulate the typical development of HCC in context of chronic liver disease.[76,77]

SB-mediated gene delivery provides an efficient method useful for studying candidate cancer genes *in vivo*.[102,103,106] SB can be used to excise transposon-based expression vectors for genes of interest or shRNA sequences for gene knockdown from plasmids and integrate them randomly at TA dinucleotides in the genome for stable expression.[106] SB-mediated gene delivery to hepatocytes of fumaryl acetoacetate hydrolase (*Fah*) mutant mice is a useful model for studying liver cancer genes.[48,102,108] *Fah* mutant mice have a defect in the tyrosine metabolic pathway and die from liver failure unless maintained on nitisinone. Plasmids with expression cassettes for genes of interest and an *Fah* rescue cDNA within SB transposons are delivered to hepatocytes by hydrodynamic tail vein injection.[107] Withdrawal of nitisinone treatment causes the death of hepatocytes lacking *Fah* and subsequent regeneration of the liver with cells stably expressing the *Fah* rescue cDNA plus the gene of interest in approximately 2 months.[102] This selective model allows the relatively rapid and inexpensive generation of mice with livers expressing a transgene of interest.

In this study, we used SB-mediated gene transfer into the livers of *Fah* mutant mice to study the roles of candidate HCC driving oncogenes either identified by forward genetic screens and altered in human cancer and or identified as variants of known HCC-promoting HBV viral genes. We did so in context of otherwise normal livers, in male and female animals to study the HCC sex bias, and in context of hepatic fibrosis, improving our understanding of the molecular drivers of HCC in various relevant contexts.

Results

Dlk1-Dio3 domain gene Rtl1 drives hepatocarcinogenesis in vivo

Because *Rtl1* was identified as a candidate oncogene in SB-induced HCCs[92] and *RTL1* was overexpressed in human HCC samples,[99] we sought to determine if hepatic *Rtl1* overexpression was sufficient to induce liver tumor formation *in vivo*. Transposon-based expression vectors for *Rtl1* and *Fah*[48] (*Rtl1* only), *Rtl1*, *Fah*, and a short hairpin directed against *Trp53* (*Rtl1*/shp53),[108] or *mCherry* and *Fah* (*mCherry* only) were delivered by hydrodynamic tail vein injection to the livers of *Fah* mutant male mice expressing SB transposase.[48,107] Nitisinone treatment was withdrawn, inducing the death of *Fah*-null hepatocytes and thereby allowing selective liver repopulation by stably transfected cells.[102]

Mice were sacrificed approximately 9 months after hydrodynamic injection and examined for tumor formation. *Rtl1* expression induced liver tumorigenesis, with 85.7% of *Rtl1* only-injected mice (12 of 14) developing tumors versus 23.1% of *mCherry* only-injected control mice (3 of 13) ($P = .002$, Fisher's exact test). (Figure 3.1A-B, Table 3.1) *Rtl1* only-injected mice developed an average of 2.86 tumors, while *mCherry* only-injected mice developed 0.23 tumors per mouse ($P < .0001$, Student's t test). (Figure 3.1C, Table 3.1) Loss of p53 function is one of the most common molecular alterations in HCC.[46] *Trp53* knockdown increased tumorigenesis in *Rtl1*-expressing animals. *Rtl1*/shp53-injected mice that were aged for approximately 9 months developed 6.67 tumors per mouse, a higher tumor burden than in mice injected with *Rtl1*-only ($P = .027$, Student's t test) and had a similar tumor penetrance, with 83% of mice (5 of 6) developing tumors. (Figure 3.1B-C, Table 3.1)

Egfr promotes male sex biased liver tumorigenesis

Since *Egfr* was identified as a male specific liver tumor CIS gene and *EGFR* gains and overexpression are associated with a subclass of HCC which occurs more frequently in men than women,[53,54] we tested the sex biased hepatocarcinogenic effects of *EGFR in vivo*. SB transposon-based expression vectors for truncated *EGFR* and full-length *EGFR* were coadministered with SB transposon-based expression vectors for *Fah* and a short hairpin directed against *Trp53* (shp53) by hydrodynamic tail vein injection to *Fah* mutant mice of both sexes expressing SB transposase. Nitisinone was withdrawn to select for cells with stable transgene expression.[48,107] Mice were sacrificed and examined for tumor formation at approximately 130 days post-hydrodynamic injection.

For both truncated and full-length *EGFR*, male injected mice developed more HCC than female mice. One hundred percent of male mice (9 of 9) and 25% of female mice (1 of 4) injected with truncated *EGFR, Fah,* and shp53 developed tumors (*P* =.014, Fisher's exact test). (Figure 3.2A-B, Table 3.1) Male and female mice had a mean tumor burden of 5.33 and 1.00 tumors per mouse, respectively (*P* = .033, Student's t test). (Figure 3.2C, Table 3.1) One hundred percent of male mice (3 of 3) and 33% of female mice (1 of 3) injected with full length *EGFR, Fah,* and shp53 developed tumors (no significant difference in tumor penetrance). (Figure 3.2B, Table 3.1) Male and female mice had a mean tumor burden of 5.67 and 0.67 tumors per mouse, respectively (*P* = .003). (Figure 3.2C, Table 3.1) Liver tumors from both sexes were classified as HCCs by histopathological analysis.

In contrast to *EGFR*, *CTNNB1* activation is associated with a subclass of HCC with relatively low sex bias.[53] As a control, we tested the hepatocarcinogenic effects of a constitutively active *CTNNB1* mutation (*CTNNB1*$_{S33Y}$) in mice of both sexes. SB transposon expression vectors for *CTNNB1*$_{S33Y}$ and shp53 were coadministered to *Fah*

mutant mice and hepatocytes with stable transgene expression were selected as described above. Mice were sacrificed and examined for tumor formation at approximately 80 days post-hydrodynamic injection.

Expression of *CTNNB1*$_{S33Y}$ induced HCC without strong sex bias. Male and female mice had comparable numbers of liver tumors, with a mean of 18.13 tumors per male and 26.50 tumors per female mouse (P = .195, Student's t test). (Figure 3.3A-B, Table 3.1) Tumor penetrance was 100% in both male and female mice (8 of 8 and 10 of 10, respectively). (Table 3.1) Liver tumors from both sexes were classified as HCCs by histopathological analysis.

Rspo2 promotes hepatomegaly and tumorigenesis in the mouse liver

Rspo2 is a gene involved in Wnt/β-catenin signaling that is altered in mouse gastrointestinal tract and breast cancers and amplified and overexpressed in human HCC (manuscript in preparation).[94,151–154] To study the effects of *Rspo2* in the mouse liver, we used hydrodynamic injection and *Fah* selection as described above to generate mice of both sexes expressing *RSPO2* alone (*RSPO2* only) and with shp53 (*RSPO2*/shp53) along with negative controls expressing *GFP* alone (*GFP* only) and with shp53 (*GFP*/shp53).

Mice were sacrificed at approximately 30 day intervals between 60 and 150 days post hydrodynamic injection to examine liver mass and tumor formation. (Table 3.1) Hepatic GFP expression was assessed by visualization with GFP goggles at necropsy for all mice. Mouse livers injected with *RSPO2* only and *RSPO2*/shp53 displayed hepatomegaly. The liver mass as a percent of the total body mass of *RSPO2* only-injected mice was 1.6 fold higher than *GFP* only controls at all time points tested (P < .05 for all time points. P < .0001 at 150 days). The liver body mass percent of *RSPO2*/shp53 injected mice was 1.7

to 1.9 fold higher than *GFP*/shp53 controls ($P < .05$ for all time points. $P < .0001$ at 150 days). (Figure 3.4A-B)

At 150 days post hydrodynamic injection, the rate of background tumor formation in *GFP* only and *GFP*/shp53 injected mice was low, with 4.3% to 5.0% penetrance and average tumor burden of 0.05 to 0.09. (Figure 3.4D-E) Mice injected with *RSPO2* only had a non-significant increase in tumor formation, with 18.2% penetrance and a mean of 0.27 tumors per mouse (no significant difference in tumor penetrance or burden). (Figure 3.4D-E) *RSPO2*/shp53 injected mice had significantly increased tumor formation compared to *GFP*/shp53. Sixty-five percent of *RSPO2*/shp53 injected mice developed tumors vs 4.3% of *GFP*/shp53 control mice ($P < .0001$, Fisher's exact test). (Figure 3.4C-D) *RSPO2*/shp53 injected mice developed an average of 1.15 tumor per mouse, significantly more than 0.09 tumors per *GFP*/shp53 injected moue ($P = .001$, Student's t test). (Figure 3.4E) Similarly to what was observed for $CTNNB1_{S33Y}$ induced tumors, there was no significant difference in tumor penetrance or burden between male and female *RSPO2*/shp53 injected mice. Seventy percent of male and 60% of female mice developed tumors ($P = 1.000$, Fisher's exact test). (Figure 3.4F) Male mice had an average tumor burden of 1.60 tumors per mouse and females 0.70 tumors per mouse ($P = .127$, Student's t test). (Figure 3.4G) Tumors were classified as HCCs upon histologic examination.

Gli2 overexpression induces tumor formation in fibrotic liver

We aimed to test if *Gli2* overexpression in fibrotic livers induces HCC, because *Gli2* was identified as a candidate fibrosis-associated liver oncogene in an SB screen (manuscript under review), and GLI2 protein overexpression is associated with poor survival in human HCC.[155,156] Mice with stable *Gli2* expression and control mice expressing *mCherry* in hepatocytes were generated using SB-mediated gene delivery of a *Gli2* or *mCherry*

expression vector and *Fah* rescue transgene to *Fah*-mutant male mice as described above.

Approximately 90% of the *Gli2* injected mice died within 75 days of hydrodynamic injection. (Table 3.2) The morbidity of this cohort was likely not due to technical failure in delivery of the *Fah* rescue transgene, as transgene delivery was verified in a subset of 7 animals by imaging for a luciferase reporter included in the *Fah* rescue transgene cassette and, of these animals, 100% died within 30 days of hydrodynamic injection. Morbidity was also likely not due to tumor formation, since none of these animals showed evidence of tumor formation upon examination at time of death. (Data not shown) We attribute the lethality, therefore, to a possible interference of *Gli2* overexpression with liver repopulation or function.

Of the remaining seven *Gli2* injected mice, 3 were treated with CCl4 to induce liver fibrosis and 4 were left untreated. Half of the control *mCherry* injected mice were treated with CCl4 and the other half untreated. (Table 3.1) These were all aged for 150 days post-hydrodynamic injection. *Gli2* expression induced more tumors in mouse livers than *mCherry* (Figure 3.5A-B). All untreated *Gli2* expressing mice had developed tumors by 150 days, with an average of 39.5 per mouse ($P < 0.0001$, *Gli2* vs. *mCherry* ANOVA). (Figure 3.5B) As expected, the addition of CCl4 treatment increased tumor burden to 57.0 tumors per mouse ($P = .006$, *Gli2* CCl4 vs. *Gli2* untreated Tukey post-hoc test). (Figure 3.5B) Our model showed *Gli2* expression can promote tumor formation *in vivo* with increased multiplicity in context of hepatic fibrosis.

Mutant HBx has higher oncogenic potential than wildtype HBx

Two point mutations in *HBx* resulting 2 amino acid substitutions (150M to K and 151 V to I) (*HBx*$_M$) is associated with liver damage and HCC more strongly than wildtype *HBx*.[161] To determine the relative oncogenic potential of *HBx*$_M$ and *HBx*, we generated male and female mice with hepatic *HBx*$_M$ and *HBx* expression along with a short hairpin directed against *Trp53* (*HBx*$_M$/shp53 and *HBx*/shp53) and control mice expressing *GFP* and shp53 (*GFP*/shp53) using the *Fah*-mutant mouse model as described above.

HBx$_M$ induced hepatomegaly. Both *HBx*/shp53 and *HBx*$_M$ /shp53 injected male mice had higher liver body mass percent than *GFP*/shp53 injected mice (7.8 and 7.7 vs 6.2, respectively; *P* = .001 and .0003, respectively, Student's t test). (Figure 3.6B) *HBx*$_M$ injected female mice also had a significant increase in liver body mass percent compared to *GFP*/shp53 injected mice (6.2 vs 5.5, respectively; *P* = .029, Student's t test). (Figure 3.6B)

HBx$_M$ induced more tumors than *HBx*. Both *HBx*$_M$ and *HBx* induced tumor formation in *Fah* mutant male mice by approximately 180 days post-injection. Tumor penetrance was 80% and 100% in *HBx*$_M$/shp53- and *HBx/*shp53-injected mice and 0% in *GFP*/shp53-injected mice (*P* = .007 and P = .001, respectively, Fisher's exact test). (Figure 3.6A, 3.6C, Table 3.1) No significant increase in tumor penetrance was seen in female mice, although 57.1% of *HBx*$_M$/shp53-injected female mice developed tumors vs 12.5% of *GFP*/shp53-injected control mice (*P* = .119, Fisher's exact test). (Figure 3.6A, 3.6C) Male mice injected with *HBx*$_M$/shp53 developed a mean of 7.6 tumors per mouse, significantly more than mice injected with *HBx*/shp53, which developed a mean of 3.1 tumors (*P* = .032, Student's t test) and than mice injected with *GFP*/shp53, with 0 tumors per mouse (*P* = .006, Student's

t test). No significant differences in tumor burden were observed in female mice. (Figure 3.6D)

Methods

Generation and maintenance of Fah-deficient mice

All animal studies were conducted using procedures approved and monitored by the Institutional Animal Care and Use Committee at the University of Minnesota. Doubly transgenic mice deficient for *Fah* and expressing the *SB11* transposase (*Fah*$^{-/-}$*; Rosa26-SB11*$^{Tg/WT}$)[88,162] were generated and maintained as described.[108] Mice were maintained on 2-(2-nitro-4-trifluoromethylbenzoyl)-1,3-cyclohexanedione (nitisinone) drinking water until hydrodynamic injection with plasmid DNA at 6-8 weeks of age, then maintained on normal drinking water. Injected animals were observed for weight changes. At 150-180 days post-injection, liver tumor analysis was performed as described below.

Hydrodynamic injection of plasmid DNA into Fah-deficient mice

The following plasmids have been described previously: a plasmid expressing mouse *Rtl1* from the human *EF-1α* promoter,[99] a plasmid with an expression cassette for *mCherry* driven by the human *EF-1α* promoter (manuscript under review), a plasmid containing an SB IR/DR flanked expression cassette for mouse *Fah* and firefly luciferase under the control of the phosphoglycerate kinase (*PGK*) promoter,[102] a plasmid containing an expression cassette for *GFP* and a short hairpin RNA directed against *Trp53,*[108] full length human *EGFR* complementary DNA (cDNA) driven by the *PGK* promoter,[54] human truncated *EGFR* (exon 1 to exon 24) cDNA driven by the *PGK* promoter,[54] a plasmid expressing mouse *Fah* and *GFP* from the *PGK* promoter and human *CTNNB1*$_{S33Y}$ and firefly luciferase from the Caggs promoter,[54] a plasmid with an *EF-1α* promoter driven

expression cassette for mouse *Gli2* (manuscript under review), a plasmid expressing mouse *Fah* and *GFP* from the *PGK* promoter and human *RSPO2* and firefly luciferase from the Caggs promoter (manuscript in preparation), a plasmid expressing *GFP* driven by the *PGK* promoter and mouse *Fah* and firefly luciferase from the *Caggs* promoter[108] and a plasmid expressing D genotype *HBx* from the *PGK* promoter and mouse *Fah* and firefly luciferase from the *Caggs* promoter (pKT2/GD-HBx),[108] all flanked by SB transposon inverted repeat/direct repeats. A plasmid with an SB transposon inverted repeat/direct repeat flanked cassette for mutant D genotype *HBx* with 2 nucleotide substitutions at 389 and 391 of *HBx* coding sequence (A389 to T and G391 to A) under control of the *PGK* promoter and mouse *Fah* and firefly luciferase under control of the *Caggs* promoter was generated as follows: Two fragments containing *HBx* coding sequence and flanking plasmid backbone sequences were PCR amplified from pKT2/GD-HBx with primers encoding the point mutations using ReddyMix PCR Master Mix (ThermoFisher Scientific) according to the manufacturer's instructions with an initial denaturing step of 94°C for 5 min; 35-cycles of denaturing at 94°C for 30 sec, annealing at 56° C (fragment 1) or 52° C (fragment 2) for 1 min, and extension at 72°C for 1.5 min; and a final extension at 72°C for 5 min. Primers were 5'-TGTTCATGATGCAACTGGATCCAG-3' and 5'-AGGTTAATGATCTTTGTACTAGGAGGCTGTAG-3' for fragment 1 and 5'-CTAGTACAAAGATCATTAACCTAATCTCC-3' and 5'-TCGAGACCATGGCTGCTAG-3' for fragment 2. These fragments were joined by PCR amplification using HotStar HiFidelity Polymerase (Qiagen) according to the manufacturer's instructions with an initial denaturing step of 95°C for 5 min; 40-cycles of denaturing at 94°C for 15 sec, annealing at 47° C for 1 min, and extension at 72°C for 1.5 min; and a final extension at 72°C for 10 min. Primers used were 5'-GTTGGAGTCATTAAAACTCG-3' and 5'-CGTCCTTTGTTTACGTCC-3'. This sequence was cloned into the pKT2/GD-HBx vector,

replacing the corresponding wildtype *HBx* sequence using standard cloning techniques. All plasmids used for hydrodynamic tail vein injections were prepared using NucleoBond Xtra Maxi EF DNA Maxi-preparation kits (Macherey-Nagel) following the manufacturer's instructions. Twenty µg of each plasmid was delivered by hydrodynamic tail vein injection as described.[107]

CCl4 treatment for fibrosis induction

Starting at 6 weeks post-hydrodynamic injection, half of the surviving mice injected with *Gli2* or *mCherry* were given 2.5 µl per gram body weight of a 10% CCl4 solution in mineral oil by intraperitoneal injections twice weekly for a total of 12 weeks to induce hepatic inflammation and fibrosis.

Liver tumor analysis

After euthanasia by CO2, the whole mouse was weighed. The liver was removed, weighed, and placed in cold phosphate buffered saline. Macroscopic hyperplastic liver nodules were counted. When applicable, livers were examined using GFP goggles (BLS-ltd), and GFP-positive tumors were counted and collected. Tumors greater than 1mm in diameter were collected and processed for histological examination. Tissues for histological examination were fixed in 10% formalin, paraffin-embedded, sectioned at 5 microns on a standard microtome (Leica), mounted, and heat-fixed onto glass slides. Slides were dewaxed, rehydrated through a gradual decrease in ethanol concentration, stained with hematoxylin and eosin (H&E) following a standard protocol, and analyzed by color brightfield microscopy by two board-certified pathologists (KA and ML, American Board of Pathology).

Discussion

Molecular characterization of HCC has revealed a great amount of genetic complexity, making the identification of cancer drivers difficult. Comparative studies using forward genetic screening in mice have identified large numbers of candidate driver alterations in human HCC, but establishing their roles as HCC drivers requires functional validation. HBV is a known HCC-promoting virus, but the roles of individual HBV genetic components in promoting HCC are not fully understood. The SB transposon system can be used not only for forward genetic screening for HCC drivers, but also for reverse genetic studies testing candidate HCC drivers *in vivo*. In this study, we used SB based gene delivery to hepatocytes of *Fah*-deficient mice to rapidly generate mice with hepatic expression of several candidate oncogenes.

A SB transposon-based forward genetic screen identified the Dlk-Dio3 domain gene *Rtl1* as a candidate hepatic oncogene. Several studies have correlated Dlk-Dio3 domain alterations with HCC,[144–147] and through SB-mediated gene delivery, we directly showed *Rtl1* overexpression results in liver tumor formation in mice. Thus, the role of Dlk-Dio3 domain alterations in promoting HCC may be explained, at least in part, by the oncogenic role of *Rtl1* validated in our mouse model.

Many mouse models of HCC include only males because HCC occurs most commonly in men.[64] Sex distributions vary in different subclasses of HCC,[53] however, making the inclusion of both males and females relevant in HCC studies. Males are highly enriched in a subclass of HCC with chromosome 7 polysomy and *EGFR* overexpression,[53] and SB transposon mutations in *EGFR* in a forward genetic screen for HCC drivers were enriched in male mice.[54] Using an SB gene delivery mouse model of HCC, we showed *EGFR* overexpression promotes HCC in a male sex biased manner. In contrast, activated

CTNNB1 and *RSPO2* both drove HCC in both sexes of mice with similar frequencies, confirming the non-sex biased role of Wnt/β-catenin signaling in HCC development.

The HBV *HBx* gene has been shown to promote liver cancer.[108] We functionally validated the role of a mutant *HBx* variant associated with increased liver damage and HCC,[161] showing it to have stronger oncogenic potential than wildtype *HBx*. Interestingly, another *HBx* variant with a truncation of the same region of C-terminal transactivation domain altered by the mutations we studied is also associated with increased liver damage and HCC.[163] This suggests the C-terminal transactivation domain of *HBx* may have an important role in tumorigenesis.

HCC almost always develops in context of chronic liver damage and fibrosis.[18,19,31] The selective *Fah* mutant mouse model can be used with CCl4-induced hepatic fibrosis to model the conditions under which HCC most commonly occurs. We showed *Gli2* expression can induce liver tumors in a mouse model with hepatic fibrosis, confirming its predicted role as a fibrosis-associated oncogene based on mutations in fibrosis-associated SB-induced mouse liver tumors and on its overexpression in human HCC (manuscript under review).[155,156] This is the first direct evidence, to our knowledge, that *Gli2* overexpression can drives liver tumor formation *in vivo*.

By performing reverse genetic studies using SB transposon- based gene delivery to *Fah* deficient mouse livers, we modeled HCC induced by a variety of genes discovered in forward genetic screens or as variants of oncogenic viral genes. We used this method to study HCC in both males and females, and in the highly relevant context of hepatic fibrosis. This method has also been used to study drivers of fatty liver associated HCC, another highly relevant context (manuscript in preparation). This is a versatile mouse model that can be used to study HCC drivers in a variety of highly relevant contexts.

Table 3.1: Liver tumors in hydrodynamically injected mice

Mouse ID	Sex	Experimental Group	Treatment	Days post-injection	Liver Nodules
M1381	Male	*Rtl1*	None	240	4
M1382	Male	*Rtl1*	None	240	1
M1383	Male	*Rtl1*	None	240	0
M1384	Male	*Rtl1*	None	240	6
M1375	Male	*Rtl1*	None	251	1
M1376	Male	*Rtl1*	None	251	3
M1482	Male	*Rtl1*	None	251	5
M1483	Male	*Rtl1*	None	251	1
M1484	Male	*Rtl1*	None	251	4
M1485	Male	*Rtl1*	None	251	3
M1491	Male	*Rtl1*	None	251	5
M1492	Male	*Rtl1*	None	251	4
M1501	Male	*Rtl1*	None	251	0
M1502	Male	*Rtl1*	None	251	3
				Mean	**2.86**

Mouse ID	Sex	Experimental Group	Treatment	Days post-injection	Liver Nodules
M1391	Male	*Rtl1* /shp53	None	251	5
M1392	Male	*Rtl1* /shp53	None	251	0
M1394	Male	*Rtl1* /shp53	None	251	6
M1451	Male	*Rtl1* /shp53	None	254	5
M1454	Male	*Rtl1* /shp53	None	254	16
M1455	Male	*Rtl1* /shp53	None	254	8
				Mean	**6.67**

Mouse ID	Sex	Experimental Group	Treatment	Days post-injection	Liver Nodules
M3062	Male	*mCherry*	None	198	0
M3063	Male	*mCherry*	None	198	0
M3065	Male	*mCherry*	None	200	0
M3066	Male	*mCherry*	None	200	0
M3067	Male	*mCherry*	None	200	0
M4181	Male	*mCherry*	None	201	0
M4182	Male	*mCherry*	None	201	1
M4183	Male	*mCherry*	None	201	1
M4391	Male	*mCherry*	None	201	1
M4402	Male	*mCherry*	None	201	0
M4403	Male	*mCherry*	None	201	0
M4404	Male	*mCherry*	None	201	0
M4406	Male	*mCherry*	None	201	0
				Mean	**0.23**

Mouse ID	Sex	Experimental Group	Treatment	Days post-injection	Liver Nodules
M2683	Male	*mCherry*	CCl4	202	2
M2686	Male	*mCherry*	CCl4	203	0
M2687	Male	*mCherry*	CCl4	203	0
M2693	Male	*mCherry*	CCl4	205	0
M2701	Male	*mCherry*	CCl4	204	0
M2702	Male	*mCherry*	CCl4	204	0
M2703	Male	*mCherry*	CCl4	206	0
M3132	Male	*mCherry*	CCl4	192	0
M3136	Male	*mCherry*	CCl4	202	0
M3138	Male	*mCherry*	CCl4	202	1
				Mean	**0.30**

Mouse ID	Sex	Experimental Group	Treatment	Days post-injection	Liver Nodules

M3854	Male	*Gli2*	None	157	27
M4022	Male	*Gli2*	None	152	30
M4041	Male	*Gli2*	None	152	52
M4042	Male	*Gli2*	None	152	49
				Mean	**39.5**

Mouse ID	Sex	Experimental Group	Treatment	Days post-injection	Liver Nodules
M3743	Male	*Gli2*	CCl4	153	41
M3761	Male	*Gli2*	CCl4	157	65
M3762	Male	*Gli2*	CCl4	161	65
				Mean	**57**

Mouse ID	Sex	Experimental Group	Treatment	Days post-injection	Liver Nodules
F1141	Female	Trunc *EGFR*/shp53	None	129	0
F1142	Female	Trunc *EGFR*/shp53	None	129	0
F1143	Female	Trunc *EGFR*/shp53	None	129	4
F1144	Female	Trunc *EGFR*/shp53	None	129	0
				Mean	**1.00**

Mouse ID	Sex	Experimental Group	Treatment	Days post-injection	Liver Nodules
M1131	Male	Trunc *EGFR*/shp53	None	129	3
M1132	Male	Trunc *EGFR*/shp53	None	129	3
M1133	Male	Trunc *EGFR*/shp53	None	129	6
M1141	Male	Trunc *EGFR*/shp53	None	132	6
M932	Male	Trunc *EGFR*/shp53	None	134	4
M933	Male	Trunc *EGFR*/shp53	None	134	5
M961	Male	Trunc *EGFR*/shp53	None	134	1
M962	Male	Trunc *EGFR*/shp53	None	137	12
M963	Male	Trunc *EGFR*/shp53	None	137	8
				Mean	**5.33**

Mouse ID	Sex	Experimental Group	Treatment	Days post-injection	Liver Nodules
F1195	Female	WT *EGFR*/shp53	None	128	0
F1181	Female	WT *EGFR*/shp53	None	133	2
F1183	Female	WT *EGFR*/shp53	None	133	0
				Mean	**0.67**

Mouse ID	Sex	Experimental Group	Treatment	Days post-injection	Liver Nodules
M1201	Male	WT *EGFR*/shp53	None	133	6
M1202	Male	WT *EGFR*/shp53	None	133	5
M1212	Male	WT *EGFR*/shp53	None	133	6
				Mean	**5.67**

Mouse ID	Sex	Experimental Group	Treatment	Days post-injection	Liver Nodules
F1351	Female	*CTNNB1* $_{S33Y}$/shp53	None	80	15
F1353	Female	*CTNNB1* $_{S33Y}$/shp53	None	80	11
F1471	Female	*CTNNB1* $_{S33Y}$/shp53	None	80	50
F1472	Female	*CTNNB1* $_{S33Y}$/shp53	None	80	50
F1473	Female	*CTNNB1* $_{S33Y}$/shp53	None	80	30
F1491	Female	*CTNNB1* $_{S33Y}$/shp53	None	80	12
F1493	Female	*CTNNB1* $_{S33Y}$/shp53	None	80	50
F1543	Female	*CTNNB1* $_{S33Y}$/shp53	None	80	12
F1311	Female	*CTNNB1* $_{S33Y}$/shp53	None	83	20
F1312	Female	*CTNNB1* $_{S33Y}$/shp53	None	83	15
				Mean	**26.50**

Mouse ID	Sex	Experimental Group	Treatment	Days post-injection	Liver Nodules
M1341	Male	*CTNNB1* $_{S33Y}$/shp53	None	80	16
M1343	Male	*CTNNB1* $_{S33Y}$/shp53	None	80	18

M1541	Male	*CTNNB1* $_{S33Y}$/shp53	None	80	15	
M1551	Male	*CTNNB1* $_{S33Y}$/shp53	None	80	20	
M1552	Male	*CTNNB1* $_{S33Y}$/shp53	None	80	15	
M1553	Male	*CTNNB1* $_{S33Y}$/shp53	None	80	15	
M1331	Male	*CTNNB1* $_{S33Y}$/shp53	None	83	24	
M1332	Male	*CTNNB1* $_{S33Y}$/shp53	None	83	22	
				Mean	**18.13**	

Mouse ID	Sex	Experimental Group	Treatment	Days post-injection	Liver Nodules	Liver mass % of body weight
F2051	Female	*RSPO2*	None	79	0	8.4%
M2053	Male	*RSPO2*	None	79	0	10.1%
				Mean	**0.00**	**9.3%**

Mouse ID	Sex	Experimental Group	Treatment	Days post-injection	Liver Nodules	Liver mass % of body weight
F2052	Female	*RSPO2*	None	120	1	8.7%
F2053	Female	*RSPO2*	None	120	2	8.7%
M3331	Male	*RSPO2*	None	128	0	8.8%
M3332	Male	*RSPO2*	None	128	0	11.5%
				Mean	**0.75**	**9.4%**

Mouse ID	Sex	Experimental Group	Treatment	Days post-injection	Liver Nodules	Liver mass % of body weight
F2054	Female	*RSPO2*	None	149	0	9.4%
F2055	Female	*RSPO2*	None	149	0	9.1%
M2871	Male	*RSPO2*	None	150	0	7.9%
M2872	Male	*RSPO2*	None	150	0	7.2%
M2873	Male	*RSPO2*	None	150	1	8.0%
M3054	Male	*RSPO2*	None	155	0	8.7%
M3055	Male	*RSPO2*	None	155	0	8.6%
F2861	Female	*RSPO2*	None	156	0	9.6%
F2863	Female	*RSPO2*	None	156	0	10.4%
F2883	Female	*RSPO2*	None	156	0	10.1%
F2884	Female	*RSPO2*	None	156	0	10.8%
F3382	Female	*RSPO2*	None	156	1	11.0%
F3383	Female	*RSPO2*	None	156	0	9.9%
M3402	Male	*RSPO2*	None	156	1	11.5%
F3052	Female	*RSPO2*	None	158	3	13.3%
F3053	Female	*RSPO2*	None	158	0	10.6%
F2182	Female	*RSPO2*	None	159	0	8.5%
F2183	Female	*RSPO2*	None	159	0	8.1%
M2191	Male	*RSPO2*	None	159	0	10.2%
M2192	Male	*RSPO2*	None	159	0	10.0%
M2182	Male	*RSPO2*	None	160	0	8.8%
M2185	Male	*RSPO2*	None	160	0	10.6%
				Mean	**0.27**	**9.7%**

Mouse ID	Sex	Experimental Group	Treatment	Days post-injection	Liver Nodules	Liver mass % of body weight
F2131	Female	*RSPO2*/shp53	None	59	0	10.0%
M2131	Male	*RSPO2*/shp53	None	59	0	10.2%
				Mean	**0.00**	**10.1%**

Mouse ID	Sex	Experimental Group	Treatment	Days post-injection	Liver Nodules	Liver mass % of body weight
F2864	Female	*RSPO2*/shp53	None	77	0	9.6%
F3331	Female	*RSPO2*/shp53	None	80	0	11.4%
M3391	Male	*RSPO2*/shp53	None	80	0	9.8%
				Mean	**0.00**	**10.3%**

Mouse ID	Sex	Experimental Group	Treatment	Days post-injection	Liver Nodules	Liver mass % of body weight
F2132	Female	*RSPO2*/shp53	None	120	0	8.5%
M2134	Male	*RSPO2*/shp53	None	120	4	9.9%

				Mean	**2.00**	**9.2%**
Mouse ID	Sex	Experimental Group	Treatment	Days post-injection	Liver Nodules	Liver mass % of body weight
M2201	Male	*RSPO2*/shp53	None	152	1	13.6%
M2204	Male	*RSPO2*/shp53	None	152	5	10.3%
F2191	Female	*RSPO2*/shp53	None	153	0	8.0%
F2192	Female	*RSPO2*/shp53	None	153	0	7.4%
F2193	Female	*RSPO2*/shp53	None	153	0	9.0%
F2201	Female	*RSPO2*/shp53	None	153	1	9.4%
M2202	Male	*RSPO2*/shp53	None	153	1	11.8%
M2203	Male	*RSPO2*/shp53	None	153	1	11.2%
M3041	Male	*RSPO2*/shp53	None	153	0	9.7%
M3043	Male	*RSPO2*/shp53	None	153	2	9.6%
F3041	Female	*RSPO2*/shp53	None	154	1	11.0%
F2133	Female	*RSPO2*/shp53	None	155	1	9.0%
F2865	Female	*RSPO2*/shp53	None	155	1	9.7%
F3043	Female	*RSPO2*/shp53	None	155	0	11.1%
M2133	Male	*RSPO2*/shp53	None	155	3	9.0%
M3392	Male	*RSPO2*/shp53	None	155	3	18.5%
M2135	Male	*RSPO2*/shp53	None	156	0	9.3%
M2136	Male	*RSPO2*/shp53	None	156	0	9.2%
F2101	Female	*RSPO2*/shp53	None	160	2	8.4%
F2102	Female	*RSPO2*/shp53	None	160	1	8.5%
				Mean	**1.15**	**10.2%**
Mouse ID	Sex	Experimental Group	Treatment	Days post-injection	Liver Nodules	Liver mass % of body weight
F2271	Female	*GFP*	None	63	0	5.2%
F2272	Female	*GFP*	None	63	0	5.0%
M2271	Male	*GFP*	None	63	0	6.0%
M2272	Male	*GFP*	None	63	0	5.5%
M2273	Male	*GFP*	None	63	0	5.4%
				Mean	**0.00**	**5.4%**
Mouse ID	Sex	Experimental Group	Treatment	Days post-injection	Liver Nodules	Liver mass % of body weight
M271	Male	*GFP*	None	82	0	5.2%
M272	Male	*GFP*	None	82	0	5.9%
M2883	Male	*GFP*	None	106	0	6.4%
				Mean	**0.00**	**5.8%**
Mouse ID	Sex	Experimental Group	Treatment	Days post-injection	Liver Nodules	Liver mass % of body weight
F3401	Female	*GFP*	None	127	0	5.8%
F3402	Female	*GFP*	None	127	0	6.3%
				Mean	**0.00**	**6.0%**
Mouse ID	Sex	Experimental Group	Treatment	Days post-injection	Liver Nodules	Liver mass % of body weight
F2641	Female	*GFP*	None	153	0	5.7%
F2642	Female	*GFP*	None	153	1	5.8%
F2643	Female	*GFP*	None	153	0	not meaured; appeared normal
F2644	Female	*GFP*	None	154	0	5.9%
M2643	Male	*GFP*	None	154	0	6.1%
F2691	Female	*GFP*	None	155	0	5.3%
F2692	Female	*GFP*	None	155	0	5.6%
F2693	Female	*GFP*	None	155	0	5.3%
F3072	Female	*GFP*	None	155	0	6.3%
M2661	Male	*GFP*	None	155	0	6.5%
M2672	Male	*GFP*	None	155	0	6.3%
F3403	Female	*GFP*	None	156	0	7.2%
M2884	Male	*GFP*	None	156	0	5.5%
M3384	Male	*GFP*	None	156	0	6.1%

M3094	Male	*GFP*	None	157	0	5.6%
M2621	Male	*GFP*	None	158	0	6.2%
M2622	Male	*GFP*	None	158	0	5.4%
M3095	Male	*GFP*	None	158	0	6.7%
F2701	Female	*GFP*	None	161	0	5.3%
F2702	Female	*GFP*	None	161	0	not meaured; appeared normal
				Mean	**0.05**	**5.9%**

Mouse ID	Sex	Experimental Group	Treatment	Days post-injection	Liver Nodules	Liver mass % of body weight
M702	Male	*GFP*/shp53	None	70	0	6.3%
M721	Male	*GFP*/shp53	None	70	0	6.3%
				Mean	**0.00**	**6.3%**

Mouse ID	Sex	Experimental Group	Treatment	Days post-injection	Liver Nodules	Liver mass % of body weight
M701	Male	*GFP*/shp53	None	80	0	5.8%
M703	Male	*GFP*/shp53	None	80	0	6.1%
F3391	Female	*GFP*/shp53	None	81	0	5.4%
F3392	Female	*GFP*/shp53	None	81	0	5.1%
				Mean	**0.00**	**5.6%**

Mouse ID	Sex	Experimental Group	Treatment	Days post-injection	Liver Nodules	Liver mass % of body weight
F3393	Female	*GFP*/shp53	None	127	0	5.1%
F3394	Female	*GFP*/shp53	None	127	0	6.0%
				Mean	**0.00**	**5.5%**

Mouse ID	Sex	Experimental Group	Treatment	Days post-injection	Liver Nodules	Liver mass % of body weight
F2651	Female	*GFP*/shp53	None	151	0	6.4%
F2652	Female	*GFP*/shp53	None	151	0	5.6%
F2653	Female	*GFP*/shp53	None	151	0	6.1%
F2662	Female	*GFP*/shp53	None	151	0	5.7%
F2663	Female	*GFP*/shp53	None	151	0	5.6%
F2664	Female	*GFP*/shp53	None	151	0	4.8%
F2665	Female	*GFP*/shp53	None	151	2	5.4%
F2666	Female	*GFP*/shp53	None	151	0	6.0%
M2291	Male	*GFP*/shp53	None	154	0	5.5%
M2292	Male	*GFP*/shp53	None	154	0	4.5%
M2293	Male	*GFP*/shp53	None	154	0	4.1%
M2294	Male	*GFP*/shp53	None	154	0	4.7%
F3395	Female	*GFP*/shp53	None	156	0	6.5%
M3111	Male	*GFP*/shp53	None	156	0	5.4%
M3404	Male	*GFP*/shp53	None	156	0	5.9%
M3405	Male	*GFP*/shp53	None	156	0	5.9%
M1991	Male	*GFP*/shp53	None	157	0	5.6%
M1992	Male	*GFP*/shp53	None	157	0	4.9%
M3112	Male	*GFP*/shp53	None	157	0	5.8%
F3111	Female	*GFP*/shp53	None	158	0	5.5%
F3112	Female	*GFP*/shp53	None	158	0	5.2%
M1993	Male	*GFP*/shp53	None	160	0	5.5%
F2671	Female	*GFP*/shp53	None	161	0	8.3%
				Mean	**0.09**	**5.6%**

Mouse ID	Sex	Experimental Group	Treatment	Days post-injection	Liver Nodules	Liver mass % of body weight
M1991	Male	*GFP*/shp53	None	157	0	5.6%
M1992	Male	*GFP*/shp53	None	157	0	4.9%
M1993	Male	*GFP*/shp53	None	160	0	5.5%
M2481	Male	*GFP*/shp53	None	169	0	5.6%
M2482	Male	*GFP*/shp53	None	169	0	5.7%
				Mean	**0.00**	**5.5%**

Mouse ID	Sex	Experimental Group	Treatment	Days post-injection	Liver Nodules	Liver mass % of body weight

F1992	Female	*GFP*/shp53	None	175	0	5.7%
F1993	Female	*GFP*/shp53	None	176	0	5.9%
F1994	Female	*GFP*/shp53	None	176	1	5.2%
F2461	Female	*GFP*/shp53	None	170	0	not meaured; appeared normal
F2482	Female	*GFP*/shp53	None	171	0	5.8%
F2483	Female	*GFP*/shp53	None	171	0	5.6%
F2484	Female	*GFP*/shp53	None	171	0	5.6%
F2485	Female	*GFP*/shp53	None	171	0	4.9%
				Mean	**0.13**	**5.5%**

Mouse ID	Sex	Experimental Group	Treatment	Days post-injection	Liver Nodules	Liver mass % of body weight
M2522	Male	*HBx* $_M$/shp53	None	168	8	7.9%
M2523	Male	*HBx* $_M$/shp53	None	168	15	9.2%
M2571	Male	*HBx* $_M$/shp53	None	174	11	6.9%
M2572	Male	*HBx* $_M$/shp53	None	175	13	8.0%
M2573	Male	*HBx* $_M$/shp53	None	175	4	8.0%
M3251	Male	*HBx* $_M$/shp53	None	168	0	6.1%
M3252	Male	*HBx* $_M$/shp53	None	169	0	7.7%
M3253	Male	*HBx* $_M$/shp53	None	169	9	7.4%
M3281	Male	*HBx* $_M$/shp53	None	172	6	6.8%
M3282	Male	*HBx* $_M$/shp53	None	174	10	9.1%
				Mean	**7.60**	**7.7%**

Mouse ID	Sex	Experimental Group	Treatment	Days post-injection	Liver Nodules	Liver mass % of body weight
F2521	Female	*HBx* $_M$/shp53	None	169	0	6.5%
F2522	Female	*HBx* $_M$/shp53	None	169	1	6.2%
F2531	Female	*HBx* $_M$/shp53	None	171	0	5.3%
F2533	Female	*HBx* $_M$/shp53	None	171	0	5.6%
F2571	Female	*HBx* $_M$/shp53	None	175	1	6.3%
F2572	Female	*HBx* $_M$/shp53	None	177	1	6.5%
F2573	Female	*HBx* $_M$/shp53	None	177	2	7.4%
				Mean	**0.71**	**6.2%**

Mouse ID	Sex	Experimental Group	Treatment	Days post-injection	Liver Nodules	Liver mass % of body weight
M2711	Male	*HBx* /shp53	None	167	3	8.2%
M2712	Male	*HBx* /shp53	None	167	4	7.0%
M3214	Male	*HBx* /shp53	None	169	1	6.4%
M3216	Male	*HBx* /shp53	None	169	2	7.1%
M3222	Male	*HBx* /shp53	None	170	3	6.6%
M3223	Male	*HBx* /shp53	None	170	2	9.5%
M3231	Male	*HBx* /shp53	None	168	2	9.2%
M3291	Male	*HBx* /shp53	None	170	1	7.6%
M3292	Male	*HBx* /shp53	None	170	10	8.6%
				Mean	**3.11**	**7.9%**

Mouse ID	Sex	Experimental Group	Treatment	Days post-injection	Liver Nodules	Liver mass % of body weight
F2711	Female	*HBx* /shp53	None	166	0	6.0%
F2713	Female	*HBx* /shp53	None	166	0	6.1%
F3191	Female	*HBx* /shp53	None	168	0	5.4%
F3192	Female	*HBx* /shp53	None	168	0	5.5%
F3193	Female	*HBx* /shp53	None	168	0	5.4%
F3194	Female	*HBx* /shp53	None	168	0	5.2%
F3195	Female	*HBx* /shp53	None	168	0	5.8%
F3211	Female	*HBx* /shp53	None	170	0	5.4%
F3212	Female	*HBx* /shp53	None	170	1	6.1%
F3231	Female	*HBx* /shp53	None	171	0	5.5%
F3232	Female	*HBx* /shp53	None	171	0	5.4%
F3233	Female	*HBx* /shp53	None	171	2	5.8%
				Mean	**0.25**	**5.6%**

Table 3.2: *Gli2* -injected mice

Mouse	Died prematurely?[a]	Day PHI of premature death	Luciferase confirmed by imaging
M3711	Yes	40	N/A
M3712	Yes	37	N/A
M3713	Yes	71	N/A
M3732	Yes	31	N/A
M3733	Yes	28	N/A
M3734	Yes	33	N/A
M3742	Yes	67	N/A
M3743	No	N/A	N/A
M3761	No	N/A	N/A
M3762	No	N/A	N/A
M3851	Yes	38	N/A
M3852	Yes	38	N/A
M3853	Yes	38	N/A
M3854	No	N/A	N/A
M3862	Yes	24	N/A
M3863	Yes	24	N/A
M3871	Yes	38	N/A
M3872	Yes	37	N/A
M3873	Yes	37	N/A
M3901	Yes	26	N/A
M3902	Yes	26	N/A
M3903	Yes	26	N/A
M3904	Yes	26	N/A
M3973	Yes	35	N/A
M3974	Yes	35	N/A
M3992	Yes	33	N/A
M3993	Yes	33	N/A
M3994	Yes	33	N/A
M4012	Yes	29	N/A
M4013	Yes	29	N/A
M4014	Yes	23	N/A
M4015	Yes	6	N/A
M4021	Yes	41	N/A
M4022	No	N/A	N/A
M4023	Yes	41	N/A
M4024	Yes	29	N/A
M4032	Yes	6	N/A
M4033	Yes	9	N/A
M4034	Yes	27	N/A

M4041	No	N/A	N/A
M4042	No	N/A	N/A
M4061	Yes	42	N/A
M4062	Yes	28	N/A
M4063	Yes	38	N/A
M4064	Yes	42	N/A
M4071	Yes	30	N/A
M4072	Yes	30	N/A
M4073	Yes	31	N/A
M4075	Yes	36	N/A
M4076	Yes	35	N/A
M4091	Yes	39	N/A
M4092	Yes	33	N/A
M4101	Yes	27	N/A
M4102	Yes	29	N/A
M4103	Yes	29	N/A
M4111	Yes	31	N/A
M4112	Yes	36	N/A
M4113	Yes	38	N/A
M4114	Yes	30	N/A
M4291	Yes	25	Yes
M4292	Yes	26	Yes
M4293	Yes	26	Yes
M4301	Yes	27	Yes
M4302	Yes	27	Yes
M4303	Yes	27	Yes
M4304	Yes	27	Yes

[a] Died prematurely defined as dying before experiment endpoint

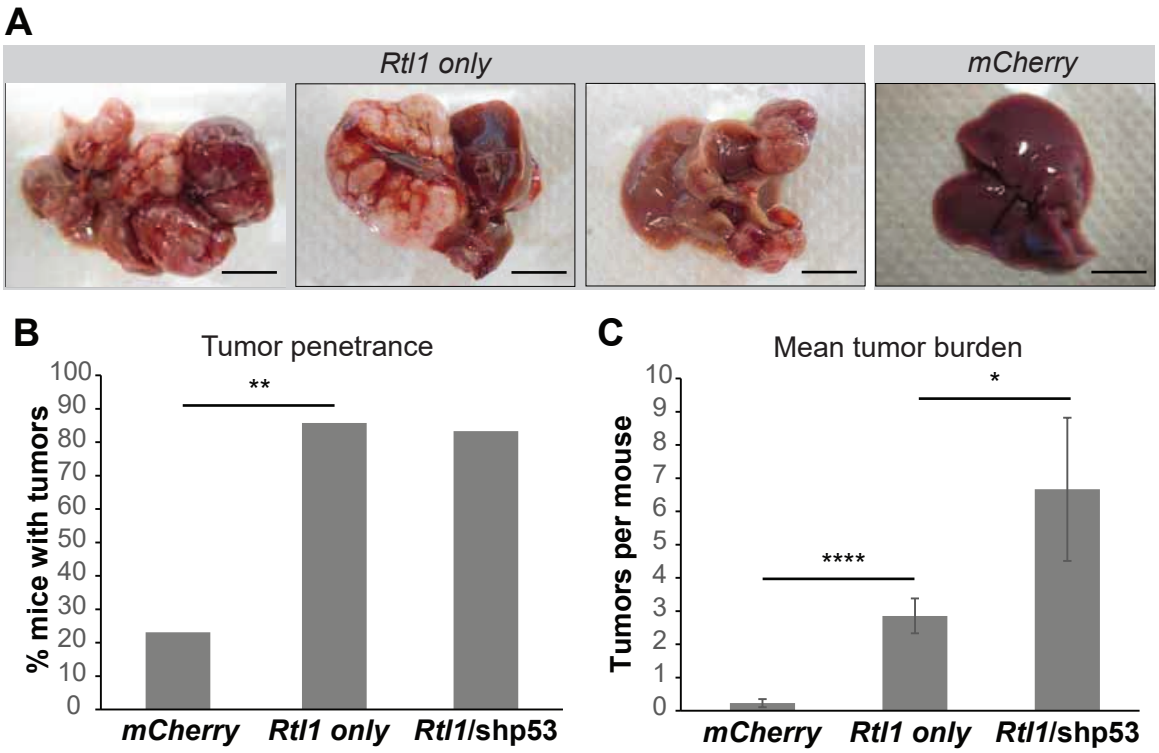

Figure 3.1. *In vivo* hepatic *Rtl1* expression of drives tumor formation. (A) Macroscopic images of representative tumor-containing whole livers from mice injected with *Rtl1* and control expression SB transposon constructs via hydrodynamic tail vein injection. Scale bars, 1 cm. (B) Tumor penetrance and (C) mean tumor burden in mice injected with *mCherry* only, *Rtl1* only, or *Rtl1*/shp53 expression SB transposon constructs. **P* < .05. ***P* < .01. *****P* < .0001. Error bars represent SEM.

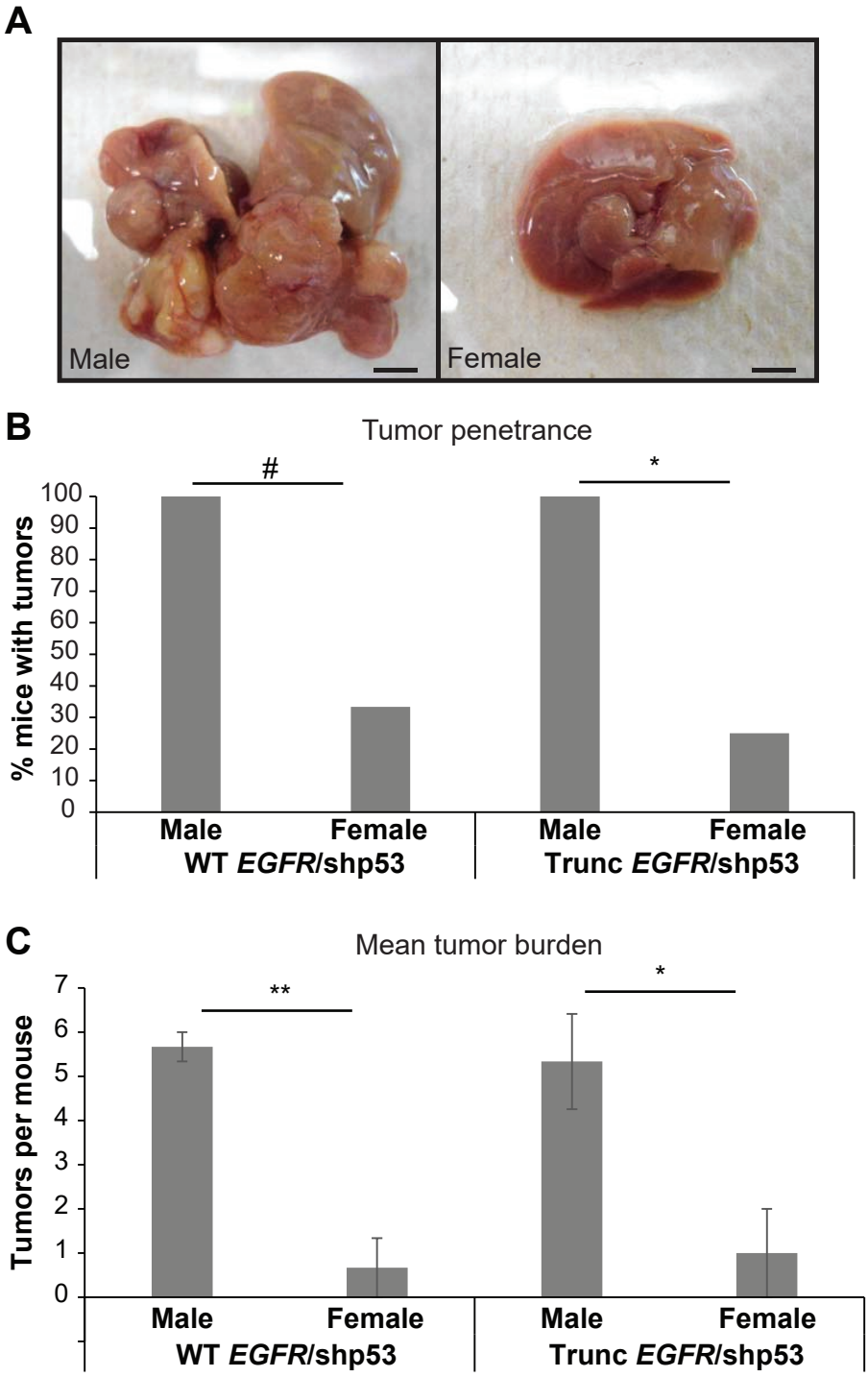

Figure 3.2. Validating the sex biased oncogenic potential of *EGFR in vivo*. (A) Representative images of gross liver from male and female *Fah* mutant mice injected with truncated *EGFR* and shp53. Scale bars, 0.5 cm. (B) Tumor penetrance and (C) mean tumor burden in male and female mice injected with full length *EGFR* and shp53 (WT *EGFR*/shp53) or truncated *EGFR* and shp53 (Trunc *EGFR*/shp53). #$P > .05$. *$P < .05$. **$P < .01$. Error bars represent SEM.

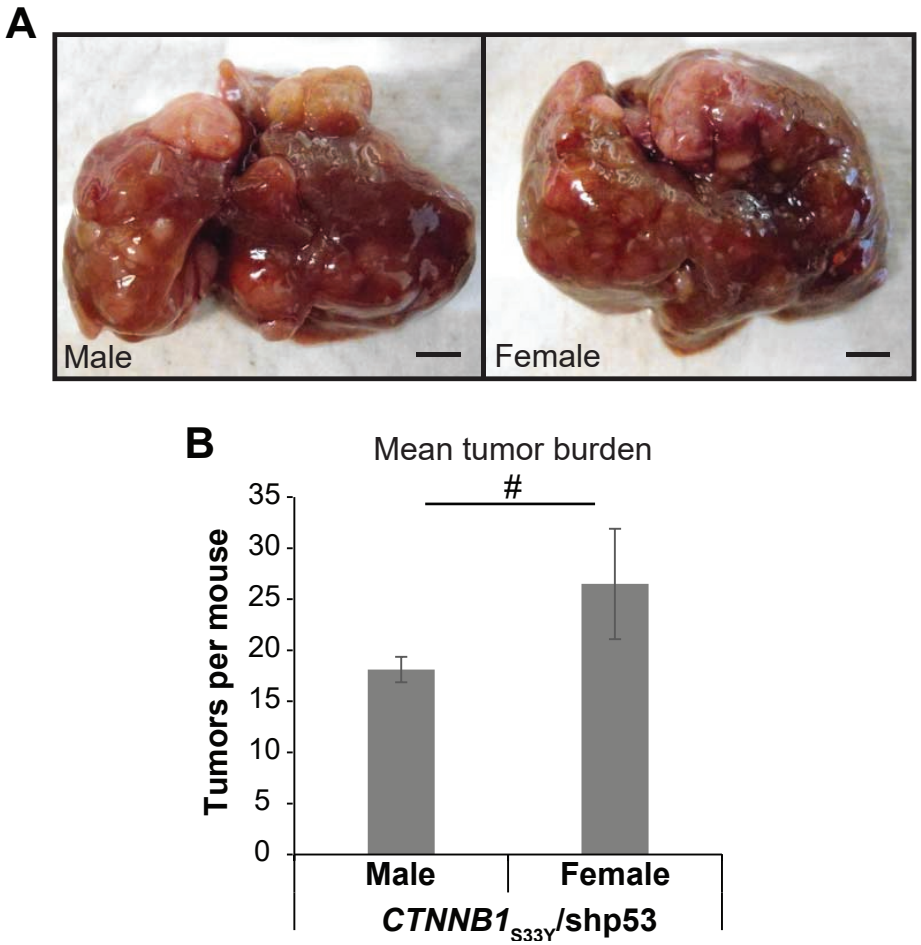

Figure 3.3. Oncogenic potential of *CTNNB1*$_{S33Y}$ in male and female mice *in vivo*. (A) Representative images of gross livers from male and female *Fah* mutant mice injected with *CTNNB1*$_{S33Y}$ and shp53. Scale bars, 0.5 cm. (B) Mean tumor burden in male and female mice injected with *CTNNB1*$_{S33Y}$ and shp53 (*CTNNB1*$_{S33Y}$/shp53). #*P* > .05. Error bars represent SEM.

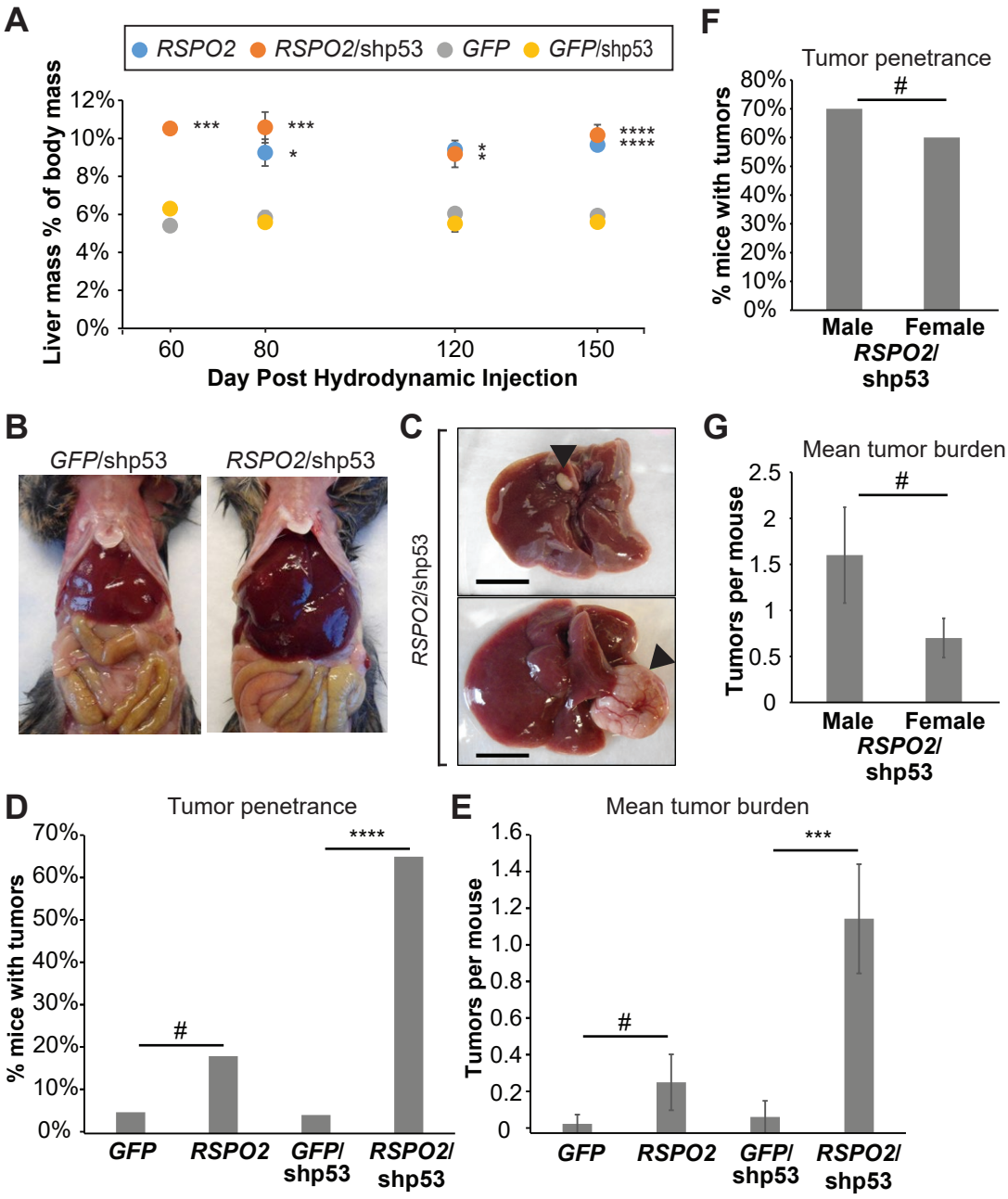

Figure 3.4. *RSPO2* promotes hepatomegaly and HCC. (A) Liver mass percent of body mass for *RSPO2*, *RSPO2*/shp53, and control injected mice. (B) Representative gross images of livers *in situ* from *RSPO2*/shp53 and *GFP*/shp53 injected mice at 150 days post-hydrodynamic injection. (C) Representative gross images of livers isolated from *RSPO2*/shp53 injected mice at 150 days post-hydrodynamic injection. Tumors are indicated by black arrowheads. Scale bars, 1cm. (D) Tumor penetrance and (E) mean tumor burden in *RSPO2*, *RSPO2*/shp53, and control injected mouse livers at 150 days post-hydrodynamic injection. (F) Tumor penetrance and (G) mean tumor burden in male *RSPO2*/shp53 injected mouse livers at 150 days post-hydrodynamic injection by sex. #$P > .05$. *$P < .05$. ***$P < .001$. ****$P < .0001$. Error bars represent SEM.

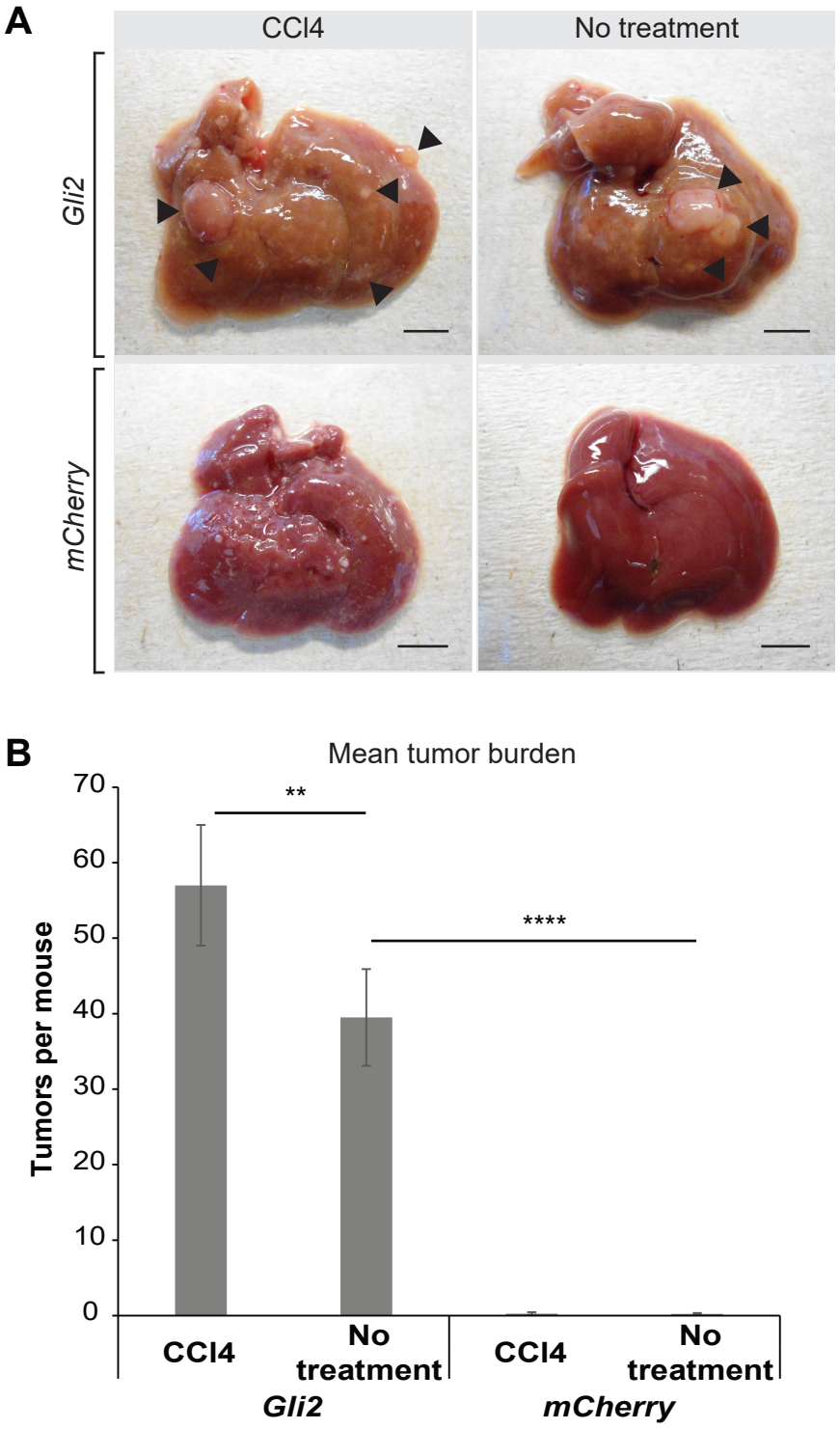

Figure 3.5. *Gli2* overexpression induces tumor formation. (A) Representative gross livers from *Gli2* and *mCherry* injected mice treated with CCl4 or no treatment. Black arrowheads indicate tumors. Scale bars, 0.5 cm. (B) Mean tumor burden in *Gli2* or *mCherry* injected mice treated with CCl4 or no treatment. ***P* < .01. *****P* < .0001. Error bars represent SEM.

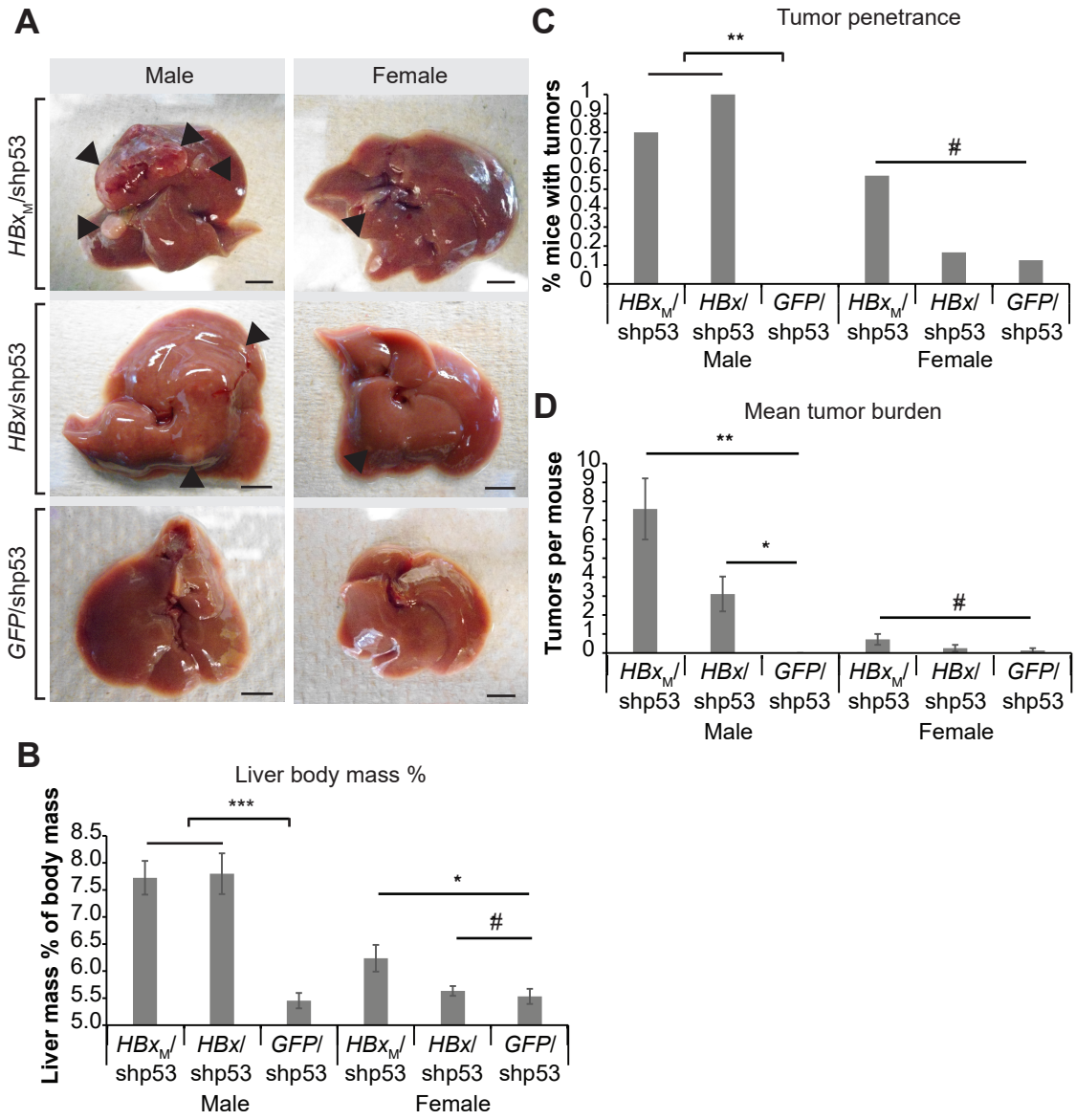

Figure 3.6. Mutant *HBx* is more oncogenic than *HBx* in the mouse liver. (A) Representative gross liver images from male and female mice injected with HBx_M/shp53, *HBX*-/shp53, or *GFP*/shp53. Scalebars, 0.5 cm. (B) Liver mass percent of body mass from HBx_M/shp53, *HBX*/shp53, or *GFP*/shp53 injected mice. (C) Tumor penetrance and (D) mean tumor burden in HBx_M/shp53, *HBX*/shp53, or *GFP*/shp53 injected mice. #$P > .05$. *$P < .05$. **$P < .01$. ****$P < .001$. Error bars represent SEM.

CHAPTER 4: SUMMARY

Significance of *Sleeping Beauty* transposon-based forward and reverse genetic liver cancer studies and potential future advancements

*Contains material from previously published work:

Tschida BR, Largaespada DA, Keng VW. Mouse models of cancer: Sleeping Beauty transposons for insertional mutagenesis screens and reverse genetic studies. Semin Cell Dev Biol 2014;27:86–95.

Distinct applications of the Sleeping Beauty transposon system for forward and reverse genetic studies of liver cancer in contexts relevant to the human disease are described in the preceding chapters. SB transposon insertional mutagenesis and SB transposon-based gene delivery are useful tools for modeling HCC. Applying these technologies to study liver cancer drivers in a variety of contexts can advance our understanding of the molecular pathogenesis of this disease. Since HCC does not usually arise in normal livers,[8] the relevance of these models is increased dramatically by applying these technologies in relevant conditions, by including both male and female animals, and modeling liver damage due to hepatic steatosis and fibrosis.

SB insertional mutagenesis has been established as a method to discover HCC associated genes in otherwise normal livers or in context of tumor-predisposing mutations.[48,54,92,95] HCC, however, almost always develops in context of chronic liver damage.[8] We used SB insertional mutagenesis to model HCC in context of diet and alcohol- induced hepatic steatosis, since steatosis is one of the most common risk factors for HCC and this risk is further increased with alcohol consumption.[36–39] This SB mutagenesis-driven model HCC is likely more relevant to the human disease than previous models. One particularly interesting finding of this study was the increase in tumor burden observed in female mice with hepatic steatosis, which modeled the higher representation of females we found in human steatosis-associated HCC cases than in the overall cohort examined. This finding highlights the importance of including both sexes of animals when modeling HCC, particularly in context of steatosis.

In this study, we found a distinct set of mutations from previous SB screens for liver cancer drivers,[48,54,92,95] which could lead to the development of new targeted therapies. The PKA/cAMP signaling pathway was specifically associated with the steatosis-associated CIS genes and with genes with expression changes in human

steatosis and alcohol-associated HCC. This pathway is activated in other cancers including fibrolamellar hepatocellular carcinoma, where a *DNAJB1-PRKACA* fusion leading to *PRKACA* upregulation may be the sole driver.[117,121,164] Inhibition of downsteam targets of PKA/cAMP signaling could be investigated for efficacy in inhibiting HCC growth. This pathway is also commonly activated by upstream signaling through β-adrenergic *receptors,*[122] leading to augmented lipid accumulation in hepatocytes[165] and alterations in hepatic autophagy, which is involved in non-alcoholic fatty liver disease and HCC.[166] Non-selective beta-blocker (NSBB) use in patients with cirrhosis has been linked to reduced HCC incidence in retrospective studies, but, to our knowledge, the effect of NSBB use of HCC development has not been functionally evaluated.[123–125] Both upstream and downstream inhibition of PKA/cAMP signaling could be tested in steatotic livers *in vivo* using the types mouse models described in the preceding chapters. Adrenergic signaling activates hepatic stem cells to proliferate in response to liver damage.[167] If the pathway is activated upstream in tumor cells in response to liver damage from steatosis, blocking activation of this pathway upstream by NSBBs could inhibit tumor formation in steatotic livers. If genetic or epigenetic alterations downstream of adrenergic receptor activation allows steatotic liver tumor cells to sustain signaling through this pathway in the absence of adrenergic receptor stimulation, the NSBBs would be ineffective, but expression of a dominant negative *PKA* mutation, *Prkar1a* glycine to aspartate substitution at position 325[168] would still inhibit tumor formation. Similarly, if this pathway is activated upstream in tumor cells in response to liver damage, then reversal of steatosis by diet alteration[169–171] could inhibit tumor progression.

We also identified *Nat10* as a HCC oncogene in our hepatic steatosis mouse model. NAT10 protein was found in both our study and another published study[126] to be

overexpressed in more than half of human HCC cases examined, and *NAT10* knockdown has been demonstrated to inhibit growth of several cancer cell types.[130,133] NAT10 acetyltransferase activity can be inhibited by a chemical compound, Remodelin.[134] Ribosome biogenesis, a process affected by NAT10 activity, can be inhibited using the RNA polymerase I specific inhibitor, CX-5461.[135,136] NAT10, therefore, provides another potential drug target for HCC treatment or prevention.

In addition to *Nat10*, we found 203 candidate liver cancer driving mutations, many of which are altered in human steatosis and alcohol associated HCC. Almost half of the steatosis-associated candidate liver cancer genes we found were enriched for mutations in mice with diet and alcohol-induced hepatic steatosis compared to mice on a normal diet.[48] This distinct set of mutations in the context of steatosis shows the interactions between the tumor predisposing environment of liver damage and the mutations promoting cancer are complex, and may alter the target cell for transformation. It has been suggested that the mechanism by which predisposing liver damage may increase cancer risk is by increasing the frequency of target cells for transformation.[172] If this were the case, the same liver cancer-promoting mutations would be found regardless of the predisposing conditions. We observed, however, a distinct set of mutations driving liver cancer in context of hepatic steatosis. One steatosis-enriched cancer gene, *Nat10,* was validated as an oncogene in a mouse model of hepatic steatosis. Other candidate oncogenes could be tested using the same method. Candidate tumor suppressors could be tested in steatotic *Fah*-deficient mouse livers using shRNA knockdown or CRISPR/CAS mutation, which has been used to edit *Fah*-deficient hepatocytes *in vivo*.[173]

Forward genetic screens and human mutational data are revealing a large number of liver cancer-associated genes. Reverse genetic models can be used to test the roles of

these genes in tumorigenesis and study the mechanisms by which these genes drive tumorigenesis, which may inform the development of novel therapies. In general, reverse genetic models driven by known agents may be more useful for testing therapeutic agents than non-specific models, which may not contain the molecular alteration targeted by the therapeutic agent. We used SB gene delivery and the selective *Fah* mutant mouse model to test candidate drivers and model HCC in otherwise normal livers, in mice of both sexes, in context of hepatic fibrosis, and in context of hepatic steatosis. Here, we described the use of SB gene delivery for the generation of 12 different HCC models driven by the expression of 7 different oncogenes and mutant oncogene variants, alone, in combination with knockdown of tumor suppressor gene *Trp53*, in fibrotic livers, in steatotic livers, and in otherwise normal livers. These represent different molecular subclasses of HCC including two models each of the previously described Wnt/β-catenin subclass and the Poly7 subclass.[53] Drivers of the proliferation, interferon, and unannotated subclasses[53] could be tested using similar methods to generate models of those subclasses of HCC. These findings have furthered our understanding of HCC pathogenesis in these various contexts. The HCC models we generated and this method of modeling HCC in disease-relevant contexts of chronic liver damage could be used to study the mechanisms of disease progression and could also provide useful preclinical models for therapeutic testing.

We modeled *Nat10*-induced liver cancer in context of hepatic steatosis, for example, validating the oncogenic role of *Nat10* in steatotic liver. NAT10 acetylates multiple cellular targets, and our SB reverse genetic model of *Nat10*-induced liver tumorigenesis could prove useful for further studies addressing the mechanisms by which *Nat10* drives liver cancer. NAT10 is required for a highly conserved modification of 18S

rRNAs with an important role in ribosome biogenesis.[130] NAT10 could allow cells to regulate translation in a nutrient-responsive manner, responding to the abundance of acetylCoA in steatotic livers[132] by promoting ribosome biosynthesis, which may be rate limiting for HCC, only in the presence of acetylCoA.[131] Treating mice with hepatic *Nat10* overexpression with either Remodelin,[134] an inhibitor of NAT10 acetyltransferase activity, or CX-5461,[135,136] an RNA polymerase I specific inhibitor, could address the role of ribosome biogenesis in *Nat10*-driven liver tumor formation. If CX-5461 treatment inhibits *Nat10*-driven liver tumor formation, this would reveal ribosome biogenesis is a function of *Nat10* with an important role in tumorigenesis, whereas if Remodelin but not CX-5461 inhibits liver tumor formation, this would reveal a different *Nat10* function is involved in tumor formation. At the same time, this could act as a preclinical model to test the efficacy of these drugs in inhibiting *Nat10*-driven liver tumorigenesis.

Drivers of HCC developing in chronic liver damage contexts can be addressed with the SB gene delivery system and the selective *Fah* mutant mouse model. We modeled fibrosis, alcohol-associated steatosis, and Hepatitis B Virus (HBV)-associated liver cancer. Other dietary models of hepatic steatosis could be used to test drivers of steatosis-associated HCC. Several different dietary models of non-alcoholic fatty liver disease have been described, including high fat diets, which induce obesity, hepatic steatosis and fibrosis, and high fat-high fructose and/or sucrose diets, which induces a similar degree obesity and hepatic steatosis as high fat diets but with more severe fibrosis and HCC.[174,175] Expression vectors for HBV or Hepatitis C Virus (HCV) viral proteins could be co-administered with candidate oncogenes to evaluate host genetic alterations promoting HCC in context of viral infection. This model could also be improved using

conditional expression vectors to investigate the role of candidate oncogenes in tumor initiation versus maintenance.

The mosaic mouse model of HCC in which liver progenitor cells are genetically modified in culture and transplanted into syngeneic recipient mice livers[76] could also be used to test candidate HCC genes in disease-relevant liver damage contexts like fibrosis and steatosis. This would allow candidate HCC genes to be expressed in a smaller population of hepatocytes in livers that have not undergone full regeneration. Livers of *Fah*-deficient, immunodeficient mice have been repopulated with human hepatocytes, generating mice with humanized livers.[176] This model could also be used in conjunction with liver damage to model HCC developing in relevant disease conditions, with the major advantage of testing candidate cancer drivers in human hepatocytes *in vivo*. Since the humanized mouse liver model lacks a functioning immune system but allows the study of tumor development in human hepatocytes *in vivo*,[176] it would be a useful complementary approach to SB gene delivery to *Fah*-deficient mouse livers or mosaic mouse livers with genetically modified which liver progenitor cells, both of which are purely mouse models, but allow the study of liver tumor progression in context of a functioning immune system.[76,102]

The application of SB to generate forward and reverse genetic models of cancer in context of disease-relevant damaged tissue, while especially important in the liver given the close connection between chronic liver damage and HCC, is not exclusively relevant to the study of liver cancer. Obesity is a risk factor for many cancer types including liver, colorectal, pancreatic, kidney, esophageal, thyroid, melanoma, leukemia, breast, endometrial, cervical, ovarian, and prostate cancers.[177] Genetic studies could be conducted in these tissue types using SB for insertional mutagenesis or delivery of

oncogenes in context of diet-induced obesity to study the interaction between molecular cancer drivers and the selective pressures caused by obesity-induced changes in cytokines, adipokines, insulin resistance, hormones, and inflammation.[177] Certain infectious agents are also linked to cancer risk, including HBV and HCV increasing the risk for liver cancer, human papillomavirus for cervical and oropharanx cancer, Epstein-Barr virus for Hodgkin's and Burkitt's lymphomas, and *Helicobacter pylori* for gastric cancer.[159] SB genetic studies of these cancers could be conducted in the presence of viral components or bacterial infection to identify or study the genetic drivers of these cancers in context of a relevant infection. The studies we conducted have improved our understanding of the molecular drivers of HCC in relevant liver environments, and could provide new models for preclinical therapeutic testing. Similar methods might be employed to study other cancer types in relevant environments.

BIBLIOGRAPHY

1. Alison MR. Liver Stem Cells: Implications for Hepatocarcinogenesis. Stem Cell Rev 2005;1:253–260.
2. Zhang S-H, Cong W-M, Wu M-C. Focal nodular hyperplasia with concomitant hepatocellular carcinoma: a case report and clonal analysis. J Clin Pathol 2004;57:556–9.
3. Govindarajan S, Craig J, Valinluck B. Clonal origin of hepatitis B virus-associated hepatocellular carcinoma. Hum Pathol 1988;19:403–5.
4. Yamamoto T, Kajino K, Kudo M, et al. Determination of the clonal origin of multiple human hepatocellular carcinomas by cloning and polymerase chain reaction of the integrated hepatitis B virus DNA. Hepatology 1999;29:1446–52.
5. Ng IO, Guan XY, Poon RT, et al. Determination of the molecular relationship between multiple tumour nodules in hepatocellular carcinoma differentiates multicentric origin from intrahepatic metastasis. J Pathol 2003;199:345–53.
6. Lowes KN, Brennan BA, Yeoh GC, et al. Oval cell numbers in human chronic liver diseases are directly related to disease severity. Am J Pathol 1999;154:537–41.
7. Roskams TA, Libbrecht L, Desmet VJ. Progenitor cells in diseased human liver. Semin Liver Dis 2003;23:385–96.
8. El-Serag HB. Hepatocellular carcinoma. N Engl J Med 2011;365:1118–27.
9. Libbrecht L, Desmet V, Roskams T. Preneoplastic lesions in human hepatocarcinogenesis. Liver Int 2005;25:16–27.
10. Schlageter M, Terracciano LM, D'Angelo S, et al. Histopathology of hepatocellular carcinoma. World J Gastroenterol 2014;20:15955–15964.
11. Edmondson HA, Steiner PE. Primary carcinoma of the liver: a study of 100 cases among 48,900 necropsies. Cancer 1954;7:462–503.
12. Pawlik TM, Gleisner AL, Anders RA, et al. Preoperative assessment of hepatocellular carcinoma tumor grade using needle biopsy: implications for transplant eligibility. Ann Surg 2007;245:435–42.
13. Ferlay J, Soerjomataram I, Ervik M, et al. GLOBOCAN 2012 v1.0, Cancer Incidence and Mortality Worldwide: IARC CancerBase No. 11 [Internet]. Lyon, Fr Int Agency Res Cancer 2013. Available at: http://globocan.iarc.fr [Accessed February 27, 2017].
14. Torre LA, Bray F, Siegel RL, et al. Global Cancer Statistics, 2012. CA A cancer J Clin 2015;65:87–108.
15. Howlader N, Noone A, Krapcho M, et al. SEER Cancer Statistics Review, 1975-2011, National Cancer Institute. Bethesda, MD 2014:based on November 2013 SEER data submission, poste.

16. White DL, Thrift AP, Kanwal F, et al. Incidence of Hepatocellular Carcinoma in all 50 United States, From 2000 Through 2012. Gastroenterology 2016:pii: S0016-5085(16)35389-6.

17. Naugler WE, Sakurai T, Kim S, et al. Gender disparity in liver cancer due to sex differences in MyD88-dependent IL-6 production. Science (80-) 2007;317:121–4.

18. Lee UE, Friedman SL. Mechanisms of hepatic fibrogenesis. Best Pr Res Clin Gastroenterol 2011;25:195–206.

19. Caldwell SH, Oelsner DH, Iezzoni JC, et al. Cryptogenic cirrhosis: clinical characterization and risk factors for underlying disease. Hepatology 1999;29:664–669.

20. Parkin DM. The global health burden of infection-associated cancers in the year 2002. Int J Cancer 2006;118:3030–3044.

21. Ghany M, Liang TJ. Drug targets and molecular mechanisms of drug resistance in chronic hepatitis B. Gastroenterology 2007;132:1574–85.

22. But DYK, Lai CL, Yuen MF. Natural history of hepatitis-related hepatocellular carcinoma. World J Gastroenterol 2008;14:1652–1656.

23. El-Serag HB. Epidemiology of viral hepatitis and hepatocellular carcinoma. Gastroenterology 2012;142:1264–1273.

24. Kawai-Kitahata F, Asahina Y, Tanaka S, et al. Comprehensive analyses of mutations and hepatitis B virus integration in hepatocellular carcinoma with clinicopathological features. J Gastroenterol 2016;51:473–486.

25. Sung W-K, Zheng H, Li S, et al. Genome-wide survey of recurrent HBV integration in hepatocellular carcinoma. Nat Genet 2012;44:765–9.

26. Levrero M, Zucman-Rossi J. Mechanisms of HBV-induced hepatocellular carcinoma. J Hepatol 2016;64:S84–S101.

27. Sanyal AJ, Yoon SK, Lencioni R. The etiology of hepatocellular carcinoma and consequences for treatment. Oncologist 2010;15:14–22.

28. Lonardo A, Adinolfi LE, Petta S, et al. Hepatitis C and diabetes: the inevitable coincidence? Expert Rev Anti Infect Ther 2009;7:293–308.

29. Cua IHY, Hui JM, Bandara P, et al. Insulin resistance and liver injury in hepatitis C is not associated with virus-specific changes in adipocytokines. Hepatology 2007;46:66–73.

30. Heidelbaugh JJ, Bruderly M. Cirrhosis and chronic liver failure: part I. Diagnosis and evaluation. Am Fam Physician 2006;74:756–62.

31. Seitz HK, Stickel F. Risk factors and mechanisms of hepatocarcinogenesis with special emphasis on alcohol and oxidative stress. Biol Chem 2006;387:349–360.

32. IARC. Acetaldehyde IARC monographs on the evaluation of the carcinogenic risk to humans. Reevaluation of some organic chemicals, hydrazine and hydrogen peroxides. Lyon Int Agency Res Cancer 1999;71:319–335.

33. Lieber CS. Alcoholic fatty liver: its pathogenesis and mechanism of progression to inflammation and fibrosis. Alcohol 2004;34:9–19.

34. Lieber CS, Jones DP, DeCarli LM. Effects of Prolonged Ethanol Intake: Production of Fatty Liver Despite Adequate Diets. J Clin Invest 1965;44:1009–1021.

35. Becker U, Deis A, Sørensen T, et al. Prediction of risk of liver disease by alcohol intake, sex, and age: a prospective population study. Hepatology 1996;23:1025–9.

36. Ong JP, Younossi ZM. Epidemiology and Natural History of NAFLD and NASH. Clin Liver Dis 2007;11:1–16.

37. Ascha MS, Hanouneh IA, Lopez R, et al. The incidence and risk factors of hepatocellular carcinoma in patients with nonalcoholic steatohepatitis. Hepatology 2010;51:1972–1978.

38. Pekow JR, Bhan AK, Zheng H, et al. Hepatic steatosis is associated with increased frequency of hepatocellular carcinoma in patients with hepatitis C-related cirrhosis. Cancer 2007;109:2490–2496.

39. Lazo M, Clark JM. The Epidemiology of Nonalcoholic Fatty Liver Disease : A Global Perspective. Semin Liver Dis 2008;28:339–50.

40. Yu J, Shen J, Sun TT, et al. Obesity, insulin resistance, NASH and hepatocellular carcinoma. Semin Cancer Biol 2013;E pub ahea.

41. Calle EE, Thun MJ. Obesity and cancer. Oncogene 2004;23:6365–78.

42. Falck-Ytter Y, Younossi ZM, Marchesini G, et al. Clinical features and natural history of nonalcoholic steatosis syndromes. Semin Liver Dis 2001;21:17–26.

43. Hanahan D, Weinberg RA, Francisco S. The hallmarks of cancer [Review]. Cell 2000;100:57–70.

44. Hanahan D, Weinberg RA. Hallmarks of cancer: the next generation. Cell 2011;144:646–74.

45. Boyault S, Rickman DS, Reynies A de, et al. Transcriptome classification of HCC is related to gene alterations and to new therapeutic targets. Hepatology 2007;45:42–52.

46. Totoki Y, Tatsuno K, Covington KR, et al. Trans-ancestry mutational landscape of hepatocellular carcinoma genomes. Nat Genet 2014;46:1267–73.

47. Polakis P. Wnt Signaling in Cancer. Cold Spring Harb Perspect Biol 2012;4:a008052.

48. Keng VW, Villanueva A, Chiang DY, et al. A conditional transposon-based insertional mutagenesis screen for hepatocellular carcinoma-associated genes in mice. Nat Biotechnol 2009;27:264–274.

49. Chu JS, Ge FJ, Zhang B, et al. Expression and prognostic value of VEGFR-2, PDGFR-β, and c-Met in advanced hepatocellular carcinoma. J Exp Clin Cancer Res 2013;3:16.

50. Wilhelm SM, Adnane L, Newell P, et al. Preclinical overview of sorafenib, a multikinase inhibitor that targets both Raf and VEGF and PDGF receptor tyrosine kinase signaling. Mol Cancer Ther 2008;7:3129–3140.

51. Zucman-Rossi J, Villanueva A, Nault JC, et al. Genetic Landscape and Biomarkers of Hepatocellular Carcinoma. Gastroenterology 2015;149:1226–1239.

52. Buendia MA. Genetics of hepatocellular carcinoma. Semin Cancer Biol 2000;10:185–200.

53. Chiang DY, Villanueva A, Hoshida Y, et al. Focal gains of VEGFA and molecular classification of hepatocellular carcinoma. Cancer Res 2008;68:6779–88.

54. Keng VW, Sia D, Sarver AL, et al. Sex bias occurrence of hepatocellular carcinoma in Poly7 molecular subclass is associated with EGFR. Hepatology 2013;57:120–30.

55. Raza A, Sood GK. Hepatocellular carcinoma review: Current treatment, and evidence-based medicine. World J Gastroenterol 2014;20:4115–4127.

56. Bruix J, Qin S, Merle P, et al. Regorafenib for patients with hepatocellular carcinoma who progressed on sorafenib treatment (RESORCE): a randomised, double-blind, placebo-controlled, phase 3 trial. Lancet 2017;389:56–66.

57. Llovet J, Ricci S, Mazzaferro V, et al. Sorafenib in Advanced Hepatocellular Carcinoma. N Engl J Med 2008;359:378–90.

58. Wilhelm SM, Dumas J, Adnane L, et al. Regorafenib (BAY 73-4506): A new oral multikinase inhibitor of angiogenic, stromal and oncogenic receptor tyrosine kinases with potent preclinical antitumor activity. Int J Cancer 2011;129:245–255.

59. Ho DWH, Kai AKL, Ng IOL. TCGA whole-transcriptome sequencing data reveals significantly dysregulated genes and signaling pathways in hepatocellular carcinoma. Front Med 2015;9:322–330.

60. Woo HG, Park ES, Thorgeirsson SS, et al. Exploring Genomic Profiles of Hepatocellular Carcinoma. Mol Carcinog 2011;50:235–243.

61. Schulze K, Imbeaud S, Letouzé E, et al. Exome sequencing of hepatocellular carcinomas identifies new mutational signatures and potential therapeutic targets. Nat Genet 2015;47:505–511.

62. Zimmermann U, Feneux D, Mathey G, et al. Chromosomal aberrations in hepatocellular carcinomas: relationship with pathological features. Hepatology 1997;26:1492–8.

63. Thorgeirsson SS, Grisham JW. Molecular pathogenesis of human hepatocellular carcinoma. Nat Genet 2002;31:339–46.

64. Heindryckx F, Colle I, Vlierberghe H Van. Experimental mouse models for hepatocellular carcinoma research. Int J Exp Pathol 2009;90:367–386.

65. Araki K, Miyazaki J, Hino O, et al. Expression and replication of hepatitis B virus genome in transgenic mice. Proc Natl Acad Sci U S A 1989;86:207–11.

66. Babinet C, Farza H, Morello D, et al. Specific expression of hepatitis-B surface-antigen (Hbsag) in transgenic mice. Science (80-) 1985;230:1160–3.

67. Xiong J, Yao YC, Zi XY, et al. Expression of hepatitis B virus X protein in transgenic mice. World J Gastroenterol 2003;9:112–6.

68. Lerat H, Honda M, Beard MR, et al. Steatosis and liver cancer in transgenic mice expressing the structural and nonstructural proteins of hepatitis C virus. Gastroenterology 2002;122:352–65.

69. Moriya K, Fujie H, Shintani Y, et al. The core protein of hepatitis C virus induces hepatocellular carcinoma in transgenic mice. Nat Med 1998;4:1065–7.

70. Tanaka N, Moriya K, Kiyosawa K, et al. Hepatitis C virus core protein induces spontaneous and persistent activation of peroxisome proliferator-activated receptor alpha in transgenic mice: implications for HCV-associated hepatocarcinogenesis. Int J Cancer 2008;122:124–31.

71. Naas T, Ghorbani M, Alvarez-Maya I, et al. Characterization of liver histopathology in a transgenic mouse model expressing genotype 1a hepatitis C virus core and envelope proteins 1 and 2. J Gen Virol 2005;86:2185–96.

72. Lee JS, Chu IS, Mikaelyan A, et al. Application of comparative functional genomics to identify best-fit mouse models to study human cancer. Nat Genet 2004;36:1306–11.

73. Harada N, Oshima H, Katoh M, et al. Hepatocarcinogenesis in mice with beta-catenin and Ha-ras gene mutations. Cancer Res 2004;64:48–54.

74. Borlak J, Meier T, Halter R, et al. Oncogene. 2005 Mar 10;24(11):1809-19. Epidermal growth factor-induced hepatocellular carcinoma: gene expression profiles in precursor lesions, early stage and solitary tumours. Oncogene 2005;24:1809–19.

75. Watanabe S, Horie Y, Kataoka E, et al. Non-alcoholic steatohepatitis and hepatocellular carcinoma: lessons from hepatocyte-specific phosphatase and tensin homolog (PTEN)-deficient mice. J Gastroenterol Hepatol 2007;22:S96–S100.

76. Zender L, Xue W, Cordon-Cardo C, et al. Generation and Analysis of Genetically Defined Liver Carcinomas Derived from Bipotential Liver Progenitors. Cold Spring Harb Symp Quant Biol 2005;70:251–261.

77. Zender L, Spector MS, Xue W, et al. Identification and validation of oncogenes in liver cancer using an integrative oncogenomic approach. Cell 2006;125:1253–67.

78. Zender L, Xue W, Zuber J, et al. An oncogenomics-based in vivo RNAi screen identifies tumor suppressors in liver cancer. Cell 2008;135:852–864.

79. Sawey ET, Chanrion M, Cai C, et al. Identification of a Therapeutic Strategy Targeting Amplified FGF19 in Liver Cancer by Oncogenomic Screening. Cancer Cell 2011;19:347–358.

80. Kornek M, Raskopf E, Tolba R, et al. Accelerated orthotopic hepatocellular carcinomas growth is linked to increased expression of pro-angiogenic and prometastatic factors in murine liver fibrosis. Liver Int 2008;28:509–18.

81. Nakatani T, Roy G, Fujimoto N, et al. Sex hormone dependency of diethylnitrosamine-induced liver tumors in mice and chemoprevention by leuprorelin. Japanese J cancer Res 2001;92:249–56.

82. Yoshida LS, Miyazawa T, Hatayama I, et al. Phosphatidylcholine peroxidation and liver cancer in mice fed a choline-deficient diet with ethionine. Free Radic Biol Med 1993;14:191–199.

83. Gyamfi MA, Damjanov I, French S, et al. The pathogenesis of ethanol versus methionine and choline deficient diet-induced liver injury. Biochem Pharmacol 2008;75:981–95.

84. Croager EJ, Smith PGJ, Yeoh GCT. Ethanol interactions with a choline-deficient, ethionine-supplemented feeding regime potentiate pre-neoplastic cellular alterations in rat liver. Carcinogenesis 2002;23:1685–93.

85. Ivics Z, Hackett PB, Plasterk RH, et al. Molecular reconstruction of Sleeping Beauty, a Tc1-like transposon from fish, and its transposition in human cells. Cell 1997;91:501–10.

86. Keng VW, Yae K, Hayakawa T, et al. Region-specific saturation germline mutagenesis in mice using the Sleeping Beauty transposon system. Nat Methods 2005;2:763–769.

87. Collier LS, Carlson CM, Ravimohan S, et al. Cancer gene discovery in solid tumours using transposon-based somatic mutagenesis in the mouse. Nature 2005;436:272–6.

88. Dupuy AJ, Akagi K, Largaespada DA, et al. Mammalian mutagenesis using a highly mobile somatic Sleeping Beauty transposon system. Nature 2005;436:221–226.

89. Dupuy AJ, Fritz S, Largaespada DA. Transposition and Gene Disruption in the Male Germline of the Mouse. Genesis 2001;30:82–88.

90. Copeland NG, Jenkins NA. Harnessing transposons for cancer gene discovery. Nat Rev Cancer 2010;10:696–706.

91. Howell VM. Sleeping Beauty - A mouse model for all cancers? Cancer Lett 2012;317:1–8.

92. Dupuy AJ, Rogers LM, Kim J, et al. A modified sleeping beauty transposon system that can be used to model a wide variety of human cancers in mice. Cancer Res 2009;69:8150–6.

93. Geurts A. Gene transfer into genomes of human cells by the sleeping beauty transposon system. Mol Ther 2003;8:108–117.

94. Starr TK, Allaei R, Silverstein KAT, et al. A Transposon-Based Genetic Screen in Mice Identifies Genes Altered in Colorectal Cancer. Science (80-) 2009;323:1747–1750.

95. O'Donnell KA, Keng VW, York B, et al. A Sleeping Beauty mutagenesis screen reveals a tumor suppressor role for Ncoa2/Src-2 in liver cancer. Proc Natl Acad Sci U S A 2012;109:E1377-86.

96. Rahrmann EP, Collier LS, Knutson TP, et al. Identification of PDE4D as a proliferation promoting factor in prostate cancer using a Sleeping Beauty transposon-based somatic mutagenesis screen. Cancer Res 2009;69:4388–97.

97. Rahrmann EP, Watson AL, Keng VW, et al. Forward genetic screen for malignant peripheral nerve sheath tumor formation identifies new genes and pathways driving tumorigenesis. Nat Genet 2013;45:756–66.

98. Vries A de, Flores ER, Miranda B, et al. Targeted point mutations of p53 lead to dominant-negative inhibition of wild-type p53 function. Proc Natl Acad Sci U S A 2002;99:2948–53.

99. Riordan JD, Keng VW, Tschida BR, et al. Identification of rtl1, a retrotransposon-derived imprinted gene, as a novel driver of hepatocarcinogenesis. PLoS Genet 2013;9:e1003441.

100. Bard-Chapeau EA, Nguyen A-T, Rust AG, et al. Transposon mutagenesis identifies genes driving hepatocellular carcinoma in a chronic Hepatitis B mouse model. Nat Genet 2014;46:24–32.

101. Kodama T, Bard-Chapeau EA, Newberg JY, et al. Two-Step Forward Genetic Screen in Mice Identifies Ral GTPase-Activating Proteins as Suppressors of Hepatocellular Carcinoma. Gastroenterology 2016;151:324–337.e12.

102. Wangensteen KJ, Wilber A, Keng VW, et al. A facile method for somatic, lifelong manipulation of multiple genes in the mouse liver. Hepatology 2008;47:1714–24.

103. Wiesner SM, Decker S a, Larson JD, et al. De novo induction of genetically engineered brain tumors in mice using plasmid DNA. Cancer Res 2009;69:431–9.

104. Belur L. Gene insertion and long-term expression in lung mediated by the sleeping beauty transposon system. Mol Ther 2003;8:501–507.

105. Ohlfest JR, Demorest ZL, Motooka Y, et al. Combinatorial antiangiogenic gene therapy by nonviral gene transfer using the sleeping beauty transposon causes tumor regression and improves survival in mice bearing intracranial human glioblastoma. Mol Ther 2005;12:778–88.

106. Ivics Z, Kaufman CD, Zayed H, et al. The Sleeping Beauty transposable element: evolution, regulation and genetic applications. Curr Issues Mol Biol 2004;6:43–56.

107. Bell JB, Podetz-Pedersen KM, Aronovich EL, et al. Preferential delivery of the Sleeping Beauty transposon system to livers of mice by hydrodynamic injection. Nat Protoc 2007;2:3153–3165.

108. Keng VW, Tschida BR, Bell JB, et al. Modeling hepatitis B virus X-induced hepatocellular carcinoma in mice with the Sleeping Beauty transposon system. Hepatology 2011;53:781–90.

109. Yang JD, Harmsen WS, Slettedahl SW, et al. Factors That Affect Risk for Hepatocellular Carcinoma and Effects of Surveillance. Clin Gastroenterol Hepatol 2011;9:617–623.

110. Li Z, Tuteja G, Schug J, et al. Foxa1 and Foxa2 are essential for sexual dimorphism in liver cancer. Cell 2012;148:72–83.

111. Moya M, Benet M, Guzmán C, et al. Foxa1 reduces lipid accumulation in human hepatocytes and is down-regulated in nonalcoholic fatty liver. PLoS One 2012;7.

112. Howell JJ, Stoffel M. Nuclear export-independent inhibition of Foxa2 by insulin. J Biol Chem 2009;284:24816–24824.

113. Gan L, Chitturi S, Farrell GC. Mechanisms and implications of age-related changes in the liver: Nonalcoholic fatty liver disease in the elderly. Curr Gerontol Geriatr Res 2011;2011.

114. Honma T, Yanaka M, Tsuduki T, et al. Increased Lipid Accumulation in Liver and White Adipose Tissue in Aging in the SAMP10 Mouse. J Nutr Sci Vitaminol (Tokyo) 2011;57:123–129.

115. Sarver A, Erdman J, Starr T, et al. TAPDANCE: An Automated tool to identify and annotate Transposon insertion CISs and associations between CISs from next generation sequence data. BMC Bioinformatics 2012;13:154.

116. Cauthron RD, Carter KB, Liauw S, et al. Physiological Phosphorylation of Protein Kinase A at Thr-197 Is by a Protein Kinase A Kinase. Mol Cell Biol 1998;18:1416–1423.

117. Cheung J, Ginter C, Cassidy M, et al. Structural insights into mis-regulation of protein kinase A in human tumors. Proc Natl Acad Sci U S A 2015;112:1374–9.

118. Yang H, Yang L. Targeting cAMP/PKA pathway for glycemic control and type 2 diabetes therapy. J Mol Endocrinol 2016;57:R93–R108.

119. Woo CWH, Siow YL, Karmin O. Homocysteine activates cAMP-response element binding protein in HepG2 through cAMP/PKA signaling pathway. Arterioscler Thromb Vasc Biol 2006;26:1043–1050.

120. Ji H, Shen X, Zhang Y, et al. Activation of cyclic adenosine monophosphate-dependent protein kinase a signaling prevents liver ischemia/reperfusion injury in mice. Liver Transplant 2012;18:659–670.

121. Honeyman JN, Simon EP, Robine N, et al. Detection of a recurrent DNAJB1-PRKACA chimeric transcript in fibrolamellar hepatocellular carcinoma. Science (80-) 2014;343:1010–4.

122. Cole SW, Sood AK. Molecular pathways: Beta-adrenergic signaling in cancer. Clin Cancer Res 2012;18:1201–1206.

123. Thiele M, Albillos A, Abazi R, et al. Non-selective beta-blockers may reduce risk of hepatocellular carcinoma: A meta-analysis of randomized trials. Liver Int 2015;35:2009–2016.

124. Patel H, Kumar A, Shah N, et al. Role of Non-Selective Beta Blockers in Hepatocellular Carcinoma: An Analysis in Patients with Cirrhosis and Portal Hypertenrion. North Am J Med Sci 2015;8:105–108.

125. Nkontchou G, Aout M, Mahmoudi A, et al. Effect of long-term propranolol treatment on hepatocellular carcinoma incidence in patients with HCV-associated cirrhosis. Cancer Prev Res 2012;5:1007–1014.

126. Zhang X, Liu J, Yan S, et al. High expression of N-acetyltransferase 10: a novel independent prognostic marker of worse outcome in patients with hepatocellular carcinoma. Int J Clin Exp Pathol 2015;8:14765–71.

127. Ma R, Chen J, Jiang S, et al. Up regulation of NAT10 promotes metastasis of hepatocellular carcinoma cells through epithelial-to-mesenchymal transition. Am J Transl Re 2016;8:4215–4223.

128. Lv J, Liu H, Wang Q, et al. Molecular cloning of a novel human gene encoding histone acetyltransferase-like protein involved in transcriptional activation of hTERT. Biochem Biophys Res Commun 2003;311:506–513.

129. Shen Q, Zheng X, McNutt MA, et al. NAT10, a nucleolar protein, localizes to the midbody and regulates cytokinesis and acetylation of microtubules. Exp Cell Res 2009;315:1653–1667.

130. Ito S, Horikawa S, Suzuki T, et al. Human NAT10 is an ATP-dependent rna acetyltransferase responsible for N4-acetylcytidine formation in 18 S ribosomal RNA (rRNA). J Biol Chem 2014;289:35724–35730.

131. Lee C-D, Tu BP. Metabolic influences on RNA biology and translation. Crit Rev Biochem Mol Biol 2017;Feb:1–9.

132. Gusdon AM, Song K-X, Qu S. Nonalcoholic Fatty liver disease: pathogenesis and therapeutics from a mitochondria-centric perspective. Oxid Med Cell Longev 2014;2014:637027.

133. Tan TZ, Miow QH, Huang RYJ, et al. Functional genomics identifies five distinct molecular subtypes with clinical relevance and pathways for growth control in epithelial ovarian cancer. EMBO Mol Med 2013;5:1051–66.

134. Larrieu D, Britton S, Demir M, et al. Chemical inhibition of NAT10 corrects defects of laminopathic cells. Science (80-) 2014;344:527–32.

135. Drygin D, Lin A, Bliesath J, et al. Targeting RNA polymerase I with an oral small molecule CX-5461 inhibits ribosomal RNA synthesis and solid tumor growth. Cancer Res 2011;71:1418–1430.

136. Haddach M, Schwaebe MK, Michaux J, et al. Discovery of CX-5461, the first direct and selective inhibitor of RNA polymerase I, for cancer therapeutics. ACS Med Chem Lett 2012;3:602–606.

137. Shu J, Dolman GE, Duan J, et al. Statistical colour models: an automated digital image analysis method for quantification of histological biomarkers. Biomed Eng Online 2016;15.

138. Janik C, Starr T. Identification of Sleeping Beauty transposon insertions in solid tumors using linker-mediated PCR. J Vis Exp 2013;72:e5015.

139. Gao J, Aksoy BA, Dogrusoz U, et al. Integrative analysis of complex cancer genomics and clinical profiles using the cBioPortal. Sci Signal 2013;6:pl1.

140. Cerami E, Gao J, Dogrusoz U, et al. The cBio Cancer Genomics Portal: An open platform for exploring multidimensional cancer genomics data. Cancer Discov 2012;2:401–404.

141. Bray, Nicolas L Pimentel, Harold Melsted P, Pachter L. Near-optimal probabilistic RNA-seq quantification. Nat Biotechnol 2016;34:525–7.

142. Tschida BR, Largaespada DA, Keng VW. Mouse models of cancer: Sleeping Beauty transposons for insertional mutagenesis screens and reverse genetic studies. Semin Cell Dev Biol 2014;27:86–95.

143. Rocha ST da, Edwards CA, Ito M, et al. Genomic imprinting at the mammalian Dlk1-Dio3 domain. Trends Genet 2008;24:306–316.

144. Braconi C, Kogure T, Valeri N, et al. microRNA-29 can regulate expression of the long non-coding RNA gene MEG3 in hepatocellular cancer. Oncogene 2011;30:4750–6.

145. Huang J, Zhang X, Zhang M, et al. Up-regulation of DLK1 as an imprinted gene could contribute to human hepatocellular carcinoma. Carcinogenesis 2007;28:1094–1103.

146. Luk JM, Burchard J, Zhang C, et al. DLK1-DIO3 genomic imprinted microRNA cluster at 14q32.2 defines a stemlike subtype of hepatocellular carcinoma associated with poor survival. J Biol Chem 2011;286:30706–30713.

147. Yu F, Hao X, Zhao H, et al. Delta-like 1 contributes to cell growth by increasing the interferon-inducible protein 16 expression in hepatocellular carcinoma. Liver Int 2010;30:703–714.

148. Lachenmayer A, Alsinet C, Savic R, et al. Wnt-pathway activation in two molecular classes of hepatocellular carcinoma and experimental modulation by sorafenib. Clin Cancer Res 2012;18:4997–5007.

149. Guichard C, Amaddeo G, Imbeaud S, et al. Integrated analysis of somatic mutations and focal copy-number changes identifies key genes and pathways in hepatocellular carcinoma. Nat Genet 2012;44:694–698.

150. Lau WB de, Snel B, Clevers HC. The R-spondin protein family. Genome Biol 2012;13:242.

151. Takeda H, Wei Z, Koso H, et al. Transposon mutagenesis identifies genes and evolutionary forces driving gastrointestinal tract tumor progression. Nat Genet 2015;47:142–150.

152. Lowther W, Wiley K, Smith GH, et al. A new common integration site, Int7, for the mouse mammary tumor virus in mouse mammary tumors identifies a gene whose product has furin-like and thrombospondin-like sequences. J Virol 2005;79:10093–6.

153. Theodorou V, Kimm MA, Boer M, et al. MMTV insertional mutagenesis identifies genes, gene families and pathways involved in mammary cancer. Nat Genet 2007;39:759–769.

154. Ahn S-M, Jang SJ, Shim JH, et al. Genomic portrait of resectable hepatocellular carcinomas: Implications of RB1 and FGF19 aberrations for patient stratification. Hepatology 2014;60:1972–1982.

155. Shi C, Huang D, Lu N, et al. Aberrantly activated Gli2-KIF20A axis is crucial for growth of hepatocellular carcinoma and predicts poor prognosis. Oncotarget 2016;7:26206–19.

156. Zhang D, Cao L, Li Y, et al. Expression of glioma-associated oncogene 2 (Gli 2) is correlated with poor prognosis in patients with hepatocellular carcinoma undergoing hepatectomy. World J Surg Oncol 2013;11:25.

157. Huang S, He J, Zhang X, et al. Activation of the hedgehog pathway in human hepatocellular carcinomas. Carcinogenesis 2006;27:1334–1340.

158. Sicklick JK, Li Y-X, Jayaraman A, et al. Dysregulation of the Hedgehog pathway in human hepatocarcinogenesis. Carcinogenesis 2006;27:748–757.

159. Plummer M, Martel C de, Vignat J, et al. Global burden of cancers attributable to infections in 2012: a synthetic analysis. Lancet Glob Heal 2016;4:e609–e616.

160. Bisceglie AM Di. Hepatitis B And Hepatocellular Carcinoma. Hepatology 2009;49:S56-60.

161. Lindh M, Gustavson C, Mårdberg K, et al. Mutation of nucleotide 1,762 in the core promoter region during hepatitis B e seroconversion and its relation to liver damage in hepatitis B e antigen carriers. J Med Virol 1998;55:185–90.

162. Grompe M, Al-Dhalimy M, Finegold M, et al. Loss of fumarylacetoacetate hydrolase is responsible for the neonatal hepatic dysfunction phenotype of lethal albino mice. Genes Dev 1993;7:2298–2307.

163. Sze KMF, Chu GKY, Lee JMF, et al. C-terminal truncated hepatitis B virus x protein is associated with metastasis and enhances invasiveness by C-Jun/matrix metalloproteinase protein 10 activation in hepatocellular carcinoma. Hepatology 2013;57:131–9.

164. Cornella H, Alsinet C, Sayols S, et al. Unique genomic profile of fibrolamellar hepatocellular carcinoma. Gastroenterology 2016;148:806–18.

165. Ghosh PM, Shu Z-J, Zhu B, et al. Role of β-adrenergic receptors in regulation of hepatic fat accumulation during aging. J Endocrinol 2012;213:251–61.

166. Farah BL, Sinha R a., Wu Y, et al. β-adrenergic agonist and antagonist regulation of autophagy in HepG2 cells, primary mouse hepatocytes, and mouse liver. PLoS One 2014;9.

167. Mizuno K, Ueno Y. Hepatol Res. 2016 Jun 7. doi: 10.1111/hepr.12760. [Epub ahead of print] Autonomic Nervous System and the Liver. Hepatol Res 2016;Jun 7:[Epub ahead of print].

168. Niswender CM, Willis BS, Wallen A, et al. Cre recombinase-dependent expression of a constitutively active mutant allele of the catalytic subunit of Protein Kinase A. Genesis 2005;43:109–119.

169. Mu Y, Ogawa T, Kawada N. Reversibility of fibrosis, inflammation, and endoplasmic reticulum stress in the liver of rats fed a methionine-choline-deficient diet. Lab Invest 2010;90:245–256.

170. Buchman A, Ament M, Sohel M, et al. Choline deficiency causes reversible hepatic abnormalities in patients receiving parenteral nutrition: proof of a human choline requirement: a placebo-controlled trial. JPEN J Parenter Enter Nutr 2001;25:260–268.

171. Costa K da, Garner S, Chang J, et al. Effects of prolonged (1 year) choline deficiency and subsequent re-feeding of choline on 1,2-sn-diradylglycerol, fatty acids and protein kinase C in rat liver. Carcinogenesis 1995;16:327–334.

172. Zhu L, Finkelstein D, Gao C, et al. Multi-organ Mapping of Cancer Risk. Cell 2016;166:1132–1146.e7.

173. Pankowicz FP, Barzi M, Legras X, et al. Reprogramming metabolic pathways in vivo with CRISPR/Cas9 genome editing to treat hereditary tyrosinaemia. Nat Commun 2016;30:12642.

174. Lau JKC, Zhang X, Yu J. Animal models of non-alcoholic fatty liver disease: current perspectives and recent advances. J Pathol 2017;241:36–44.

175. Dowman JK, Hopkins LJ, Reynolds GM, et al. Development of hepatocellular carcinoma in a murine model of nonalcoholic steatohepatitis induced by use of a high-fat/fructose diet and sedentary lifestyle. Am J Pathol 2014;184:1550–61.

176. Azuma H, Paulk N, Ranade A, et al. Robust expansion of human hepatocytes in Fah-/-/Rag2-/-/Il2rg-/- mice. Nat Biotechnol 2007;25:903–10.

177. Gallagher EJ, LeRoith D. Obesity and Diabetes: The Increased Risk of Cancer and Cancer-Related Mortality. Physiol Rev 2015;95:727–748.

APPENDIX

Permission letters

Excerpts of text and figures from the following publications were re-printed in this work.

1. **Tschida BR**, Largaespada DA, Keng VW. Mouse models of cancer: *Sleeping Beauty* transposons for insertional mutagenesis screens and reverse genetic studies. Semin Cell Dev Biol 2014;27:86–95.
   (http://www.sciencedirect.com.ezp2.lib.umn.edu/science/article/pii/S108495211400007X)

2. Riordan JD, Keng VW, **Tschida BR**, Scheetz TE, Bell JB, Podetz-Pedersen KM, Moser CD, Copeland NG, Jenkins NA, Roberts LR, Largaespada DA, Dupuy AJ. Identification of rtl1, a retrotransposon-derived imprinted gene, as a novel driver of hepatocarcinogenesis. PLoS Genet 2013;9:e1003441.
   Open access publication.
   (http://journals.plos.org.ezp2.lib.umn.edu/plosgenetics/article/related?id=10.1371/journal.pgen.1003441)

3. Keng VW, Sia D, Sarver AL, **Tschida BR**, Fan D, Alsinet C, Solé M, Lee WL, Kuka TP, Moriarity BS, Villanueva A, Dupuy AJ, Riordan JD, Bell JB, Silverstein KA, Llovet JM, Largaespada DA. Sex bias occurrence of hepatocellular carcinoma in Poly7 molecular subclass is associated with EGFR. Hepatology 2013;57:120–30.
   (http://onlinelibrary.wiley.com.ezp2.lib.umn.edu/doi/10.1002/hep.26004/full)

ELSEVIER LICENSE
TERMS AND CONDITIONS

Mar 16, 2017

This Agreement between Barbara R Tschida ("You") and Elsevier ("Elsevier") consists of your license details and the terms and conditions provided by Elsevier and Copyright Clearance Center.

License Number	4071000945057
License date	Mar 16, 2017
Licensed Content Publisher	Elsevier
Licensed Content Publication	Seminars in Cell & Developmental Biology
Licensed Content Title	Mouse models of cancer: Sleeping Beauty transposons for insertional mutagenesis screens and reverse genetic studies
Licensed Content Author	Barbara R. Tschida,David A. Largaespada,Vincent W. Keng
Licensed Content Date	March 2014
Licensed Content Volume	27
Licensed Content Issue	n/a
Licensed Content Pages	10
Start Page	86
End Page	95
Type of Use	reuse in a thesis/dissertation
Portion	excerpt
Number of excerpts	13
Format	both print and electronic
Are you the author of this Elsevier article?	Yes
Will you be translating?	No
Order reference number	
Title of your thesis/dissertation	THE SLEEPING BEAUTY TRANSPOSON SYSTEM FOR FORWARD AND REVERSE GENETIC STUDIES OF LIVER CANCER
Expected completion date	Apr 2017
Estimated size (number of pages)	140
Elsevier VAT number	GB 494 6272 12
Requestor Location	Barbara R Tschida 1527 Sargent Ave SAINT PAUL, MN 55105 United States Attn: Barbara R Tschida
Publisher Tax ID	98-0397604
Total	0.00 USD
Terms and Conditions	

INTRODUCTION

1. The publisher for this copyrighted material is Elsevier. By clicking "accept" in connection with completing this licensing transaction, you agree that the following terms and conditions apply to this transaction (along with the Billing and Payment terms and conditions established by Copyright Clearance Center, Inc. ("CCC"), at the time that you opened your Rightslink account and that are available at any time at http://myaccount.copyright.com).

GENERAL TERMS

2. Elsevier hereby grants you permission to reproduce the aforementioned material subject to

the terms and conditions indicated.
3. Acknowledgement: If any part of the material to be used (for example, figures) has appeared in our publication with credit or acknowledgement to another source, permission must also be sought from that source. If such permission is not obtained then that material may not be included in your publication/copies. Suitable acknowledgement to the source must be made, either as a footnote or in a reference list at the end of your publication, as follows:
"Reprinted from Publication title, Vol /edition number, Author(s), Title of article / title of chapter, Pages No., Copyright (Year), with permission from Elsevier [OR APPLICABLE SOCIETY COPYRIGHT OWNER]." Also Lancet special credit - "Reprinted from The Lancet, Vol. number, Author(s), Title of article, Pages No., Copyright (Year), with permission from Elsevier."
4. Reproduction of this material is confined to the purpose and/or media for which permission is hereby given.
5. Altering/Modifying Material: Not Permitted. However figures and illustrations may be altered/adapted minimally to serve your work. Any other abbreviations, additions, deletions and/or any other alterations shall be made only with prior written authorization of Elsevier Ltd. (Please contact Elsevier at permissions@elsevier.com). No modifications can be made to any Lancet figures/tables and they must be reproduced in full.
6. If the permission fee for the requested use of our material is waived in this instance, please be advised that your future requests for Elsevier materials may attract a fee.
7. Reservation of Rights: Publisher reserves all rights not specifically granted in the combination of (i) the license details provided by you and accepted in the course of this licensing transaction, (ii) these terms and conditions and (iii) CCC's Billing and Payment terms and conditions.
8. License Contingent Upon Payment: While you may exercise the rights licensed immediately upon issuance of the license at the end of the licensing process for the transaction, provided that you have disclosed complete and accurate details of your proposed use, no license is finally effective unless and until full payment is received from you (either by publisher or by CCC) as provided in CCC's Billing and Payment terms and conditions. If full payment is not received on a timely basis, then any license preliminarily granted shall be deemed automatically revoked and shall be void as if never granted. Further, in the event that you breach any of these terms and conditions or any of CCC's Billing and Payment terms and conditions, the license is automatically revoked and shall be void as if never granted. Use of materials as described in a revoked license, as well as any use of the materials beyond the scope of an unrevoked license, may constitute copyright infringement and publisher reserves the right to take any and all action to protect its copyright in the materials.
9. Warranties: Publisher makes no representations or warranties with respect to the licensed material.
10. Indemnity: You hereby indemnify and agree to hold harmless publisher and CCC, and their respective officers, directors, employees and agents, from and against any and all claims arising out of your use of the licensed material other than as specifically authorized pursuant to this license.
11. No Transfer of License: This license is personal to you and may not be sublicensed, assigned, or transferred by you to any other person without publisher's written permission.
12. No Amendment Except in Writing: This license may not be amended except in a writing signed by both parties (or, in the case of publisher, by CCC on publisher's behalf).
13. Objection to Contrary Terms: Publisher hereby objects to any terms contained in any purchase order, acknowledgment, check endorsement or other writing prepared by you, which terms are inconsistent with these terms and conditions or CCC's Billing and Payment terms and conditions. These terms and conditions, together with CCC's Billing and Payment terms and conditions (which are incorporated herein), comprise the entire agreement between you and publisher (and CCC) concerning this licensing transaction. In the event of any conflict between your obligations established by these terms and conditions and those established by CCC's Billing and Payment terms and conditions, these terms and conditions shall control.
14. Revocation: Elsevier or Copyright Clearance Center may deny the permissions described in this License at their sole discretion, for any reason or no reason, with a full refund payable

to you. Notice of such denial will be made using the contact information provided by you. Failure to receive such notice will not alter or invalidate the denial. In no event will Elsevier or Copyright Clearance Center be responsible or liable for any costs, expenses or damage incurred by you as a result of a denial of your permission request, other than a refund of the amount(s) paid by you to Elsevier and/or Copyright Clearance Center for denied permissions.

LIMITED LICENSE

The following terms and conditions apply only to specific license types:

15. **Translation**: This permission is granted for non-exclusive world **English** rights only unless your license was granted for translation rights. If you licensed translation rights you may only translate this content into the languages you requested. A professional translator must perform all translations and reproduce the content word for word preserving the integrity of the article.

16. **Posting licensed content on any Website**: The following terms and conditions apply as follows: Licensing material from an Elsevier journal: All content posted to the web site must maintain the copyright information line on the bottom of each image; A hyper-text must be included to the Homepage of the journal from which you are licensing at http://www.sciencedirect.com/science/journal/xxxxx or the Elsevier homepage for books at http://www.elsevier.com; Central Storage: This license does not include permission for a scanned version of the material to be stored in a central repository such as that provided by Heron/XanEdu.

Licensing material from an Elsevier book: A hyper-text link must be included to the Elsevier homepage at http://www.elsevier.com . All content posted to the web site must maintain the copyright information line on the bottom of each image.

Posting licensed content on Electronic reserve: In addition to the above the following clauses are applicable: The web site must be password-protected and made available only to bona fide students registered on a relevant course. This permission is granted for 1 year only. You may obtain a new license for future website posting.

17. **For journal authors:** the following clauses are applicable in addition to the above:

Preprints:

A preprint is an author's own write-up of research results and analysis, it has not been peer-reviewed, nor has it had any other value added to it by a publisher (such as formatting, copyright, technical enhancement etc.).

Authors can share their preprints anywhere at any time. Preprints should not be added to or enhanced in any way in order to appear more like, or to substitute for, the final versions of articles however authors can update their preprints on arXiv or RePEc with their Accepted Author Manuscript (see below).

If accepted for publication, we encourage authors to link from the preprint to their formal publication via its DOI. Millions of researchers have access to the formal publications on ScienceDirect, and so links will help users to find, access, cite and use the best available version. Please note that Cell Press, The Lancet and some society-owned have different preprint policies. Information on these policies is available on the journal homepage.

Accepted Author Manuscripts: An accepted author manuscript is the manuscript of an article that has been accepted for publication and which typically includes author-incorporated changes suggested during submission, peer review and editor-author communications.

Authors can share their accepted author manuscript:

- immediately
  - via their non-commercial person homepage or blog
  - by updating a preprint in arXiv or RePEc with the accepted manuscript
  - via their research institute or institutional repository for internal institutional uses or as part of an invitation-only research collaboration work-group
  - directly by providing copies to their students or to research collaborators for their personal use
  - for private scholarly sharing as part of an invitation-only work group on commercial sites with which Elsevier has an agreement
- After the embargo period

- via non-commercial hosting platforms such as their institutional repository
- via commercial sites with which Elsevier has an agreement

In all cases accepted manuscripts should:

- link to the formal publication via its DOI
- bear a CC-BY-NC-ND license - this is easy to do
- if aggregated with other manuscripts, for example in a repository or other site, be shared in alignment with our hosting policy not be added to or enhanced in any way to appear more like, or to substitute for, the published journal article.

Published journal article (JPA): A published journal article (PJA) is the definitive final record of published research that appears or will appear in the journal and embodies all value-adding publishing activities including peer review co-ordination, copy-editing, formatting, (if relevant) pagination and online enrichment.
Policies for sharing publishing journal articles differ for subscription and gold open access articles:
Subscription Articles: If you are an author, please share a link to your article rather than the full-text. Millions of researchers have access to the formal publications on ScienceDirect, and so links will help your users to find, access, cite, and use the best available version.
Theses and dissertations which contain embedded PJAs as part of the formal submission can be posted publicly by the awarding institution with DOI links back to the formal publications on ScienceDirect.
If you are affiliated with a library that subscribes to ScienceDirect you have additional private sharing rights for others' research accessed under that agreement. This includes use for classroom teaching and internal training at the institution (including use in course packs and courseware programs), and inclusion of the article for grant funding purposes.
Gold Open Access Articles: May be shared according to the author-selected end-user license and should contain a CrossMark logo, the end user license, and a DOI link to the formal publication on ScienceDirect.
Please refer to Elsevier's posting policy for further information.
18. **For book authors** the following clauses are applicable in addition to the above:
Authors are permitted to place a brief summary of their work online only. You are not allowed to download and post the published electronic version of your chapter, nor may you scan the printed edition to create an electronic version. **Posting to a repository:** Authors are permitted to post a summary of their chapter only in their institution's repository.
19. **Thesis/Dissertation**: If your license is for use in a thesis/dissertation your thesis may be submitted to your institution in either print or electronic form. Should your thesis be published commercially, please reapply for permission. These requirements include permission for the Library and Archives of Canada to supply single copies, on demand, of the complete thesis and include permission for Proquest/UMI to supply single copies, on demand, of the complete thesis. Should your thesis be published commercially, please reapply for permission. Theses and dissertations which contain embedded PJAs as part of the formal submission can be posted publicly by the awarding institution with DOI links back to the formal publications on ScienceDirect.

Elsevier Open Access Terms and Conditions
You can publish open access with Elsevier in hundreds of open access journals or in nearly 2000 established subscription journals that support open access publishing. Permitted third party re-use of these open access articles is defined by the author's choice of Creative Commons user license. See our open access license policy for more information.
Terms & Conditions applicable to all Open Access articles published with Elsevier:
Any reuse of the article must not represent the author as endorsing the adaptation of the article nor should the article be modified in such a way as to damage the author's honour or reputation. If any changes have been made, such changes must be clearly indicated.
The author(s) must be appropriately credited and we ask that you include the end user license and a DOI link to the formal publication on ScienceDirect.
If any part of the material to be used (for example, figures) has appeared in our publication with credit or acknowledgement to another source it is the responsibility of the user to ensure their reuse complies with the terms and conditions determined by the rights holder.

Additional Terms & Conditions applicable to each Creative Commons user license:
CC BY: The CC-BY license allows users to copy, to create extracts, abstracts and new works from the Article, to alter and revise the Article and to make commercial use of the Article (including reuse and/or resale of the Article by commercial entities), provided the user gives appropriate credit (with a link to the formal publication through the relevant DOI), provides a link to the license, indicates if changes were made and the licensor is not represented as endorsing the use made of the work. The full details of the license are available at http://creativecommons.org/licenses/by/4.0.
CC BY NC SA: The CC BY-NC-SA license allows users to copy, to create extracts, abstracts and new works from the Article, to alter and revise the Article, provided this is not done for commercial purposes, and that the user gives appropriate credit (with a link to the formal publication through the relevant DOI), provides a link to the license, indicates if changes were made and the licensor is not represented as endorsing the use made of the work. Further, any new works must be made available on the same conditions. The full details of the license are available at http://creativecommons.org/licenses/by-nc-sa/4.0.
CC BY NC ND: The CC BY-NC-ND license allows users to copy and distribute the Article, provided this is not done for commercial purposes and further does not permit distribution of the Article if it is changed or edited in any way, and provided the user gives appropriate credit (with a link to the formal publication through the relevant DOI), provides a link to the license, and that the licensor is not represented as endorsing the use made of the work. The full details of the license are available at http://creativecommons.org/licenses/by-nc-nd/4.0.
Any commercial reuse of Open Access articles published with a CC BY NC SA or CC BY NC ND license requires permission from Elsevier and will be subject to a fee.
Commercial reuse includes:

- Associating advertising with the full text of the Article
- Charging fees for document delivery or access
- Article aggregation
- Systematic distribution via e-mail lists or share buttons

Posting or linking by commercial companies for use by customers of those companies.

20. **Other Conditions**:

v1.9

Questions? customercare@copyright.com or +1-855-239-3415 (toll free in the US) or +1-978-646-2777.

ELSEVIER LICENSE
TERMS AND CONDITIONS

Mar 16, 2017

This Agreement between Barbara R Tschida ("You") and Elsevier ("Elsevier") consists of your license details and the terms and conditions provided by Elsevier and Copyright Clearance Center.

License Number	4071001169479
License date	Mar 16, 2017
Licensed Content Publisher	Elsevier
Licensed Content Publication	Seminars in Cell & Developmental Biology
Licensed Content Title	Mouse models of cancer: Sleeping Beauty transposons for insertional mutagenesis screens and reverse genetic studies
Licensed Content Author	Barbara R. Tschida,David A. Largaespada,Vincent W. Keng
Licensed Content Date	March 2014
Licensed Content Volume	27
Licensed Content Issue	n/a
Licensed Content Pages	10
Start Page	86
End Page	95
Type of Use	reuse in a thesis/dissertation
Intended publisher of new work	other
Portion	figures/tables/illustrations
Number of figures/tables /illustrations	2
Format	both print and electronic
Are you the author of this Elsevier article?	Yes
Will you be translating?	No
Order reference number	
Original figure numbers	figures 1 and 2
Title of your thesis/dissertation	THE SLEEPING BEAUTY TRANSPOSON SYSTEM FOR FORWARD AND REVERSE GENETIC STUDIES OF LIVER CANCER
Expected completion date	Apr 2017
Estimated size (number of pages)	140
Elsevier VAT number	GB 494 6272 12
Requestor Location	Barbara R Tschida 1527 Sargent Ave SAINT PAUL, MN 55105 United States Attn: Barbara R Tschida
Publisher Tax ID	98-0397604
Total	0.00 USD
Terms and Conditions	

INTRODUCTION

1. The publisher for this copyrighted material is Elsevier. By clicking "accept" in connection with completing this licensing transaction, you agree that the following terms and conditions apply to this transaction (along with the Billing and Payment terms and conditions established by Copyright Clearance Center, Inc. ("CCC"), at the time that you

opened your Rightslink account and that are available at any time at http://myaccount.copyright.com).

GENERAL TERMS

2. Elsevier hereby grants you permission to reproduce the aforementioned material subject to the terms and conditions indicated.

3. Acknowledgement: If any part of the material to be used (for example, figures) has appeared in our publication with credit or acknowledgement to another source, permission must also be sought from that source. If such permission is not obtained then that material may not be included in your publication/copies. Suitable acknowledgement to the source must be made, either as a footnote or in a reference list at the end of your publication, as follows:

"Reprinted from Publication title, Vol /edition number, Author(s), Title of article / title of chapter, Pages No., Copyright (Year), with permission from Elsevier [OR APPLICABLE SOCIETY COPYRIGHT OWNER]." Also Lancet special credit - "Reprinted from The Lancet, Vol. number, Author(s), Title of article, Pages No., Copyright (Year), with permission from Elsevier."

4. Reproduction of this material is confined to the purpose and/or media for which permission is hereby given.

5. Altering/Modifying Material: Not Permitted. However figures and illustrations may be altered/adapted minimally to serve your work. Any other abbreviations, additions, deletions and/or any other alterations shall be made only with prior written authorization of Elsevier Ltd. (Please contact Elsevier at permissions@elsevier.com). No modifications can be made to any Lancet figures/tables and they must be reproduced in full.

6. If the permission fee for the requested use of our material is waived in this instance, please be advised that your future requests for Elsevier materials may attract a fee.

7. Reservation of Rights: Publisher reserves all rights not specifically granted in the combination of (i) the license details provided by you and accepted in the course of this licensing transaction, (ii) these terms and conditions and (iii) CCC's Billing and Payment terms and conditions.

8. License Contingent Upon Payment: While you may exercise the rights licensed immediately upon issuance of the license at the end of the licensing process for the transaction, provided that you have disclosed complete and accurate details of your proposed use, no license is finally effective unless and until full payment is received from you (either by publisher or by CCC) as provided in CCC's Billing and Payment terms and conditions. If full payment is not received on a timely basis, then any license preliminarily granted shall be deemed automatically revoked and shall be void as if never granted. Further, in the event that you breach any of these terms and conditions or any of CCC's Billing and Payment terms and conditions, the license is automatically revoked and shall be void as if never granted. Use of materials as described in a revoked license, as well as any use of the materials beyond the scope of an unrevoked license, may constitute copyright infringement and publisher reserves the right to take any and all action to protect its copyright in the materials.

9. Warranties: Publisher makes no representations or warranties with respect to the licensed material.

10. Indemnity: You hereby indemnify and agree to hold harmless publisher and CCC, and their respective officers, directors, employees and agents, from and against any and all claims arising out of your use of the licensed material other than as specifically authorized pursuant to this license.

11. No Transfer of License: This license is personal to you and may not be sublicensed, assigned, or transferred by you to any other person without publisher's written permission.

12. No Amendment Except in Writing: This license may not be amended except in a writing signed by both parties (or, in the case of publisher, by CCC on publisher's behalf).

13. Objection to Contrary Terms: Publisher hereby objects to any terms contained in any purchase order, acknowledgment, check endorsement or other writing prepared by you, which terms are inconsistent with these terms and conditions or CCC's Billing and Payment terms and conditions. These terms and conditions, together with CCC's Billing and Payment terms and conditions (which are incorporated herein), comprise the entire agreement between you and publisher (and CCC) concerning this licensing transaction. In the event of any conflict between your obligations established by these terms and conditions and those

established by CCC's Billing and Payment terms and conditions, these terms and conditions shall control.
14. Revocation: Elsevier or Copyright Clearance Center may deny the permissions described in this License at their sole discretion, for any reason or no reason, with a full refund payable to you. Notice of such denial will be made using the contact information provided by you. Failure to receive such notice will not alter or invalidate the denial. In no event will Elsevier or Copyright Clearance Center be responsible or liable for any costs, expenses or damage incurred by you as a result of a denial of your permission request, other than a refund of the amount(s) paid by you to Elsevier and/or Copyright Clearance Center for denied permissions.

LIMITED LICENSE

The following terms and conditions apply only to specific license types:
15. **Translation**: This permission is granted for non-exclusive world **English** rights only unless your license was granted for translation rights. If you licensed translation rights you may only translate this content into the languages you requested. A professional translator must perform all translations and reproduce the content word for word preserving the integrity of the article.
16. **Posting licensed content on any Website**: The following terms and conditions apply as follows: Licensing material from an Elsevier journal: All content posted to the web site must maintain the copyright information line on the bottom of each image; A hyper-text must be included to the Homepage of the journal from which you are licensing at http://www.sciencedirect.com/science/journal/xxxxx or the Elsevier homepage for books at http://www.elsevier.com; Central Storage: This license does not include permission for a scanned version of the material to be stored in a central repository such as that provided by Heron/XanEdu.
Licensing material from an Elsevier book: A hyper-text link must be included to the Elsevier homepage at http://www.elsevier.com . All content posted to the web site must maintain the copyright information line on the bottom of each image.

Posting licensed content on Electronic reserve: In addition to the above the following clauses are applicable: The web site must be password-protected and made available only to bona fide students registered on a relevant course. This permission is granted for 1 year only. You may obtain a new license for future website posting.
17. **For journal authors:** the following clauses are applicable in addition to the above:
Preprints:
A preprint is an author's own write-up of research results and analysis, it has not been peer-reviewed, nor has it had any other value added to it by a publisher (such as formatting, copyright, technical enhancement etc.).
Authors can share their preprints anywhere at any time. Preprints should not be added to or enhanced in any way in order to appear more like, or to substitute for, the final versions of articles however authors can update their preprints on arXiv or RePEc with their Accepted Author Manuscript (see below).
If accepted for publication, we encourage authors to link from the preprint to their formal publication via its DOI. Millions of researchers have access to the formal publications on ScienceDirect, and so links will help users to find, access, cite and use the best available version. Please note that Cell Press, The Lancet and some society-owned have different preprint policies. Information on these policies is available on the journal homepage.
Accepted Author Manuscripts: An accepted author manuscript is the manuscript of an article that has been accepted for publication and which typically includes author-incorporated changes suggested during submission, peer review and editor-author communications.
Authors can share their accepted author manuscript:

- immediately
  - via their non-commercial person homepage or blog
  - by updating a preprint in arXiv or RePEc with the accepted manuscript
  - via their research institute or institutional repository for internal institutional uses or as part of an invitation-only research collaboration work-group
  - directly by providing copies to their students or to research collaborators for

their personal use
    - for private scholarly sharing as part of an invitation-only work group on commercial sites with which Elsevier has an agreement
- After the embargo period
    - via non-commercial hosting platforms such as their institutional repository
    - via commercial sites with which Elsevier has an agreement

In all cases accepted manuscripts should:

- link to the formal publication via its DOI
- bear a CC-BY-NC-ND license - this is easy to do
- if aggregated with other manuscripts, for example in a repository or other site, be shared in alignment with our hosting policy not be added to or enhanced in any way to appear more like, or to substitute for, the published journal article.

Published journal article (JPA): A published journal article (PJA) is the definitive final record of published research that appears or will appear in the journal and embodies all value-adding publishing activities including peer review co-ordination, copy-editing, formatting, (if relevant) pagination and online enrichment.
Policies for sharing publishing journal articles differ for subscription and gold open access articles:
Subscription Articles: If you are an author, please share a link to your article rather than the full-text. Millions of researchers have access to the formal publications on ScienceDirect, and so links will help your users to find, access, cite, and use the best available version.
Theses and dissertations which contain embedded PJAs as part of the formal submission can be posted publicly by the awarding institution with DOI links back to the formal publications on ScienceDirect.
If you are affiliated with a library that subscribes to ScienceDirect you have additional private sharing rights for others' research accessed under that agreement. This includes use for classroom teaching and internal training at the institution (including use in course packs and courseware programs), and inclusion of the article for grant funding purposes.
Gold Open Access Articles: May be shared according to the author-selected end-user license and should contain a CrossMark logo, the end user license, and a DOI link to the formal publication on ScienceDirect.
Please refer to Elsevier's posting policy for further information.
18. **For book authors** the following clauses are applicable in addition to the above:
Authors are permitted to place a brief summary of their work online only. You are not allowed to download and post the published electronic version of your chapter, nor may you scan the printed edition to create an electronic version. **Posting to a repository:** Authors are permitted to post a summary of their chapter only in their institution's repository.
19. **Thesis/Dissertation**: If your license is for use in a thesis/dissertation your thesis may be submitted to your institution in either print or electronic form. Should your thesis be published commercially, please reapply for permission. These requirements include permission for the Library and Archives of Canada to supply single copies, on demand, of the complete thesis and include permission for Proquest/UMI to supply single copies, on demand, of the complete thesis. Should your thesis be published commercially, please reapply for permission. Theses and dissertations which contain embedded PJAs as part of the formal submission can be posted publicly by the awarding institution with DOI links back to the formal publications on ScienceDirect.

Elsevier Open Access Terms and Conditions
You can publish open access with Elsevier in hundreds of open access journals or in nearly 2000 established subscription journals that support open access publishing. Permitted third party re-use of these open access articles is defined by the author's choice of Creative Commons user license. See our open access license policy for more information.
Terms & Conditions applicable to all Open Access articles published with Elsevier:
Any reuse of the article must not represent the author as endorsing the adaptation of the article nor should the article be modified in such a way as to damage the author's honour or reputation. If any changes have been made, such changes must be clearly indicated.
The author(s) must be appropriately credited and we ask that you include the end user

OPEN ACCESS Freely available online

PLOS | GENETICS

Identification of *Rtl1*, a Retrotransposon-Derived Imprinted Gene, as a Novel Driver of Hepatocarcinogenesis

Jesse D. Riordan [1], Vincent W. Keng [2¤], Barbara R. Tschida [2], Todd E. Scheetz [3], Jason B. Bell [4], Kelly M. Podetz-Pedersen [4], Catherine D. Moser [5], Neal G. Copeland [6], Nancy A. Jenkins [6], Lewis R. Roberts [5], David A. Largaespada [2], Adam J. Dupuy [1]*

1 Department of Anatomy and Cell Biology, Roy J. and Lucille A. Carver College of Medicine, University of Iowa, Iowa City, Iowa, United States of America, 2 Masonic Cancer Center, Department of Genetics, Cell Biology and Development and Center for Genome Engineering, University of Minnesota, Minneapolis, Minnesota, United States of America, 3 Center for Bioinformatics and Computational Biology, Department of Opthalmology and Visual Sciences, Roy J. and Lucille A. Carver College of Medicine, University of Iowa, Iowa City, Iowa, United States of America, 4 Department of Genetics, Cell Biology and Development and Center for Genome Engineering, University of Minnesota, Minneapolis, Minnesota, United States of America, 5 Division of Gastroenterology and Hepatology, College of Medicine, Mayo Clinic and Mayo Clinic Cancer Center, Rochester, Minnesota, United States of America, 6 Cancer Research Program, The Methodist Hospital Research Institute, Houston, Texas, United States of America

Abstract

We previously utilized a Sleeping Beauty (SB) transposon mutagenesis screen to discover novel drivers of HCC. This approach identified recurrent mutations within the Dlk1-Dio3 imprinted domain, indicating that alteration of one or more elements within the domain provides a selective advantage to cells during the process of hepatocarcinogenesis. For the current study, we performed transcriptome and small RNA sequencing to profile gene expression in SB–induced HCCs in an attempt to clarify the genetic element(s) contributing to tumorigenesis. We identified strong induction of Retrotransposon-like 1 (Rtl1) expression as the only consistent alteration detected in all SB–induced tumors with Dlk1-Dio3 integrations, suggesting that Rtl1 activation serves as a driver of HCC. While previous studies have identified correlations between disrupted expression of multiple Dlk1-Dio3 domain members and HCC, we show here that direct modulation of a single domain member, Rtl1, can promote hepatocarcinogenesis in vivo. Overexpression of Rtl1 in the livers of adult mice using a hydrodynamic gene delivery technique resulted in highly penetrant (86%) tumor formation. Additionally, we detected overexpression of RTL1 in 30% of analyzed human HCC samples, indicating the potential relevance of this locus as a therapeutic target for patients. The Rtl1 locus is evolutionarily derived from the domestication of a retrotransposon. In addition to identifying Rtl1 as a novel driver of HCC, our study represents one of the first direct in vivo demonstrations of a role for such a co-opted genetic element in promoting carcinogenesis.

Citation: Riordan JD, Keng VW, Tschida BR, Scheetz TE, Bell JB, et al. (2013) Identification of Rtl1, a Retrotransposon-Derived Imprinted Gene, as a Novel Driver of Hepatocarcinogenesis. PLoS Genet 9(4): e1003441. doi:10.1371/journal.pgen.1003441

Editor: Kent W. Hunter, National Cancer Institute, United States of America

Received November 5, 2012; Accepted February 22, 2013; Published April 4, 2013

Funding: This work was funded by a grant from the National Cancer Institute (R01CA132962). The funders had no role in study design, data collection and analysis, decision to publish, or preparation of the manuscript.

Competing Interests: The authors have declared that no competing interests exist.

* E-mail: adam-dupuy@uiowa.edu

¤ Current address: Department of Applied Biology and Chemical Technology, The Hong Kong Polytechnic University, Hung Hom, Kowloon, Hong Kong

Introduction

Hepatocellular carcinoma (HCC) is the third leading cause of cancer-related deaths worldwide [1]. In contrast to the downward trends in incidence observed for most cancer types, that of HCC continues to rise, particularly in the United States [2]. This is due in part to increases in obesity and hepatitis C viral infection, both of which have been implicated in HCC pathogenesis. Treatment options for patients are limited, particularly for those with advanced disease, and the five-year survival rate remains low at , 10%.

A major goal of HCC research is to develop therapies targeted at the molecular mechanisms underlying tumor development and progression. This type of approach is expected to be much more efficacious, increasing survival rates for HCC patients. Consistent with this idea, treatment with sorafenib, a multi-kinase inhibitor, has shown survival benefits for late-stage patients [3] – a rare achievement in HCC treatment. Nevertheless, sorafenib treatment is only able to extend median survival by three months, underlying the need for improved targeted therapies. Unfortunately, the molecular drivers of HCC remain poorly characterized, precluding the development of such therapeutics. Large-scale sequencing efforts currently being undertaken by The Cancer Genome Atlas (TCGA) project will likely characterize the recurrent genetic alterations present in human liver tumors and may identify novel therapeutic targets. However, it is becoming increasingly clear that human tumors are incredibly complex, and identifying molecular drivers of carcinogenesis among the larger number of background events has proven difficult. Comparative analysis of the information gained from human tumor profiling with data from animal

Creative Commons

Creative Commons License Deed

Attribution 4.0 International (CC BY 4.0)

This is a human-readable summary of (and not a substitute for) the license.
Disclaimer

You are free to:

Share — copy and redistribute the material in any medium or format

Adapt — remix, transform, and build upon the material

for any purpose, even commercially.

The licensor cannot revoke these freedoms as long as you follow the license terms.

Under the following terms:

Attribution — You must give appropriate credit, provide a link to the license, and indicate if changes were made. You may do so in any reasonable manner, but not in any way that suggests the licensor endorses you or your use.

No additional restrictions — You may not apply legal terms or technological measures that legally restrict others from doing anything the license permits.

Notices:

You do not have to comply with the license for elements of the material in the public domain or where your use is permitted by an applicable exception or limitation.

No warranties are given. The license may not give you all of the permissions necessary for your intended use. For example, other rights such as publicity, privacy, or moral rights may limit how you use the material.

Creative Commons — Attribution 4.0 International — CC BY 4.0

Creative Commons Legal Code

Attribution 4.0 International

Official translations of this license are available in other languages.

Creative Commons Corporation (“Creative Commons”) is not a law firm and does not provide legal services or legal advice. Distribution of Creative Commons public licenses does not create a lawyer-client or other relationship. Creative Commons makes its licenses and related information available on an “as-is” basis. Creative Commons gives no warranties regarding its licenses, any material licensed under their terms and conditions, or any related information. Creative Commons disclaims all liability for damages resulting from their use to the fullest extent possible.

Using Creative Commons Public Licenses

Creative Commons public licenses provide a standard set of terms and conditions that creators and other rights holders may use to share original works of authorship and other material subject to copyright and certain other rights specified in the public license below. The following considerations are for informational purposes only, are not exhaustive, and do not form part of our licenses.

Considerations for licensors: *Our public licenses are intended for use by those authorized to give the public permission to use material in ways otherwise restricted by copyright and certain other rights. Our licenses are irrevocable. Licensors should read and understand the terms and conditions of the license they choose before applying it. Licensors should also secure all rights necessary before applying our licenses so that the public can reuse the material as expected. Licensors should clearly mark any material not subject to the license. This includes other CC-licensed material, or material used under an exception or limitation to copyright. More considerations for licensors.*

Considerations for the public: *By using one of our public licenses, a licensor grants the public permission to use the licensed material under specified terms and conditions. If the licensor’s permission is not necessary for any reason–for example, because of any applicable exception or limitation to copyright–then that use is not regulated by the license. Our licenses grant only permissions under copyright and certain other rights that a licensor has authority to grant. Use of the licensed material may still be restricted for other reasons, including because others have copyright or other rights in the material. A licensor may make special requests, such as asking that all changes be marked or described. Although not required by our licenses, you are encouraged to respect those requests where reasonable. More considerations for the public.*

Creative Commons Attribution 4.0 International Public License

By exercising the Licensed Rights (defined below), You accept and agree to be bound by the terms and conditions of this Creative Commons Attribution 4.0 International Public License ("Public License"). To the extent this Public License may be interpreted as a contract, You are granted the Licensed Rights in consideration of Your acceptance of these terms and conditions, and the Licensor grants You such rights in consideration of benefits the Licensor receives from making the Licensed Material available under these terms and conditions.

Section 1 – Definitions.

a. **Adapted Material** means material subject to Copyright and Similar Rights that is derived from or based upon the Licensed Material and in which the Licensed Material is translated, altered, arranged, transformed, or otherwise modified in a manner requiring permission under the Copyright and Similar Rights held by the Licensor. For purposes of this Public License, where the Licensed Material is a musical work, performance, or sound recording, Adapted Material is always produced where the Licensed Material is synched in timed relation with a moving image.
b. **Adapter's License** means the license You apply to Your Copyright and Similar Rights in Your contributions to Adapted Material in accordance with the terms and conditions of this Public License.
c. **Copyright and Similar Rights** means copyright and/or similar rights closely related to copyright including, without limitation, performance, broadcast, sound recording, and Sui Generis Database Rights, without regard to how the rights are labeled or categorized. For purposes of this Public

License, the rights specified in Section 2(b)(1)-(2) are not Copyright and Similar Rights.

d. **Effective Technological Measures** means those measures that, in the absence of proper authority, may not be circumvented under laws fulfilling obligations under Article 11 of the WIPO Copyright Treaty adopted on December 20, 1996, and/or similar international agreements.

e. **Exceptions and Limitations** means fair use, fair dealing, and/or any other exception or limitation to Copyright and Similar Rights that applies to Your use of the Licensed Material.

f. **Licensed Material** means the artistic or literary work, database, or other material to which the Licensor applied this Public License.

g. **Licensed Rights** means the rights granted to You subject to the terms and conditions of this Public License, which are limited to all Copyright and Similar Rights that apply to Your use of the Licensed Material and that the Licensor has authority to license.

h. **Licensor** means the individual(s) or entity(ies) granting rights under this Public License.

i. **Share** means to provide material to the public by any means or process that requires permission under the Licensed Rights, such as reproduction, public display, public performance, distribution, dissemination, communication, or importation, and to make material available to the public including in ways that members of the public may access the material from a place and at a time individually chosen by them.

j. **Sui Generis Database Rights** means rights other than copyright resulting from Directive 96/9/EC of the European Parliament and of the Council of 11 March 1996 on the legal protection of databases, as amended and/or succeeded, as well as other essentially equivalent rights anywhere in the world.

k. **You** means the individual or entity exercising the Licensed Rights under this Public License. **Your** has a corresponding meaning.

Section 2 – Scope.

a. **License grant**.

1. Subject to the terms and conditions of this Public License, the Licensor hereby grants You a worldwide, royalty-free, non-sublicensable, non-exclusive, irrevocable license to exercise the Licensed Rights in the Licensed Material to:
   A. reproduce and Share the Licensed Material, in whole or in part; and
   B. produce, reproduce, and Share Adapted Material.
2. Exceptions and Limitations. For the avoidance of doubt, where Exceptions and Limitations apply to Your use, this Public License does not apply, and You do not need to comply with its terms and conditions.
3. Term. The term of this Public License is specified in Section 6(a).
4. Media and formats; technical modifications allowed. The Licensor authorizes You to exercise the Licensed Rights in all media and formats whether now known or hereafter created, and to make technical modifications necessary to do so. The Licensor waives and/or agrees not to assert any right or authority to forbid You from making technical modifications necessary to exercise the Licensed Rights, including technical modifications necessary to circumvent Effective Technological Measures. For purposes of this Public License, simply making modifications authorized by this Section 2(a)(4) never produces Adapted Material.
5. Downstream recipients.
   A. Offer from the Licensor – Licensed Material. Every recipient of the Licensed Material automatically receives an offer from the Licensor to exercise the Licensed Rights under the terms and conditions of this Public License.
   B. No downstream restrictions. You may not offer or impose any additional or different terms or conditions on, or apply any Effective Technological Measures to, the Licensed Material if doing so restricts exercise of the Licensed Rights by any recipient of the Licensed Material.
6. No endorsement. Nothing in this Public License constitutes or may be construed as permission to assert or imply that You are, or that Your use of the Licensed Material is, connected with, or sponsored, endorsed, or granted official status by, the Licensor or others designated to receive attribution as provided in Section 3(a)(1)(A)(i).

b. **Other rights**.

1. Moral rights, such as the right of integrity, are not licensed under this Public License, nor are publicity, privacy, and/or other similar personality rights; however, to the extent possible, the Licensor waives and/or agrees not to assert any such rights held by the Licensor to the limited extent necessary to allow You to exercise the Licensed Rights, but not otherwise.
2. Patent and trademark rights are not licensed under this Public License.
3. To the extent possible, the Licensor waives any right to collect royalties from You for the exercise of the Licensed Rights, whether directly or through a collecting society under any voluntary or waivable statutory or compulsory licensing scheme. In all other cases the Licensor expressly reserves any right to collect such royalties.

Section 3 – License Conditions.

Your exercise of the Licensed Rights is expressly made subject to the following conditions.

a. **Attribution**.

1. If You Share the Licensed Material (including in modified form), You must:

A. retain the following if it is supplied by the Licensor with the Licensed Material:
   i. identification of the creator(s) of the Licensed Material and any others designated to receive attribution, in any reasonable manner requested by the Licensor (including by pseudonym if designated);
   ii. a copyright notice;
   iii. a notice that refers to this Public License;
   iv. a notice that refers to the disclaimer of warranties;
   v. a URI or hyperlink to the Licensed Material to the extent reasonably practicable;

B. indicate if You modified the Licensed Material and retain an indication of any previous modifications; and

C. indicate the Licensed Material is licensed under this Public License, and include the text of, or the URI or hyperlink to, this Public License.

2. You may satisfy the conditions in Section 3(a)(1) in any reasonable manner based on the medium, means, and context in which You Share the Licensed Material. For example, it may be reasonable to satisfy the conditions by providing a URI or hyperlink to a resource that includes the required information.
3. If requested by the Licensor, You must remove any of the information required by Section 3(a)(1)(A) to the extent reasonably practicable.
4. If You Share Adapted Material You produce, the Adapter's License You apply must not prevent recipients of the Adapted Material from complying with this Public License.

Section 4 – Sui Generis Database Rights.

Where the Licensed Rights include Sui Generis Database Rights that apply to Your use of the Licensed Material:

a. for the avoidance of doubt, Section 2(a)(1) grants You the right to extract, reuse, reproduce, and Share all or a substantial portion of the contents of the database;
b. if You include all or a substantial portion of the database contents in a database in which You have Sui Generis Database Rights, then the database in which You have Sui Generis Database Rights (but not its individual contents) is Adapted Material; and
c. You must comply with the conditions in Section 3(a) if You Share all or a substantial portion of the contents of the database.

For the avoidance of doubt, this Section 4 supplements and does not replace Your obligations under this Public License where the Licensed Rights include other Copyright and Similar Rights.

Section 5 – Disclaimer of Warranties and Limitation of Liability.

a. **Unless otherwise separately undertaken by the Licensor, to the extent possible, the Licensor offers the Licensed Material as-is and as-available, and makes no representations or warranties of any kind concerning the Licensed Material, whether express, implied, statutory, or other. This includes, without limitation, warranties of title, merchantability, fitness for a particular purpose, non-infringement, absence of latent or other defects, accuracy, or the presence or absence of errors, whether or not known or discoverable. Where disclaimers of warranties are not allowed in full or in part, this disclaimer may not apply to You.**
b. **To the extent possible, in no event will the Licensor be liable to You on any legal theory (including, without limitation, negligence) or otherwise for any direct, special, indirect, incidental, consequential, punitive, exemplary, or other losses, costs, expenses, or damages arising out of this Public License or use of the Licensed Material, even if the Licensor has been advised of the possibility of such losses, costs, expenses, or damages. Where a limitation of liability is not allowed in full or in part, this limitation may not apply to You.**

c. The disclaimer of warranties and limitation of liability provided above shall be interpreted in a manner that, to the extent possible, most closely approximates an absolute disclaimer and waiver of all liability.

Section 6 – Term and Termination.

a. This Public License applies for the term of the Copyright and Similar Rights licensed here. However, if You fail to comply with this Public License, then Your rights under this Public License terminate automatically.

b. Where Your right to use the Licensed Material has terminated under Section 6(a), it reinstates:

   1. automatically as of the date the violation is cured, provided it is cured within 30 days of Your discovery of the violation; or
   2. upon express reinstatement by the Licensor.

   For the avoidance of doubt, this Section 6(b) does not affect any right the Licensor may have to seek remedies for Your violations of this Public License.

c. For the avoidance of doubt, the Licensor may also offer the Licensed Material under separate terms or conditions or stop distributing the Licensed Material at any time; however, doing so will not

terminate this Public License.

d. Sections 1, 5, 6, 7, and 8 survive termination of this Public License.

Section 7 – Other Terms and Conditions.

a. The Licensor shall not be bound by any additional or different terms or conditions communicated by You unless expressly agreed.
b. Any arrangements, understandings, or agreements regarding the Licensed Material not stated herein are separate from and independent of the terms and conditions of this Public License.

Section 8 – Interpretation.

a. For the avoidance of doubt, this Public License does not, and shall not be interpreted to, reduce, limit, restrict, or impose conditions on any use of the Licensed Material that could lawfully be made without permission under this Public License.
b. To the extent possible, if any provision of this Public License is deemed unenforceable, it shall be automatically reformed to the minimum extent necessary to make it enforceable. If the provision cannot be reformed, it shall be severed from this Public License without affecting the enforceability of the remaining terms and conditions.
c. No term or condition of this Public License will be waived and no failure to comply consented to unless expressly agreed to by the Licensor.
d. Nothing in this Public License constitutes or may be interpreted as a limitation upon, or waiver of, any privileges and immunities that apply to the Licensor or You, including from the legal processes of any jurisdiction or authority.

JOHN WILEY AND SONS LICENSE TERMS AND CONDITIONS

Apr 12, 2017

This Agreement between Barbara R Tschida ("You") and John Wiley and Sons ("John Wiley and Sons") consists of your license details and the terms and conditions provided by John Wiley and Sons and Copyright Clearance Center.

License Number	4086600254807
License date	Apr 12, 2017
Licensed Content Publisher	John Wiley and Sons
Licensed Content Publication	Hepatology
Licensed Content Title	Sex bias occurrence of hepatocellular carcinoma in Poly7 molecular subclass is associated with EGFR
Licensed Content Author	Vincent W. Keng,Daniela Sia,Aaron L. Sarver,Barbara R. Tschida,Danhua Fan,Clara Alsinet,Manel Solé,Wai L. Lee,Timothy P. Kuka,Branden S. Moriarity,Augusto Villanueva,Adam J. Dupuy,Jesse D. Riordan,Jason B. Bell,Kevin A. T.Silverstein,Josep M. Llovet,David A. Largaespada
Licensed Content Date	Oct 19, 2012
Licensed Content Pages	11
Type of use	Dissertation/Thesis
Requestor type	Author of this Wiley article
Format	Print and electronic
Portion	Figure/table
Number of figures/tables	2
Original Wiley figure/table number(s)	Figure 3 and Figure 4
Will you be translating?	No
Title of your thesis / dissertation	THE SLEEPING BEAUTY TRANSPOSON SYSTEM FOR FORWARD AND REVERSE GENETIC STUDIES OF LIVER CANCER
Expected completion date	Apr 2017
Expected size (number of pages)	140
Requestor Location	Barbara R Tschida 1527 Sargent Ave SAINT PAUL, MN 55105 United States Attn: Barbara R Tschida
Publisher Tax ID	EU826007151
Billing Type	Invoice
Billing Address	Barbara R Tschida 1527 Sargent Ave SAINT PAUL, MN 55105 United States Attn: Barbara R Tschida
Total	0.00 USD
Terms and Conditions	

TERMS AND CONDITIONS

This copyrighted material is owned by or exclusively licensed to John Wiley & Sons, Inc. or one of its group companies (each a"Wiley Company") or handled on behalf of a society with which a Wiley Company has exclusive publishing rights in relation to a particular work (collectively "WILEY"). By clicking "accept" in connection with completing this licensing

transaction, you agree that the following terms and conditions apply to this transaction (along with the billing and payment terms and conditions established by the Copyright Clearance Center Inc., ("CCC's Billing and Payment terms and conditions"), at the time that you opened your RightsLink account (these are available at any time at http://myaccount.copyright.com).

Terms and Conditions

- The materials you have requested permission to reproduce or reuse (the "Wiley Materials") are protected by copyright.

- You are hereby granted a personal, non-exclusive, non-sub licensable (on a stand-alone basis), non-transferable, worldwide, limited license to reproduce the Wiley Materials for the purpose specified in the licensing process. This license, **and any CONTENT (PDF or image file) purchased as part of your order,** is for a one-time use only and limited to any maximum distribution number specified in the license. The first instance of republication or reuse granted by this license must be completed within two years of the date of the grant of this license (although copies prepared before the end date may be distributed thereafter). The Wiley Materials shall not be used in any other manner or for any other purpose, beyond what is granted in the license. Permission is granted subject to an appropriate acknowledgement given to the author, title of the material/book/journal and the publisher. You shall also duplicate the copyright notice that appears in the Wiley publication in your use of the Wiley Material. Permission is also granted on the understanding that nowhere in the text is a previously published source acknowledged for all or part of this Wiley Material. Any third party content is expressly excluded from this permission.

- With respect to the Wiley Materials, all rights are reserved. Except as expressly granted by the terms of the license, no part of the Wiley Materials may be copied, modified, adapted (except for minor reformatting required by the new Publication), translated, reproduced, transferred or distributed, in any form or by any means, and no derivative works may be made based on the Wiley Materials without the prior permission of the respective copyright owner.**For STM Signatory Publishers clearing permission under the terms of the STM Permissions Guidelines only, the terms of the license are extended to include subsequent editions and for editions in other languages, provided such editions are for the work as a whole in situ and does not involve the separate exploitation of the permitted figures or extracts,** You may not alter, remove or suppress in any manner any copyright, trademark or other notices displayed by the Wiley Materials. You may not license, rent, sell, loan, lease, pledge, offer as security, transfer or assign the Wiley Materials on a stand-alone basis, or any of the rights granted to you hereunder to any other person.

- The Wiley Materials and all of the intellectual property rights therein shall at all times remain the exclusive property of John Wiley & Sons Inc, the Wiley Companies, or their respective licensors, and your interest therein is only that of having possession of and the right to reproduce the Wiley Materials pursuant to Section 2 herein during the continuance of this Agreement. You agree that you own no right, title or interest in or to the Wiley Materials or any of the intellectual property rights therein. You shall have no rights hereunder other than the license as provided for above in Section 2. No right, license or interest to any trademark, trade name, service mark or other branding ("Marks") of WILEY or its licensors is granted hereunder, and you agree that you shall not assert any such right, license or interest with respect thereto

- NEITHER WILEY NOR ITS LICENSORS MAKES ANY WARRANTY OR REPRESENTATION OF ANY KIND TO YOU OR ANY THIRD PARTY, EXPRESS, IMPLIED OR STATUTORY, WITH RESPECT TO THE MATERIALS OR THE ACCURACY OF ANY INFORMATION CONTAINED IN THE MATERIALS, INCLUDING, WITHOUT LIMITATION, ANY IMPLIED WARRANTY OF MERCHANTABILITY, ACCURACY, SATISFACTORY

QUALITY, FITNESS FOR A PARTICULAR PURPOSE, USABILITY, INTEGRATION OR NON-INFRINGEMENT AND ALL SUCH WARRANTIES ARE HEREBY EXCLUDED BY WILEY AND ITS LICENSORS AND WAIVED BY YOU.

- WILEY shall have the right to terminate this Agreement immediately upon breach of this Agreement by you.
- You shall indemnify, defend and hold harmless WILEY, its Licensors and their respective directors, officers, agents and employees, from and against any actual or threatened claims, demands, causes of action or proceedings arising from any breach of this Agreement by you.
- IN NO EVENT SHALL WILEY OR ITS LICENSORS BE LIABLE TO YOU OR ANY OTHER PARTY OR ANY OTHER PERSON OR ENTITY FOR ANY SPECIAL, CONSEQUENTIAL, INCIDENTAL, INDIRECT, EXEMPLARY OR PUNITIVE DAMAGES, HOWEVER CAUSED, ARISING OUT OF OR IN CONNECTION WITH THE DOWNLOADING, PROVISIONING, VIEWING OR USE OF THE MATERIALS REGARDLESS OF THE FORM OF ACTION, WHETHER FOR BREACH OF CONTRACT, BREACH OF WARRANTY, TORT, NEGLIGENCE, INFRINGEMENT OR OTHERWISE (INCLUDING, WITHOUT LIMITATION, DAMAGES BASED ON LOSS OF PROFITS, DATA, FILES, USE, BUSINESS OPPORTUNITY OR CLAIMS OF THIRD PARTIES), AND WHETHER OR NOT THE PARTY HAS BEEN ADVISED OF THE POSSIBILITY OF SUCH DAMAGES. THIS LIMITATION SHALL APPLY NOTWITHSTANDING ANY FAILURE OF ESSENTIAL PURPOSE OF ANY LIMITED REMEDY PROVIDED HEREIN.
- Should any provision of this Agreement be held by a court of competent jurisdiction to be illegal, invalid, or unenforceable, that provision shall be deemed amended to achieve as nearly as possible the same economic effect as the original provision, and the legality, validity and enforceability of the remaining provisions of this Agreement shall not be affected or impaired thereby.
- The failure of either party to enforce any term or condition of this Agreement shall not constitute a waiver of either party's right to enforce each and every term and condition of this Agreement. No breach under this agreement shall be deemed waived or excused by either party unless such waiver or consent is in writing signed by the party granting such waiver or consent. The waiver by or consent of a party to a breach of any provision of this Agreement shall not operate or be construed as a waiver of or consent to any other or subsequent breach by such other party.
- This Agreement may not be assigned (including by operation of law or otherwise) by you without WILEY's prior written consent.
- Any fee required for this permission shall be non-refundable after thirty (30) days from receipt by the CCC.
- These terms and conditions together with CCC's Billing and Payment terms and conditions (which are incorporated herein) form the entire agreement between you and WILEY concerning this licensing transaction and (in the absence of fraud) supersedes all prior agreements and representations of the parties, oral or written. This Agreement may not be amended except in writing signed by both parties. This Agreement shall be binding upon and inure to the benefit of the parties' successors, legal representatives, and authorized assigns.
- In the event of any conflict between your obligations established by these terms and conditions and those established by CCC's Billing and Payment terms and conditions, these terms and conditions shall prevail.

- WILEY expressly reserves all rights not specifically granted in the combination of (i) the license details provided by you and accepted in the course of this licensing transaction, (ii) these terms and conditions and (iii) CCC's Billing and Payment terms and conditions.

- This Agreement will be void if the Type of Use, Format, Circulation, or Requestor Type was misrepresented during the licensing process.

- This Agreement shall be governed by and construed in accordance with the laws of the State of New York, USA, without regards to such state's conflict of law rules. Any legal action, suit or proceeding arising out of or relating to these Terms and Conditions or the breach thereof shall be instituted in a court of competent jurisdiction in New York County in the State of New York in the United States of America and each party hereby consents and submits to the personal jurisdiction of such court, waives any objection to venue in such court and consents to service of process by registered or certified mail, return receipt requested, at the last known address of such party.

WILEY OPEN ACCESS TERMS AND CONDITIONS

Wiley Publishes Open Access Articles in fully Open Access Journals and in Subscription journals offering Online Open. Although most of the fully Open Access journals publish open access articles under the terms of the Creative Commons Attribution (CC BY) License only, the subscription journals and a few of the Open Access Journals offer a choice of Creative Commons Licenses. The license type is clearly identified on the article.

The Creative Commons Attribution License

The Creative Commons Attribution License (CC-BY) allows users to copy, distribute and transmit an article, adapt the article and make commercial use of the article. The CC-BY license permits commercial and non-

Creative Commons Attribution Non-Commercial License

The Creative Commons Attribution Non-Commercial (CC-BY-NC)License permits use, distribution and reproduction in any medium, provided the original work is properly cited and is not used for commercial purposes.(see below)

Creative Commons Attribution-Non-Commercial-NoDerivs License

The Creative Commons Attribution Non-Commercial-NoDerivs License (CC-BY-NC-ND) permits use, distribution and reproduction in any medium, provided the original work is properly cited, is not used for commercial purposes and no modifications or adaptations are made. (see below)

Use by commercial "for-profit" organizations

Use of Wiley Open Access articles for commercial, promotional, or marketing purposes requires further explicit permission from Wiley and will be subject to a fee.

Further details can be found on Wiley Online Library http://olabout.wiley.com/WileyCDA/Section/id-410895.html

Other Terms and Conditions:

v1.10 Last updated September 2015

Questions? customercare@copyright.com or +1-855-239-3415 (toll free in the US) or +1-978-646-2777.